

Dissertation
submitted to the
Combined Faculty of Natural Sciences and Mathematics
of the Ruperto Carola University Heidelberg, Germany
for the degree of
Doctor of Natural Sciences

**Analysis of CENP-A loading and
misincorporation in *Drosophila melanogaster***

Presented by
M.Sc. Engin Demirdizen
born in: Ankara, Turkey
Oral examination: 05.07.2018

Dissertation
submitted to the
Combined Faculty of Natural Sciences and Mathematics
of the Ruperto Carola University Heidelberg, Germany
for the degree of
Doctor of Natural Sciences

Presented by
M.Sc. Engin Demirdizen
born in: Ankara, Turkey
Oral examination: 05.07.2018

Analysis of CENP-A loading and misincorporation in *Drosophila melanogaster*

Referees: Prof. Dr. Frauke Melchior

Prof. Dr. Sylvia Erhardt

To my family and my love

ZUSAMMENFASSUNG

Das Zentromerische Protein-A (CENP-A, auch bekannt als ‚Centromere Identifier‘ oder CID in *Drosophila melanogaster*) ist eine epigenetische Markierung im Genom, die essentiell für die Identität von Zentromeren und deren Übertragung in die nächste Generation ist (Allshire & Karpen, 2008). Sobald CENP-A überexprimiert ist, lokalisiert das Protein ektopisch und dies kann zur Entstehung von neuen, sogenannten Neozentromeren führen. Dies resultiert fast ausnahmslos in einem instabilen Genom (Heun et al., 2006; Shrestha et al., 2017; Tomonaga, Matsushita, Yamaguchi, et al., 2003). Daher ist willkürlich lokalisiertes CENP-A ein prognostisches und prädiktives Kennzeichen für Tumorentwicklung (Filipescu et al., 2017). Um das bestehende Wissen um den detaillierten Mechanismus dieser inkorrekten Lokalisierung zu erweitern, untersuchte ich in dieser Arbeit alternative Signalwege für CENP-A Inkorporierung und Eliminierung, wobei ich kultivierte Fruchtfliegen S2 Zellen, wie auch ausgewachsene Fruchtfliegen verwendete. Studien deuten bisher darauf hin, dass RbAp48, generell ein Chromatin-Assemblierungs Faktor, eine Rolle beim ektopischen Einbau von CENP-A (Furuyama, Dalal, & Henikoff, 2006; Spiller-Becker, unpublished) und dessen *de novo* Lokalisierung in mehreren eukaryotischen Organismen spielt (Fujita et al., 2007; Hayashi et al., 2004; Lee, Lin, & Yuen, 2016). RbAp48 ist Teil von verschiedenen Chromatin-Assemblierungs/-Umgestaltungs und -Modifizierungs Komplexen (Doyen et al., 2013; Rai et al., 2013). Es ist jedoch noch nicht bekannt, ob RbAp48 seine Funktionen innerhalb eines größeren Komplexes bestehend aus mehreren Untereinheiten ausübt. Beispielsweise bildet RbAp48 eine Untereinheit des ‚Chromatin Assembly Factors-1‘ (CAF-1) Komplexes (Tyler, Bulger, Kamakaka, Kobayashi, & Kadonaga, 1996). Daher testete ich zu Anfang welche Rolle CAF-1 bei der Fehllokalisierung von CID spielt. Ich konnte jedoch keine überzeugenden Beweise dafür finden, dass CAF-1 am ektopischen Einbau von CID beteiligt ist, denn beispielsweise blieb die Quantität an ektopisch exprimiertem und lokalisiertem CID Protein nach der experimentellen Reduzierung von CAF-1 unverändert. Darüber hinaus konnte keine physische Interaktion der beiden Proteine nachgewiesen werden. Aufgrund dessen entschied ich, mit Hilfe von ‚Crosslinked Immunoprecipitation Mass Spec‘ (Xlink-IP-MS) weitere potentielle RbAp48-beinhaltende Komplexe zu finden, die in die Fehllokalisierung von CID verwickelt sein könnten. Interessanterweise identifizierte ich einen zweifach katalytischen und RbAp48-beinhaltenden Komplex – den ‚Nucleosome Remodelling and Deacetylase‘ (NuRD) Komplex. NuRD hat demnach zwei katalytische Funktionen: Zum einen Umgestaltung von Nukleosomen und zum anderen Deacetylierung von Histonen (Denslow & Wade, 2007). Ich konnte die physische Interaktion von CID mit den NuRD Hauptkomponenten Mi-2, MTA1-like und RbAp48 bestätigen. Wenn der katalytisch aktive Bestandteil Mi-2 und das Gerüstprotein MTA1-like dezimiert wurden, sank das Protein Level an mis-exprimierten CID sowie dessen Einbau in das Chromatin. Darüberhinaus war der nukleare Transport von CID und sein irrtümlicher Einbau ins Chromatin vermindert, sobald die Interaktionsplattform von RbAp48 mit MTA1-like modifiziert wurde. Zusammenfassend deuten diese Resultate darauf hin, dass die Interaktion mit RbAp47/MTA1-like für den Einbau von überexprimiertem CID wichtig ist und dass die katalytischen Bestandteile und Gerüst-Komponenten des NuRD Komplexes essentiell zur Fehllokalisierung von CID beitragen. Durch Xlink-IP-MS konnte außerdem auch, *hyperplastic discs*‘ (hyd), eine E3 Ubiquitin Ligase (Moncrieff, Moncan, Scialpi, & Ditzel, 2015), als CID-interagierendes Protein detektiert werden. Fälschlich lokalisiertes CID ist der Literatur zufolge ein Substrat für E3

Ligasen (Hewawasam et al., 2010; Moreno-Moreno, Medina-Giró, Torras-Llort, & Azorín, 2011; Ranjitkar et al., 2010). Demnach untersuchte ich auch die Hypothese, ob CID durch hyd gezielt proteolytisch abgebaut wird und konnte die genetische wie auch physische Interaktion beider Proteine nachweisen. Die Überexpression von Hyd resultierte in Poly-Ubiquitinierung und Destabilisierung von CID. Des Weiteren stieg die Proteinmenge von endo- wie auch exogenem CID nach der Depletion von hyd. Diese Ergebnisse demonstrieren, dass die hyd E3 Ligase CID Proteinmengen durch Ubiquitin vermittelte Proteolyse reguliert. Zusammenfassend konnte ich zeigen, dass der NuRD Komplex eine essentielle Rolle bei der nuklearen Lokalisation und willkürlichen Inkorporierung von fehlerhaft exprimiertem CID spielt, und dass dessen Stabilität durch die hyd E3 Ligase reguliert wird. Die Ergebnisse dieser Doktorarbeit tragen möglicherweise dazu bei, genauer zu verstehen wie dereguliertes CENP-A zu Krebsentwicklung führt und helfen potentiell dabei, neue Strategien zu entwickeln, die die verheerenden Folgen von irrtümlich eingebautem CENP-A in verschiedenen Tumorformen eindämmen.

SUMMARY

Centromeric Protein-A (CENP-A, known as Centromere Identifier (CID) in *Drosophila melanogaster*) is an epigenetic marker for centromere identity and propagation (Allshire & Karpen, 2008). Upon elevated expression, CENP-A mislocalizes to ectopic sites and can give rise to neocentromeres, thereby leading to genome instability (Heun et al., 2006; Shrestha et al., 2017; Tomonaga, Matsushita, Yamaguchi, et al., 2003). Promiscuously-incorporated CENP-A is a prognostic and predictive marker for tumor progression (Filipescu et al., 2017). To gain further understanding on this mechanism of mislocalization, I explored alternative CENP-A incorporation and elimination pathways, using cultured fly S2 cells and adult flies. Previous studies suggested that component of general assembly factors RbAp48 is involved in CENP-A ectopic incorporation (Furuyama, Dalal, & Henikoff, 2006; Spiller-Becker, unpublished) and *de novo* deposition in multiple eukaryotic lineages (Fujita et al., 2007; Hayashi et al., 2004; Lee et al., 2016). RbAp48 is found in several chromatin assembly, remodelling, and modification complexes (Doyen et al., 2013; Rai et al., 2013), but it is yet unknown whether RbAp48 carries out this function together with a multi-subunit complex. RbAp48 is a subunit of Chromatin Assembly Factor-1 (CAF-1) complex (Tyler et al., 1996). Thus, I first tested the role of CAF-1 in CID mislocalization but did not find convincing evidence for an involvement of CAF-1 in CID ectopic loading. Levels of ectopically expressed and misincorporated CID were stable upon CAF-1 depletion and no physical interaction was detected. Hence, I decided to search for the role of other potential RbAp48-containing complexes in CID misincorporation, using a Crosslinked Immunoprecipitation Mass Spec (Xlink-IP-MS) approach. Interestingly, I identified a dual catalytic and RbAp48-containing multi-subunit complex so called Nucleosome Remodelling and Deacetylase (NuRD) complex. NuRD has two catalytic functions, namely nucleosome remodelling and histone deacetylation (Denslow & Wade, 2007). I detected a physical interaction of overexpressed CID with the NuRD complex core components Mi-2, MTA1-like and RbAp48 and misexpressed CID protein levels decreased and chromatin incorporation upon depletion of the catalytic component Mi-2 and MTA1-like scaffold protein. Moreover, upon disruption of the RbAp48 interaction surface with MTA1-like, the nuclear transport and misincorporation of CID were impaired. Taken together, these results suggest that RbAp48/MTA1-like binding is required for nuclear incorporation of overexpressed CID, and catalytic and scaffold components of the NuRD complex are essential for the mislocalization of CID. Xlink-IP-MS also detected *hyperplastic discs* (hyd), an E3 ubiquitin ligase (Moncrieff et al., 2015) as CID interacting component. Mislocalized CENP-A is known to be targeted by E3 ligases in several eukaryotes (Hewawasam et al., 2010; Moreno-Moreno et al., 2011; Ranjitkar et al., 2010). Thus, I also tested the hypothesis that CID is targeted by hyd for proteasomal degradation. The genetic and physical interaction between CID and hyd were determined. Hyd overexpression resulted in poly-ubiquitination and destabilization of CID. Endogenous and ectopically expressed CID protein levels were found to increase upon hyd depletion. Collectively, these results demonstrated that hyd E3 ligase regulates CID protein levels through ubiquitin-mediated proteolysis. In summary, I found that the NuRD complex plays an essential role in nuclear localization and misincorporation of misexpressed CID, and its stability and incorporation are controlled by hyd E3 ligase. The findings presented in this work may contribute to our understanding of misregulated CENP-A in cancer and new strategies for tackling the detrimental misincorporation in many different tumor entities.

TABLE OF CONTENTS

ZUSAMMENFASSUNG	8
SUMMARY	10
1 INTRODUCTION	14
1.1 CHROMATIN	14
1.1.1 <i>Epigenetic Information</i>	14
1.1.1.1 Histone Variants	17
1.1.1.1.1 H3 variant CENP-A	17
1.1.1.1.1.1 Centromere and Kinetochore	18
1.1.1.2 Histone Assembly	21
1.1.1.2.1 Histone Variant Assembly	21
1.1.1.2.1.1 Replication-Coupled Chaperone CAF-1 Complex	22
1.1.1.2.1.2 CENP-A Assembly at Centromeres	22
1.1.1.2.1.3 CENP-A Misincorporation and Neocentromere Formation	25
1.1.1.2.1.3.1 CENP-A Regulation in Cancer	25
1.1.1.3 Chromatin Remodelling	26
1.1.1.3.1 Nucleosome Remodelling and Deacetylase (NuRD) Complex	28
1.1.1.3.1.1 NuRD Regulation in Cancer	30
1.1.1.4 Elimination of Mislocalized CENP-A	31
1.1.1.4.1 Hyd E3 Ubiquitin Ligase	32
2 AIM	32
3 RESULTS	34
3.1 CAF1 IS DISPENSABLE FOR CENP-A MISINCORPORATION IN <i>DROSOPHILA</i>	34
3.1.1 <i>RbAp48 physically interacts with CID</i>	34
3.1.2 <i>RbAp48 is required for loading of newly synthesized CID</i>	36
3.1.3 <i>Investigation of CID ectopic loading by RbAp48-tethering at LacO array</i>	36
3.1.4 <i>CID protein levels do not decrease upon depletion of CAF1 subunits</i>	38
3.2 NURD COMPLEX IS REQUIRED FOR MISLOCALIZATION OF CID	41
3.2.1 <i>Investigation of RbAp48-dependent CID loading complexes by IP-MS based approaches</i>	41
3.2.2 <i>B3 (A) is integrated into chromatin under RbAp48 overexpression</i>	46
3.2.3 <i>RbAp48-containing NuRD complex emerges as a candidate CID-interacting partner</i>	46
3.2.4 <i>CID and NuRD complex physically interacts</i>	48
3.2.5 <i>Ectopically expressed CID levels are reduced under silencing of Mi-2 and HDAC inhibition</i>	50
3.2.6 <i>CID ectopic localization goes down upon knockdown of Mi-2 and MTA1-like</i>	51
3.2.7 <i>CID ectopic loading requires interaction with NuRD complex</i>	54
3.2.8 <i>MTA1-like plays a role in nuclear translocation of ectopically expressed CID</i>	57
3.2.9 <i>Physical interaction with MTA1-like and NuRD complex is critical for nuclear localization of CID</i>	57
3.3 HYD E3 UBIQUITIN LIGASE IS INVOLVED IN DESTABILIZATION OF CID	60
3.3.1 <i>CID has a physical and genetic interaction with hyd</i>	60
3.3.2 <i>CID is poly-ubiquitinated and destabilized by hyd induction</i>	62
3.3.3 <i>Cellular CID levels increase upon hyd knockdown in interphase cells</i>	64
3.3.4 <i>Centromeric CID levels increase upon hyd knockdown in mitotic chromosomes</i>	67
4 DISCUSSION	70
4.1 CAF-1/CID INTERACTION IS MOST LIKELY NOT PRESENT IN <i>DROSOPHILA</i>	70
4.2 RBAP48 IS NECESSARY AND SUFFICIENT FOR PRIMING <i>DE NOVO</i> CID DEPOSITION AT CENTROMERES AND ECTOPIC SITES	71
4.3 CAF-1 DOES NOT PLAY AN OBVIOUS ROLE IN CID MISINCORPORATION	71
4.4 HYD E3 LIGASE IS A NOVEL CANDIDATE CID INTERACTING PARTNER	72
4.5 NURD COMPLEX IS AN INTERESTING CANDIDATE FOR REGULATION OF CID LOADING	72
4.6 CID INTERACTS WITH NURD CORE SUBUNITS	74

4.7 TARGETING OF NURD CATALYTIC AND SCAFFOLD COMPONENTS ABROGATES CID MISLOCALIZATION AND STABILITY	74
4.8 RBAP48-MTA1-LIKE BINDING POCKET IS REQUIRED FOR CID NUCLEAR LOCALIZATION	76
4.9 HYD IS INVOLVED IN THE REGULATION OF CID SYNTHESIS AND INCORPORATION	76
4.10 POTENTIALLY NON-CONSERVED CAF-1-MEDIATED CID MISINCORPORATION MECHANISM IN <i>DROSOPHILA</i>	77
4.11 THE POTENTIAL ROLE OF REMODELING AND DEACETYLATION IN CENP-A MISLOCALIZATION BY THE NURD COMPLEX	78
4.12 THE CRITICAL ROLE OF RBAP48-MTA1-LIKE BINDING INTERFACE IN NUCLEAR LOCALIZATION OF OVEREXPRESSED CID	79
4.13 THE CONTROL OF CID LEVELS AND LOADING BY HYD E3 LIGASE	79
4.14 POTENTIAL WORKING MODEL FOR NURD-MEDIATED CENP-A MISLOCALIZATION IN <i>DROSOPHILA</i> AND SUMMARY	80
5 CONCLUSIONS	83
6 FUTURE PERSPECTIVES	84
7 MATERIALS AND METHODS	86
7.1 MATERIALS	86
7.2 METHODS	95
7.2.1 <i>Molecular Biology Techniques</i>	95
7.2.1.1 Molecular cloning	95
7.2.1.2 Preparation of double-stranded RNA for RNA interference studies	95
7.2.1.3 Inducible gene constructs: the pMT-V5-His vector system	95
7.2.1.4 Mutagenesis	96
7.2.1.5 RNA Isolation and RT-PCR	96
7.2.1.6 Yeast two hybrid	96
7.2.2 <i>Tissue culture methods using Drosophila S2 cells</i>	97
7.2.2.1 Growing and maintaining S2 cells	97
7.2.2.2 Thawing <i>Drosophila</i> S2 cells	97
7.2.2.3 Freezing S2 cells	97
7.2.2.4 Transfection of S2 cells	98
7.2.2.5 Drug treatment of S2 cells	98
7.2.2.6 RNAi in S2 cells	98
7.2.3 <i>Microscopy</i>	98
7.2.3.1 Image acquisition on Deltavision microscope	98
7.2.3.2 Image quantification using ImageJ software	99
7.2.3.3 Indirect immuno-fluorescence (IF)	99
7.2.3.4 Preparation of mitotic spreads	99
7.2.4 <i>Biochemical methods</i>	100
7.2.4.1 Preparation of S2 cell lysates	100
7.2.4.2 Co-immunoprecipitation of GFP-tagged proteins	100
7.2.4.3 Xlink-IP	100
7.2.4.4 Co-immunoprecipitation of V5 or His-tagged proteins	100
7.2.4.5 SDS PAGE and western blot analysis	101
7.2.4.6 Mass spectrometry of proteins and data analysis	101
7.2.5 <i>Fly Genetics</i>	102
7.2.5.1 Fly culture	102
7.2.5.2 Virgin collection	102
7.2.5.3 Genetic interaction using CID overexpression flies	102
7.2.5.4 Induction of RNAi in flies	102
8 APPENDICES	103
9 BIBLIOGRAPHY	111
LIST OF ABBREVIATIONS	132
ACKNOWLEDGMENTS	136

1 INTRODUCTION

1.1 Chromatin

Chromatin is the heritable material of living organisms consisting of DNA and histones (Soshnev, Josefowicz, & Allis, 2016). From yeast to human, linear DNA is made up of several megabases to gigabases of nucleotides (Schwartz & Cavalli, 2017). This long molecule needs to be packed into hierarchical structural units so that it fits into the nucleus of about 10 μm size, for instance in human (Schwartz & Cavalli, 2017). Chromatin is packed into 10 nm fibers, further folding of which builds up higher order chromatin structures (Sitbon, Podsypanina, Yadav, & Almouzni, 2017), as depicted in Figure 1.1 (modified from Feinberg, 2018). Another corresponding term so called “beads on a string” is also commonly used to define this 10 nm fiber structure (Grigoryev, 2018). This term comes from single nucleosomal subunits with 147 bp DNA wrapped around it (Sequeira-Mendes & Gutierrez, 2016). As the basic unit of chromatin, nucleosome structure contains a histone octamer, which comprises of duplicate H2A, H2B, H3 and H4 core histones (Waldmann & Schneider, 2013). Linker DNA and a linker histone H1 also participates into this complex to form a complete nucleosome structure (Sequeira-Mendes & Gutierrez, 2016). In terms of transcription, chromatin can be divided into two main subgroups (Figure 1.1): Transcriptionally highly active so called euchromatin and transcriptionally less active so called heterochromatin (Allis & Jenuwein, 2016). Epigenetic marks underlie the labeling and discrimination of those regions (Schwartz & Cavalli, 2017).

1.1.1 Epigenetic Information

The term epigenetics, first introduced by Waddington (Waddington, 1942), was originally used to define the relationships between genes and their products, which ultimately influences the phenotypic outcome (Waddington, 1957). His definition was fundamentally based on the perspective that final consequences of tissue development are determined by genetics rather than environment (Waddington, 1957). He also used the term “epigenetic landscape” to define the paths that a pluripotent cell goes around, ending up with its ultimate destiny (Waddington, 1957). The recent view on epigenetics has been changed by noticing that environmental factors influence developmental dynamics (Feinberg, 2018). Epigenetics is currently described as the sources of information, which is retained in the chromatin except for DNA sequence, propagated to daughter cells, modulated by environmental effects, and leads to permanent impacts on gene expression (Feinberg, 2018; Steven Henikoff & Greally, 2016). The epigenetic phenomena are best described with a well-known calico cat example (Steven Henikoff & Greally, 2016). The calico cat has orange or black furs due to the inactivation of one or the other X chromosome for dosage compensation in females (Steven Henikoff & Greally, 2016). These two states are stably inherited through development, bringing about phenotypically different two cell lineages from same genetic background (Feinberg, 2018; Steven Henikoff & Greally, 2016). This familiar example of epigenetic processes elegantly illustrates that epigenetic information influenced by environmental or developmental inputs stably alters gene expression, and this cellular memory is maintained during development and translated into phenotype (Feinberg, 2018; Steffen & Ringrose, 2014; Turner, 2002).

There are different sources of epigenetic information (Feinberg, 2018). The first one discovered was DNA methylation (Holliday & Pugh, 1975). This has been followed by histone modification, histone variants, chromatin remodeling, non-coding RNAs and higher order chromatin structures (Allis & Jenuwein, 2016; Feinberg, 2018; Soshnev et al., 2016). DNA methylation and histone modification (Figure 1.1) can be controlled by enzymatic factors so called writers, erasers and readers (Jones, Issa, & Baylin, 2016; Sequeira-Mendes & Gutierrez, 2016), and they also determine transcription activity (Allis & Jenuwein, 2016). For instance, DNA hypermethylation regulated by DNA methyl transferases (DNMTs) and ten-eleven translocation methyl cytosine dioxygenase (TETs) at promoters are usually associated with transcription inhibition (Jones et al., 2016). As one of the most common histone modifications, acetylation, modulated by histone acetyltransferases (HATs) and histone deacetylases (HDACs), is usually associated with active chromatin (Ribich, Harvey, & Copeland, 2017). On the other hand, methylation, controlled by histone methyltransferases (HMTs) and histone demethylases (HDMs) is associated with either active or inactive chromatin depending on which lysine is modified (Allis & Jenuwein, 2016). All those epigenetic labels on a given genetic material collectively form the epigenetic code or epigenome (Kelly & Issa, 2017). Epigenomic alterations, similar to genetic mutations, can also be linked to diseases and globally targeted by certain type of drugs for therapeutic reasons (Kelly & Issa, 2017; Ribich et al., 2017).

Recent advances in 3C-based techniques and imaging of 3D chromatin architecture elucidated yet another epigenetic source of information known as higher-order chromatin structures (Bonev & Cavalli, 2016), including chromosome territories, chromatin loops and topologically associated domains (TADs) (Schwartz & Cavalli, 2017). In these special organization units, several chromatin processes can be regulated such as transcription, replication and repair (Bonev & Cavalli, 2016). Long non-coding RNAs are also involved in structural architecture and maintenance of these higher-order structures (Rošić & Erhardt, 2016; Sitbon et al., 2017). Remaining epigenetic sources of information, including histone variants and chromatin remodeling, will be discussed in detail in the following sections.

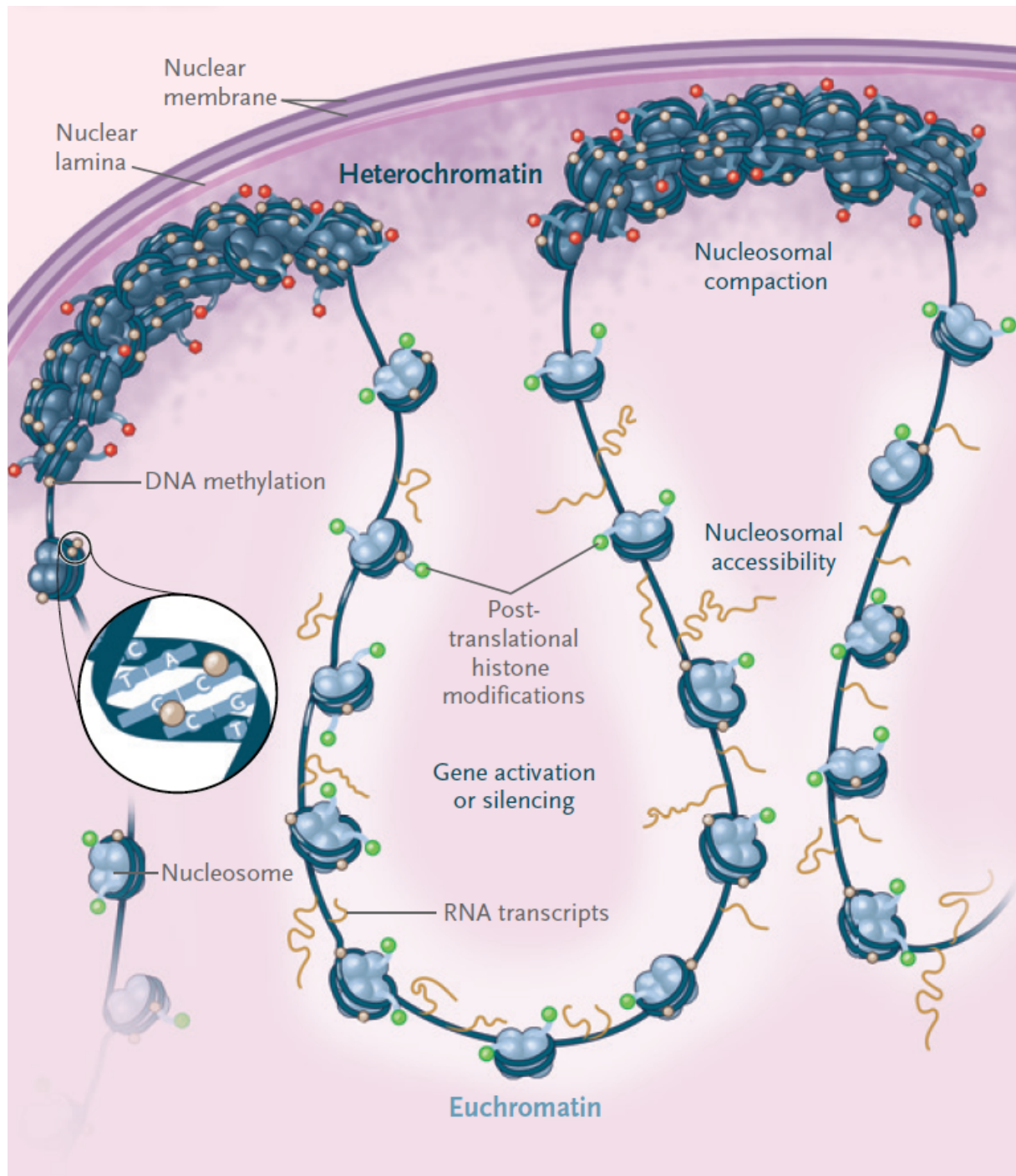


Figure 1.1 The epigenetic information in the cell, modified from Feinberg (2018). DNA is wrapped around histone octamer, making nucleosomes. Chromatin is organized into two subcompartments in the nucleus: silent heterochromatin and active euchromatin. Epigenetic elements regulate this organization. Marked by predominantly repressive marks, such as DNA methylation (light brown balls) and histone methylation (red balls), heterochromatin undergoes higher order chromatin compaction and inhibits the accessibility for transcription machinery. On the other hand, marked by active marks, such as histone acetylation (green balls), euchromatin is accessible for transcription machinery, and there is ongoing synthesis of mRNA. Nuclear periphery is sometimes permissive but mostly repressive for transcription.

1.1.1.1 Histone Variants

Histone variants together with their respective chaperones are considered as ‘bricks of chromatin architecture’, which label particular chromatin area with a distinctive signature in a cell cycle-dependent manner (Sitbon et al., 2017). In human somatic cells, eight H2A variants have been revealed up to date, whereas two H2B variants have been testis-specific (Buschbeck & Hake, 2017). They are involved in critical biological roles. For instance, phosphorylated H2A.X marks sites of DNA damage and is involved in the initiation of damage signaling (Buschbeck & Hake, 2017; Singh et al., 2012). Another well-studied example H2A.Z, as a placeholder variant, occupies nucleosome-depleted promoter, enhancer and insulator regions, and is therefore involved in transcriptional activation (P. Chen, Wang, & Li, 2014; Jin et al., 2009). In addition, MacroH2A-containing nucleosomes were shown to be recognized by PARP1 (Timinszky et al., 2009), which then recruits histone acetyltransferase CBP and leads to acetylation of neighboring histones (Chen *et al.*, 2014). Another well-described class of histone variants are H3 variants. In humans, eight H3 variants have been found so far (Waterborg, 2012), with evolutionary conservation across several species (Sitbon et al., 2017). H3.1 and H3.3 variants share 96.3 % sequence conservation with only 5 different amino acids, while the centromeric histone H3 variant CENP-A is highly dissimilar to H3.1, with only 45.1 % conservation (Buschbeck & Hake, 2017). Those H3 variants are functionally associated with replication, repair and chromosome stability (Ray-Gallet et al., 2002). H3.3 has many functions, including transcription, telomere silencing, pericentric transcription, regulation of sperm chromatin and functions as a placeholder at centromeres (Gibbons, Picketts, Villard, & Higgs, 1995; Goldberg et al., 2010; Lewis, Elsaesser, Noh, Stadler, & Allis, 2010). Centromeric protein A (CENP-A) acts as an epigenetic determinant of centromeres (Allshire & Karpen, 2008). Interestingly, there are no H4 variants identified so far in higher eukaryotes (Maze, Noh, Soshnev, & Allis, 2014).

1.1.1.1.1 H3 variant CENP-A

One of the most interesting epigenetic sources of Information is CENP-A, contributing to stable transmission of a biological process through cell divisions (Müller & Almouzni, 2017a). In majority of eukaryotes, CENP-A acts as a marker and epigenetic identifier of centromeres (Sitbon et al., 2017) and maintains genome stability (Bodor, Valente, Mata, Black, & Jansen, 2013; Nechemia-Arbely et al., 2017). Lack of CENP-A results in mitotic defects and senescence (Bodor et al., 2014). The change of centromeric chromatin architecture by the presence of an H3 variant CENP-A demonstrates the importance of epigenetic features in shaping the chromatin (Sitbon et al., 2017). Furthermore, the maintenance of this mechanism is essential for chromatin stability during the cell cycle stages and survival of the organism in the long term (Allshire & Karpen, 2008). Thus, timing and abundance are critical concepts for the control of CENP-A and its biological roles (Müller & Almouzni, 2017a). After introducing the roles of CENP-A in centromere and kinetochore functions, I will focus on timing and abundance issues, which may result in catastrophic consequences upon misregulation.

1.1.1.1.1 Centromere and Kinetochore

During cell division, the center of condensed chromosomes appear as primary constrictions (Flemming, 1882), as depicted in Figure 1.2a (modified from Przewloka and Glover, 2009). These special chromatin structures called centromeres provide the platform for multi-subunit kinetochore complex and the microtubule spindle attachment as seen in Figure 1.2c (modified from Allshire and Karpen, 2008), which is required for chromosome segregation during mitosis and meiosis (Sevim, Bashir, Chin, & Miga, 2016). Centromere identity in most eukaryotes is determined by the H3 variant CENP-A (Henikoff, Ahmad, Platero, & van Steensel, 2000; Pauleau & Erhardt, 2011), or CID in flies, (Talbert & Henikoff, 2010), which replaces H3 in centromeric nucleosomes (Amor *et al.*, 2004). CENP-A protein marks the centromeric DNA and is evolutionarily conserved through all eukaryotes (Amor *et al.*, 2004). In *S. cerevisiae*, 125 bp centromeric DNA defines the point centromere with single CENP-A-containing nucleosome and single microtubule attachment site (Sullivan, Boivin, Mravinac, Song, & Sullivan, 2011). In majority of eukaryotes, there are regional centromeres, which enable multiple spindles to attach (Sullivan & Karpen, 2004). In fission yeast, CENP-A nucleosomes located in the centromeric site are surrounded by H3 nucleosome-containing heterochromatin (Malik & Henikoff, 2003). In flies and vertebrates, CENP-A nucleosomes are interspersed with H3 nucleosomes with distinct modifications along the megabases-long arrays of centromeric satellite repeats (Malik & Henikoff, 2003). The alternating distribution of CENP-A nucleosomes enables spindle microtubules to contact with the centromere only at the outer surface (Black & Cleveland, 2011; Guse, Carroll, Moree, Fuller, & Straight, 2011; Steven Henikoff & Furuyama, 2012; Mendiburo, Padeken, Fülöp, Schepers, & Heun, 2011). In worms, CENP-A is dispersed along the whole chromosome, creating special holocentromeres, to which individual spindle fibers can attach (Buschbeck & Hake, 2017). Overall, there is now a consensus on the notion that CENP-A is required and sufficient for centromere establishment and inheritance (Buschbeck and Hake, 2017).

Most eukaryotic centromeres are located at repetitive sequences, which are called α -satellite sequences in human (Amor *et al.*, 2004; Melters *et al.*, 2013). These sequences are variable among the species and even among different chromosomes (Steven Henikoff & Smith, 2015), as indicated in Figure 1.2b (modified from Allshire and Karpen, 2008). Exceptionally, in budding yeast, a specific centromeric sequence consisting of 125 bp is required and adequate for centromere formation (Amor *et al.*, 2004). Unlike in budding yeast, centromeres consist of several megabases of tandemly repeating short sequences in most plants and animals (Allshire & Ekwall, 2015; Steven Henikoff & Smith, 2015). In those higher eukaryotes, neocentromeres can occur at completely different non-centromeric DNA regions (Müller & Almouzni, 2017b), suggesting that DNA sequence does not appear to underlie centromere specification (Allshire & Ekwall, 2015; Steven Henikoff & Smith, 2015). Argumentatively, recent evidence suggest that centromeric satellite repeats in plants and animals form a non-B form of DNA structure, thereby playing a role in centromere identification (Kasinathan & Henikoff, 2017). Despite the controversy, collectively, the conservation of centromere identity is thought to be through epigenetic rather than genetic mechanisms (Allshire and Ekwall, 2015; Henikoff and Smith, 2015).

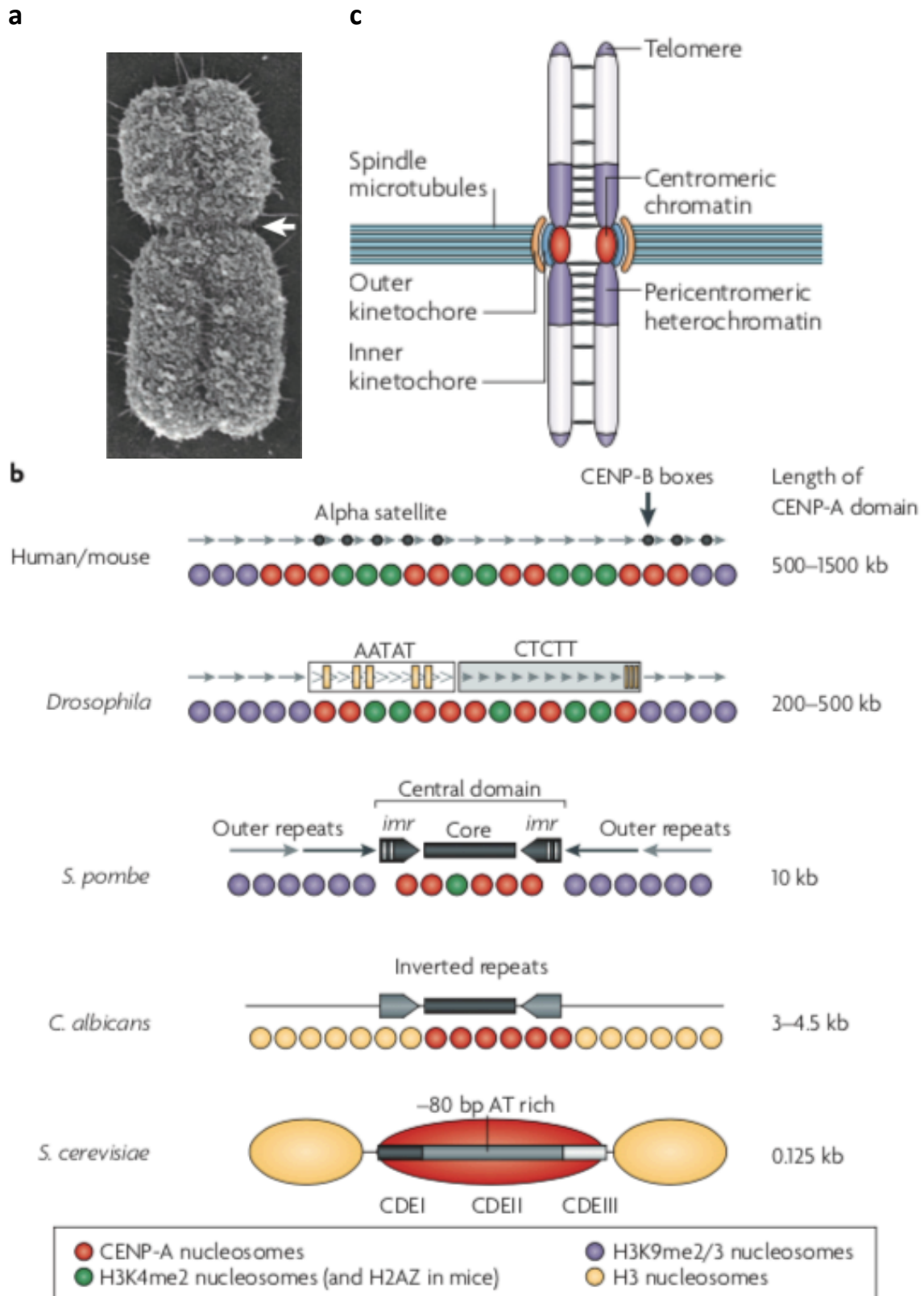


Figure 1.2 Centromeres are functionally conserved primary constriction sites for kinetochore assembly during chromosome segregation.

A Metaphase chromosome image taken by scanning electron microscope modified from Przewlaka and Glover (2009). The centromere is marked by arrow. **B** Schematic illustration of variable centromeric chromatin elements from human/mouse, *Drosophila*, *S. pombe*, *C. albicans* and *S.*

cerevisiae modified from Allshire and Karpen (2008). Imr: innermost repeat, CDE: centromere DNA element. **C** Representative image of a mitotic chromosome with kinetochore and spindle fiber attachment modified from Allshire and Karpen (2008). Centromeres are initially identified by CENP-A, and then inner-outer kinetochore and microtubule binding follows, which ensures proper segregation of chromosomes.

In addition to CENP-A, other epigenetic regulatory mechanisms contribute to centromere identity and function. A long non-coding RNA, known as satellite III in *Drosophila*, has been found to be involved in assembly of kinetochore assembly and function in humans and flies (Quénet & Dalal, 2014; Rošić, Köhler, & Erhardt, 2014). Moreover, in several biological systems, including *Drosophila*, centromeric transcription rather than the transcript itself has been shown to be critical for de novo CENP-A deposition (Müller and Almouzni, 2017a). Transcription at pericentric regions is also required for pericentric heterochromatin (PHC) formation and inheritance (Maison & Almouzni, 2004). PHC is labelled by the repressive marks and factors, including H3K9me₂, H3K9me₃, H4K20me₃ and heterochromatin protein 1 HP1 (Probst & Almouzni, 2011). HP1 is not only essential for heterochromatin establishment but also for cohesion interaction, which is important for chromosome segregation (Hahn et al., 2013). PHC has been suggested to act as a barrier to block propagation of centromere into other gene regions (Scott, White, & Willard, 2007). Centromeric regions, on the other hand, possesses marks which enable open chromatin and transcription, including H3K4me₃ and H3K36me (Bergmann et al., 2011). FACT complex also facilitates transcription and H2A-H2B turnover at centromeres (Chen et al., 2015). H4K20me₁ also plays a role in stabilization of kinetochore attachment following CENP-A assembly (Hori et al., 2014). Phosphorylation at N-terminal S16 and S18 of CENP-A, on the other hand, leads to stronger intranucleosomal interactions (Bailey et al., 2013). Collectively, all these epigenetic elements, including CENP-A, play essential roles for centromere identity and kinetochore attachment.

Kinetochore is the huge protein assembly that mediates microtubule attachment to centromeres (Westhorpe and Straight, 2013). Kinetochore complex consists of inner kinetochore, also known as constitutive centromere associated network (CCAN), and outer kinetochore (Musacchio & Desai, 2017). Most CCAN components are loaded at centromeres in G2 and M phases and involved in stabilization rather than incorporation of CENP-A (Müller & Almouzni, 2017a). For instance, CCAN component CENP-B interaction with both CENP-B box and the N-tail of CENP-A improves the centromere stability but is non-essential for CENP-A assembly (Fachinetti et al., 2015). CENP-A nucleosomes are more compact in the sense that 121 bp DNA sequence is wrapped around, creating flexible DNA ends (Tachiwana et al., 2011). The linker histone H1 is intriguingly excluded from those flexible ends of CENP-A nucleosomes (Roulland et al., 2016), which is thought to contribute to the establishment of kinetochores (Müller & Almouzni, 2017a). CENP-C is required for further structural compacting and bridging with other components (Falk et al., 2015). Both CENP-C and CENP-T play critical roles in recruitment of the outer kinetochore (Klare et al., 2015; Tachiwana et al., 2015). The interaction between CENP-T and CENP-W, which is mediated by CENPH/I/K/M, is also important for inner kinetochore assembly in human (Musacchio & Desai, 2017). The outer kinetochore is required to transfer the pulling forces exerted by microtubules to centromere and chromosome (Cheeseman, Chappie, Wilson-Kubalek, & Desai, 2006). The outer kinetochore core complex consists of KMN network, including Knl1 complex, Mis12 complex and Ndc80 complex (Musacchio & Desai, 2017). Ndc80 complex is

the initial receiver of the microtubule attachment (Cheeseman et al., 2006; DeLuca et al., 2006). Mis12 complex enables the interaction of CENP-C-/CENP-T with KMN network and plays a bridging role between Knl1 and Ndc80 complexes (Suzuki, Badger, & Salmon, 2015).

1.1.1.2 Histone Assembly

Canonical histones are assembled into a nucleosome core complex in a replication- or repair-dependent manner (Sitbon et al., 2017). H2A-H2B heterodimer complex is recognized and delivered to nucleosome core complex by NAP1 and FACT chaperones (Andrews, Chen, Zevin, Stargell, & Luger, 2010; Belotserkovskaya et al., 2003; Mosammaparast, Ewart, & Pemberton, 2002). H3 and H4 interaction gives rise to a heterodimer complex, which is recognized by the general H3 chaperone ASF1 (Natsume et al., 2007). Acetylation, carried out by HATs, is also required for the nuclear import and assembly of canonical H3-H4 histone complex (Hewawasam, Dhatchinamoorthy, Mattingly, Seidel, & Gerton, 2018; Kaufman, Kobayashi, Kessler, & Stillman, 1995; Tyler et al., 2001, 1996). ASF1 carries this complex into the nucleus and transfers it to CAF-1 complex or HIRA H3 chaperones (Buschbeck & Hake, 2017; Natsume et al., 2007; Talbert & Henikoff, 2016). CAF-1 can locate at replication forks and then deposit (H3-H4)₂ heterotetramer into histone octamer (Liu, Roemer, Port, & Churchill, 2012; Shibahara & Stillman, 1999; Winkler, Zhou, Dar, Zhang, & Luger, 2012). FACT complex also contributes in parallel to CAF-1 for replication-coupled assembly process (Kaufman et al., 1995). FACT can recognize both H3K56Ac-acetylated, newly-synthesized H3-H4 dimers (Yang et al., 2016) as well as H2A-H2B dimers and recruit them into the replicating chromatin through interaction with MCM helicase (Foltman et al., 2013).

1.1.1.2.1 Histone Variant Assembly

Similar to canonical histones, histone variants are also loaded by their dedicated chaperones. Loading of H2A.X is regulated by FACT chaperone complex (Belotserkovskaya et al., 2003). SRCAP and p400 remodelers, on the other hand, are involved in H2A.Z incorporation (Bönisch et al., 2012). ATRX was reported to assemble another H2A variant MacroH2A (Ratnakumar et al., 2012). In terms of their assembly pathways, H3 variants can be divided into two subgroups as replication-coupled or uncoupled (Gaillard et al., 1996; Polo, Roche, & Almouzni, 2006). H3.1/2 variants reach their peak expression level in S phase (Ahmad & Henikoff, 2002; Hamiche & Shuaib, 2012) and deposited into chromatin by CAF-1 histone chaperone complex in a replication (Hamiche & Shuaib, 2012) or repair-dependent manner (Ahmad & Henikoff, 2002), as illustrated in Figure 1.3 (modified from Filipescu, Szenker and Almouzni, 2013). H3.3 placeholder variant, on the other hand, is synthesized at every cell cycle stage (Ahmad & Henikoff, 2002; Hamiche & Shuaib, 2012) and loaded in a replication-independent way (Figure 1.3) (Ray-Gallet et al., 2002; Tagami, Ray-Gallet, Almouzni, & Nakatani, 2004) by two different chaperones. HIRA chaperone complex for instance is involved in loading of H3.3 variant at promoters, gene bodies and regulatory elements (Figure 1.3) (Nye, Melters, & Dalal, 2018). DAXX complex on the other hand is responsible for H3.3 incorporation at telomeres and pericentric heterochromatin (Figure 1.2) (Jansen, Black, Foltz, & Cleveland, 2007; Shelby, Monier, & Sullivan, 2000). DAXX is accompanied by a SWI/SNF type remodeler ATRX for the H3.3 loading (Nye et al., 2018). Unlike other H3 variants, centromeric protein A (CENP-A) loading is different in terms of cell

cycle regulation and chaperone specificity (Dunleavy et al., 2009; Foltz et al., 2009; Shuaib, Ouararhni, Dimitrov, & Hamiche, 2010), which will be discussed later in detail.

1.1.1.2.1.1 Replication-Coupled Chaperone CAF-1 Complex

One of the major chaperones that incorporate newly-synthesized H3-H4 dimer into replicating genome is CAF-1 (Kaufman et al., 1995). The CAF-1 complex is conserved among eukaryotes and consists of three components from yeast to humans (G. S. Hewawasam et al., 2018; Kaufman et al., 1995; Tyler et al., 2001, 1996). CAF-1 is responsible for replication-coupled loading of H3-H4 histones (Kaufman et al., 1995; Tyler et al., 2001). CAF-1 also plays essential roles in DNA repair pathways (Gaillard et al., 1996), including nucleotide excision repair (Green & Almouzni, 2003; Moggs et al., 2000; Polo et al., 2006), mismatch repair coupled assembly of H3 and H4 histones (Blanko, Kadyrova, & Kadyrov, 2016) and repair of double strand breaks (Linger & Tyler, 2005). Through heterochromatin maintenance, CAF-1 also contributes to protection against retrotransposons and genome stability (Hatanaka et al., 2015). Influencing critical biological processes, it is an essential complex for *Drosophila* development (Y. Song et al., 2007).

In human, CAF-1 is made up of p150, p60 and RbAp48 (p48) subunits (Kaufman et al., 1995). In flies, CAF-1 complex consists of p180, p105 and RbAp48 (p55) subunits (Tyler et al., 2001). The largest component p180 is known to interact with PCNA and HP1, connecting CAF-1 with DNA replication and heterochromatin maintenance (Gurard-Levin, Quivy, & Almouzni, 2014; Huang et al., 2010). CAF-1-p105 mediates the interaction between CAF-1 and ASF1 (Tyler et al., 2001). CAF-1-p105 is not only important for the link between CAF-1 and H3-H4 complex but also for the stability of the complex as a scaffold protein (Ye *et al.*, 2003). RbAp48, a 55 kDa protein also known as p55 or Caf1, has homology to human RbAp46 and RbAp48 proteins (Tyler et al., 1996). In *Drosophila*, proper RbAp48 function is essential for fundamental biological processes, survival and preservation of the cellular identity (Anderson et al., 2011; Cheloufi et al., 2015). It directly interacts with H4 (Murzina et al., 2008; Song, Garlick, & Kingston, 2008). Interestingly, RbAp48 participates into several chromatin assembly, remodelling and modification complexes, such as NuRD, NuRF, PRC2 and dREAM (Doyen et al., 2013; Rai et al., 2013). It is unclear whether CAF-1 is involved in CENP-A assembly in *Drosophila*.

1.1.1.2.1.2 CENP-A Assembly at Centromeres

CENP-A incorporation is tightly regulated during the cell cycle (Müller & Almouzni, 2017b). In mammals, and most higher eukaryotes, CENP-A is diluted in S phase between the daughter centromeres, synthesized in G2 phase (Müller & Almouzni, 2014) and deposited between late telophase and early G1 (Jansen et al., 2007). Distinctively, CID is loaded in M phase in flies (Mellone et al., 2011; Schuh, Lehner, & Heidmann, 2007). Intriguingly, CENP-A loading occurs in S phase in *S. cerevisiae* (Pearson et al., 2004) and in S-G2 phase in *S. pombe* (Lando et al., 2012; Takayama et al., 2007). The reason why the timing of CENP-A deposition has evolved in such a way as to exclude S phase in higher eukaryotes could be to avoid promiscuous incorporation during DNA replication (Müller & Almouzni, 2017b). *De novo* CENP-A deposition is preceded by a licensing phase, which requires acetylation (Bergmann et al., 2012) and chromatin remodelling (Okada, Okawa, Isobe, & Fukagawa,

2009). Licensing in humans is controlled by loading of RBAP46 or RBAP48 together with MIS18 complex, comprising of MIS18BP1, MIS18 α and MIS18 β at early anaphase (Fujita et al., 2007). In *Drosophila*, RbAp48/CID/H4/Hat1 complex has been shown to regulate centromere licensing, acetylation (Furuyama et al., 2006; Hayashi et al., 2004), nuclear import and deposition at centromeres (Boltengagen et al., 2015; Shang et al., 2016a).

The domains and PTMs of CENP-A are critical for chaperone specificity and cell cycle-dependent loading. The HFD (histone fold domain) of CENP-A, which contains the CATD (CENP-A targeting domain), is responsible for chaperone specificity and centromeric targeting (Shuaib et al., 2010). Arginine and lysine-rich motifs in the N-tail of CENP-A have been shown to be required for nuclear import, DNA contact and centromeric targeting in human cells (Jing, Xi, Leng, Chen, Wang, & Jia, 2017). This is in accordance with the observations from a previous student that the deletion of the N-tail (Δ NCID mutant) or the conversion of particular arginines to alanines (B3-A mutant) prevents nuclear and centromeric localization of *Drosophila* CENP-A (Spiller-Becker, unpublished). In humans, HJURP plays a critical role in centromere formation, maintenance and propagation through *de novo* CENP-A incorporation (Silva et al., 2018; Stankovic et al., 2017) in a cell cycle-dependent manner (Dunleavy et al., 2009; Foltz et al., 2009). CDK/Cyclin A phosphorylation regulates HJURP positioning and licensing (Zasadzińska, Barnhart-Dailey, Kuich, & Foltz, 2013). HJURP interacts with CENP-A both in the prenucleosomal complex and nucleosomal complex, to ensure proper targeting at centromeres (Stoler et al., 2007). CENP-A phosphorylation at S68 inhibits binding of prenucleosomal assembly complex and premature assembly (Stoler et al., 2007). CENP-A K124 ubiquitination regulates stability of HJURP-CENP-A complex and assembly (Niikura et al., 2015a). In *Drosophila*, the HJURP orthologue CAL1 is responsible for the incorporation of CENP-A, also called CID, together with CENP-C into centromeric chromatin (Chen et al., 2014). The stability of CAL1/CID complex in *Drosophila* is controlled by mono-ubiquitination of CENP-A in a CUL3/RDX-dependent manner (Bade, Pauleau, Wendler, & Erhardt, 2014a). Scm3 is the dedicated chaperone for CENP-A, also called Cse4, centromeric loading in budding yeast (Allshire & Karpen, 2008). In *C. elegans*, RbAp48 homologue LIN-53 functions in transport and deposition of holocentric CENP-A, known as HCP-3 (Lee, Lin and Yuen, 2016). Even though the names and amino acid homology vary between species, CENP-A chaperone is functionally conserved and required for centromeric targeting.

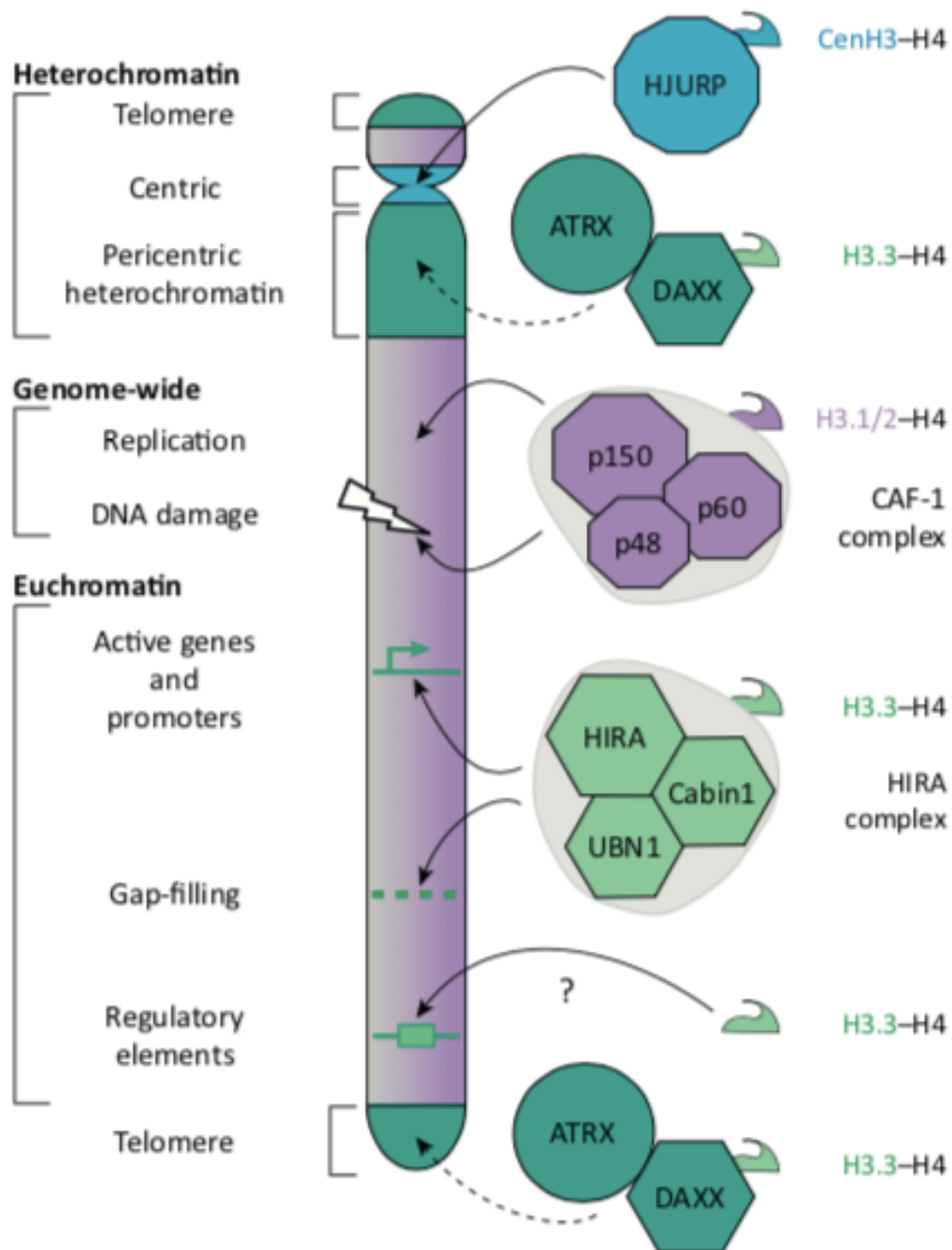


Figure 1.3 Loading pathways of H3 variants in mammals by their specific chaperone complexes, modified from Filipescu, Szenker and Almouzni (2013). Canonical H3.1/2-H4 histones are incorporated by CAF-1 complex, consisting of p150, p60 and p48 subunits in mammals, into chromatin genome-wide in a replication or repair-dependent manner. H3.3-H4 heterodimer histone complex is loaded by DAXX/ATRX complex into telomeres and pericentric heterochromatin independent of replication. HIRA, which is made up of HIRA, Cabin1 and UBN1 components, deposits H3.3-H4 dimer into active genes and promoters, gap-filling sites and regulatory elements irrespective of S phase. HJURP is involved in loading of centromeric H3 variant CenH3 (CENP-A) at centromeres in late mitosis-early G1 phase in mammals.

1.1.1.2.1.3 CENP-A Misincorporation and Neocentromere Formation

In most eukaryotes, only one specialized regional centromere is functional (Miga et al., 2014). The presence of another active centromere at non-centromeric site is called neocentromere, which very rarely occurs on X and Y chromosomes (Miga et al., 2014), and can lead to segregation defects and aneuploidy if the actual centromere is still active (Benito et al., 2015; Gu et al., 2014; Li et al., 2011; Ma et al., 2003; Qiu et al., 2013; Tomonaga, Matsushita, & Yamaguchi, 2003). Neocentromeres can be observed due to chromosome rearrangements in a cell (Voullaire, Slater, Petrovic, & Choo, 1993), or alternatively, occur by inactivation of the endogenous centromere (Scott & Sullivan, 2014) and be inherited through several generations (Amor et al., 2004). A particular chromatin environment containing a threshold level of CENP-A (Bodor et al., 2014) and heterochromatin might favour neocentromere formation (Olszak et al., 2011). Ectopic localization of yeast CENP-A occurs in active histone turnover sites in the absence of yeast CAF-1 and HIRA complexes due to the lack of CENP-A eviction from those sites (Rosa, Holik, Green, Rando, & Kaufman, 2011). By contrast, a recent report suggested that mislocalized CENP-A is incorporated by CAF-1 complex in budding yeast (Hewawasam et al., 2018). In yeast, upon loss of old centromeres, neocentromeres are formed in H2A.Z-depleted regions and activated by the recruitment of Scm3 (Ogiyama, Ohno, Kubota, & Ishii, 2013). CENP-A in fission yeast was also shown to spread into ectopic sites by redundant actions of Ino80 and Chd1 chromatin remodelers (Choi, Cheon, Kang, & Lee, 2017a). There could be an interesting link between chromatin remodelling and CENP-A mislocalization.

In *Drosophila*, CID mislocalization is enough to create neocentromeres (Mendiburo et al., 2011). CENP-A misincorporation is thought to stem from defects in cell cycle-dependent synthesis or loading of CENP-A (Müller & Almouzni, 2017a). Overexpressed CENP-A is recruited to ectopic sites in human cells, flies and yeast (Müller & Almouzni, 2017a; Pauleau & Erhardt, 2011). Those mislocalized CENP-A foci can cause formation of functional ectopic kinetochores and segregation defects, leading to genome instability (Heun et al., 2006; Shrestha et al., 2017). Recent reports indicated that overexpressed CENP-A is incorporated into sites of active histone turnover by H3.3 chaperone DAXX (Lacoste et al., 2014) in a heteromeric tetramer complex containing CENP-A/H4 with H3.3/H4 (Arimura et al., 2014), affecting gene expression and improving DNA damage resistance (Sun et al., 2016). A previous study in our lab further suggested that the general assembly factor RbAp48 might also be involved in stability and mislocalization of overexpressed CENP-A in *Drosophila*, upon either truncation of CID N-tail or mutation of its NLS (Spiller-Becker et al., unpublished). Therefore, it is crucial to address RbAp48-dependent CENP-A misincorporation mechanism.

1.1.1.2.1.3.1 CENP-A Regulation in Cancer

There is an interesting correlation between excess of CENP-A, HJURP chaperone or both and tumorigenic changes (Sitbon et al., 2017). It is yet to be understood whether it is a cause or consequence of cancer (Athwal et al., 2015). CENP-A has been reported to be upregulated in a broad spectra of aggressive tumors, including breast cancer, ovarian cancer, hepatocellular carcinoma, colorectal cancer, osteosarcoma and acute leukemia (Shrestha et al., 2017). Knockout of the tumor suppressor p53 results in elevated levels of CENP-A and

HJURP due to derepression of transcription at CENP-A and HJURP promoters (Sitbon et al., 2017). Moreover, HJURP depletion in p53-null background results in apoptosis, suggesting that p53 knockout-driven tumorigenesis requires HJURP and CENP-A for survival (Filipescu et al., 2017). In cancer cells, CENP-A has also been found to be misincorporated at ectopic sites (Lacoste et al., 2014), bringing about chromosome instability (Nye et al., 2018; Sitbon et al., 2017). Thus, overexpressed and mislocalized CENP-A is proposed to be a prognostic and predictive marker for cancer progression (Filipescu et al., 2017).

The plasticity of histone chaperone binding between different H3 variants is thought to be exploited by cancer cells (Filipescu et al., 2017). For instance, surplus CENP-A can be localized at centromeres as well as mislocalized at chromosome arms (Nye et al., 2018). DAXX, a H3.3 chaperone under normal conditions, functions in the promiscuous incorporation of non-centromeric CENP-A (Lacoste et al., 2014). In oncogene-induced MEFs (mouse embryonic fibroblasts), overexpressed HJURP loads excessive amount of CENP-A at centromeres, suggesting HJURP is the limiting factor for centromeric restriction of CENP-A (Filipescu et al., 2017). Posttranslational modifications also regulate the ectopic localization of CENP-A in cancer (Nye et al., 2018; Zhao, Winogradoff, Bui, Dalal, & Papoian, 2016). K124 ubiquitylation is required for HJURP interaction and centromeric targeting (Niikura, Kitagawa, & Kitagawa, 2017), whereas S68 phosphorylation is necessary for dissociation of HJURP (Yu *et al.*, 2015). Misregulation of those modifications alters the HJURP binding and results in CENP-A mislocalization (Heo, Cho, & Kim, 2013; Maehara, Takahashi, & Saitoh, 2010; Valente et al., 2013). Taken together, it is necessary to understand alternative loading pathways of excessive CENP-A upon bypass of HJURP interaction. In this context, it is required to further investigate the potential roles of RbAp48 and chromatin remodelling.

1.1.1.3 Chromatin Remodelling

To render DNA accessible for transcription, replication and repair, nucleosomes must be moved or evicted (Steven Henikoff, 2016). Remodeling by several types of DNA translocases (chromatin remodelers) is required for the disruption of nucleosomes (Clapier & Cairns, 2009). Using histone variants, histone modifications, DNA methylation and ATP-dependent remodeling either individually or in combination, chromatin remodelers make DNA accessible (G. G. Wang, Allis, & Chi, 2007). Depending on their action mechanisms, chromatin remodelers are divided into two subclasses: (1) changing histone posttranslational modifications, (2) loosening histone-DNA binding through ATP hydrolysis (Clapier & Cairns, 2009). ATP-dependent chromatin remodelers are further divided into distinct subfamilies: SWI/SNF (switch/sucrose non-fermenting), ISWI (imitation switch), CHD (chromo-helicase-DNA binding) and INO80 (inositol requiring 80) (Steven Henikoff, 2016; Tyagi, Imam, Verma, & Patel, 2016). SWI/SNF group of remodelers interfere with nucleosomes to stimulate gene expression, ISWI group regulates rearrangement and equal distribution of nucleosomes, and CHD group facilitates RNAPII enzyme movement along the nucleosome (Steven Henikoff, 2016) and INO80 favors DNA repair and replication by helicase activity (Tyagi et al., 2016). Except for ATPase domains, bromodomains in SWI/SNF group, SANT/SLIDE modules in ISWI family, chromodomains in CHD class and HAS domains in INO80 remodelers are present in order to recognize histone modifications, recruit the remodeler on the chromatin or regulate ATPase activity (Clapier & Cairns, 2009).

Nucleosome sliding and ejection can be mechanistically explained by the stepwise action of SWI/SNF group of remodelers, as described previously (Wilson & Roberts, 2011). SWI/SNF remodeler complexes first attach tightly to DNA and nucleosome, then starts loosening the DNA-histone contacts by the action of several subunits and ATP hydrolysis, which is then followed by loop formation and nucleosome sliding (Wilson & Roberts, 2011). Then histone eviction takes place by an unknown mechanism, thereby creating an empty chromatin region for RNAPII to initiate transcription (Steven Henikoff, 2016; Wilson & Roberts, 2011).

SWI/SNF type remodelers, co-operating with HAT complexes, are usually involved in transcription activation (Roberts & Winston, 1997). There are two members of SWI/SNF family in yeast: Swi2/Snf2 and Sth1, which form γ SWI/SNF and RSC complexes (Cairns et al., 1996). The only SWI/SNF remodeler in *Drosophila* is called Brahma (BRM) and participates into BAP and PBAP complexes (Tamkun et al., 1992). In humans, two SWI/SNF members so called human Brahma (hBRM) and Brahma-related gene 1 (BRG1) take part in BAF and PBAF complexes (Toto, D'Angelo, & Corona, 2014).

ISWI family remodelers regulate nucleosome positioning by ATPase-dependent remodeling activity, thereby mediating novel deposition of nucleosomes as well as transcription inhibition (Tyagi et al., 2016). They also play roles in DNA replication and repair (Erdel & Rippe, 2011). Isw1 and Isw2 form four distinct complexes in yeast (Toto et al., 2014). In *Drosophila*, only one ISWI ATPase has been identified, which is involved in CHRAC, ACF and NURF complexes (Bouazoune & Brehm, 2006; Varga-Weisz et al., 1997). ACF functions in nucleosome sliding (Chioda, Vengadasalam, Kremmer, Eberharder, & Becker, 2010), whereas CHRAC and NURF, apart from chromatin remodeling, are involved in histone variant exchange (Cherry & Matunis, 2010; Mathew et al., 2014). In mammals, two ISWI ATPases, the so called SNF2H and SNF2L, constitute eight large complexes (Yadon & Tsukiyama, 2011).

INO80 family of remodelers localize at replication forks and holiday junctions, thereby playing a role in DNA damage repair (Tsukuda, Fleming, Nickoloff, & Osley, 2005; Van Attikum, Fritsch, & Gasser, 2007). They recognize H2A variants H2A.X and H2A.Z and provide histone exchange at DNA damage sites (Krogan et al., 2003; Mizuguchi et al., 2004; Tsukuda et al., 2005; Van Attikum et al., 2007). The family consist of Ino80 and Swr1 in yeast, INO80 and p400 in *Drosophila* and SRCAP and p400 in mammals, which gives rise to a very large individual complex with the involvement of 14-15 subunits (Kanemaki et al., 1999).

CHD class constitutes a large group of ATPase-dependent chromatin remodelers with various submodules and actions (Hall & Georgel, 2007; Marfella & Imbalzano, 2007). CHD family members are primarily involved in transcriptional suppression or activation (Becker & Hörz, 2002; Shimono, Shimono, Shimokata, Ishiguro, & Takahashi, 2005). Tandem chromodomains are found in CHD family members as signature motifs, which are capable of binding to H3K9me2/3 or H3K27me2/3 modifications (Tyagi et al., 2016). The only family member in *S. cerevisiae* is γ Chd1 (Tyagi et al., 2016). CHD1 and CHD2 in mammals were shown to interact with AT-rich DNA sequences through a DNA-binding motif (Stokes & Perry, 1995). Human CHD1 can also interact with H3K4me2/3 through chromodomains (Flanagan et al., 2005). CHD3 and CHD4 (Mi-2 α , Mi-2 β) were reported to associate with histone deacetylase HDAC1 component of NuRD complex through PHD finger domain (Xue

et al., 1998). On the other hand, PHD domain of CHD4 interacts with H3K9Ac or H3K9me, but is prevented from binding to H3K4me (R. E. Mansfield et al., 2011). SANT domain, responsible for histone tail binding, is present in CHD5, and Brahma and Kismet (BRK) domain was found in Kismet, CHD7, CHD8 and CHD9 (Daubresse et al., 1999; Hall & Georgel, 2007; Marfella & Imbalzano, 2007). In summary, chromatin remodelers are essential for chromatin accessibility, duplication, correction and modification (Henikoff, 2016). RbAp48-containing NuRD complex might be interesting for CENP-A mislocalization and will be discussed in detail in the following section.

1.1.1.3.1 Nucleosome Remodelling and Deacetylase (NuRD) Complex

Chromatin remodelling and deacetylase (NuRD) complex, highly conserved among higher eukaryotes (Denslow & Wade, 2007), is one of the major ATP-dependent chromatin remodelling complexes (Lai & Wade, 2011). Resembling other remodelling complexes, NuRD plays crucial roles in transcription (mostly repression), nucleosome deposition, cell cycle regulation and genome stability (Clapier & Cairns, 2009). Moreover, NuRD complex is also important during development, such as differentiation of haematopoietic cells, and tumor progression, such as metastasis (Ramírez & Hagman, 2009; Yoshida et al., 2008). NuRD has further been associated with PCNA and CAF-1 during DNA synthesis at pericentromeric heterochromatin in quickly growing lymphocytes, suggesting a potential role in DNA replication and chromatin assembly (Chadwick, Chadwick, Jaye, & Wade, 2009). Several lines of evidence further indicated that NuRD complex modulates both transition from G1 to S phase and G2/M arrest (Larsen et al., 2010; Polo, Kaidi, Baskcomb, Galanty, & Jackson, 2010; Smeenk et al., 2010). Regarding genomic stability, NuRD complex was suggested to aid in incorporating repair proteins and suppressing transcription to let DNA repair occur (Chou et al., 2010; Larsen et al., 2010; Smeenk et al., 2010). Recent evidences further identified more complex regulatory mechanisms occurring by the crosstalk of NuRD and other modification complexes. For instance, in embryonic stem cells, NuRD-dependent deacetylation of H3K27 leads to PRC2-mediated H3K27 methylation and silencing at target genes, regulating embryonic stem cell differentiation (Reynolds et al., 2012).

NuRD multi-subunit complex contains several accessory components which are involved in targeting the complex to specific genomic loci and performing the context-dependent functions (Lai & Wade, 2011). It consists of six core components, two of which have catalytic activities. CHD3 or CHD4 (also called Mi-2 α and Mi-2 β , respectively) possesses ATPase-dependent chromatin remodelling function, whereas HDAC1 and HDAC2 subunits retain histone deacetylase function (Denslow & Wade, 2007; Lai & Wade, 2011). The reason for those dual enzymatic roles is not entirely clear (Denslow & Wade, 2007), but one possibility is that chromatin remodelling activity might facilitate penetration of the complex and histone deacetylation (Torchy, Hamiche, & Klaholz, 2015). The non-catalytic core subunits of the complex contain methyl-CpG-binding domain 2 or 3 (MBD2 or MBD3); metastasis-associated gene 1, 2 or 3 (MTA1, MTA2 or MTA3); retinoblastoma binding protein 4 (RBBP4, also called RbAp48) or 7 (RBBP7, also called RbAp46); GATAD2A or GATAD2B (also called p66 α or p66 β , respectively) (Brackertz, Boeke, Zhang, & Renkawitz, 2002; Feng et al., 2002; Wade et al., 1999). MBD proteins are involved in localizing the complex at methylated-CpG sites (Hendrich & Bird, 1998), while MTA components recruit the complex at transcription factor binding regions (N. Fujita et al., 2004). On the other hand, RBBP and GATAD subunits

are considered to be required for structural assembly of NuRD complex and play a role in binding to histone tails (Brackertz et al., 2002; Loyola & Almouzni, 2004; Joachim Marhold, Brehm, & Kramer, 2004). Recent studies also discovered an additional subunit called deleted in oral cancer 1 (DOC1), whose function remains uncharacterized (Smits, Jansen, Poser, Hyman, & Vermeulen, 2013; Spruijt et al., 2010).

NuRD-related research has recently gained more focus into structural understanding of its assembly. MTA1 has been shown to associate with RbAp48 and inhibit RbAp48-H4 interaction, thereby playing an essential role in the NuRD assembly acting as a scaffold protein (Alqarni et al., 2014). MTA-RBBP form a stable sub-complex in human and *Drosophila*, which then plays an intermediate role for the assembly of the whole complex (Brasen et al., 2017; Zhang et al., 2016). MBD2 also establishes a critical binding interface between CHD4 catalytic component and histone deacetylation core, consisting of HDAC/MTA/RBBP (Zhang et al., 2016; Brasen et al., 2017). Furthermore, it has been shown that MTA1 can recruit two RBBP subunits (Torchy et al., 2015), and there is a 2:2 stoichiometric ratio between MTA1 and HDAC1 (Torchy, Hamiche and Klaholz, 2015). NuRD complex was found to stoichiometrically consist of one CHD3/4, one HDAC1/2, one MBD2/3, three MTA1/2/3, two p66 α / β , six RbAp46/48 and two DOC1 (Smits et al., 2013), as demonstrated in Figure 1.4 (modified from Torchy, Hamiche and Klaholz, 2015), even though this stoichiometry is still under debate.

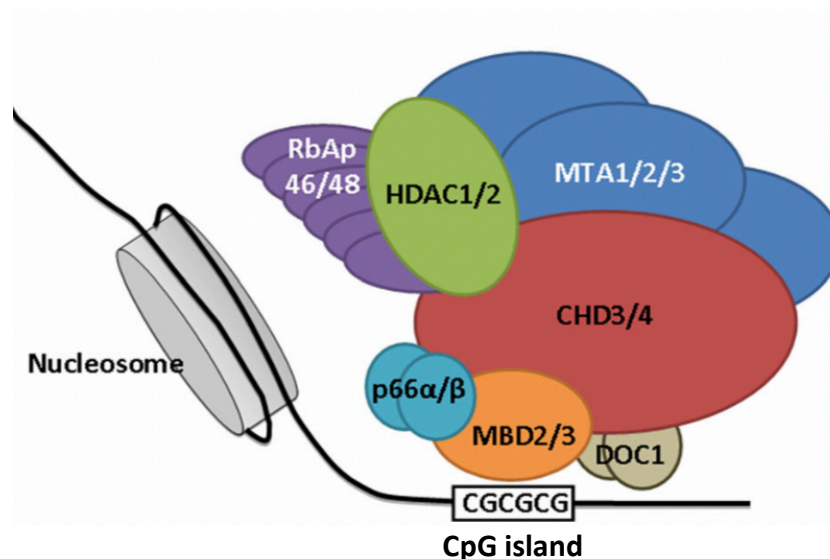


Figure 1.4 Chromatin localization and stoichiometric composition of mammalian multi-subunit NuRD complex, modified from Torchy, Hamiche and Klaholz (2015). NuRD complex located at a CpG island through interaction of MBD2/3 component with methylated DNA is illustrated. According to (Smits et al., 2013), mammalian NuRD complex consists of one CHD3/4, one HDAC1/2, one MBD2/3, two p66 α / β , two DOC1, three MTA1/2/3 and six RbAp46/48 subunits.

Non-enzymatic components of the NuRD complex constitute distinct NuRD complexes with different functionality (Lai & Wade, 2011). For instance, MBD3 cannot recognize DNA methylation; instead, it has been shown to interact with an oncoprotein JUN, in turn forming an alternative NuRD complex to the one with MBD2 (Aguilera et al., 2011). MTA3 also mediates the interaction between BCL-6 transcription repressor and NuRD, thereby

maintaining the cellular identity in B cells (Fujita et al., 2004). Therefore, NuRD complexes have variable subunit composition with distinct functional roles, suggesting cell type- or species-specific roles of this complex (Lai & Wade, 2011). RBBP subunits are also involved in multiple other complexes and thought to support structural assembly of NuRD complex by providing protein contact surfaces rather than functional roles (Loyola & Almouzni, 2004). In addition HDAC1 and HDAC2 subunits participate into other co-repressor complexes, such as CoREST and Sin3 (Yang & Seto, 2008).

All NuRD components are conserved in *Drosophila* and highly homologous to their mammalian counterparts (Lai & Wade, 2011). There are two types of NuRD complexes in *Drosophila*: dNuRD and dMec (MEP-1 containing complex) (Kunert & Brehm, 2009). The most abundant one is the dMec complex, which is involved in SUMO-dependent transcriptional repression (Kunert et al., 2009). dNuRD complex consists of Mi-2, MTA1-like, Rpd3, MBD-like, Simjang and RbAp48 subunits (Marhold, 2004; Joachim Marhold et al., 2004; Zhang et al., 2016), and each individual component is encoded by a single gene (Zhang et al., 2016). Earlier studies to understand the structural architecture of the complex found that MBD2/3 protein interacts with RbAp48 and Mi-2 and creates an interaction interface between methylated DNA and dNuRD complex (Joachim Marhold et al., 2004). Structural and MS-based approaches later identified that dNuRD is comprised of a stable preformed subcomplex containing RbAp48, MTA1-like, Rpd3 and MBD2/3 in 4:2:2:1 stoichiometric ratio (Smits et al., 2013). Mi-2, Simjang and Doc are not consistently present (Zhang et al., 2016). Interestingly, dNuRD is required for maintenance of pericentric heterochromatin (Zhang et al., 2016), regulates chromosome compaction and cohesion attachment (Fasulo et al., 2012). By dual catalytic roles, it can both activate and repress transcription (Alqarni et al., 2014). The recruitment of dNuRD has been observed to the actively-transcribed heat shock genes (Mathieu et al., 2012). Tramtrack69 is involved in targeting of dMec to the Tramtrack69-regulated downstream genes (Reddy et al., 2010). It is also involved in development, differentiation and DNA damage repair (Basta & Rauchman, 2017).

1.1.1.3.1.1 NuRD Regulation in Cancer

The MTA family is the most studied component of NuRD complex in regards to cancer (Lai & Wade, 2011). MTA1, associated with high metastatic potential and poor prognosis, has been reported to be upregulated in many types of cancer from wide range of human tissues (Toh & Nicolson, 2009). MTA1 and MTA2 suppress oestrogen functions, promoting breast tumor malignancy (Nicolson et al., 2003). In contrast, MTA3 inhibits epithelial to mesenchymal transition (EMT) (Fujita et al., 2003), which is a process thought to lead to metastasis (Kalluri & Weinberg, 2009). Several studies implicated that NuRD complex associates with oncogenic transcription factors to suppress transcription of downstream genes (Lai & Wade, 2011). For instance, MBD3-dependent recruitment of NuRD through direct physical interaction with BCL-6, an oncogenic transcription repressor, plays a critical role in B cell lymphoma (Kusam & Dent, 2007). In breast cancer, MTA2-containing NuRD complex was shown to interact with TWIST, a key mediator of EMT, to repress E-Cadherin expression (Fu et al., 2011). Apart from transcriptional regulation, NuRD complex also influences cancer by applying posttranslational modification on target proteins through HDAC component (Lai & Wade, 2011). MTA1-dependent NuRD complex performs deacetylation of HIF1 α , a factor promoting angiogenesis and tumor survival and under low oxygen conditions, in turn

stabilizing HIF1 α and increasing breast tumor growth (Yoo, Kong, & Lee, 2006). Likewise, p53 deacetylation takes place in a MTA1 and HDAC-dependent manner, leading to inhibition of p53-mediated cell cycle arrest or cell death (Luo, Su, Chen, Shiloh, & Gu, 2000; Moon, Cheon, & Lee, 2007). MBD2 has also been shown to associate with hypermethylated *CDKN1A* locus, bringing about HDAC-mediated inactivation of INK4A and ARF tumor suppressor proteins in colon cancer (Magdinier & Wolffe, 2001; Sansom, Maddison, & Clarke, 2007). Furthermore, CHD4 was observed to suppress tumor suppressor genes in colorectal cancer (Xia et al., 2017), and CHD4 knockdown decreased tumorigenicity in acute myeloid leukemia (Sperlazza et al., 2015). Altogether, with two catalytic activities, several binding modules, including RbAp48, and critical functions in tumor progression like CENP-A, NuRD complex is an interesting tool to study CENP-A mislocalization.

1.1.1.4 Elimination of Mislocalized CENP-A

As well as histone assembly and chromatin remodelling, eviction and degradation is equally critical for the regulation of mislocalized CENP-A. CENP-A is restricted to the centromeres and eliminated from the non-centromeric chromatin by counteracting chaperones (Dong et al., 2016; Mathew et al., 2014), or via targeting by specific E3 ubiquitin ligases to proteasomal degradation in yeasts and flies (Hewawasam et al., 2010; Moreno-Moreno, Torras-Llort, & Azorín, 2006; Ranjitkar et al., 2010). Psh1 was first found to be responsible for elimination of ectopic budding yeast CENP-A (Cse4) (Hewawasam et al., 2010; Ranjitkar et al., 2010). Later, it was discovered that Psh1 is accompanied by other E3 ubiquitin ligases, including Ubr1, Slx5 and Rcy1, to ubiquitylate mislocalized Cse4 (Cheng, Bao, Gan, Luo, & Rao, 2017). Cse4 mislocalizes at promoter regions upon deletion of Psh1, and this is enhanced by Ino80-mediated eviction of H2A.Z (Hildebrand & Biggins, 2016). Mislocalized *Drosophila* CENP-A (CID) is eliminated by SCF^{Ppa} ubiquitin ligase-dependent degradation (Moreno-Moreno et al., 2011). Elimination of misincorporated CENP-A mostly occurs in G1 phase, pointing to a cell cycle-dependent surveillance mechanism (Müller & Almouzni, 2017a). Psh1 is phosphorylated by casein kinase 2 and activated for Cse4 proteolysis (G. S. Hewawasam et al., 2014). The interaction between Psh1 and Cse4 is facilitated by H4-R36 residue (Deyter, Hildebrand, Barber, & Biggins, 2017) and FACT complex, in turn enabling Cse4 degradation (Deyter & Biggins, 2014). Following sumoylation at the N-terminal tail of Cse4, SUMO-targeted ubiquitin ligase (STUbL) Slx5 is also involved in the Cse4 elimination process (Ohkuni et al., 2016). Concomitantly, deletion of N-terminal tail results in more ectopic CENP-A (Cnp1) foci in fission yeast, further illustrating the importance of N-terminal tail in ubiquitin-mediated proteolysis of mislocalized CENP-A (Gonzalez, He, Dong, Sun, & Li, 2014). In addition, Doa1-mediated ubiquitination at the N-terminal tail of Cse4 further augmented the Psh1-mediated degradation (Au et al., 2013). Previous work in our lab also found that the N-terminal tail truncated mutant (Δ NCID) and nuclear localization signal (NLS)-deficient mutant (B3-A) are unstable and targeted by proteolytic degradation (Spiller-Becker, unpublished). In order to protect degradation of centromeric Cse4 by Psh1 in budding yeast, the deubiquitinase Ubp8 counteracts this degradation (Canzonetta et al., 2016). Those findings overall illustrate the complexity of regulatory mechanisms on clearance of mislocalized CENP-A. Recent report also suggested that HECT domain containing hyd E3 ligase might have a regulatory role on *Drosophila* CENP-A (Barth et al., 2014). It is yet unclear whether hyd plays a role in elimination of ectopic CID by ubiquitination and degradation.

1.1.1.4.1 Hyd E3 Ubiquitin Ligase

Hyd (hyperplastic discs, CG9484), homologue of mammalian UBR5, is a highly conserved *Drosophila* HECT domain-containing N-end rule E3 ubiquitin ligase (Shearer, Iconomou, Watts, & Saunders, 2015; Wang et al., 2014). Its mammalian counterpart UBR5 plays an essential role during development and is mutated or aberrantly expressed in cancer (Clancy et al., 2003). UBR5 has been shown to be involved in regulation of critical proteins, such as p53, ATM, CHK2, TopBP1, OCT4, Cyclin D, β -Catenin, thereby regulating many important biological processes, including cell cycle, genomic stability, cell death, transcription, pluripotency, angiogenesis and metabolism (Shearer et al., 2015). Intriguingly, it has been associated with resistance of cancer cells against chemotherapeutics (Alps, Yasa, & Gündüz, 2014; Matsuura, Huang, Cocce, Zhang, & Kornbluth, 2017). Moreover, certain kinds of human-infecting viruses hijack UBR5-dependent proteolysis mechanism to arrest cell cycle (Mori et al., 2015; Tomaić et al., 2011; Wang et al., 2013).

On the other hand, hyd is also essential for development after 2nd instar larvae, gives rise to hyperplastic growth in imaginal discs upon its depletion (Mansfield, Hersperger, Biggs, & Shearn, 1994) and is required for spermatogenesis (Pertceva et al., 2010). Furthermore, hyd is involved in poly-ubiquitination and degradation of Cubitus interruptus (Ci), a downstream transcription factor in sonic hedgehog (shh) pathway, in the cytosol (Lee, 2002). Hyd was also shown to degrade Groucho/TLE repressor in Wnt signalling, thereby activating expression of downstream Wnt-dependent genes (Flack, Mieszczanek, Novcic, & Bienz, 2017). It was also detected in MS pulldown study of full length *Drosophila* CENP-A; and its depletion causes mitotic defects (Barth et al., 2014). This further suggests that hyd might act on ubiquitin-dependent proteasomal degradation of CENP-A in *D. melanogaster*. Hence, it is important to find out whether hyd regulates CENP-A and centromere biology.

2 AIM

CENP-A is a key player in genome integrity, cellular homeostasis, cell division, survival and development due to its functions in centromere identity and kinetochore attachment. CENP-A expression and loading are tightly regulated in order to restrict its localization to centromeres and avoid mislocalization at ectopic sites (Müller & Almouzni, 2017b). CENP-A has been reported to be upregulated and misincorporated in several type of aggressive cancers, which drives the cell into malignancy (Shrestha et al., 2017). CENP-A overexpression in *Drosophila* is sufficient for ectopic centromere and kinetochore formation (Mendiburo et al., 2011), thereby causing chromosome segregation defects and genomic instability (Heun et al., 2006; Shrestha et al., 2017). CENP-A has been suggested to be a predictive and prognostic marker of cancer (Filipescu et al., 2017). Indeed, it is also considered as a cause for malignant transformation and metastasis (Athwal et al., 2015). Thus, it is crucial to elucidate the mechanism for promiscuous incorporation of CENP-A.

Previous work has found that RbAp48, a co-factor in multiple chromatin remodeling and histone modification complexes (Doyen et al., 2013; Rai et al., 2013), physically interacts with CENP-A (Dunleavy et al., 2009; Foltz et al., 2009), and enables CENP-A/H4 incorporation into chromatin (Furuyama et al., 2006). RbAp48 has been associated with CENP-A licensing complex (Fujita et al., 2007; Hayashi et al., 2004), nuclear import and centromeric deposition (Boltengagen et al., 2015; Shang et al., 2016a) in several organisms. Intriguingly, previous work in our lab found that in *Drosophila* RbAp48 is involved in stabilization and mislocalization of nuclear localization-deficient CENP-A mutants (Δ NCID and B3-A) (Spiller-Becker, unpublished). This suggests that RbAp48 might play a role in CENP-A misincorporation. It is yet unclear in which complex RbAp48 acts on CENP-A ectopic loading. Intriguingly, a recent report showed that the evolutionarily conserved RbAp48-containing CAF-1 complex regulates CENP-A mislocalization in budding yeast (Hewawasam et al., 2018), making it a potential candidate for CENP-A misincorporation in other species, including *Drosophila melanogaster*. Thus, in this study, I firstly aimed to address the role of CAF-1 complex in *Drosophila* CENP-A misincorporation. However, recent studies in human cells have reported that DAXX chaperone is also involved in CENP-A mislocalization (Arimura et al., 2014; Lacoste et al., 2014; Athwal et al., 2015). This suggests that other players might be involved in CENP-A mistargeting. Considering the plasticity of histone exchange and loading factors (Sitbon et al., 2017), I aimed to identify alternative RbAp48-dependent CID ectopic assembly complexes.

Due to its toxicity, living organisms eliminate excessive or mislocalized CENP-A through eviction (Dong et al., 2016; Mathew et al., 2014) and ubiquitin-mediated proteolysis (Hewawasam et al., 2010; Moreno-Moreno et al., 2011; Ranjitkar et al., 2010). Ubiquitination plays essential roles in CENP-A stability and targeting, and several ubiquitin ligases in different biological systems have been found to regulate CENP-A stability and degradation ((Bade et al., 2014; Niikura et al., 2015; Hewawasam et al., 2010; Ranjitkar et al., 2010; Moreno-Moreno et al., 2011; Cheng et al., 2017). In this study, I secondly aimed to elucidate the function of the E3 ligase Hyd, which I as well as other have identified in Mass spectrometry approaches (Barth et al., 2014). Taken together, the major objective of this study is to discover the mechanisms of ectopic CENP-A loading and removal in *Drosophila melanogaster*.

3 RESULTS

3.1 CAF1 is dispensable for CENP-A misincorporation in *Drosophila*

3.1.1 RbAp48 physically interacts with CID

Histone variants physically associate with their dedicated chaperones and deposited into chromatin (Gurard-Levin et al., 2014). Several lines of evidences reported an interaction between CENP-A and the chaperone complex CAF1 subunits, particularly RbAp48, in several organisms (Boltengagen et al., 2015; Dunleavy et al., 2009; Foltz et al., 2009; Furuyama et al., 2006; Hayashi et al., 2004; Shang et al., 2016b), suggesting a functional role of CAF1 in regulation of CENP-A loading, including CID in *Drosophila*. I hypothesized that if CID stably or transiently interacts with CAF1 components CAF1 complex may be responsible for CID loading in addition or in combination with its loading factor Cal1. In order to test this, reciprocal Co-IP's against overexpressed CID and RbAp48 were performed (Figure 3.1a). For this purpose, CuSO₄-inducible pMT-CID-V5-His and pMT-RbAp48-V5-His overexpressing *Drosophila* Schneider (S2) cell lines, available in AG Erhardt cell lines stock, were used. Both type of cells were induced with 0.5 mM CuSO₄ overnight. The CID-specific chaperone CAL1, which stably interacts with CID (Chen et al., 2014), was used as a positive control and indicated that CID-V5 co-IP worked (Figure 3.1a). I found a weak physical interaction with RbAp48 but no interaction with p180 subunit of CAF1 upon CID-V5 co-IP (Figure 3.1a). On the other hand, for the reciprocal RbAp48 pulldown, I used p180, which is a known interacting partner of RbAp48, as a positive control. I detected a physical interaction with p180, implicating RbAp48 co-IP also worked (Figure 3.1a). However, I did not observe a physical interaction with CID (Figure 3.1a). The reason might be unidirectional interaction of CID and RbAp48 only upon pulldown of overexpressed CID or hindrance of interaction due to technical reasons. CENP-A as well as CAF-1 components are part of multiprotein complexes. To test the direct protein-protein interactions between different combinations of CAF-1, CID, CAL1 I performed yeast two hybrid (Y2H) assay using RDX, Cul3-adaptor protein for CAL1/CID complex as a positive control (Bade, Pauleau, Wendler, & Erhardt, 2014b),. Similar to the co-IP experiment, no interaction was detected between p180 and CID (data not shown). Physical interactions were only observed between CAL1 – RbAp48 and CAL1 – p180 (Figure 3.1b). Those interactions, however, could not be confirmed by co-IPs (Figure 3.1c). Previously reported CENP-A - RbAp48 physical interaction in yeast, chicken and *Drosophila* (Boltengagen et al., 2015; Dunleavy et al., 2009; Foltz et al., 2009; Furuyama et al., 2006; Hayashi et al., 2004; Shang et al., 2016b) was consistently detectable by co-IP against CID-GFP (Figure 3.1d). Overall, these results confirm the physical interaction between CID and RbAp48 in *Drosophila* cultured S2 cells.

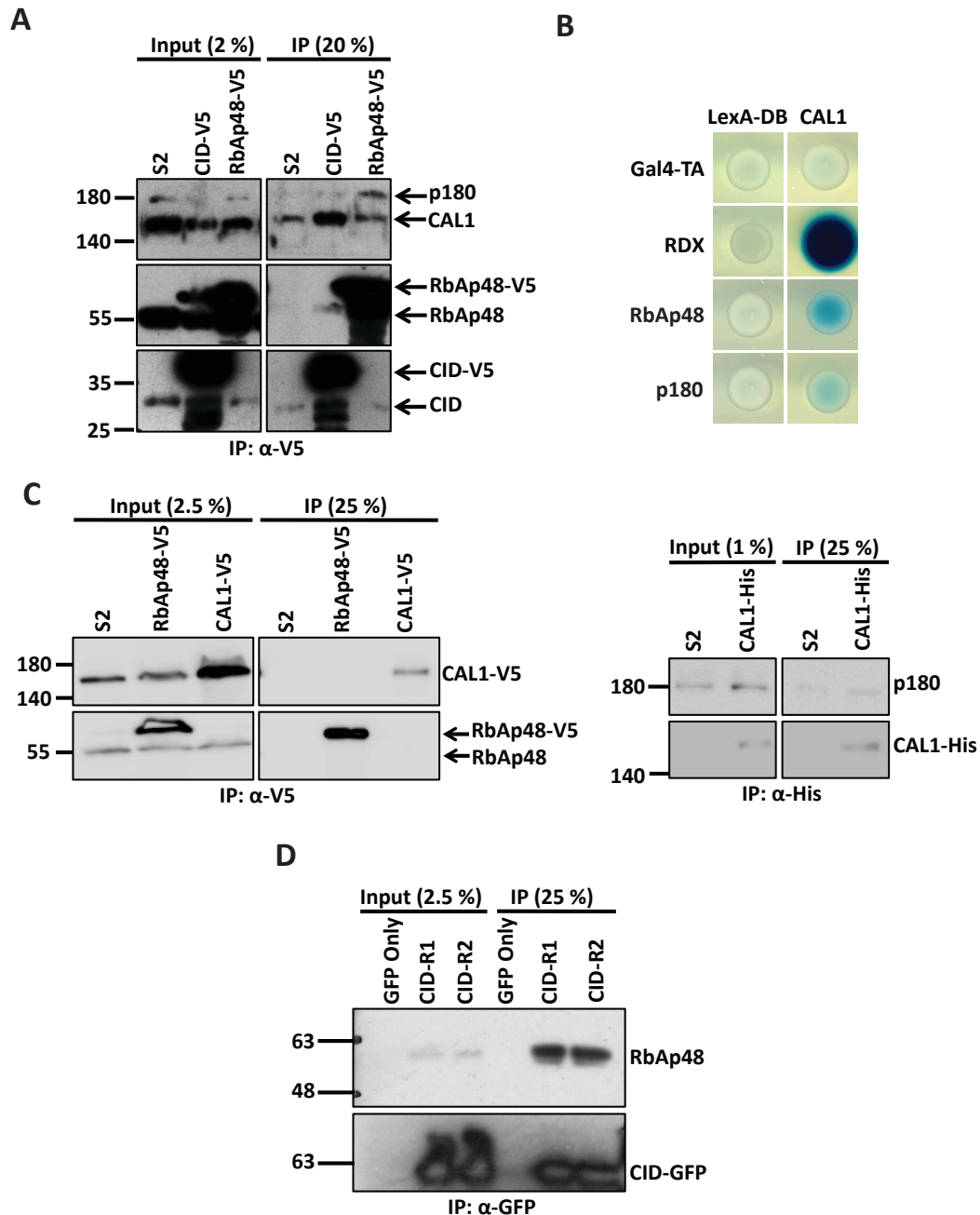


Figure 3.1 There is a physical interaction between CID and RbAp48 subunit of CAF1 complex.

A Western blot of co-IP against V5 probed for p180, CAL1, RbAp48 and CID using CID-V5 or RbAp48-overexpressing cell lines. S2 cells served as negative control for co-IP. **B** Y2H assay to test direct physical interactions between the CAL1/RbAp48 and CAL1/p180. CAL1/RDX interaction served as positive control. LexA-DB/Gal4-TA served as negative control. DB: DNA-binding and TA: Transcription-activating. **C** Western blots of co-IPs against V5 (left panel) and His (right panel) probed for CAL1, RbAp48 and p180 using RbAp48-V5 or CAL1-V5-His overexpressing cell lines. S2 cells served as negative control for co-IP. **D** Western blot of co-IP against GFP probed for RbAp48 and CID-GFP using CID-GFP-overexpressing cells. GFP only served as negative control for co-IP. CID-R1 and CID-R2 represent two replicate experiments.

3.1.2 RbAp48 is required for loading of newly synthesized CID

Next, I addressed the role of RbAp48 in loading of CID by SNAP-tag pulse-labelling approach (Jansen et al., 2007). This technique is used to detect newly synthesized proteins in a quantitative and qualitative manner. The experimental protocol contains following steps: (1) blocking the available SNAP-tagged protein with a SNAP inhibitor, (2) washout of block, (3) chase to allow production of new SNAP-tagged protein and (4) detection of it (Jansen et al., 2007). Coupling this technique with RNA interference, I tested if loading of newly synthesized CID is influenced by RbAp48 depletion. The deposition of newly synthesized CID was significantly reduced upon RbAp48 knockdown compared to control knockdown of the brown (Bw) gene that affects pigmentation of different cell types (Figure 3.2a-b). In RbAp48 depleted cells, SNAP-CID signal does not concentrate on centromeric foci and displays an increased background signal distribution throughout the entire cell (Figure 3.2a). The critical role of RbAp48 in CENP-A incorporation and centromeric targeting was previously reported in several different species (Boltengagen et al., 2015; Furuyama et al., 2006; Hayashi et al., 2004 and Shang et al., 2016). This is a further indication for the function of RbAp48 in loading of newly synthesized CID at centromeres in *Drosophila*.

3.1.3 Investigation of CID ectopic loading by RbAp48-tethering at LacO array

In order to investigate the involvement of RbAp48 in non-centromeric loading, a LacO/LacI tethering approach (Mendiburo et al., 2011) was performed (Figure 3.3). For this assay, I used a stable LacO cell line, which was provided by the Heun laboratory in Edinburgh. These cells have a Lac Operon (LacO) array inserted at non-centromeric region of the chromosomes (Mendiburo et al., 2011). Taking advantage of Lac Inhibitor (LacI) binding to LacO array, LacI-conjugated proteins could be tethered to those regions and the associating partners investigated. Hence, using this system, I tethered RbAp48 at ectopic LacO site (Figure 3.3). I used p180, a known interacting partner of RbAp48 in CAF1 complex (Tyler et al., 2001), as a positive control to check if it is recruited to RbAp48-LacI. I also used GFP-LacI tethering as a negative control to check the background co-localization levels. The recruitment of p180 took place at about 57 % of the LacO sites (Figure 3.3a-b), suggesting that our LacO/LacI approach works. Intriguingly, tethering of RbAp48 leads to the recruitment of CID at 12 % of LacO foci (Figure 3.3b),. Notably, p180 has very high background co-localization (10 %) compared to CID (3 %) upon control GFP-LacI tethering (Figure 3.3b). Overall, this result indicates that RbAp48 plays a potential role in *de novo* loading of CID at non-centromeric sites.

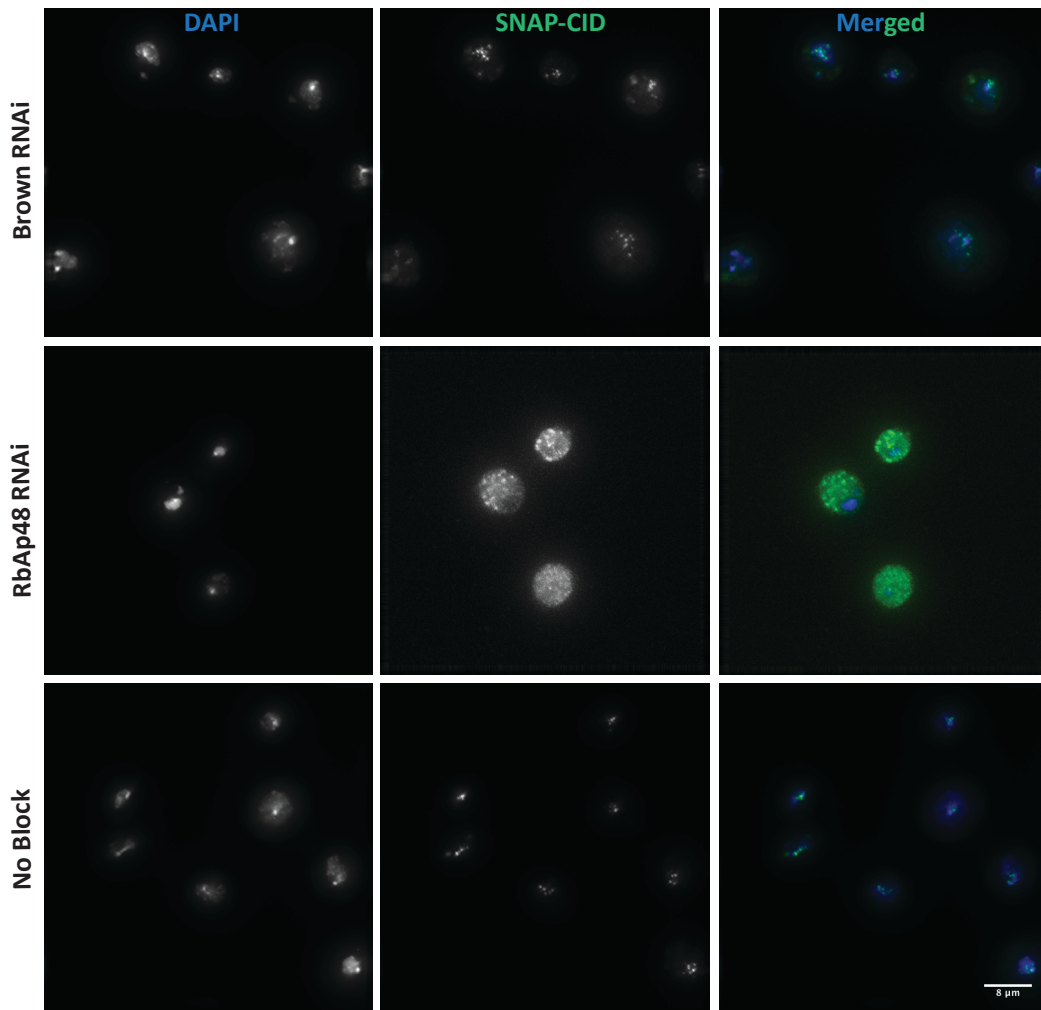
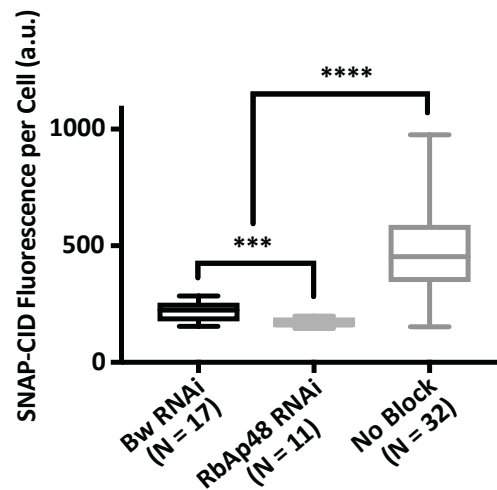
A**B**

Figure 3.2 Newly synthesized CID incorporation is reduced upon RbAp48 depletion.

A Representative IF images of SNAP-CID cells under brown RNAi, RbAp48 RNAi and no block control treatments. DAPI in blue and SNAP-CID in green. Scale bar: 8 μm. **B** Quantification of SNAP-CID fluorescence per cell in arbitrary units. Each boxplot represents the data distribution for one experiment, and the error bars represent SD. Student's t test: *** p<0.001 and **** p<0.0001.

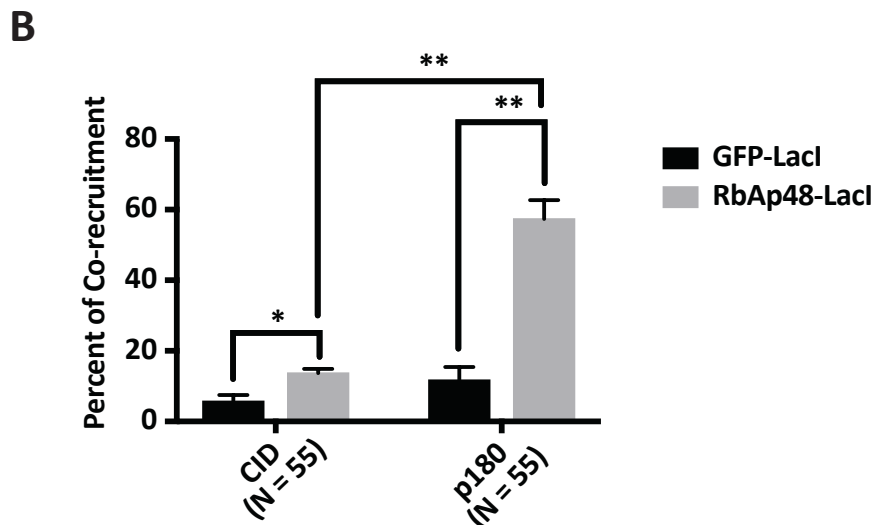
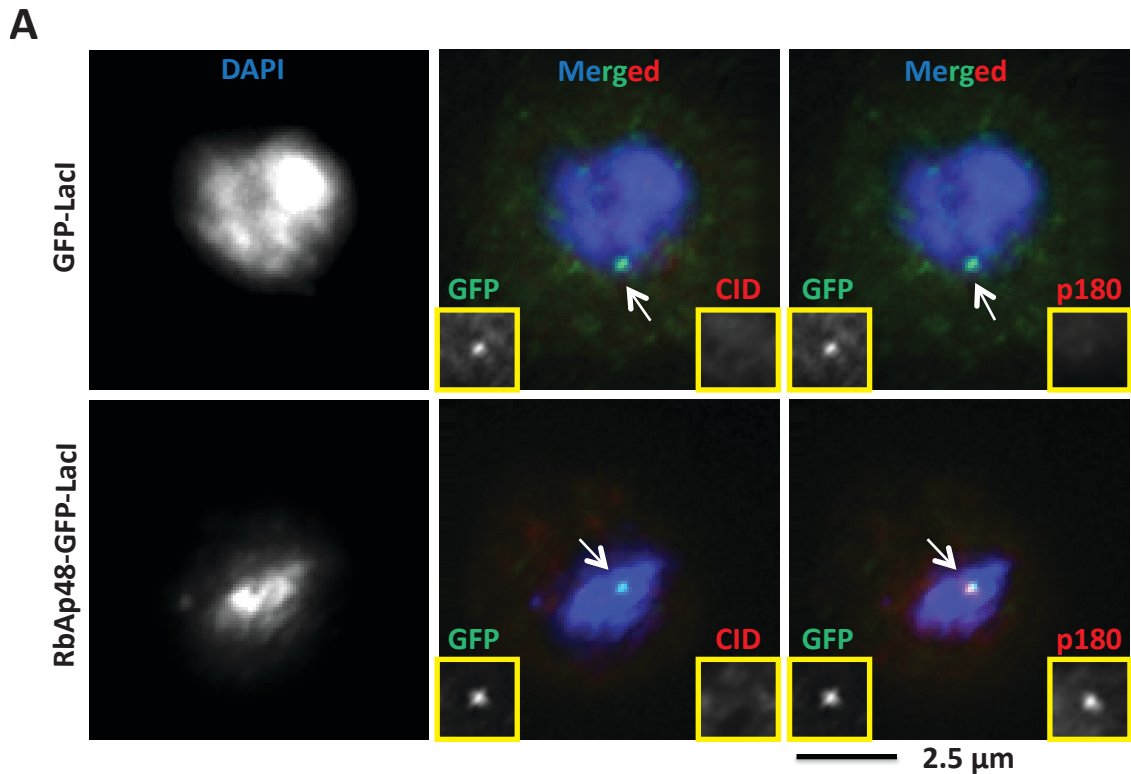


Figure 3.3 RbAp48 tethering does not recruit CID as abundantly as p180 at ectopic LacO array.

A IF images of two representative GFP-LacI-tethered or RbAp48-GFP-LacI-tethered cells. GFP-LacI tethering served as negative control. DAPI in blue, GFP in green, CID and p180 in red. LacO tethering site in each cell is marked by arrows. Scale bar: 2.5 μ m. **B** Quantification shows the percentage of RbAp48 co-recruitment with either CID or p180. Each bar represents the mean of three independent experiments, and the error bars indicate the SEM. Student's t test: * $p<0.05$ and ** $p<0.01$.

3.1.4 CID protein levels do not decrease upon depletion of CAF1 subunits

Next, I wanted to further study the specific role of CAF1 complex in CID protein stability and misincorporation. For this purpose, I tested CID nuclear levels and deposition upon knockdown of CAF-1 subunits. Single CAF1 components (p180, p105 and RbAp48) were efficiently depleted as well as a combination of p180 and RbAp48 (Figure 3.4, 3.5c).

Ectopically expressed total CID-V5 protein levels did not change significantly upon knockdown of CAF1 subunits by western blot (Figure 3.4). Since p180 is a CAF1-specific component, I focused on characterization of p180 in order to address the involvement of CAF1 complex in CID loading mechanism. I found that knockdown of p180 also does not change nuclear levels of overexpressed CID by IF staining (Figure 3.5a-b). However, nuclear CID levels increased slightly upon p180 depletion with 1 mM CuSO₄ induction (Figure 3.5b). To further address the role of p180, I tested loading of overexpressed CID on mitotic chromosome spreads upon p180 knockdown. Preliminary results indicated that the levels of mislocalized CID do not alter under p180 depletion (data not shown). Moreover, other preliminary assays also indicated that there is no detectable ectopic incorporation of endogenous CID upon p180 induction by mitotic spreads (data not shown). Together, as the preliminary assays suggested, CAF1-dependent promiscuous incorporation of CENP-A was not detected in contrast to a recent report from yeast (G. S. Hewawasam et al., 2018). This is consistent with the evidences showing that CAF1 complex is not involved in the prenucleosomal CENP-A assembly complex in humans (Dunleavy et al., 2009; Foltz et al., 2009). This discrepancy might potentially be due to various CENP-A deposition complexes in different organisms (Foltz et al., 2009). Even though additional experiments and replicates of already performed experiments would be required to fully exclude the CAF1 complex from being involved in CID loading, we decided to take a broader approach to included other RbAp48-containing complexes to our analysis as potential complexes involved in CID loading.

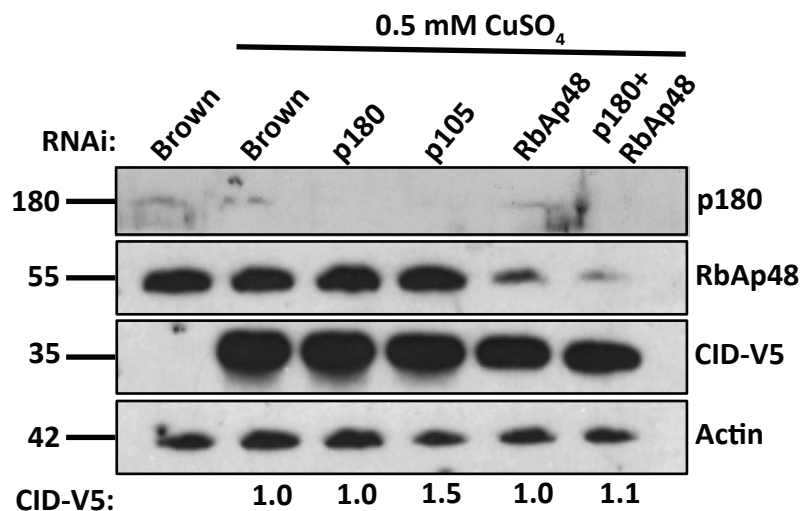


Figure 3.4 Ectopically-expressed CID protein levels do not change dramatically upon knockdown of CAF1 subunits.

Western blot of CID-V5 – overexpressing cells induced with 0.5 mM CuSO₄ under single knockdown of RbAp48, p105 and p180 or double knockdown of RbAp48/p180 probed for p180, RbAp48, CID-V5 and actin. Actin served as loading control. CID-V5 band intensity was quantified using ImageJ and normalized to actin.

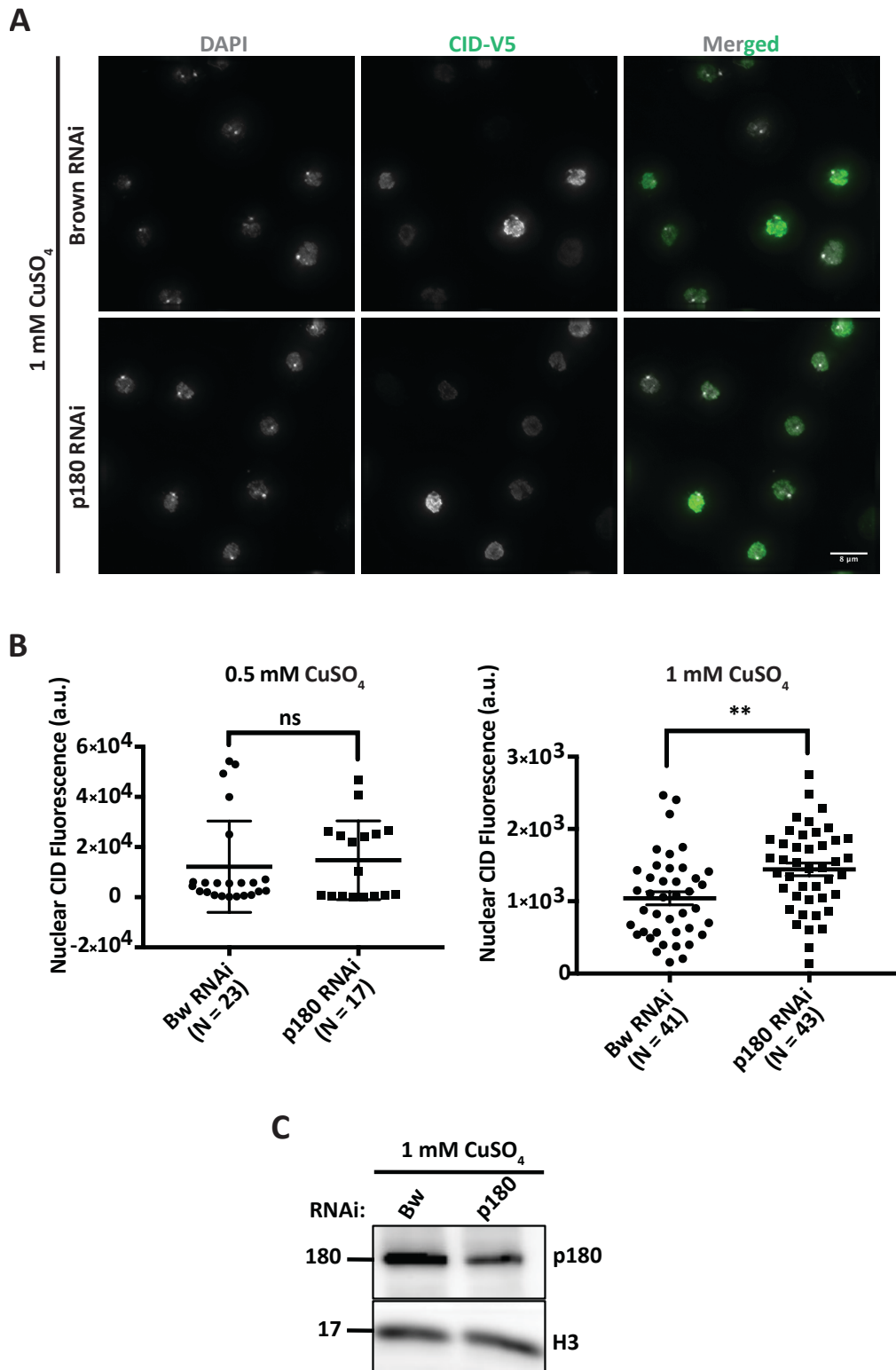


Figure 3.5 Nuclear levels of ectopically-expressed CID does not decrease upon p180 RNAi.

A Representative IF images of CID-V5 cells induced with 1 mM CuSO_4 under Brown and p180 RNAi. DAPI in blue and CID-V5 in green. Scale bar indicates 8 μm . **B** Quantification of nuclear CID-V5 fluorescence per cell in arbitrary units for 0.5 mM CuSO_4 (left) and 1 mM CuSO_4 (right) induction. Each scatterplot represents the data distribution for one experiment, and the error bars indicate the SD. Student's t test: ** $p < 0.01$ and ns: not significant. **C** Western blot of p180 RNAi under 1 mM CuSO_4 induction probed for p180 and Histone3 (H3). H3 served as loading control.

3.2 NuRD complex is required for mislocalization of CID

3.2.1 Investigation of RbAp48-dependent CID loading complexes by IP-MS based approaches

Since I could not prove that CAF1 is necessary for CID ectopic loading, I decided to perform immunoprecipitation-Mass Spec (IP-MS) based approaches in order to identify alternative RbAp48-containing complexes for CID misincorporation. I first applied native IP-MS approach using Δ NCID-overexpressing or Δ NCID-RbAp48 co-overexpressing cells (Spiller-Becker, unpublished), which were created and characterized by a previous student (Figure 3.6). Δ NCID, created by truncating 124 bp-long N-terminal tail of CID, was found to not enter into the nucleus due to the lack of nuclear localization signal (NLS) and to be degraded by proteolysis (Spiller-Becker, unpublished). Interestingly, nuclear localization-deficient and unstable Δ NCID is loaded to chromosome arms under RbAp48 co-overexpression (Spiller-Becker, unpublished), pointing to an RbAp48-dependent CID loading mechanisms to chromosome arms. RbAp48, best characterized in CAF1 (Tyler et al., 2001), is involved in multiple chromatin remodelling and modifying complexes (Deyter & Biggins, 2014; Rai et al., 2013). Thus, I aimed to pulldown RbAp48-containing ectopic loading complexes by native IP against Δ NCID under RbAp48 co-overexpression and to detect the associated proteins by MS. For this purpose, GFP only, Δ NCID-GFP and Δ NCID-GFP/RbAp48-V5 overexpressing cell lines were used (created by Dr. Spiller-Becker). GFP only cells were treated as negative control. Δ NCID-GFP co-IP by GFP-trap, according to standard AG Erhardt protocol, worked relatively efficiently as detected by CAL1 positive control (Figure 3.6a) or Coomassie staining (Figure 3.6b). Nevertheless, Δ NCID-GFP co-IP under RbAp48 co-overexpression was relatively inefficient compared to Δ NCID-GFP alone (Figure 3.6a-b). Thus, relatively fewer proteins enriched for Δ NCID/RbAp48 vs Δ NCID could be detected (Figure 3.6c). Among the detected 39 statistically enriched proteins, there was no known candidate for an RbAp48-containing complex (Table 8.1). Majority of them have metabolic enzymatic roles, which might have been detected due to non-specific interactions, or higher abundance in the cell. Only interesting candidates for centromeric functions are RbAp48 and Smt3, the only SUMO derivative in *D. melanogaster*. On the other hand, there were more proteins (102 factors) enriched for Δ NCID vs Δ NCID/RbAp48 comparison (Table 8.1). Among those, there are interacting partners with known centromeric roles, such as Cal1, Cul3, BubR1 and Spc105R (Table 8.1). There are also few histone-modifying enzymes, such as HMTs Set1 and egg or HDAC Sin3a (Table 8.1), which shows that truncated Δ NCID is capable of interacting with a few histone-associated factors. A subgroup of proteins in the list are also associated with protein stability, folding and ubiquitin-mediated proteolysis, including hyd, Cul3, Bruce, poe and DNAJ (Table 8.1). Intriguingly, hyd E3 ligase has the highest number of peptide enrichment as Δ NCID interacting partner (Figure 3.6d). Thus, hyd might be an interesting candidate to explain the proteolysis of Δ NCID, which will be examined in the following sections.

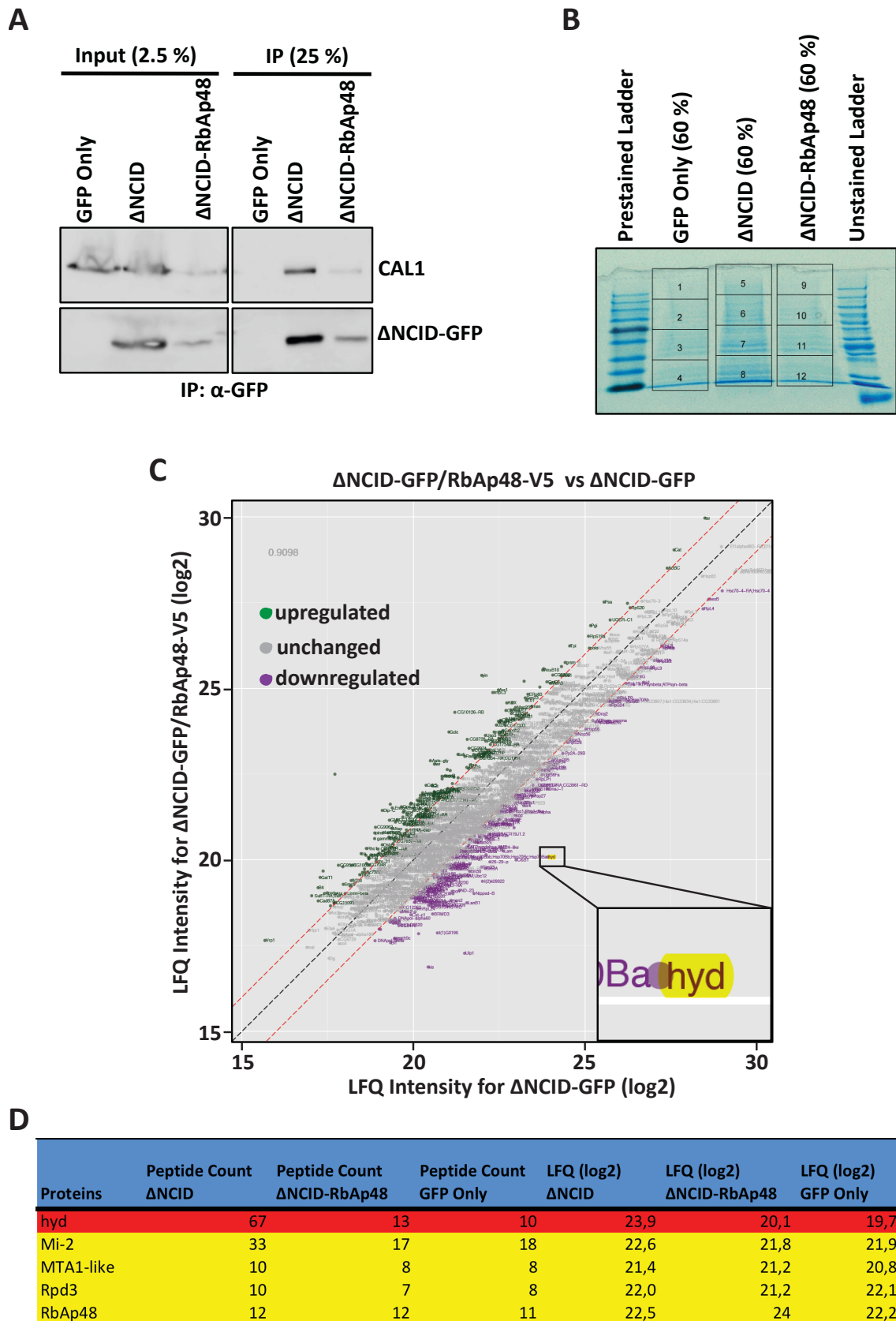


Figure 3.6 Hyd is enriched among the interacting partners of Δ NCID.

A Western blot of co-IP for Δ NCID-GFP using Δ NCID-GFP-overexpressing cells and Δ NCID-GFP/RbAp48-V5 co-overexpressing cells probed against CAL1 and Δ NCID-GFP. GFP only served as negative control for co-IP. **B** Coomassie staining of co-IP experiment in part A with 60 % of the IP

samples loaded. The gel was sliced into 4 pieces per lane as illustrated before LC/MS run. **C** Scatter plot of IP-MS experiment for LFQ (log2) values of Δ NCID-GFP/RbAp48-V5 vs Δ NCID-GFP. The candidate proteins enriched for Δ NCID-GFP/RbAp48-V5 (LFQ ratio ≥ 2) are indicated above the upper red-dashed line in green. The candidate proteins enriched for Δ NCID-GFP (LFQ ratio ≥ 2) are indicated below the lower red-dashed line in magenta. The candidate proteins, which did not enrich for neither of the groups are indicated in gray in between the red-dashed lines. Hyd is highlighted. **D** Table showing the peptide counts and LFQ values of hyd (in red) and the subunits of the NuRD complex (in yellow).

Since Δ NCID co-IP did not work very efficiently, I decided to perform crosslinked immunoprecipitation coupled with mass spec (Xlink IP-MS) approach, as previously described (Kast & Klockenbusch, 2010) in collaboration with an Dr. Bernd Hessling a former member of the ZMBH Mass Spec facility (Figure 3.7a). Xlink-IP-MS protocol was performed according to the following workflow: (1) Xlinking of the associated protein complexes by formaldehyde, (2) pulldown of Xlinked complexes by affinity purification, (3) reverse Xlinking by heat denaturation and (4) detection of interacting partners by MS (Kast & Klockenbusch, 2010). Due to the Xlinking, this technique gives the advantage of detecting weak and transient interacting partners as well, which is not possible with native co-IP. Furthermore, I also used GFP-tagged B3 (A) mutant, which is another CID mutant created by previous student (Spiller-Becker, unpublished) to increase the sensitivity of detecting interaction partners. B3 (A) mutant contains point mutations of 119th-121st triple arginine residues, involved in the bipartite NLS sequence of CID, converted to triple alanines (Spiller-Becker, unpublished). B3 (A) also displays similar nuclear localization deficient and proteolytically unstable phenotype as Δ NCID due to the lack of NLS (Spiller-Becker, unpublished). Because it contains the complete N-terminal tail except for three mutations, it is thought to be more stable (the N-terminus is identical to the wild type protein) and have more interaction potential than Δ NCID. The pulldown was performed against GFP, using GFP-trap according to standard protocol of the Erhardt lab, and the corresponding cell lines from the Erhardt lab stocks were used. GFP only cells, only expressing GFP protein, were used as a negative control. B3 (A)-GFP, B3 (A)-GFP/RbAp48-V5 and CID-GFP overexpressing cells were treated as experimental samples, and their interaction partners were compared to each other.

Pulled-down Xlinked complexes were detectable by western blot (WB) when the Xlinks were preserved at 65 °C (Figure 3.7b) or when the Xlinks were reversed at 95 °C by coomassie stain (Figure 3.7c). Since Xlink-IP-MS is a technique particularly capable of detecting false positives, it is important to analyse the data quality of detected peptides and proteins (Figure 3.8). This analysis indicated that there is an enrichment of about 5000 peptides and about 750 proteins over GFP only control (Figure 3.8a), demonstrating quite efficient elimination of false positives. The normal distribution of the histograms for each sample (Figure 3.8b) and the linear correlation of the pairwise scatter plots (Figure 3.8c) also indicate good data quality. Like in Δ NCID co-IP experiment, the hits for B3 (A)-RbAp48 vs B3 (A) were compared. Additionally, the hits for CID vs B3 (A) were also compared to identify potential RbAp48-dependent CID ectopic loading complex. Among the detected proteins, 120 of those (Table 8.2) were either known/tested or enriched centromeric proteins in another study (for instance Barth *et al.*, 2014) and several unpublished Mass spec data sets from the Erhardt lab. Taken together, the Xlink-IP-MS data seemed of high quality and a better approach to detect CID-interacting factors than classical Mass Spec approaches.

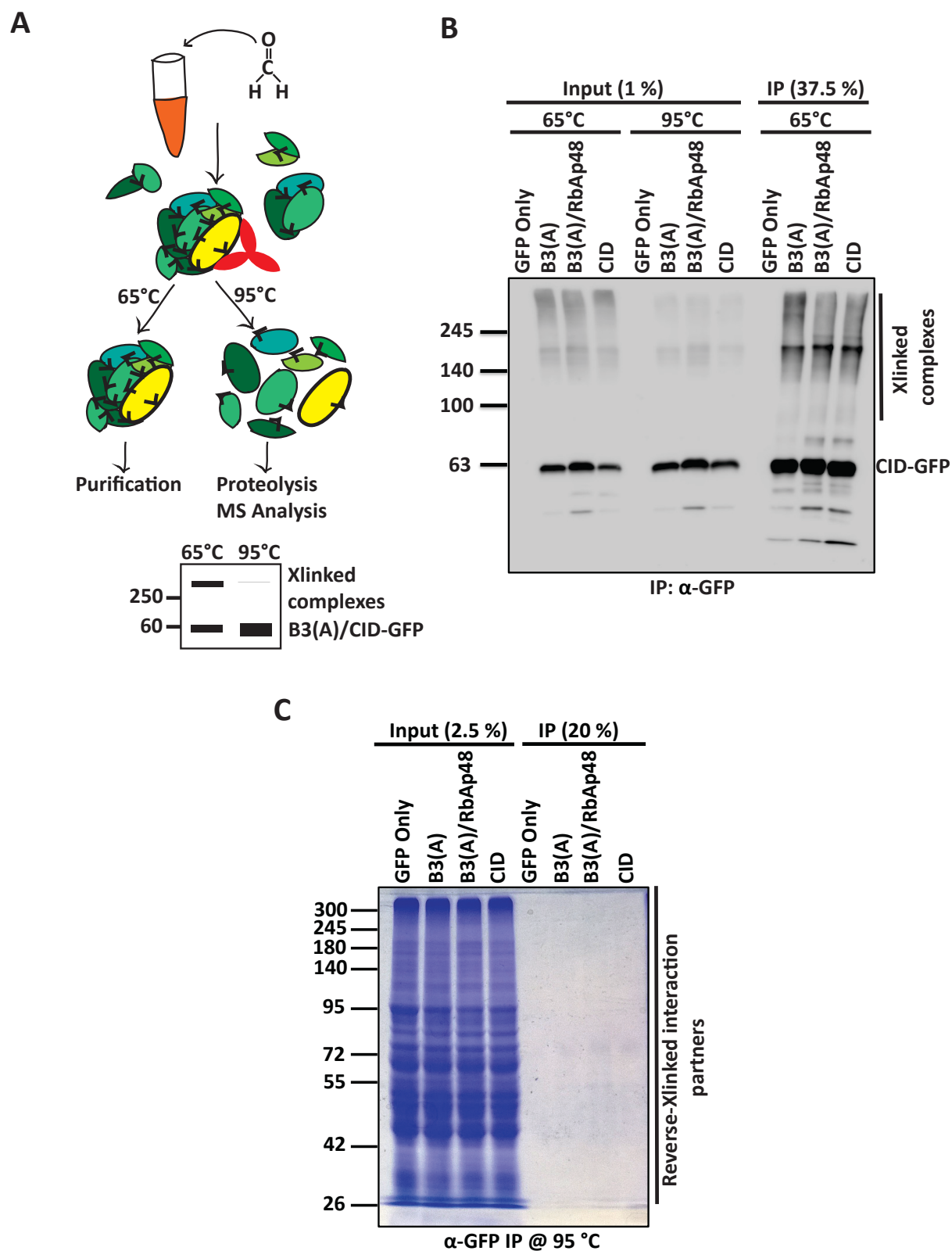


Figure 3.7 X-linked CID containing complexes are pulled down and detected.

A Schematic illustration for Xlink-IP-MS protocol adapted from Kast and Klockenbusch, 2010. **B** Western blot of GFP co-IP probed with anti-GFP after denaturing at 65°C and 95°C. GFP only served as negative control for co-IP. **C** Coomassie staining of GFP co-IP after denaturing at 95°C.

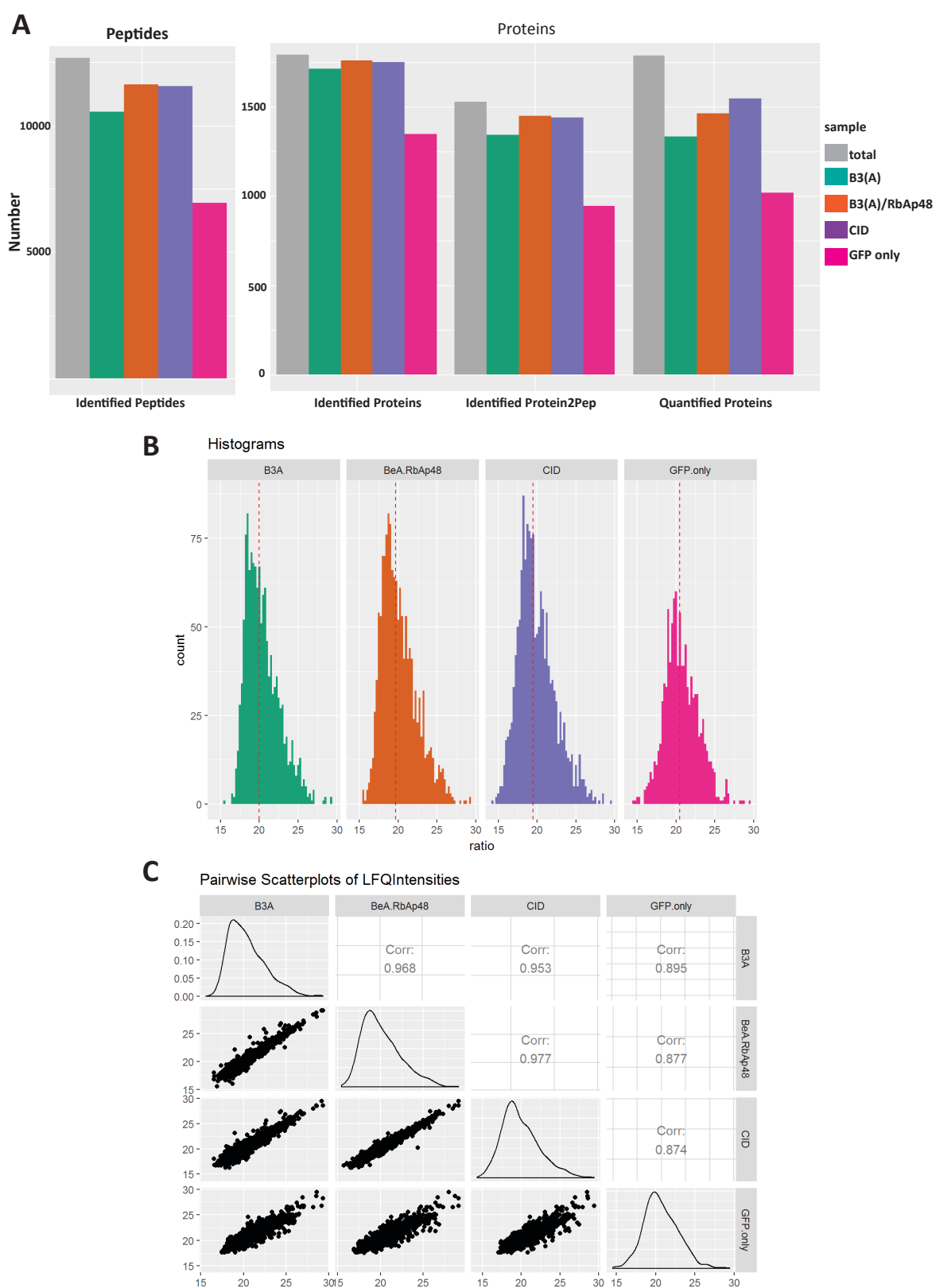


Figure 3.8 Data quality for the Xlink-IP-MS experiment

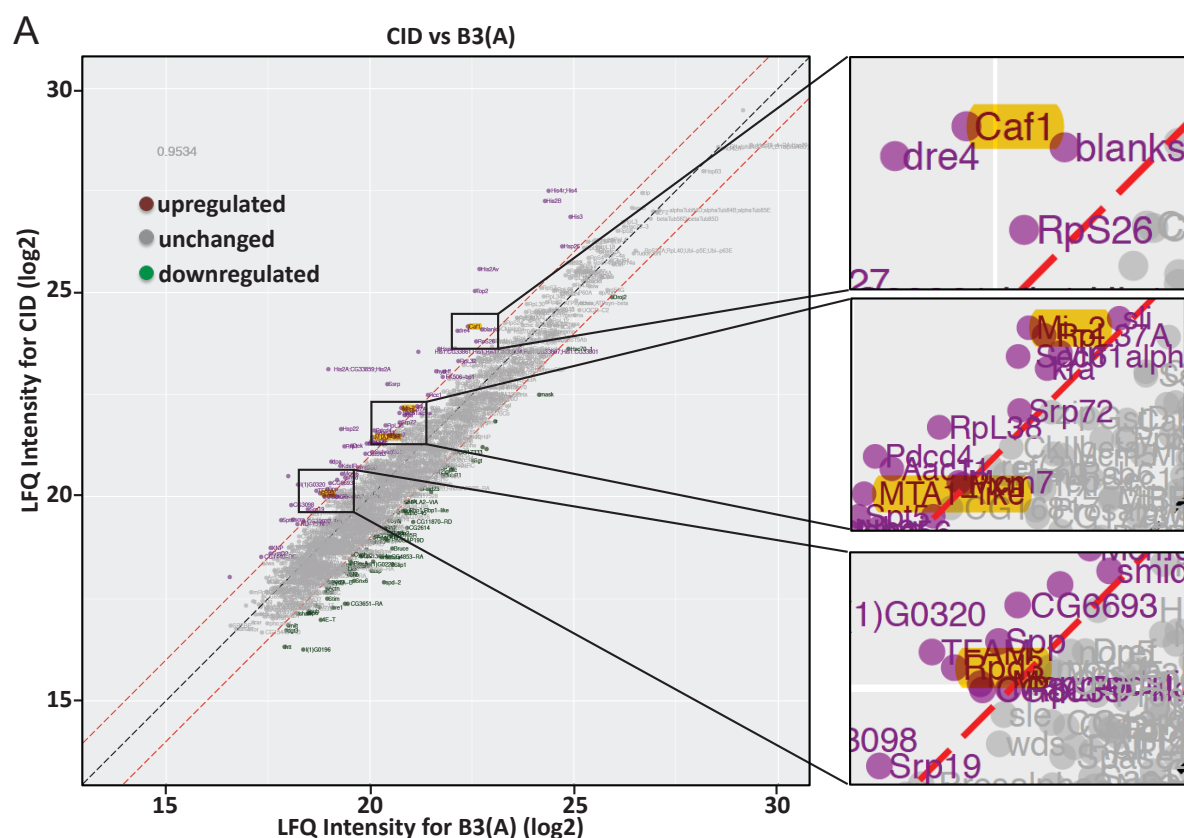
A Bar graphs of peptide and protein counts detected for all samples. **B** Histograms of peptide count versus ratio for all samples. **C** Pairwise scatterplots of LFQ intensities.

3.2.2 B3 (A) is integrated into chromatin under RbAp48 overexpression

Next, Fisher exact test was performed by Dr. Bernd Hessling to gain insights into the GO terms of the samples. CID interacts with chromatin-associated factors, whereas B3 (A) does not (Table 8.3). Intriguingly, B3 (A) interacts with chromatin-associated factors upon RbAp48 co-overexpression (Table 8.3). These results further evidence that B3 motif and RbAp48 are required for CID nuclear import and chromatin deposition as reported by previous student (Spiller-Becker, unpublished).

3.2.3 RbAp48-containing NuRD complex emerges as a candidate CID-interacting partner

To eliminate non-specific interacting factors and detect the most abundant CID-interacting complexes, stringent threshold parameters (LFQ value > 2 and peptide count increase > 4) were applied. By this filtering method, I was able to identify 120 interacting partners from pairwise comparison of the samples (Table 8.4). By B3 (A)-RbAp48 vs B3 (A) comparison, 26 enriched factors were detected, among which no known RbAp48-dependent chaperone/chromatin modification complex was present (Table 8.4). Intriguingly, by CID vs B3 (A) comparison, 48 enriched factors were detected (Figure 3.9a, Table 8.4). Among those, there are already known interacting partners which are involved in regulation of non-centromeric CENP-A (Figure 3.9b, Table 8.4). Strikingly, I obtained Dek/XNP, which is *Drosophila* homolog for DAXX/ATRX chaperone complex (Figure 3.9b, Table 8.4). DAXX is involved in ectopic loading of CENP-A in humans (Lacoste et al., 2014) even though previous preliminary work from our lab did not see DEK-dependent ectopic CID loading. Moreover, the FACT complex comprising of Spt6, Ssrp, Dre4 and Spt5 (Figure 3.9b, Table 8.4), which was previously shown to play a role in elimination of ectopic CENP-A in yeast was present (Deyter & Biggins, 2014). Most intriguingly, I was able to identify the Nucleosome Remodelling and Deacetylase (NuRD) complex core components Mi-2, MTA1-like, Rpd3 and RbAp48 (Figure 3.9, Table 8.4). Remarkably, hyd E3 ligase was also present among the top hits as in Δ NCID co-IP (Table 8.4). By CID vs B3 (A)-RbAp48 comparison, NuRD complex components including MEP-1 were again detectable (Figure 3.9b, Table 8.4). The reason why I could not detect NuRD complex by B3 (A)-RbAp48 vs B3 (A) comparison might be because of stringent threshold parameters. Nevertheless, considering the peptide counts, there was an enrichment of NuRD complex subunits in B3 (A)-RbAp48 compared to B3 (A) (Figure 3.9b). The peptide enrichment of NuRD complex subunits was also determined by the previous Δ NCID co-IP compared to control (Figure 3.6d). The enrichment of NuRD subunits was detected in an independent CID IP-MS study from our lab (Sharma, unpublished) and by another lab (Table 8.2, Barth et al., 2014). Overall, our MS approaches suggest that NuRD complex is a strong candidate for CID interaction and misincorporation.



B

Prot.names	Peptide	Peptide	Peptide	Peptide	LFQ B3(A) (log2)	LFQ B3(A)		LFQ GFP only (log2)	literature
	count B3(A)	count B3(A)	count CID	count GFP only		RbAp48 (log2)	LFQ CID (log2)		
Dek	6	6	7	4	19.6	20.4	21.2	19.5	DAXX Complex
XNP	2	4	5	0	17.6	17.9	18.7	n.a.	DAXX Complex
Spt6	3	6	8	0	17.8	17.8	19.4	n.a.	FACT Complex
dre4	13	19	24	6	22.1	23.3	24.1	19.9	FACT Complex
Ssrp	10	13	15	7	20.4	21.9	22.8	20.4	FACT Complex
RbAp48	12	20	17	7	22.4	25.8	24.2	21.9	NuRD Complex
Rpd3	2	3	3	0	18.8	18.9	20.1	n.a.:	NuRD Complex
Mi-2	11	14	17	3	20.8	20.8	22.2	19.5	NuRD Complex
MTA1-like	7	8	10	3	20.1	19.7	21.5	19.1	NuRD Complex
MEP-1	2	2	5	0	18.8	18.1	19.4	n.a.	NuRD Complex

Figure 3.9 Core components of NuRD complex are enriched among the interacting partners of CID.

A Scatter plot of Xlink-IP-MS experiment for LFQ (log2) values of CID vs B3(A). The candidate proteins enriched for CID (LFQ CID vs B3(A) ratio ≥ 2) are indicated above the upper red-dashed line in magenta. The candidate proteins enriched for B3(A) (LFQ B3(A) vs CID ratio ≥ 2) are indicated below the lower red-dashed line in green. The candidate proteins which did not enrich for neither CID nor B3(A) are indicated in gray. RbAp48 (Caf1), Mi-2, MTA1-like and Rpd3 components of the NuRD complex are highlighted and shown in a larger view. **B** Table showing the peptide counts and LFQ values of the subunits of DAXX, FACT and NuRD complexes. DAXX and FACT complexes (in green) are known interacting partners of ectopic CID. NuRD complex (in yellow) is yet to be understood.

3.2.4 CID and NuRD complex physically interacts

In order to test the physical interaction between CID and NuRD complex, I performed a co-IP against GFP-tagged CID and B3 (A) and checked by western blot (Figure 3.10). This confirmed the physical interaction between CID and NuRD complex subunits Mi-2, MTA1-like and RbAp48 (Figure 3.10). Those interactions were also in accordance with Xlink-IP-MS data, indicating stronger interaction of the NuRD complex with full length CID compared to CID-B3 (A) mutant (Figure 10). B3 (A) interaction with RbAp48 is much stronger upon RbAp48 overexpression compared to no RbAp48-overexpressing condition and equivalent to the interaction of wild type CID with endogenous RbAp48 (Figure 3.10). This further highlights the requirement of RbAp48 interaction for stability and nuclear transport of B3 (A). Moreover, CID also co-localizes with the catalytic ATPase-dependent Mi-2 helicase subunit of NuRD by IF staining under both higher (Figure 3.11a) and lower induction of CuSO₄ (Figure 3.11b). Taken together, these results indicate that ectopically expressed CID physically interacts with the core and catalytic components of NuRD complex.

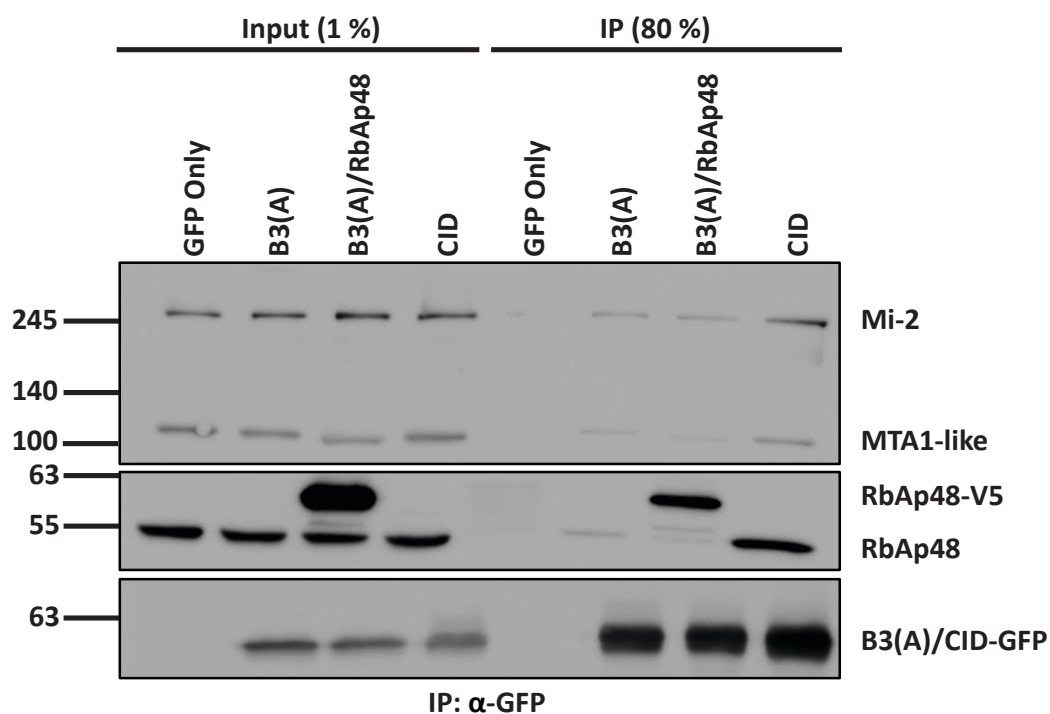


Figure 3.10 CID has a physical interaction with NuRD complex, which is stronger than B3 (A). Western blot of GFP co-IP probed with Mi-2, MTA1-like, RbAp48 and CID.

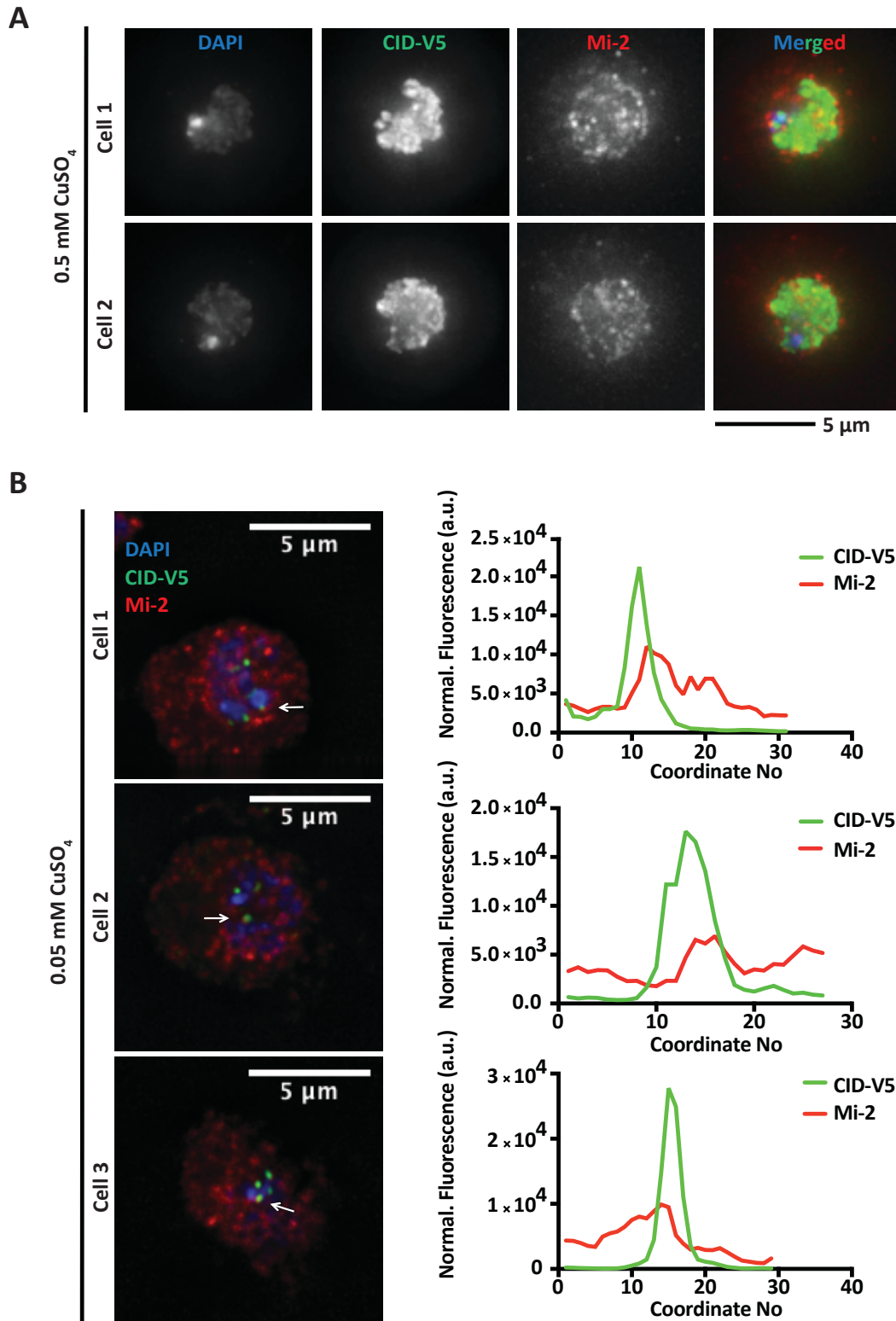


Figure 3.11 Ectopically-expressed CID co-localizes with Mi-2 on the chromatin.

A IF images of two representative inducible CID-V5 cells under 0.5 mM CuSO_4 induction. DAPI in blue, CID-V5 in green and Mi-2 in red. Scale bar indicates 5 μm . **B** IF images of three representative cells under 0.05 mM CuSO_4 induction and corresponding fluorescent intensity plots of overlapping CID-V5 and Mi-2 dots marked by arrows. DAPI in blue, CID-V5 in green and Mi-2 in red. Scale bar indicates 5 μm . Normalized fluorescence is shown in arbitrary units.

3.2.5 Ectopically expressed CID levels are reduced under silencing of Mi-2 and HDAC inhibition

Next, to address if NuRD plays a functional role in regulation of CID, I intended to target catalytic components of NuRD complex. CID is unstable and degraded upon knockdown of loading factor CAL1 (C. C. Chen et al., 2014). CENP-A mono-ubiquitination has been shown to be required for stabilization and centromeric loading in *Drosophila* and human (Bade et al., 2014; Niikura, Kitagawa and Kitagawa, 2017). Thus, I hypothesized that overexpressed CID is stabilized by NuRD complex, and overexpressed CID and mono-ubiquitinated CID levels go down upon lack of NuRD catalytic activities. Then, catalytic Mi-2 helicase component was targeted by RNAi-mediated depletion in CID-V5-His overexpressing cells. Total ectopically expressed CID and mono-ubiquitinated CID protein levels prominently decreased upon Mi-2 knockdown by western blot (Figure 3.12). To exclude the possibility that the decrease in CID-V5 levels is not due to CID-V5 transcription, semi-quantitative RT-PCR was performed by MSc student Alex Wilhelm (not shown). Preliminary results indicated no predominant change in transcription of overexpressed CID upon Mi-2 knockdown. However, this has to be further tested by qPCR. Taken together, these results suggest that Mi-2 regulates stability of overexpressed CID.

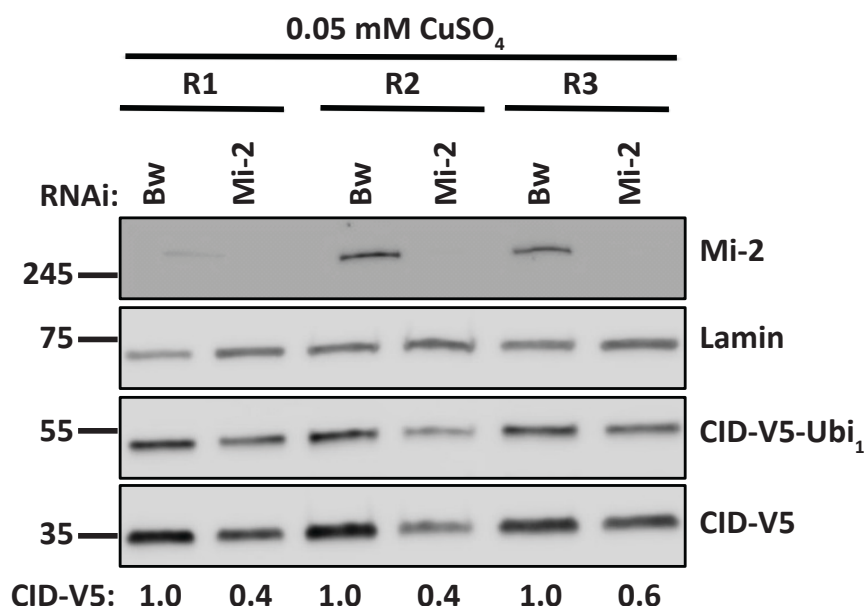


Figure 3.12 Ectopically-expressed CID protein levels decrease upon Mi-2 knockdown.

Western blot of Brown and Mi-2 RNAi depleted cells probed with Mi-2, lamin and CID-V5 for three biological replicates (R1-3). CID-V5 was induced by 0.05 mM CuSO₄ overnight. Lamin served as loading control. The intensity for each single CID-V5 band was quantified by ImageJ and normalized to lamin.

The function of other NuRD catalytic component Rpd3 in modulation of CID was also studied. Since Rpd3 histone deacetylase is part of other complexes as well, it was not targeted by siRNA depletion. Instead, a general HDAC inhibitor Trichostatin A (TSA) was used to block the histone deacetylation activity of Rpd3. TSA was shown to block CENP-A mislocalization upon Mis18α depletion in human (Fujita et al., 2007), while promoting CENP-A assembly at alphoid array (Nakano, Okamoto, Ohzeki, & Masumoto, 2003). Since TSA is

also a global epigenetic-modifying reagent (Bartsch, Truss, Bode, & Beato, 1996), potential secondary effects influences should also be taken into account. Despite not being quantitated by qPCR, preliminary semi-quantitative RT-PCR assays (Alex Wilhelm) indicated that CID-V5 transcript levels are not drastically altered upon TSA treatment compared to DMSO control (Figure 3.13a). H4-acetyl levels were prominently upregulated upon TSA treatment, indicating that the treatment works (Figure 3.13b). Intriguingly, CID-V5 protein levels decreased about 30 % upon TSA treatment (Figure 3.13b). Nuclear CID levels also significantly went down about 2-fold upon HDAC inhibition by IF staining (Figure 3.13c-d). Thus, histone deacetylation might play a role in regulation of CID misincorporation. To specifically address that and the catalytic activity of Rpd3 in CID ectopic loading, further tests are required. To sum up, these results point out that Mi-2 and histone deacetylation might have an important function in modulating mislocalized CID.

3.2.6 CID ectopic localization goes down upon knockdown of Mi-2 and MTA1-like

Next, I intended to address whether the NuRD complex is involved in ectopic CID deposition on mitotic chromosomes. In order to test this, I performed mitotic spreads technique according to the standard AG Erhardt protocol. This technique briefly depends on: (1) arresting the cells at mitosis, (2) exploding the cells with a high-salt buffer, (3) spreading the mitotic chromosomes on a microscope slide, and (4) immunofluorescent staining of proteins of interest. Mi-2, as a catalytic subunit, and MTA1-like, as a scaffold protein for the assembly of NuRD complex (Lai & Wade, 2011), were selected to target by RNAi depletion in CID-V5 overexpressing cells. By mitotic chromosome spreads, I observed a significant reduction in mislocalized CID levels (Figure 3.14a-b) under efficient knockdown of both proteins (Figure 3.14c). Notably, the reduction was even more prominent by about 7 fold under lower level of CID-V5 induction with 0.05 mM CuSO₄ (Figure 3.14a-b). Strikingly, CID was restricted only to the centromeric locations upon knockdown of NuRD subunits under 0.05 mM induction (Figure 3.14a). Of note, the reduction was more predominant upon MTA1-like RNAi under 0.5 mM CuSO₄ induction (Figure 3.14a-b). How CID mislocalization is quantitatively reduced and locally restricted only to the centromeres upon knockdown of those NuRD components stresses on the critical role of NuRD in CID ectopic localization. These results overall indicate that NuRD complex catalytic and scaffold subunits are required for CID localization to non-centromeric chromatin.

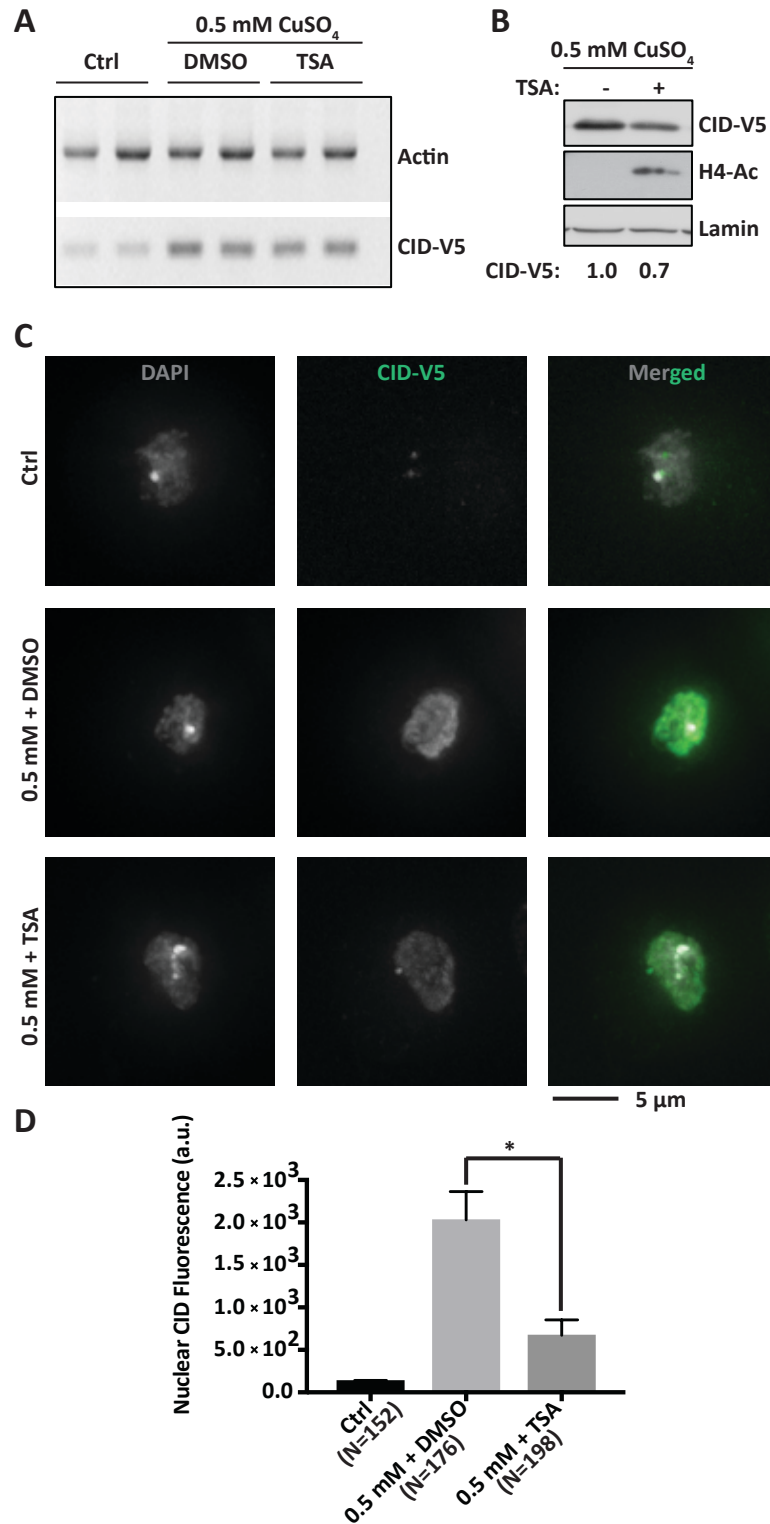


Figure 3.13 Nuclear levels of ectopically-expressed CID decreases upon HDAC inhibition.

A Agarose gel image of RT-PCR for CID-V5 expression upon DMSO and 0.25 μM TSA treatment under 0.5 mM CuSO₄ induction. Actin served as a housekeeping gene control. Ctrl served as no treatment control. **B** Western blot of CID-V5 expression upon DMSO and TSA treatment under 0.5 mM CuSO₄ induction. Lamin served as loading control. H4-Ac served as positive control for TSA treatment. Quantification was done using ImageJ, and CID bands were normalized to lamin. **C** IF images of three representative CID-V5 cells induced with 0.5 mM CuSO₄ upon DMSO and TSA treatments. DAPI in blue and CID-V5 in green. Scale bar indicates 5 μm. **D** Quantification of nuclear CID fluorescence.

Each bar represents the mean of three independent experiments, and the error bars indicate the SEM. Student's t test: * $p < 0.05$.

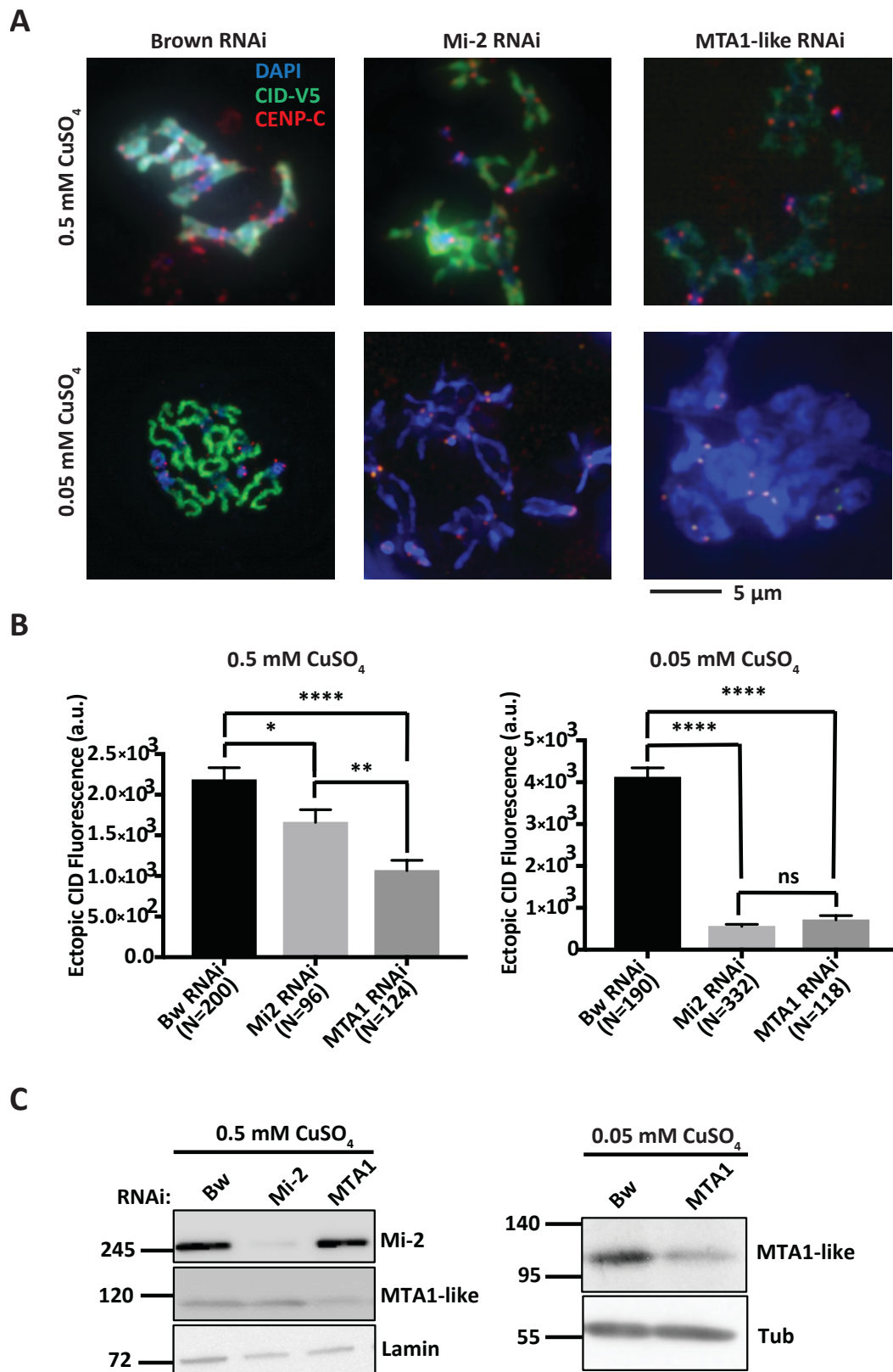


Figure 3.14 Ectopic CID localization is reduced upon Mi-2 and MTA1 depletion.

A Representative IF images of mitotic chromosomes from CID-V5 cells induced with 0.5 or 0.05 mM CuSO₄ under Brown, Mi-2 and MTA1-like knockdowns. DAPI in blue, CID-V5 in green and CENP-C in red. Scale bar indicates 5 μ m. **B** Quantification of ectopic CID fluorescence per chromosome under 0.5 mM CuSO₄ (left panel) and under 0.05 mM CuSO₄ (right panel) induction. Each bar represents the mean of three independent experiments, and the error bars indicate the SEM. Normalized fluorescence in arbitrary units. Student's t test: * $p < 0.05$, ** $p < 0.01$, **** $p < 0.0001$ and ns: not significant. **C** Western blots of Mi-2 and MTA1-like knockdowns probed for Mi-2, MTA1-like, lamin and tubulin under 0.5 mM (left) and 0.05 mM (right) CuSO₄ induction. Lamin and tubulin served as loading control.

3.2.7 CID ectopic loading requires interaction with NuRD complex

In order to further address the specific role of NuRD complex in ectopic CID incorporation mechanism, I used a RbAp48 mutant protein incapable of binding NuRD (kind gift of Professor Ernest Laue and Dr. Wei Zhang from Cambridge University). This particular RbAp48-mutant has five point mutations, E361Q D362N, E364Q, D365N and L35Y, which block its interaction with MTA1-like and all the other NuRD subunits as previously described (Alqarni et al., 2014). I confirmed those mutations by Sanger sequencing analysis. Then, I cloned this construct into inducible pMT-V5-His vector. I also employed B3 (A) mutant, which requires RbAp48 overexpression for ectopic localization, to assess the critical importance of NuRD in this mechanism. First, I created the S2 cell lines overexpressing this particular mutant alone or together with B3 (A). Next, I confirmed that this particular mutant loses the physical interaction with its direct interacting partner MTA1-like in the NuRD complex (Figure 3.15). Nevertheless, it still retains the interaction with overexpressed B3 (A), endogenous CID and CAF1-p180 (Figure 3.15). Using this system, I observed a significant decrease in ectopic B3 (A) localization by 10 fold from 33 % to 3 % of chromosomes by mitotic spreads under RbAp48-mutant overexpression (Figure 3.16). Notably, B3 (A) mislocalization of 12 % under overexpression of B3 (A) alone was not significantly different from that of 3 % under co-overexpression of RbAp48-mutant (Figure 3.16). Taken together, these outcomes suggest that NuRD-binding is required for RbAp48-dependent CID ectopic loading.

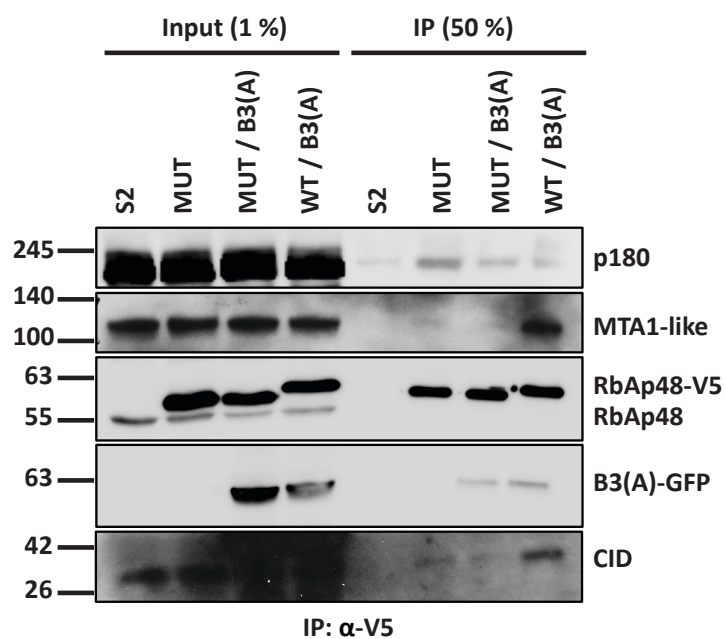


Figure 3.15 NuRD-binding incompetent RbAp48 mutant lacks MTA1-like interaction, while retaining interactions with p180 and CID.

Western blot of V5 co-IP probed with p180, MTA1-like, RbAp48 and CID. MUT: RbAp48-mutant, WT: RbAp48-wild type.

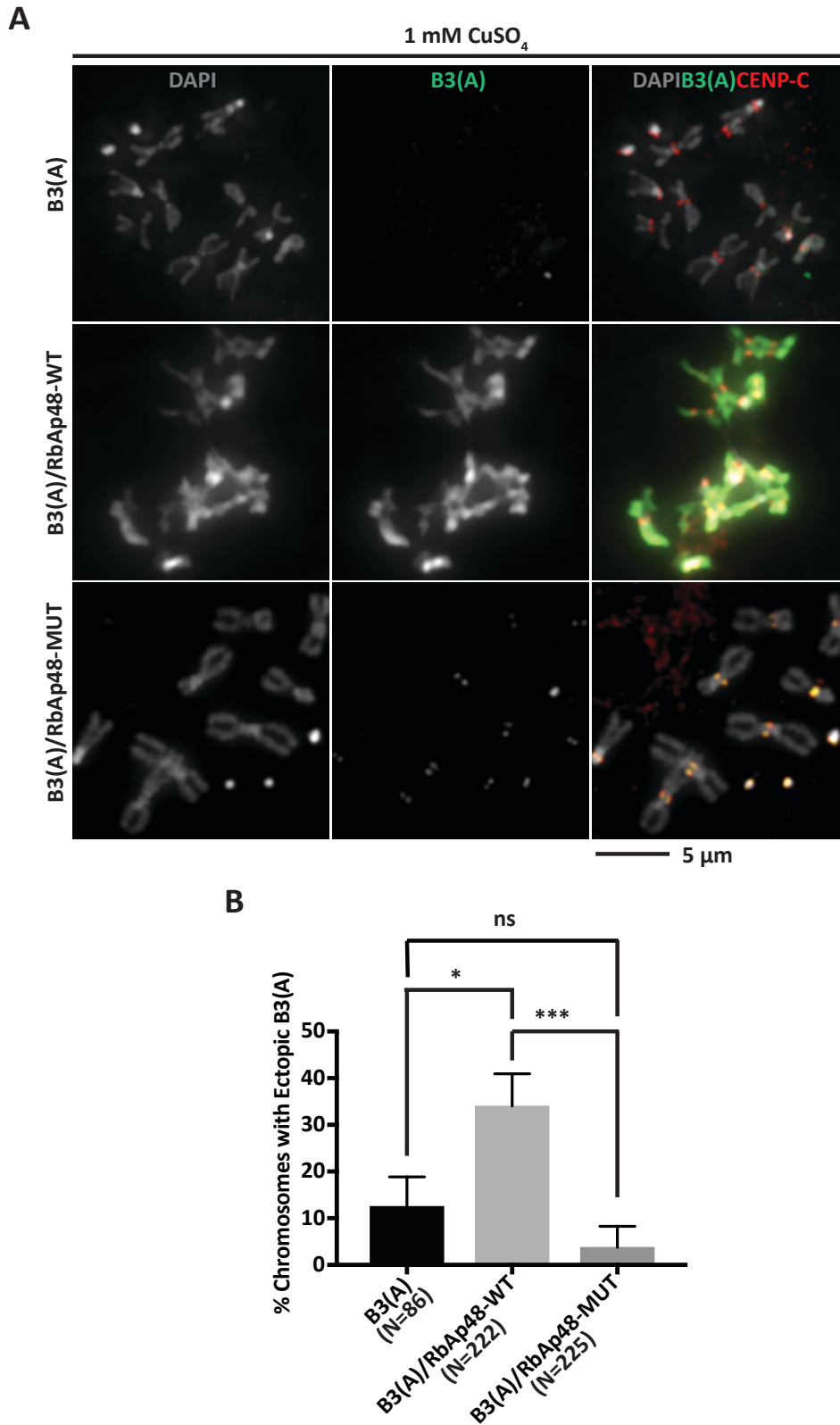


Figure 3.16 Ectopic B3 (A) localization is reduced upon NuRD-binding incapable RbAp48 mutant overexpression.

A Representative IF images of mitotic chromosomes from B3 (A)–GFP, B3 (A)–GFP/RbAp48-WT-V5 and B3 (A)–GFP/RbAp48-MUT-V5 overexpressing cell lines under 1 mM CuSO₄ induction. DAPI in gray, CID-V5 in green and CENP-C in red. Scale bar indicates 5 μm. **B** Quantification of percentage of chromosomes with ectopic B3 (A). Each bar represents the mean of three independent experiments, and the error bars indicate the SEM. Student's t test: * p<0.05, *** p<0.001 and ns: not significant.

3.2.8 MTA1-like plays a role in nuclear translocation of ectopically expressed CID

Next aim was to address the location of overexpressed CID upon depletion of NuRD components. By IF staining, I found that overexpressed CID was localized in the nucleus in almost 100 % of the cells upon brown control knockdown (Figure 3.17). Similarly, the nuclear localization was not disrupted significantly upon Mi-2 depletion (Figure 3.17). Strikingly, about half of the cells were nuclear localization deficient for overexpressed CID upon MTA1-like depletion (Figure 3.17). The reason why there is no localization-aberrant phenotype of CID under Mi-2 knockdown proposes that Mi-2 might not be involved in CID nuclear import but rather its deposition into chromatin. There might be still underlying technical problems, such as poor knockdown efficiency or poor detection capacity of the microscope, hindering the defective phenotype. Overall, this experiment shows that MTA1-like might be involved in CID nuclear import.

3.2.9 Physical interaction with MTA1-like and NuRD complex is critical for nuclear localization of CID

To test the hypothesis that MTA1-like plays a critical role in CID nuclear transport, I used the B3 (A) and RbAp48-mutant co-overexpressing system. B3 (A) cannot localize sufficiently in the nucleus without RbAp48 overexpression (Spiller-Becker, unpublished), and RbAp48-mutant does not bind to MTA1-like (Figure 3.15) as well as other NuRD subunits (Alqarni et al., 2014). Thus, this system gives the chance to test the potential role of MTA1-like and NuRD complex in CID nuclear import. Resembling B3 (A) only cells, the nuclear localization of B3 (A) was almost completely abolished under RbAp48-mutant co-overexpression compared to RbAp48 wild type by IF staining (Figure 3.18). Thus, this result strongly suggests that nuclear localization of ectopically expressed CID is impaired upon lack of physical interaction with MTA1-like and NuRD complex.

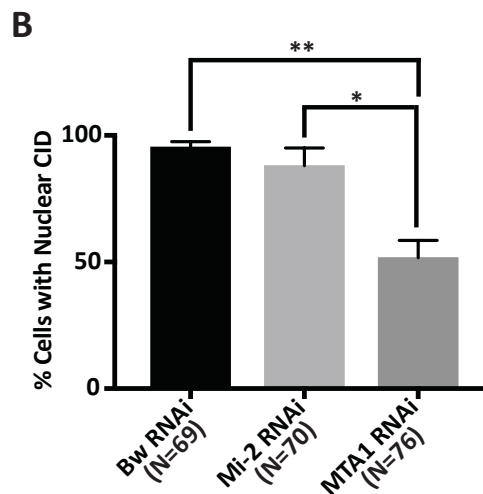
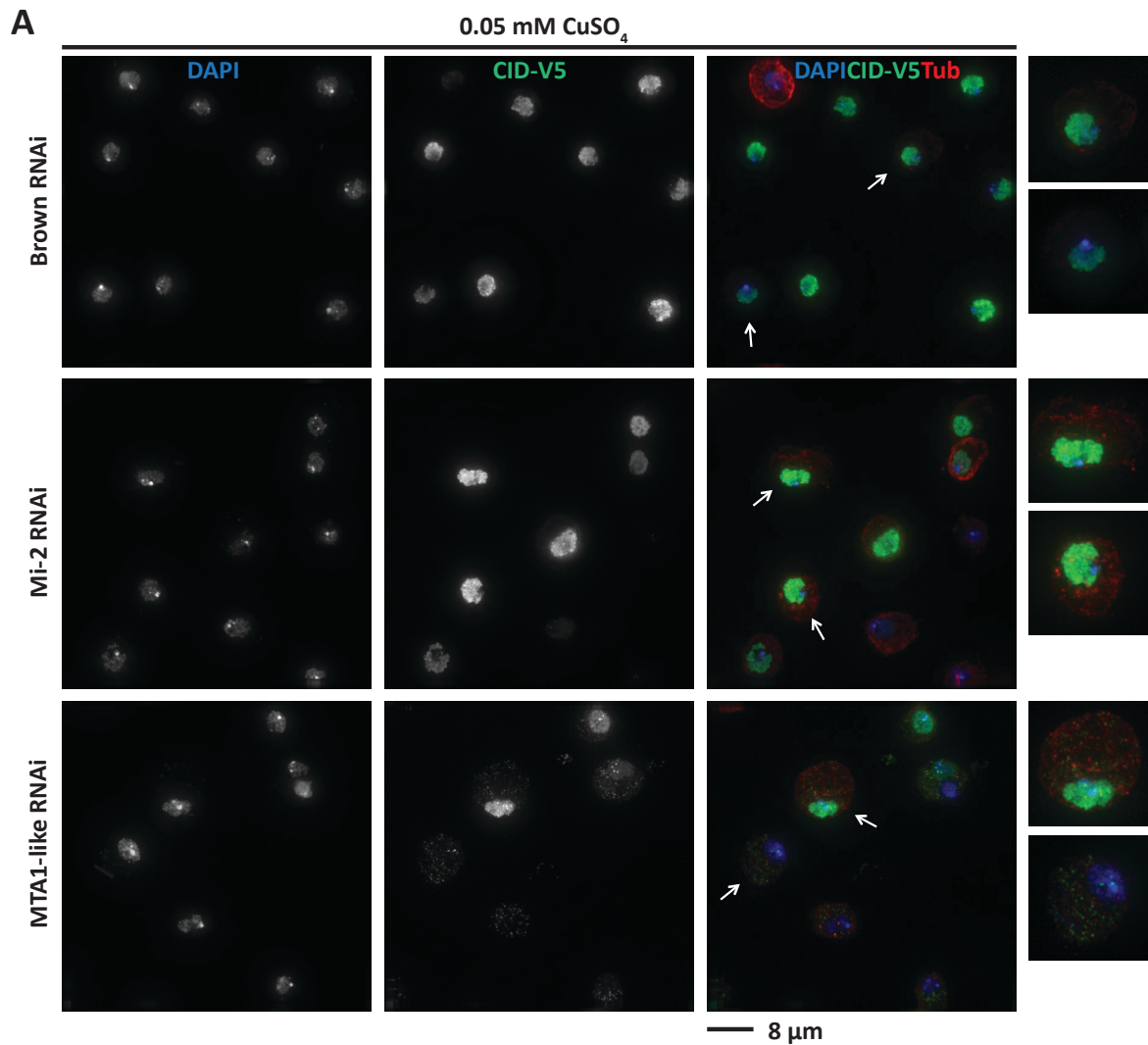


Figure 3.17 Nuclear localization of ectopically-expressed CID decreases upon MTA1-like knockdown.

A Representative IF images of inducible CID-V5 cells induced with 0.05 mM CuSO₄ under Brown, Mi-2 and MTA1-like knockdowns. Two representative cells for each condition marked by arrows are zoomed in (4X). DAPI in blue, CID-V5 in green and tubulin in red. Scale bar indicates 8 μm. **B** Quantification of percentage of cells with nuclear CID. Each bar represents the mean of three independent experiments, and the error bars indicate the SEM. Student's t test: * p<0.05, ** p<0.01.

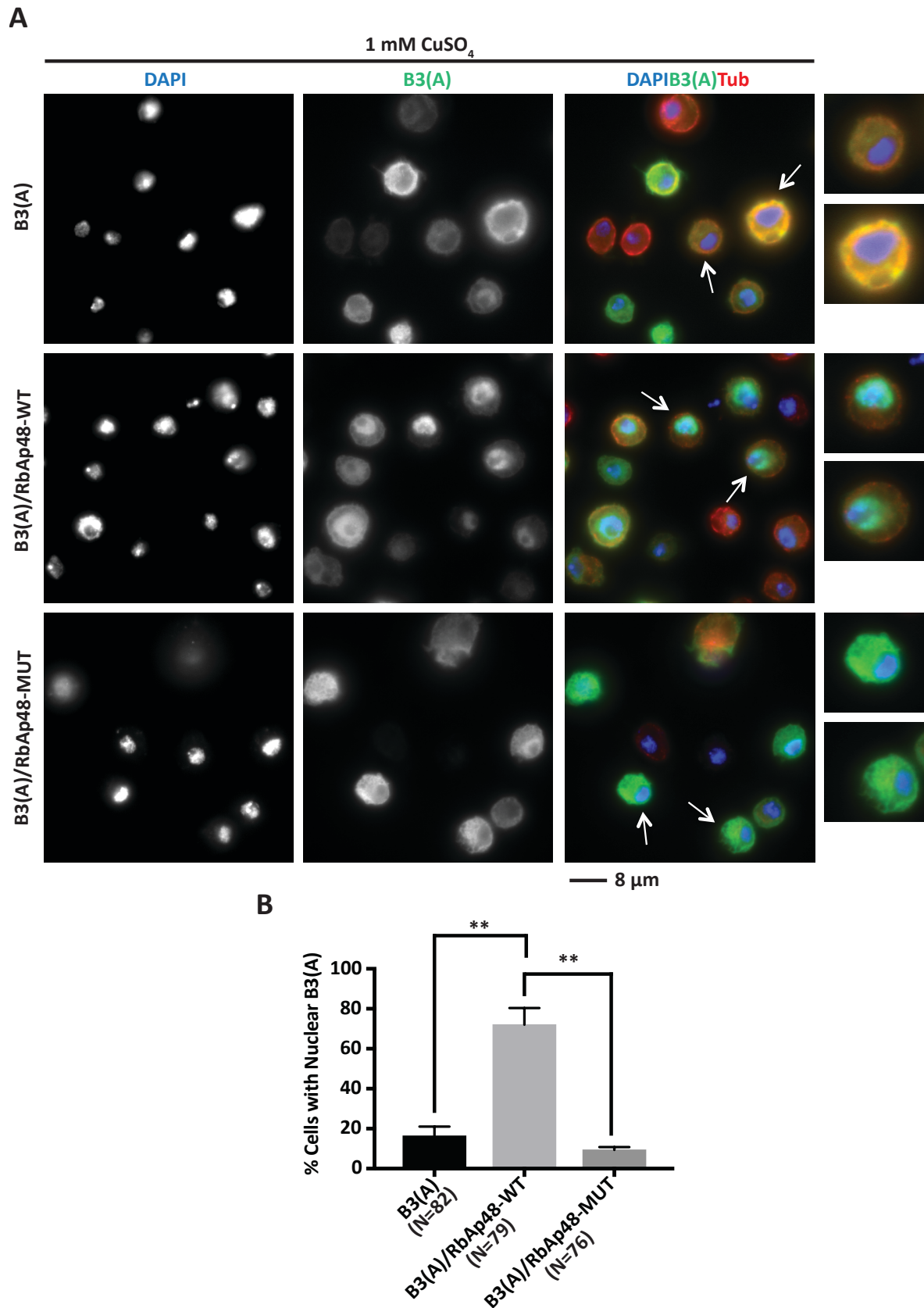


Figure 3.18 Nuclear localization of ectopically-expressed B3 (A) is abrogated upon NuRD-binding incapable RbAp48 mutant overexpression.

A Representative IF images of inducible B3 (A)–GFP, B3 (A)–GFP/RbAp48-WT-V5 and B3 (A)–GFP/RbAp48-MUT-V5 cell lines induced with 1 mM CuSO₄. Each image indicates a single z-stack. Two representative cells for each condition marked by arrows are magnified (4X). DAPI in blue, B3 (A)–

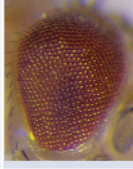
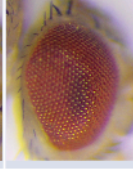
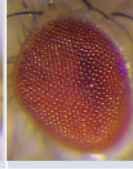
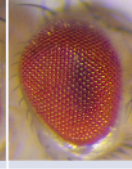
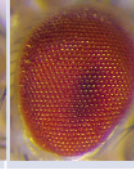
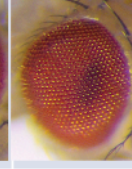
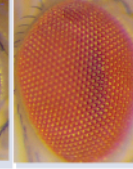
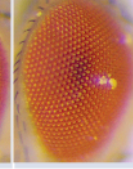
GFP in green and tubulin in red. Scale bar indicates 8 μ m. **B** Quantification of percentage of cells with nuclear B3 (A). Each bar represents the mean of three independent experiments, and the error bars indicate the SEM. Student's t test: ** $p < 0.01$.

3.3 Hyd E3 ubiquitin ligase is involved in destabilization of CID

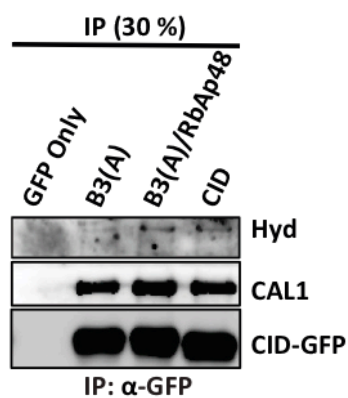
3.3.1 CID has a physical and genetic interaction with hyd

The evidences indicate that cellular levels and ectopic localization of overexpressed CID are reduced upon partial depletion of NuRD subunits or lack of NuRD-binding, and this might be partially due to the nuclear import defect. Nuclear localization deficient CID mutants are degraded by proteolysis (Spiller-Becker, unpublished). Moreover, misincorporated CENP-A is eliminated via targeting by specific E3 ubiquitin ligases and proteasomal degradation (Deyter & Biggins, 2014; G. Hewawasam et al., 2010; Hildebrand & Biggins, 2016; Moreno-Moreno et al., 2011, 2006; Ohkuni et al., 2016). Collectively, these evidences suggest that CID might be undergoing proteolysis under inhibition of NuRD-dependent loading. It is yet unclear whether full length CID is targeted by already known degradation pathways, or an alternative pathway is involved. By IP-MS and Xlink-IP-MS, I found that hyd E3 ligase is one of the most abundant Δ NCID-interacting partners (Figure 3.6d, Table 8.4). Thus, I investigated the role of hyd E3 ligase in degrading ectopic CID. To gain insight into that, I performed a genetic interaction test between CID and hyd using the rough eye phenotype that is caused by CID overexpression as described before (Mathew et al., 2014) and Jäger et al., 2005. CID overexpression by tissue-specific Gal4-drivers in the fly eye leads to rough eye phenotype due to segregation errors and genomic instability (Heun et al., 2006; Jäger, Rauch, & Heidmann, 2005), and this phenotype can be suppressed or enhanced upon changing the levels of genetic interacting partner (Jäger, Rauch and Heidmann, 2005; Bade et al., 2014; Mathew et al., 2014). Upon co-overexpression of CID and the inactive hyd¹⁵ mutant, which was created by the ethyl methansulfonate (EMS) treatment-based mutagenesis (Flybase), flies show a partial rescue of the rough eye phenotype, indicating that CID genetically interacts with hyd (Figure 3.19a). Furthermore, both endogenous and HA-tagged hyd physically interact with GFP-tagged CID by Co-IP (Figure 3.19b-c). Like CID-overexpression, hyd-depletion driven in the eye also leads to rough eyes, suggesting that hyd might also influence cell viability in the eye (Figure 3.19d). In sum, I could show that there is a physical and genetic interaction between CID and hyd.

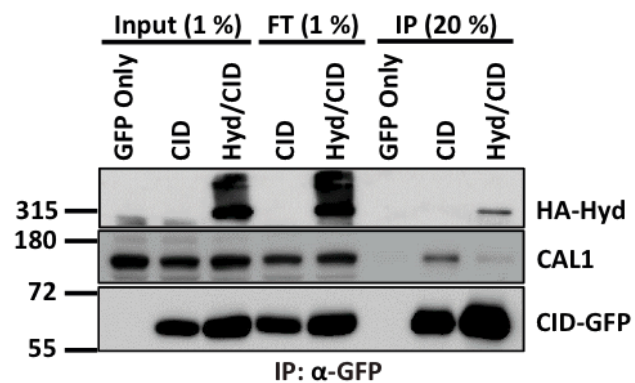
A

	Experimental fly lines				Positive control		Wild Type	
Genotype	GMR-Gal4 > UAS-CID		GMR-Gal4 > UAS-CID; GMR-Gal4 > Hyd ¹⁵		GMR-Gal4 > UAS-CID; GMR-Gal4 > CAP-G		Oregon R	
Phenotype	♀	♂	♀	♂	♀	♂	♀	♂
								
	Rough eye		Partial rescue		Rescue		Smooth eye	

B



C



D

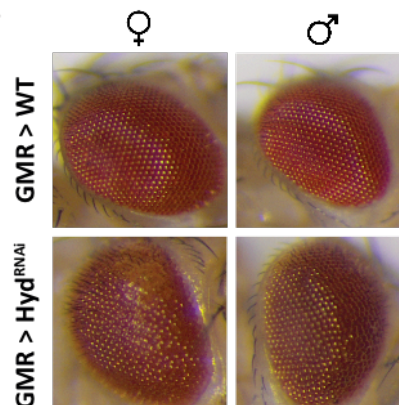


Figure 3.19 CID physically and genetically interacts with hyd.

A Genetic rescue experiment of the rough eye phenotype in CID and hyd¹⁵ – GMR-Gal4-induced co-overexpressing flies in both sexes. CID and CAP-G co-overexpressing flies served as positive control. Oregon R flies show wild type eyes. **B** Western blot of GFP co-IP probed for HA, CAL1 (positive control) and GFP. GFP only served as negative control for co-IP. **C** Western blot of GFP co-IP probed for HA, CAL1 (positive control) and GFP. GFP only served as negative control for co-IP. FT: flow-through. **D** Qualitative phenotypic analysis of hyd-depleted fly eyes in both sexes. Hyd depletion in the eye was induced by GMR-Gal4 driver.

3.3.2 CID is poly-ubiquitinated and destabilized by hyd induction

In order to mechanistically address CID and hyd interaction, I first tested how unmodified and mono-ubiquitinated CID (CID-Ubi₁) levels are altered upon hyd induction from an exogenous CuSO₄ inducible construct (Figure 3.20a-b). Endogenous CID and CID-Ubi₁ levels are gradually reduced upon stepwise increment of hyd induction (Figure 3.20a). I also observed a relative decrease in overexpressed CID-V5 and CID-V5-Ubi₁ levels under hyd co-overexpression compared to CID overexpression alone (Figure 3.20b). In order to determine whether CID is poly-ubiquitinated by hyd, I performed co-IP against ectopically expressed CID-V5 under proteasome inhibition (Figure 3.20c). Immunoblotting against ubiquitin indicated that CID co-IP complexes had substantially more poly-ubiquitination upon hyd induction (Figure 3.20c). Most intriguingly, immunoblotting against CID showed an increased level of poly-ubiquitinated CID upon hyd induction (Figure 3.20d). Notably, the mono-ubiquitinated form of CID was decreasing, suggesting that it might be converted to poly-ubiquitinated CID under hyd overexpression (Figure 3.20d). Collectively, these results suggest that hyd overexpression destabilizes CID by poly-ubiquitination and proteolysis.

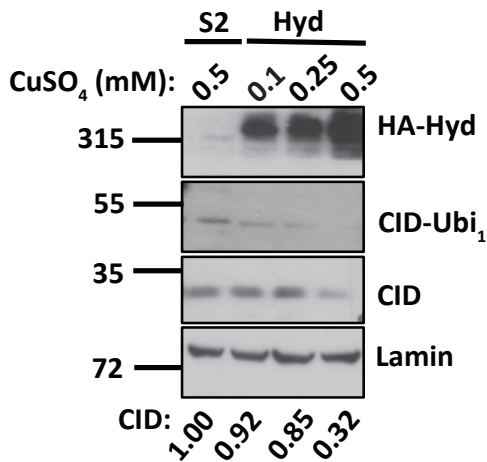
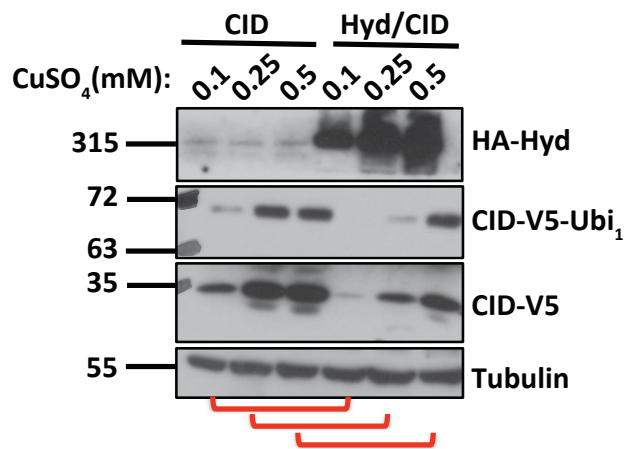
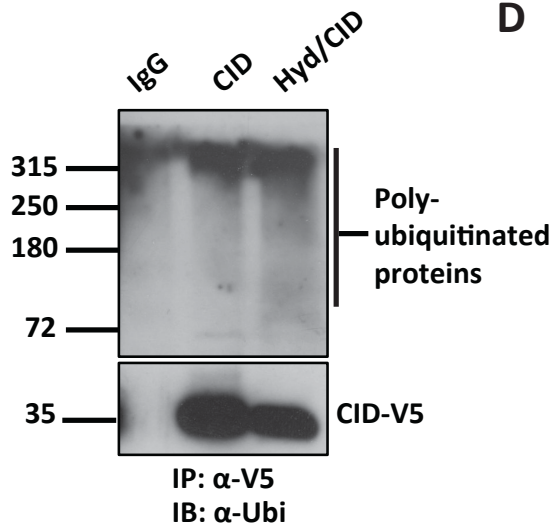
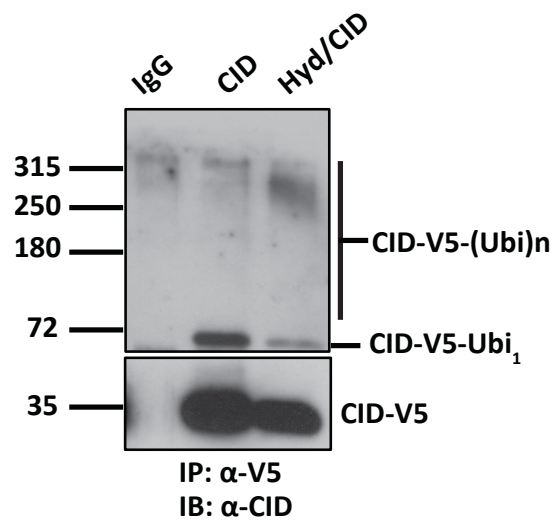
A**B****C****D**

Figure 3.20 CID is poly-ubiquitinated and destabilized upon hyd induction.

A Western blot probed for HA, CID and lamin under gradually increasing CuSO_4 induction. Lamin served as loading control. CID band intensity was quantified using ImageJ and normalized to lamin. **B** Western blot probed for HA-hyd, CID-V5 and tubulin under gradual increasing CuSO_4 induction using CID-V5 and CID-V5/HA-hyd overexpressing cell lines. Tubulin served as loading control. CID-V5 levels in two lanes marked by the same red bracket should be compared with each other. **C** Western blot of V5 co-IP using CID-V5 and CID-V5/HA-hyd-overexpressing cells under 0.1 mM CuSO_4 induction probed against ubiquitin. IgG served as negative control for co-IP. **D** Western blot of V5 co-IP in part C probed against CID. IgG served as negative control for co-IP.

3.3.3 Cellular CID levels increase upon hyd knockdown in interphase cells

Next, I intended to further test the hypothesis that CID is destabilized by hyd, performing siRNA knockdown of hyd. First, I checked if nuclear localization-deficient and unstable B3 (A) and Δ NCID is also targeted by hyd (Figure 3.21). I detected a significant increase of both total overexpressed B3 (A) and Δ NCID levels upon hyd depletion (Figure 3.21). Second, I investigated how endogenous CID is influenced from silencing of hyd (Figure 3.22). I detected by IF staining that both nuclear and total endogenous CID levels significantly increased upon hyd knockdown (Figure 3.22a-c). By western blot (Alex Wilhelm), there was also an increase in endogenous CID protein levels under hyd depletion (Figure 3.22d). Moreover, ectopically expressed CID-V5 levels were also upregulated under hyd RNAi (Figure 3.22e). Taken together, cellular CID levels are upregulated upon hyd depletion.

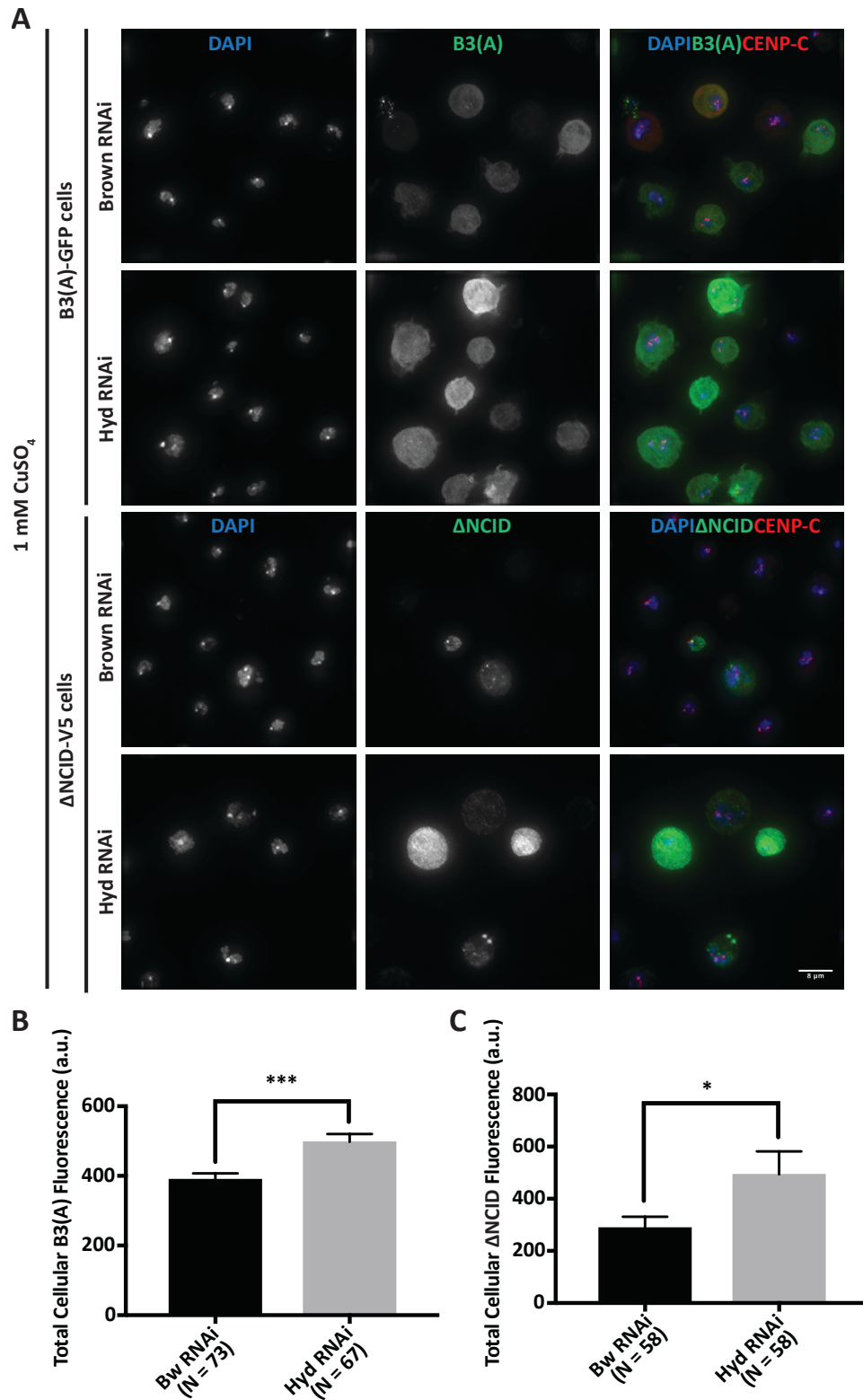


Figure 3.21 Cellular levels of nuclear localization-deficient CID constructs are upregulated under hyd depletion.

A Representative IF images of B3 (A)-GFP and ΔNCID-V5 cells under brown RNAi and hyd RNAi. DAPI in blue, B3 (A)/ΔNCID in green and CENP-C in red. Scale bar indicates 8 μm. **B** Quantification of total cellular B3 (A) (left) or ΔNCID (right) fluorescence per cell in arbitrary units. Each bar represents the mean of three independent experiments, and the error bars indicate the SEM. Student's t test: * p<0.05 and *** p<0.001.

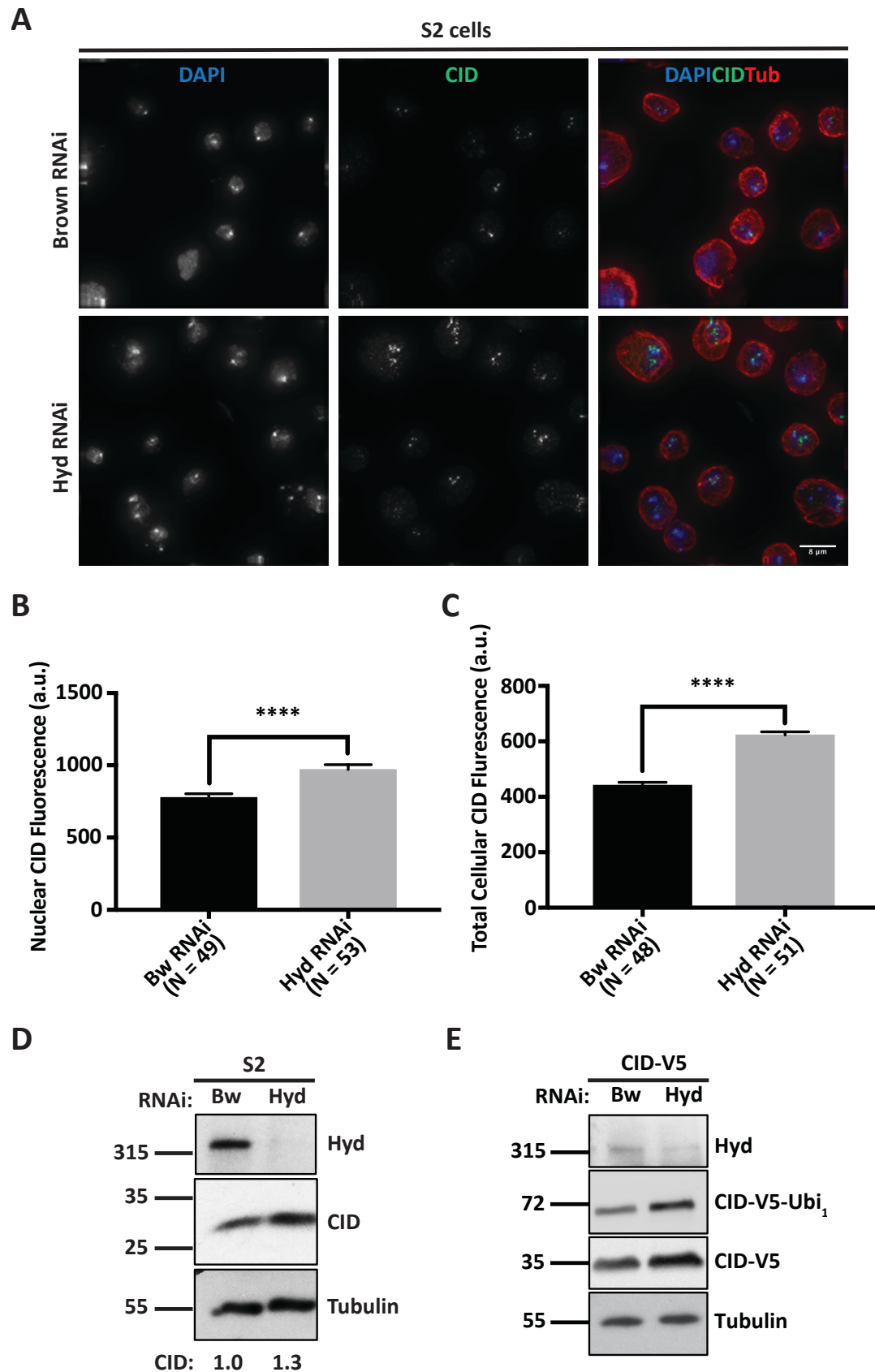


Figure 3.22 Endogenous nuclear and total cellular CID levels increased upon hyd depletion.

A Representative IF images of S2 cells under brown RNAi and hyd RNAi. DAPI in blue, CID in green and tubulin in red. Scale bar indicates 8 μ m. **B** Quantification of nuclear and **C** total cellular CID

fluorescence per cell in arbitrary units. Each bar represents the mean of three independent experiments, and the error bars indicate the SEM. Student's t test: **** $p < 0.0001$. **D** Western blot probed for hyd, CID and tubulin under brown and hyd knockdown in S2 cells. The quantification was performed using ImageJ and shows the relative band intensities of CID normalized to tubulin. **E** Western blot probed for hyd, CID-V5-Ubi₁, CID-V5 and tubulin under brown and hyd knockdown in CID-V5 cells induced with 0.05 mM CuSO₄.

3.3.4 Centromeric CID levels increase upon hyd knockdown in mitotic chromosomes

Last, I investigated if centromeric CID is also influenced by hyd E3 ligase. By mitotic spreads, I observed a significant increase in endogenous centromeric CID levels under hyd knockdown (Figure 3.23), suggesting that centromeric CID is further stabilized upon hyd depletion, which is in line with the observation that mono-ubi CID is increasing upon Hyd depletion. I also tested the incorporation of newly synthesized CID by SNAP-tag pulse-labelling approach (Jansen et al., 2007). Interestingly, I detected a significant reduction in incorporation of newly synthesized CID upon hyd RNAi (Figure 3.24). On one hand, the reason for this discrepancy might be due to saturation of centromeres with the old CID under hyd depletion, cell cycle defects, off-target effects or technical reasons. On the other hand, one can also speculate that hyd might be involved in loading of newly synthesized CID by an unknown mechanism. Overall, centromeric incorporation of physiologically available CID increases upon hyd depletion.

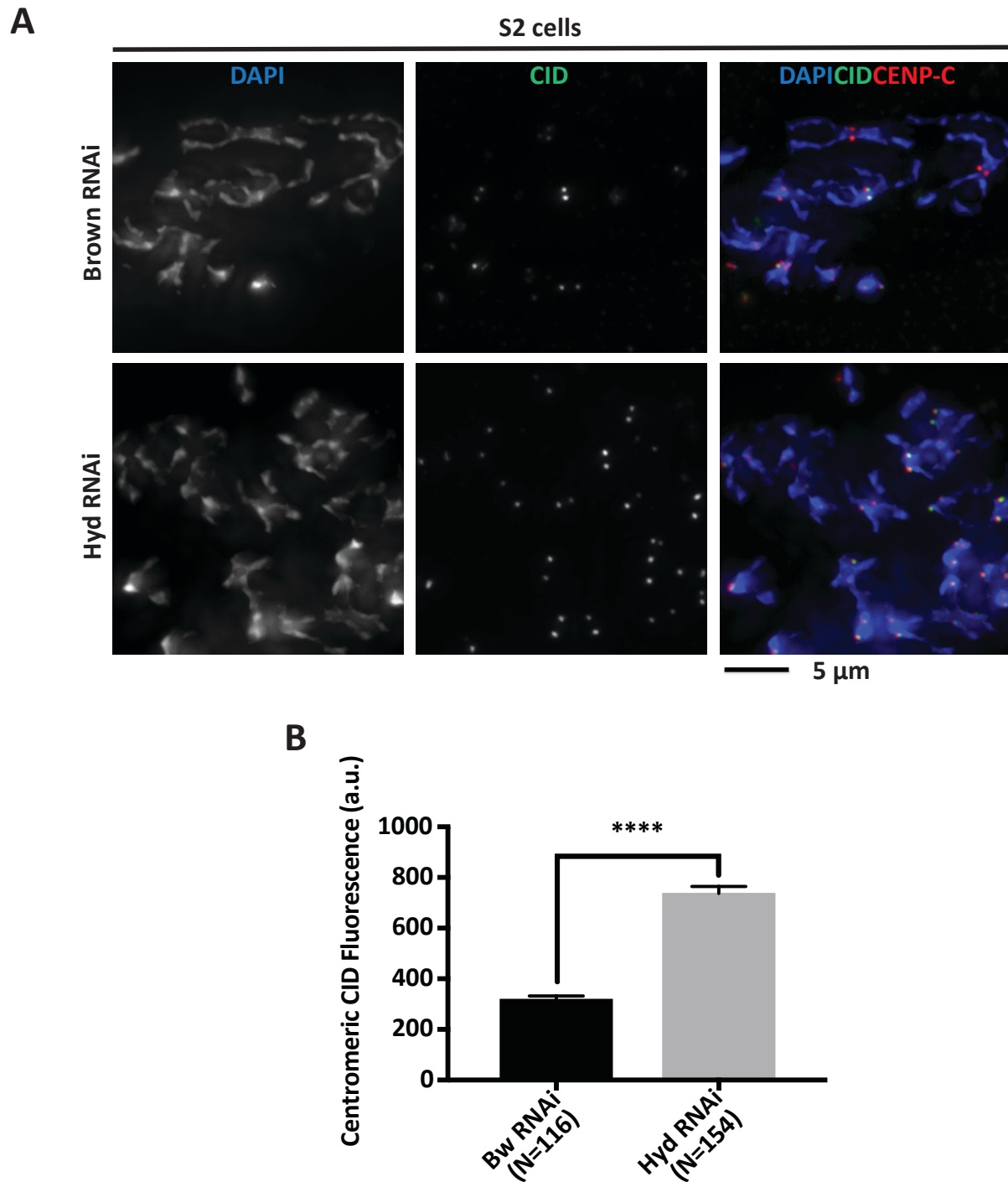


Figure 3.23 Centromeric CID levels at mitotic chromosomes increased upon hyd depletion.

A Representative IF images of mitotic chromosomes from S2 cells under Brown (control) and hyd knockdowns. DAPI in blue, CID in green and CENP-C in red. Scale bar indicates 5 μ m. **B** Quantification of centromeric CID fluorescence per chromosome in arbitrary units. Each bar represents the mean of three independent experiments, and the error bars indicate the SEM. Student's t test: **** $p < 0.0001$.

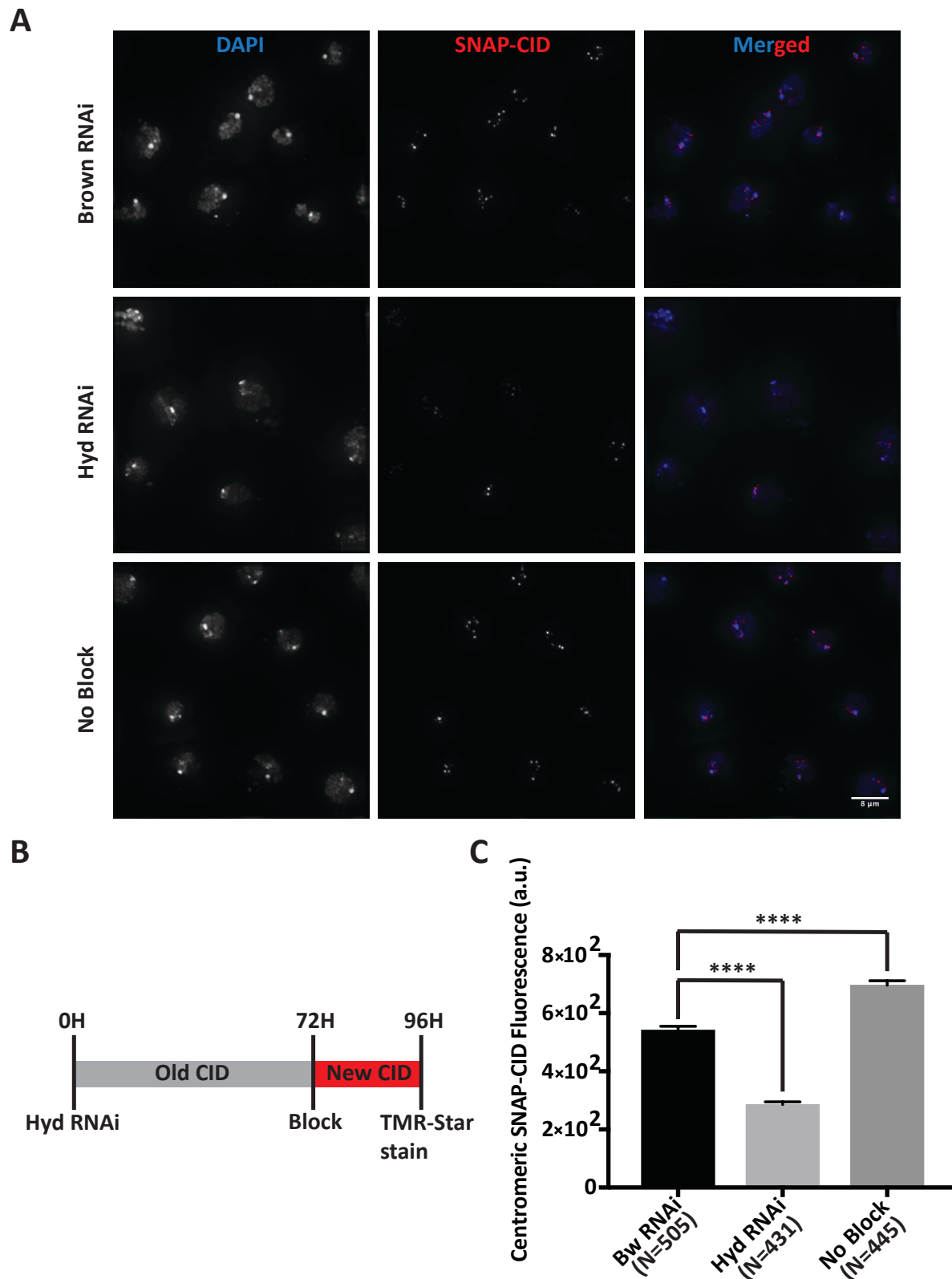


Figure 3.24 Newly synthesized CID incorporation is reduced upon hyd depletion.

A Representative IF images of SNAP-CID cells under brown RNAi, hyd RNAi and no block control treatments. DAPI in blue, SNAP-CID in red. Scale bar indicates 8 μ m. **B** Experimental workflow of RNAi-SNAP experiment. **C** Quantification of SNAP-CID fluorescence per centromere. Each bar represents the mean of three independent experiments, and the error bars indicate the SEM. Student's t test: **** $p < 0.0001$.

4 DISCUSSION

In this study, I investigated alternative mechanisms for CID mislocalization at ectopic sites and CID regulation by ubiquitin-mediated proteolysis using *Drosophila melanogaster* and cultured Schneider S2 cells. I identified NuRD complex and hyd E3 ubiquitin ligase as novel CID interacting partners. I found that NuRD complex is functionally involved in mislocalization of ectopically expressed CID. NuRD catalytic subunit Mi-2 helicase and scaffold subunit MTA1-like play essential roles in this mechanism. RbAp48 is a critical component in mediating the interaction between CID and NuRD. MTA1-like is also required for nuclear transport of overexpressed CID. On the other hand, I discovered that CID is regulated by hyd E3 ubiquitin ligase. I uncovered a genetic and physical interaction between CID and hyd. CID is poly-ubiquitinated and destabilized upon hyd induction, whereas hyd depletion leads to an upregulation of CID protein levels. Taken together, this study determined that NuRD complex is essential for CID mislocalization, and hyd E3 ligase is involved in modulating protein stability and incorporation of CID in *Drosophila*.

4.1 CAF-1/CID interaction is most likely not present in *Drosophila*

Initially, I tested the hypothesis that CAF-1 complex is required for CID misincorporation in *Drosophila*, as suggested previously (Furuyama et al., 2006). I detected a highly consistent physical interaction between ectopically expressed CID and RbAp48 (Figure 3.1d), as reported in many other studies in different model organisms (Boltengagen et al., 2015; Dunleavy et al., 2009; Foltz et al., 2009; Furuyama et al., 2006; Hayashi et al., 2004; B. C. H. Lee et al., 2016; Shang et al., 2016a). By contrast, I detected no direct or indirect physical protein-protein interactions between CID and the largest CAF-1 subunit p180 (Figure 3.1). This was consistent with previous findings in human (Dunleavy et al., 2009; Foltz et al., 2009) but in contrast to a recent finding in budding yeast (Hewawasam et al., 2018). However, plasticity between histone chaperones exist, in particular between H3 chaperones (Sitbon et al., 2017). For example, in human, HJURP and DAXX co-operate to arrange the localization of CENP-A between centromere and ectopic sites (Filipescu et al., 2017). Thus, I checked the physical interaction between CAF-1 and CAL1, the dedicated chaperone for CID loading in *Drosophila* (Chen et al., 2014). Interestingly, using yeast two hybrid technique, I detected a physical interaction between CAL1 and both RbAp48 and p180 subunits of CAF-1 (Figure 3.1b). However, I could not confirm those interactions by co-immunoprecipitation from S2 cells (Figure 3.1c). The reason for this discrepancy might be due first of all to technical problems. Y2H is a technique with high risk of detecting false positives (Serebriiskii, Estojak, Berman, & Golemis, 2000); therefore, Y2H interactions should always be confirmed by another technique. Since I did not validate those interactions by co-IP in cultured S2 cells, the interactions detected by Y2H might be false positives. Another explanation could be using two different biological model organisms for those methods. It is likely that *Drosophila* CAL1 and CAF-1 proteins might interact in yeast, as suggested for CENP-A-CAF-1 interaction in yeast (Hewawasam et al., 2018). The interaction however may not occur in *Drosophila* cells, resembling human (Dunleavy et al., 2009; Foltz et al., 2009). Overall, there is a stable and evolutionarily conserved interaction between CID and RbAp48 component of CAF-1, but the interaction of CID or CAL1 with p180 was undetectable.

4.2 RbAp48 is necessary and sufficient for priming *de novo* CID deposition at centromeres and ectopic sites

I further looked into the role of RbAp48 in priming of *de novo* CENP-A incorporation. As previously observed, I found that RbAp48 is required for loading of newly-synthesized CID (Boltengagen et al., 2015). Upon RbAp48 knockdown, CID nuclear import and concentration at centromeres decreased (Figure 3.2), as previously described (Boltengagen et al., 2015; Shang et al., 2016a). Furthermore, RbAp48-tethering at lacO site resulted in a significant enrichment of CID at those regions (Figure 3.3). This was expected because RbAp48 is involved in CENP-A licensing (Y. Fujita et al., 2007; Hayashi et al., 2004) and incorporation (Furuyama et al., 2006). Of note, p180 was more highly enriched at the lacO array when compared to CID enrichment upon RbAp48 tethering (Figure 3.3). As a major component of the CAF-1 complex (Tyler et al., 2001), such a high level of p180 co-recruitment with RbAp48 is an expected outcome. However, the difference between CID and p180 recruitment upon RbAp48 tethering implies that RbAp48 and p180 co-localization at certain chromatin regions does not necessarily lead to CID incorporation. This result is further concordant with the finding that p180 is not involved in the CENP-A pre-assembly complex (Dunleavy et al., 2009; Foltz et al., 2009). CID deposition at synthetic lacO arrays may be inefficient because a certain chromatin environment is favored for *de novo* CENP-A deposition (Athwal et al., 2015; Olszak et al., 2011). This possibility should also be taken into account and a different tethering approach instead of lacO array might be used to assess this. Another discrepant observation was that there is a very high background of p180 recruitment with GFP control (Figure 3.3b). This could possibly be explained by random co-localization due to the interspersed distribution of p180 throughout the chromatin, possibly stronger interaction affinity between p180 and GFP, and strong background GFP/p180 interaction due to the large molecular weight of p180. Collectively, those data argue that RbAp48 is involved in *de novo* deposition of CID at centromeres and at ectopic lacO site, and p180 does not appear to be required for this mechanism.

4.3 CAF-1 does not play an obvious role in CID misincorporation

To further address the role of CAF-1 in CID loading, I tested whether CID protein levels and nuclear localization are influenced upon depletion of CAF-1 components. Dedicated CID chaperone CAL1 mediates stabilization of CID through mono-ubiquitination (Bade et al., 2014a). It was further observed that CID is unstable and targeted by proteolysis upon CAL1 depletion (Chen et al., 2014). Thus, I hypothesized that if CAF-1 is acting as a loading chaperone for ectopic CID, overexpressed CID levels should decrease upon CAF-1 depletion similar to what has been observed for centromeric CID upon CAL1 depletion. Surprisingly, I found that total CID protein levels and nuclear intensity did not decrease upon CAF-1 knockdown (Figure 3.4). Those results suggest that CAF-1 is not essential for stability and misincorporation of overexpressed CID. Similarly, on mitotic chromosome spreads, I observed no change in misincorporated CID levels (Figure 3.5). However, further tests might be necessary to definitely rule out this result. One possible explanation could be that CAF-1 might have a redundant role in CID misincorporation mechanism. Upon loss of CAF-1, other ectopic loading complex for CENP-A, for instance DAXX (Lacoste et al., 2014), could take over. Since ectopically located CENP-A needs a very tight regulation (Müller and Almouzni,

2017), it is highly plausible that CENP-A mislocalization is governed by several alternative mechanisms and depletion of one pathway may not be sufficient for a robust phenotype. Moreover, several E3 ligases handle proteolysis of misincorporated CENP-A (Cheng et al., 2017), further speculating that multiple factors might also be acting on loading. To sum up, the results in this study indicated that CAF-1 does not appear to play an essential role in CID localization.

4.4 Hyd E3 ligase is a novel candidate CID interacting partner

In order to find novel CID interacting partner that may be involved in regulatory mechanisms, I performed MS-based approaches. The first MS-based approach Δ NCID-GFP co-IP did not work efficiently (Figure 3.6). Δ NCID-GFP could not be enriched in Δ NCID-GFP/RbAp48-V5 co-overexpressing cells as much as in Δ NCID-GFP overexpressing cells (Figure 3.6a). Unstable Δ NCID protein was reported to be protected from proteolysis by mediating nuclear import and chromatin loading upon RbAp48 induction (Spiller-Becker, unpublished). Thus, it is expected to observe an increase in cellular Δ NCID levels upon RbAp48 induction rather than a decrease as I observed. The reason for not observing enriched interacting partners for Δ NCID-GFP upon RbAp48 induction (Figure 3.6c, Table 8.1) could be inefficient solubility of the chromatin and poor access to the chromatin-associated complexes. On the other hand, associated centromeric proteins and histone modification enzymes from Δ NCID vs Δ NCID/RbAp48 comparison indicate that Δ NCID still retains interaction with some of the interacting partners of full-length CID. Moreover, this also suggests that N-tail of CID is important for potentiating most of the protein interactions of CID to localize at centromere (Spiller-Becker, unpublished) and perform its biological function (Jing, Xi, Leng, Chen, Wang, Jia, et al., 2017). The detection of proteins associated with proteolysis and catabolic pathways, including hyd E3 ligase, from Δ NCID vs Δ NCID/RbAp48 comparison (Figure 3.6c-d) further points out the unstable nature of Δ NCID. Hyd E3 ligase was also detected among top hits of CID-interacting partners by others (Barth et al., 2014). Several E3s were also found to regulate degradation of budding yeast mislocalized CENP-A (Cheng et al., 2017). In *Drosophila*, SCF^{Ppa} is known to target ectopically-loaded CID to proteasomal degradation (Moreno-Moreno et al., 2011). Thus, hyd E3 ligase might also be involved in an alternative pathway for clearance of CID, as found in yeast. To conclude, hyd E3 ligase is an interesting candidate for regulation of CID.

4.5 NuRD complex is an interesting candidate for regulation of CID loading

Since Δ NCID IP-MS was not very efficient, I performed Xlink-IP-MS to detect weak and transient CID interacting partners (Figure 3.7). Observing a smear instead of a single band with CID (Figure 3.7b) might be due to the complexity of CID interaction network. Histone variant CID throughout its journey from cytosol to chromatin associates with a lot of regulatory factors and complexes (Barth et al., 2014). The number of detected background proteins and peptides interacting with 'GFP-only' control was also very high (Figure 3.8a), consistent with the high rate detection of non-specific interaction partners in Xlink-IP-MS. Fortunately, the enrichment of peptide and protein counts for each sample compared to control was sufficient to distinguish real interacting partners from non-specific ones. In

order to eliminate non-specific interacting partners stringently, high threshold filtering strategy was performed in collaboration with Dr. Bernd Hessling. GO term analysis of filtered peptides performed by Dr. Bernd Hessling indicated that B3 (A) mutant mostly associates with cytosolic proteins, while B3 (A) binds to chromatin-bound factors upon RbAp48 co-overexpression (Table 8.3). This goes coherently with the finding that arginine and lysine-rich domains at the N-terminus of CENP-A is required for nuclear and centromeric localization (Jing, Xi, Leng, Chen, Wang, Jia, et al., 2017). Furthermore, it also fits with the observation that B3 (A) is cytosolic upon overexpressed alone, whereas its nuclear import and chromatin association upon co-overexpression of RbAp48 (Spiller-Becker, unpublished). This result further shows that CID-B3 motif and RbAp48 play critical roles in CID nuclear import and loading, as suggested before (Boltengagen et al., 2015; Jing, Xi, Leng, Chen, Wang, Jia, et al., 2017). RbAp48 is thought to enhance protein interactions and facilitate assembly of chromatin regulatory complexes (Lai & Wade, 2011; Torchy et al., 2015). It is also required in high quantity for the assembly of NuRD complex for instance (Smits et al., 2013). Hence, RbAp48 is probably improving and stabilizing the interactions between CID and chromatin assembly complexes, thereby leading to B3 (A) assembly into the chromatin.

CID has more chromatin-associated GO terms compared to B3 (A) even upon co-overexpression of RbAp48 with B3 (A) (Table 8.3). This further indicates that B3 (A) is actually missing many of interacting partners of full length CID, in turn potentially leading to its improper non-centromeric localization (Spiller-Becker, unpublished). After stringent filtering, not many CID loading or RbAp48-containing complexes were detected to be statistically enriched in B3 (A)/RbAp48 vs B3 (A) comparison (Table 8.4). However, the enrichment for those complexes was detectable upon comparison of peptide counts (Figure 3.9b). CID vs B3 (A) comparison, however, demonstrated much clearer statistical difference in terms of interactome (Table 8.4), better suiting our filtering method. The fact that we detected known interacting partner homologues of mislocalized CID by this comparison, such as DAXX (Lacoste et al., 2014) and FACT (Hildebrand & Biggins, 2016) (Figure 3.9b), indicates that our filtering approach is reliable for also identifying novel interacting partners of ectopic CID. Applying this strategy, core components of NuRD complex were detected (Figure 3.9, Table 8.4). NuRD complex is not only interesting because it contains RbAp48 but also because it has been previously identified as CID interacting partner in several other independent overexpressed CID pulldown studies. First of all, I observed a peptide count enrichment of the subunits in a separate Δ NCID co-IP experiment (Figure 3.6, Table 8.1). Secondly, NuRD was also detected in an analysis of CID interacting partners by others (Barth et al., 2014). Thirdly, it was also encountered in another mass pulldown study from our group (Sharma, unpublished). Of note, MEP-1 component of dMec complex, which is the most abundant type of NuRD complex in *Drosophila* (Kunert & Brehm, 2009), was also enriched (Figure 3.9b, Table 8.4). The pathways in which dMec complex is involved are not entirely clear yet (Kunert & Brehm, 2009). As the biological roles of dMec complex are further revealed, this might also give future insights into the research on CENP-A misincorporation in *Drosophila* and other species. Collectively, based on our Xlink-IP-MS results, NuRD complex was selected as a candidate complex that might regulate CID mislocalization.

4.6 CID interacts with NuRD core subunits

Mass Spec as a high throughput technique requires confirmation by other techniques as well. The physical interactions detected by Mass Spec were also confirmed by co-IP (Figure 3.10). In accordance with Mass Spec results, the interaction of NuRD components with CID is stronger than with the B3 (A) mutant (Figure 3.10). This might be due to deficient nuclear localization of B3 (A) mutant (Spiller-Becker, unpublished). The N-terminal tail of CID has been shown to possess several functional posttranslational modifications (Müller & Almouzni, 2017a). The weaker physical interactions with B3 (A) mutant compared to CID is also likely due to the loss of some posttranslational modifications upon conversion of triple arginines to alanines (Spiller-Becker, unpublished). It appears that strong RbAp48 interaction is required to compensate for B3 (A) insertion into chromatin, arguing that RbAp48 might mediate the physical contacts between CID and NuRD complex. This is again in accord with the role of RbAp48 in the multi-subunit complexes to facilitate and enhance physical interactions between the subunits (Lai & Wade, 2011; Torchy et al., 2015). Unexpectedly, I did not see much difference of B3 (A) interaction with NuRD subunits in the presence and absence of RbAp48 overexpression (Figure 3.10) although there was a detectable increase in peptide counts according to MS results upon RbAp48 induction (Figure 3.9b). This might be because the enrichment of a few peptides is not easily detectable by co-IP, as MS did. Alternatively, the stoichiometric increase in RbAp48 might be sufficient to enable physical interaction rather than increase in other components. Furthermore, CID was also detected to co-localize with Mi-2 helicase catalytic subunit (Figure 3.11). The indication that not only overexpressed CID but also transiently expressed CID co-localizes eliminates the possibility of random co-localization. The quantification of signal peaks also overlaps (Figure 3.11b). This result suggests that Mi-2 catalytic function might be required for CID ectopic localization, which needs to be tested. Moreover, the co-localization occurs site-specifically rather than ubiquitously (Figure 3.11a). This is also consistent with the observation that *de novo* CENP-A deposition requires a certain chromatin environment (Athwal et al., 2015; Olszak et al., 2011). The feature of those Mi-2 and CID co-recruiting foci should be further investigated by chromatin immunoprecipitation (ChIP) experiments. Interestingly, few CID foci under transient expression were observed to co-localize with Mi-2 (Figure 3.11b). This implies that Mi-2 might play a role in loading of centromeric CID as well.

4.7 Targeting of NuRD catalytic and scaffold components abrogates CID mislocalization and stability

CID is stabilized by its dedicated chaperone CAL1 (Erhardt et al 2008; Chen *et al.*, 2014) through Cul3/RDX-dependent mono-ubiquitination (Bade et al., 2014b). When CAL1 is depleted, CID is degraded by proteolysis (Chen et al., 2014). I observed a prominent reduction on both unmodified and mono-ubiquitinated CID levels upon Mi-2 depletion (Figure 3.12). Thus, this result showed that Mi-2 might play a role in stability and loading of CID. Preliminary results by semi-qRT-PCR further showed that this decrease is probably not due to change in CID transcription, but this should be analyzed by qPCR in the near future. Since Mi-2 helicase is the catalytic subunit of NuRD complex (Lai & Wade, 2011), this could further suggest that catalytic function of NuRD complex might be required for stability of

ectopically expressed CID. Targeting the other catalytic component of NuRD complex, the Rpd3 histone deacetylase, also resulted in similar reduction of CID protein and nuclear signal (Figure 3.13). By qualitative analysis, preliminary assay also indicated that transcription is not drastically influenced by TSA treatment (Figure 3.13a). However, it should be carefully analyzed by qPCR and further replicate experiments. Since TSA is a globally-influencing epigenetic drug (Bartsch et al., 1996), the potential off-target effects in this approach should also be taken into account. Rpd3 is also involved in other complexes as well (Torchy et al., 2015). Hence, a more specific approach, such as site-directed mutagenesis of NuRD-binding domains, is needed to target Rpd3 of the NuRD complex. Another interesting point to mention is that chromatin is supposed to decondense upon HDAC inhibition due to increase in acetylated histones (Bartsch et al., 1996). Thus, it is also possible that CID intensity quantification by IF might be affected because of decompaction. Furthermore, upon HDAC inhibition, CID ectopic localization was reduced in Mis18 α depleted cells (Fujita et al., 2007), while loading at alphoid array increased (Nakano et al., 2003). This further suggests that histone deacetylation might be required for CENP-A mislocalization. Acetylation plays essential roles for CENP-A targeting at centromeres (Shang et al., 2016b) and marking the centromere for CENP-A deposition (Bergmann et al., 2012). It is interesting to elucidate the role of deacetylation in CENP-A loading and mistargeting.

CID ectopic incorporation decreased upon silencing Mi-2 and MTA1-like components of NuRD complex (Figure 3.14). This further validates the reduced CID protein levels upon Mi-2 depletion (Figure 3.12). Observing similar phenotypes for an additional subunit of NuRD complex further emphasizes the consistent role of NuRD in CID misincorporation. Indeed, MTA1-like is the essential scaffold component for the assembly of NuRD complex (Alqarni et al., 2014). Therefore, the reduced CID mislocalization upon MTA1-like depletion illustrates the critical importance of NuRD complex in this mechanism. NuRD complex is also essential for genomic integrity and chromosome structure (Clapier & Cairns, 2009). One should exclude the possibility that the observed phenotype upon loss of NuRD components is not due to genome rearrangements. In order to address this issue and further investigate the involvement of NuRD complex in CID ectopic loading, I used an RbAp48 mutant (kind gift of Prof. Ernest Laue and Dr. Wei Zhang). This mutant cannot bind NuRD due to five point mutations at critical residues of MTA1-like binding pocket (Alqarni et al., 2014). However, except for NuRD binding, impairment in any other biological role of this protein have not been detected (Alqarni et al., 2014). The side-effects of this mutant still should be taken into account and further characterized. Thus, I also checked its binding partners, and confirmed the loss of interaction with MTA1-like (Figure 3.15). In addition, I detected the interaction with p180 and CID (Figure 3.15), which are RbAp48 interacting partners in other biological pathways (Boltengagen et al., 2015; Tyler et al., 2001). Notably, there is a reduced interaction of endogenous CID with RbAp48 mutant, while B3(A) interaction was comparable (Figure 3.15). Intriguingly, I found that B3 (A) mislocalization was lost upon induction of RbAp48-mutant (Figure 3.16), further emphasizing the requirement of NuRD complex in CID incorporation to ectopic sites.

4.8 RbAp48-MTA1-like binding pocket is required for CID nuclear localization

Nuclear incorporation of overexpressed CID was deficient in half of the cells upon MTA1-like depletion (Figure 3.17). This suggests that MTA1-like might mediate a critical role in nuclear translocation of CID. The reason for observing only 50 % reduction might be due to involvement of other complexes in CID nuclear assembly. Prenucleosomal CENP-A assembly complex, containing HJURP, RbAp48, H4 and Hat1 (Boltengagen et al., 2015; Dunleavy et al., 2009; Foltz et al., 2009; Shang et al., 2016b), and licensing complex, comprised of Mis18 components (Y. Fujita et al., 2007; Hayashi et al., 2004), are associated with CENP-A nuclear import. Thus, it is likely that excess amount of CENP-A is taken over by those complexes to be incorporated into the nucleus. Strikingly, MTA1-like might have a major contribution to this process while Mi-2 does not appear to be involved in nuclear import of CID (Figure 3.17). It could be speculated that Mi-2 might be involved in CID deposition into the chromatin, while MTA1-like might be involved in nuclear transport. Nuclear and chromatin fractionation upon Mi-2 and MTA1-like depletion should be tested by WB to further confirm this observation. I also found that overexpression of RbAp48 mutant incapable of NuRD-binding abrogates CID nuclear localization (Figure 3.18). This result also correlates with the reduced CID ectopic incorporation in mitotic spreads upon induction of this particular mutant (Figure 3.16). Altogether, these results clearly suggest that NuRD binding and assembly are required for nuclear transport and incorporation of ectopically expressed CID.

4.9 Hyd is involved in the regulation of CID synthesis and incorporation

Since misincorporation of CENP-A occurs in many species, a regulated clearance from ectopic sites is equally important. Thus, I investigated the potential hyd-dependent degradation of CID. Hyd E3 ligase interaction with CID was determined two times in Δ NCID co-IP-MS (Figure 3.6) and Xlink-IP-MS (Table 8.4) in this study and also by others (Barth et al., 2014). The physical and genetic interaction was further confirmed by other means (Figure 3.19): using the rough eye phenotype as a genetic read out, I showed that there is a suppressive interaction between CID and *hyd*¹⁵ mutant (Figure 3.19a). Even though the genetic interaction is very clear by a standard rough eye method in *Drosophila*, it is not entirely clear why it has an antagonistic nature. Possibly, more of the overexpressed CID is mono- but not poly-ubiquitinated and incorporated into centromeres therefore partially rescuing the phenotype. Further characterization of those flies and *hyd*¹⁵ mutant might be helpful to shed light on this complex phenotype. For instance, it could be investigated by measuring CID centromeric levels of eye discs from larvae. The involvement of hyd in developmental pathways (Flack et al., 2017; Mansfield et al., 1994) might also explain this phenotypic consequence. Interestingly, the rescue was stronger in the female flies, showing that there is also gender-bias. On the other hand, hyd depletion leads to a similar rough eye phenotype as CID overexpression (Figure 3.19d). This suggests that hyd and CID might be involved in the same pathway. Here, it could be speculated that hyd knockdown leads to higher CID levels, thereby bringing about segregation defects and rough eye (Jäger et al., 2005). However, this should then not lead to a rescue phenotype when CID is overexpressed in a HYD depleted background. More relevant perhaps, mitotic defects were reported upon

CID overexpression (Heun et al., 2006) and hyd knockdown (Barth et al., 2014) in S2 cells. Thus, I tested the hypothesis that CID is upregulated upon hyd depletion. I found enrichment for both endogenous and ectopically expressed CID levels upon hyd knockdown (Figure 3.22). Intriguingly, the increase in cellular levels of unstable Δ NCID and B3 (A) constructs upon hyd depletion (Figure 3.21) further suggests that those CID mutants might be targeted by hyd E3 ligase for proteasomal degradation. It is important to note that the increase in CID levels upon hyd RNAi was detected for endogenous CID and several types of exogenous CID constructs. Thus, this outcome is consistent for different experimental systems. In accord with this, hyd overexpression also leads to poly-ubiquitination and destabilization of both endogenous and overexpressed CID (Figure 3.20). One should however take into account that this result might be influenced by indirect pleiotropic effects of hyd due to alteration of multiple biological processes (Shearer et al., 2015). It is also important to rule out the possibility that overexpressed hyd might non-specifically target CID for poly-ubiquitination. Moreover, the upregulation of centromeric CID upon hyd knockdown was also observed in mitotic chromosomes (Figure 3.23). This result first suggests that hyd not only controls cytosolic or nuclear CID but also centromeric CID. Secondly, hyd regulates CID not only in interphase but also in mitosis. This further argues that hyd may globally modulate CID levels irrespective of cellular location and time. Despite the upregulated CID levels upon hyd depletion, I never detected CID mislocalization. This might be because upregulated CID levels do not reach a certain threshold to create neocentromeres (Bodor et al., 2014), ectopic CID is eliminated by another E3 ligase, such as SCF^{Ppa} (Moreno-Moreno et al., 2011), or chromatin environment does not support misincorporation as much as heterochromatin boundaries or transcription factor hotspots do (Athwal et al., 2015; Olszak et al., 2011). Incoherently, incorporation of *de novo* synthesized CID goes down upon hyd silencing (Figure 3.24). The interpretation from this result could be that hyd might be required for *de novo* CID deposition. This might occur if hyd has another regulatory action on CID. Alternatively, this unexpected result could be due to saturation of centromeres with the old CID upon hyd depletion. Pleiotropic effects of hyd (Shearer et al., 2015) should also be considered.

4.10 Potentially non-conserved CAF-1-mediated CID misincorporation mechanism in *Drosophila*

Canonical loading complexes for CENP-A are variable between species (Foltz et al., 2009). For instance, HJURP/Scm3 homologues are not found in many higher eukaryotes, including insects, nematodes, plants and fish (Chen et al., 2014). In particular, *Drosophila* CAL1 is also different in terms of homology from HJURP/Scm3 family (Chen et al., 2014). Although it was recently proposed that CAF-1 might be an evolutionarily conserved complex for CENP-A ectopic loading (Hewawasam et al., 2018), CAF-1 was not detectable in prenucleosomal CENP-A assembly complexes in human (Dunleavy et al., 2009; Foltz et al., 2009) and in *Drosophila* (Boltengagen et al., 2015), except for its RbAp48 subunit (Boltengagen et al., 2015; Furuyama et al., 2006). In a recent report, apart from RbAp48, CAF-1 p180 and p105 were also not detected among CID interacting partners in *Drosophila* (Barth et al., 2014). Here, I also did not find any interaction of overexpressed CID with p180 and p105. Consistent with other reports, I reproducibly detected CID and RbAp48 interaction. Nevertheless, a possible context-dependent and transient interaction between CID and CAF-1 complex through RbAp48 should be taken into account. Moreover, I also did not find any

evidence in support of the hypothesis that CAF-1 is involved in CENP-A misincorporation in *Drosophila*. However, further tests might help to absolutely rule out this hypothesis. Taken together, in consistence with several other reports, this study further concludes that CAF-1 is most likely not involved in CID ectopic incorporation in *Drosophila*.

4.11 The potential role of remodeling and deacetylation in CENP-A mislocalization by the NuRD complex

In this study, I identified a novel role of dual catalytic NuRD complex in CENP-A misincorporation in *Drosophila*. Remodeling activity appears to be required in this mechanism. Chromatin remodelers have long been known to play a role in loading of histone variants. SRCAP and p400 remodelers, for instance, function in H2A.Z incorporation in mammals (Bönisch et al., 2012). Another remodeler ATRX is involved in recruitment of macroH2A (Ratnakumar et al., 2012). ATRX remodeler, together with DAXX, is also responsible for loading of H3.3 (Nye et al., 2018). Chromatin remodelers are also associated with exchange of histone variants. The yeast remodeler Ino80 was shown to play a crucial role in eviction of H2A.Z (Hildebrand & Biggins, 2016). INO80 family of remodelers also enable the exchange between H2A variants H2A.X and H2A.Z at DNA damage sites (Krogan et al., 2003; Mizuguchi et al., 2004; Tsukuda et al., 2005; Van Attikum et al., 2007). Chromatin remodeling has recently been discovered to be required for licensing of *de novo* CENP-A deposition (Okada et al., 2009). Ino80 is required for replacement of H3 with CENP-A at centromeres and play redundant roles with Chd1 in ectopic centromere origination in budding yeast (Choi, Cheon, Kang, & Lee, 2017b). DAXX/ATRX chaperone and remodeling complex incorporates atypical CENP-A/H3.3 heterodimers at ectopic regions in humans (Arimura et al., 2014; Lacoste et al., 2014). Moreover, in yeast, Ino80-mediated exchange of H2A.Z with CENP-A at histone turnover sites results in neocentromere formation (Hildebrand & Biggins, 2016; Ogiyama et al., 2013). Thus, coherent with previous knowledge from other remodeling complexes, NuRD-dependent remodeling activity might be involved in CID loading. Here, I presented the evidence that Mi-2 catalytic component of NuRD complex plays an essential role for CENP-A ectopic loading in *Drosophila*. It is necessary to further characterize this catalytic function in CENP-A loading in future studies. The potential conservation of this mechanism needs to be revealed in other species as well, including human.

I also observed some traces of evidence about the potential role of histone deacetylation in CID misincorporation. Histone deacetylation is generally known to be involved in transcriptional repression (Allis & Jenuwein, 2016). Deacetylation activity of NuRD complex is also associated with transcriptional inhibition at specific foci, such as promoters of tumor suppressor genes (Denslow & Wade, 2007; Lai & Wade, 2011). Chromatin regions nearby closed heterochromatin are known to be favorable for neocentromeres (Olszak et al., 2011). Thus, we can hypothesize that NuRD-mediated histone deacetylation creates repressive chromatin regions, in turn facilitating *de novo* CENP-A incorporation. Consistently, HDAC inhibition reduces CENP-A mislocalization upon Mis18 α depletion (Fujita et al., 2007). By contrast, HDAC inhibition leads to enrichment of CENP-A at an ectopic alphoid array (Nakano et al., 2003). On the other hand, acetylation (Bergmann et al., 2012) is known to be required for licensing of *de novo* CENP-A deposition (Fujita et al., 2007; Furuyama et al., 2006; Hayashi et al., 2004) and FACT-dependent remodeling and transcription at

centromeres (Chen et al., 2015). Furthermore, Hat1-dependent acetylation is essential for nuclear transport (Boltengagen et al., 2015) and centromeric targeting of CENP-A (Shang et al., 2016b). Intriguingly, in the absence of Hat1-mediated acetylation, CENP-A is targeted to ectopic sites due to lack of HJURP binding (Shang et al., 2016b). This finding indirectly implies that histone deacetylation might be required to bypass HJURP interaction, targeting CENP-A to ectopic sites. A recent study further reported that CENP-A K124Ac is required for loading of centromeric CENP-A, but it is susceptible for nucleosome sliding if it is not converted to methylation (Bui et al., 2017). Based on this study, it could also be inferred that acetylated CENP-A nucleosomes might need deacetylation to be stabilized at centromeres, or else they might be recognized by histone remodelers and evicted. Those potential hypotheses require further investigation to elucidate the relation between deacetylation and CENP-A ectopic localization.

4.12 The critical role of RbAp48-MTA1-like binding interface in nuclear localization of overexpressed CID

Another interesting outcome of this study was that RbAp48-MTA1-like binding plays a critical role in CID nuclear transport. B3(A) is unable to accumulate in the nucleus due to the mutation of its NLS (Spiller-Becker, unpublished), and most likely due to the mutation of its arginine-rich residues at N-tail (Jing, Xi, Leng, Chen, Wang, Jia, et al., 2017). Another explanation could be that B3 (A) mutant loses the interaction with the prenucleosomal assembly complex, including H4/RbAp48/Hat1/CAL1 (Boltengagen et al., 2015). Thus, the nuclear localization defect of B3 (A) is rescued by the overexpression of RbAp48, CAL1, CID, H3 or H4 components of this complex (Spiller-Becker, unpublished). Apart from MTA1-like binding interface, RbAp48 mutant lacks the H4 binding as well (Alqarni et al., 2014). Therefore, the interaction with prenucleosomal assembly complex might be lost, which should be further checked. This might partially contribute to the nuclear localization deficiency of B3 (A) upon RbAp48-mutant overexpression. However, I also observed that full length CID also had a deficiency in nuclear transport upon MTA1 depletion (Figure 3.17). Interestingly, this was influencing about 50 % of cells, suggesting that overexpressed CID nuclear translocation is partially regulated by MTA1. This result further suggests that overexpressed CID nuclear transport is in part also regulated by other mechanisms. This alternative mechanism regulating other half of the overexpressed CID is most likely H4/RbAp48/Hat1 complex. Due to the saturation of the endogenous CID nuclear import pathway through H4/RbAp48/Hat1 complex, overexpressed CENP-A could require MTA1-like dependent pathway. Here, we can speculate that overexpressed CID nuclear transport in *Drosophila* might be handled by these two alternative mechanisms.

4.13 The control of CID levels and loading by hyd E3 ligase

The evidences suggested that hyd might target both endogenous and ectopically expressed CID for proteasomal degradation. In yeast, it has been shown that there are several alternative E3 ligases that ubiquitinate mislocalized CENP-A (Cheng et al., 2017). Thus, it is hypothesized that multiple degradation systems could also co-exist in *Drosophila* in addition to SCF^{Ppa} (Moreno-Moreno et al., 2011). However, even though overexpressed CID is destabilized upon hyd overexpression (Figure 3.20), this is also not sufficient to show the regulation of mislocalized CID by hyd. Particularly, there was no ectopic CID localization

upon hyd depletion, as observed upon Psh1 depletion in yeast (Hildebrand & Biggins, 2016). It is possible that ectopically incorporated CID might be cleared by another mechanism, such as by SCF^{Ppa} dependent proteolysis (Moreno-Moreno et al., 2011), efficiently. Therefore, it is necessary to understand if mislocalized CID is targeted by hyd E3 ligase in future studies. Moreover, it is also essential to exclude the possibility that indirect effects of hyd might lead to alteration of CENP-A proteolysis behavior. For this purpose, the catalytic ubiquitin ligase activity of hyd should specifically be targeted by site-directed mutagenesis. In addition, those multiple pathways that hyd is involved in, such as cell cycle, arrest, apoptosis, transcription, mRNA processing (Shearer et al., 2015), should also be addressed to exclude potential side-effects on CID regulation. Another possibility to exclude is whether hyd crosstalks or indirectly activates another degradation mechanism, such as Cul3/RDX. This study further illustrated the evidence that hyd regulates centromeric CID levels. Thus, it could present an additional surveillance mechanism to tightly regulate the threshold levels of centromeric and ectopic CID (Bodor et al., 2014). Interestingly, it was unclear why loading of newly synthesized CID was low upon hyd knockdown (Figure 3.24). One possible explanation could be that there might be a negative feedback loop to downregulate the expression and loading of newly synthesized CID because of saturation of centromeres with old CID. It could also be due to the indirect effects, such as cell cycle regulation. Collectively, hyd-mediated proteolysis of CID is a potential control mechanism possibly involved in centromere and neocentromere regulation.

4.14 Potential working model for NuRD-mediated CENP-A mislocalization in *Drosophila* and Summary

A model how NuRD complex mediates ectopic CID localization is summarized in the Figure 4.1. First, CID/H4 nucleosomes, expressed in excessive quantities and outside its normal timing, are deacetylated by Rpd3 or other HDACs and loses the contact with the prenucleosomal CID assembly complex and dedicated chaperone CAL1. Second, NuRD complex associates with CID/H4 dimer using the RbAp48-MTA1-like binding interface. MTA1-like most likely participates into the complex in the cytosol and is involved in nuclear translocation. Other NuRD subunits are possibly associating within the nucleus. Third, depending on the binding modules, NuRD might be targeted to a chromatin region favoring CENP-A misincorporation. For instance, the complex might be targeted to an active histone turnover region through transcription factor binding modules or p66. Alternatively, it could be targeted to a hypermethylated closed chromatin through MBD2/3. Fourth, Mi-2 enables chromatin remodeling-mediated nucleosome sliding and histone exchange, positioning CID/H4 nucleosomes at the locus. Fifth, Rpd3-mediated deacetylation leads to a closed chromatin region, inhibiting the eviction of CENP-A and stabilizing the ectopic CENP-A nucleosome.

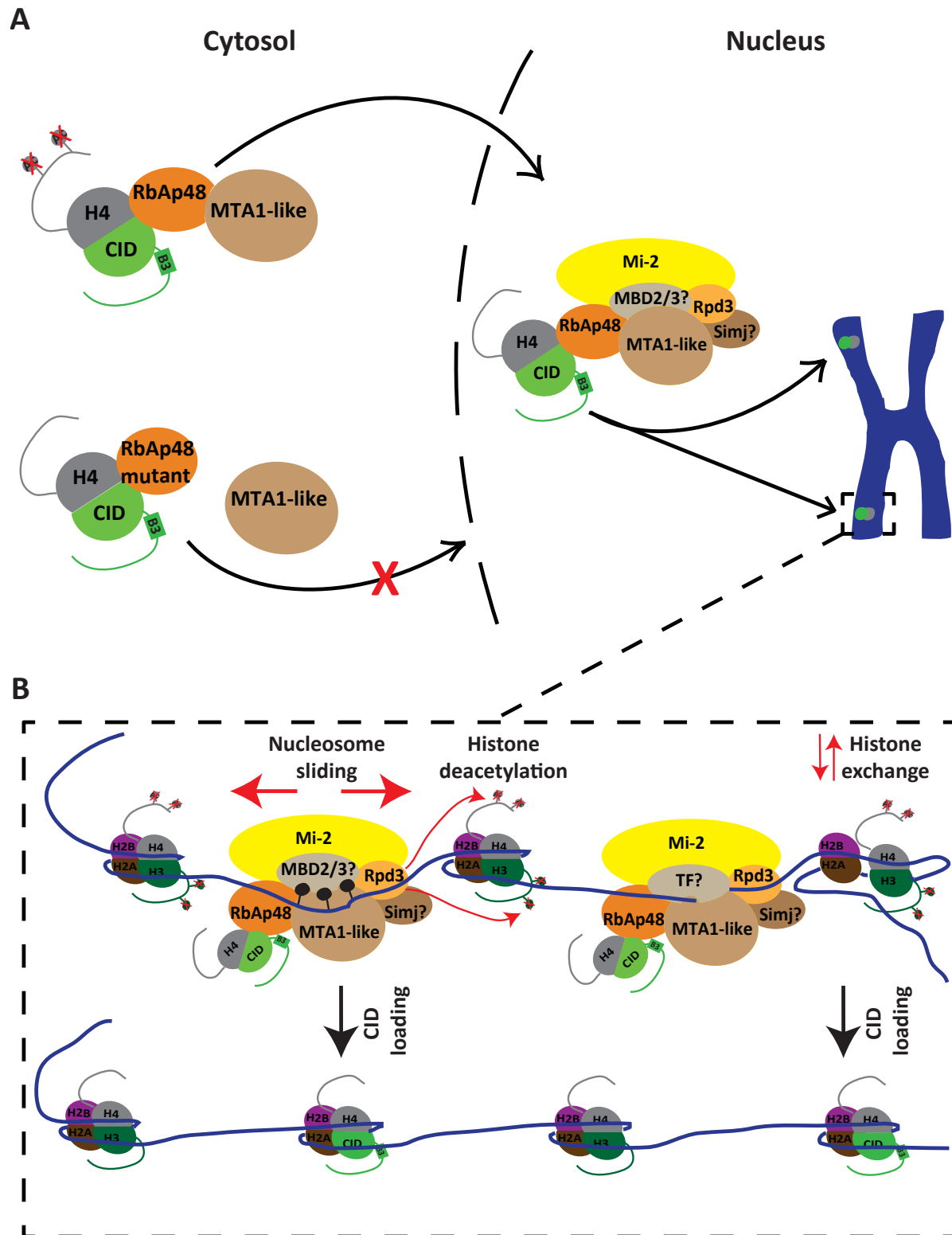


Figure 4.1 Potential working modal for NuRD complex-mediated misincorporation of overexpressed CID

A The excessively synthesized CID or B3 (A) mutant interacts with RbAp48 and MTA1-like. Hat1 and CAL1 may not be involved in this complex, resulting in loss of H4K5Ac and H4K12Ac. The physical contact of CID with RbAp48/MTA1-like interaction surface is essential for nuclear transport and association with NuRD components. Upon mutation of RbAp48/MTA1-like contact site or depletion of MTA1-like, CID or B3 (A) cannot localize in the nucleus. Once translocated into the nucleus,

CID/H4/RbAp48/MTA1-like complex is most likely accompanied by core components and different functional modules of NuRD complex. Taking advantage of NuRD targeting modules, CID might be mislocalized at ectopic sites. **B** Hypothetically, NuRD might be using MBD2/3 and transcription factor binding modules to mislocalize CID. MBD2/3 recruits NuRD complex at hypermethylated regions. Transcription factors target NuRD complex at promoters or transcription factor hotspots. Then, CID is probably deposited into the chromatin by nucleosome sliding and histone exchange activities of Mi-2. Rpd3 might deacetylate N-tails of surrounding H3/H4 and enable chromatin compaction, stabilizing the misincorporated CID at the new location. TF: transcription factor, black balls: DNA methylation

In summary, here I found that the NuRD complex and hyd E3 ligase are essential players in CENP-A regulation in *Drosophila*. Core components of NuRD complex physically interact with overexpressed CID. NuRD complex is involved in nuclear transport of ectopically expressed CID through RbAp48 and the MTA1-like contact surface. The Mi-2 helicase is required for stability of overexpressed CID levels and misincorporation. Rpd3-dependent deacetylation might potentially be involved in stabilization of mislocalized CID. Moreover, I detected a physical and genetic interaction between overexpressed CID and hyd E3 ligase. CID is poly-ubiquitinated and destabilized upon hyd overexpression. Total and centromeric CID levels increase upon hyd depletion. Endogenous and overexpressed CID levels decrease upon hyd induction. Altogether, this study sets the ground work for our understanding of the roles of NuRD complex and hyd E3 ligase in CENP-A misincorporation and stability in *Drosophila*.

5 CONCLUSIONS

This study elucidated novel regulatory mechanisms for CENP-A levels, loading and mislocalization in *Drosophila*. First of all, the essential roles of RbAp48 to escort and deliver overexpressed CID were mechanistically characterized. RbAp48 was shown to mediate the physical interaction of overexpressed CID with MTA1-like. RbAp48/MTA1-like binding was found to be essential for nuclear localization of overexpressed CID. When this binding pocket was distorted, nuclear import was impaired. In addition, nuclear localization was defective upon MTA1-like knockdown. In addition, NuRD complex core components, including Mi-2, MTA1-like and Rpd3 were detected to physically interact with overexpressed CID. Most importantly, I discovered that NuRD complex catalytic function and assembly are required for CID ectopic incorporation. I found that NuRD mislocalization was reduced upon depletion of Mi-2 catalytic component and MTA1-like scaffold component of NuRD complex. Furthermore, protein levels of overexpressed CID were downregulated upon Mi-2 depletion. These results underlined the essential involvement of NuRD complex in stability and misincorporation of overexpressed CID.

This study further shed light on CAF-1's role in CENP-A ectopic loading in *Drosophila*. Despite consistent interaction with RbAp48, no physical interaction of overexpressed CID with p180 and p105 subunits of CAF-1 was detectable nor did ectopically expressed CID protein levels change upon knockdown of CAF-1 subunits. The results obtained here lead to the conclusion that CAF-1 is most likely not essential for CID mislocalization even though some additional tests will be required for a definite answer.

Finally, this work also identified hyd E3 ligase as a major regulator of CENP-A expression, stability and loading in *Drosophila*. Here, I showed that CID physically and genetically interacts with hyd. Strikingly, CID is poly-ubiquitinated and destabilized under elevated hyd levels. On the other hand, total cellular and centromeric CID protein levels increased upon hyd knockdown. These evidences collectively suggest that CID is poly-ubiquitinated and degraded by hyd E3 ligase, thereby regulating physiological CID levels.

To conclude, in this study, I found novel mechanisms to control detrimental mislocalization of misregulated CENP-A. NuRD complex is a promising target for future research on malignant tumors to tackle with mislocalized overexpressed CENP-A. Moreover, hyd E3 ligase might also be used as a potential therapeutic instrument to fine-tune abnormal CENP-A expression. Future medical studies should also further address catalytic activities and off-target effects.

6 FUTURE PERSPECTIVES

The findings of this study are interesting for future research topics on CENP-A loading, mislocalization, homeostasis, genome integrity and cancer. The NuRD complex functions in chromatin remodeling and histone deacetylation. The involvement of those enzymatic functions in CID misincorporation need to be further characterized. Therefore, the catalytic activities of Mi-2 and Rpd3 subunits should specifically be targeted in order to identify their contributions to CID ectopic loading. For this purpose, catalytic-null mutants of Mi-2 and Rpd3 need to be created, or specific small molecule inhibitors used to inhibit the catalytic function. CID ectopic incorporation is expected to decrease in the presence of catalytic-null mutants or inhibitors. Rescue experiments will complement and validate these experiments. Moreover, the involvement of NuRD complex in *de novo* CENP-A deposition needs to be further investigated. One approach could be LacO/LacI-tethering of Mi-2 at ectopic LacO array to investigate CID mislocalization and neocentromere formation. Alternatively, human artificial chromosomes might be used to assess the CENP-A loading at synthetic alphoid arrays in the presence and absence of Mi-2. This would also shed some light on the function of NuRD complex in CENP-A loading at centromeres. In vitro binding and chromatin remodeling assays are also required to further address NuRD-dependent CID incorporation.

NuRD complex is a highly conserved multi-subunit complex and it will therefore be of interest to investigate NuRD-dependent CENP-A loading in other organisms, including human. The binding modules and composition of NuRD complex are evolutionarily highly conserved. CID mislocalization might take advantage of these various subunits of NuRD complex. For instance, MBD2/3 and transcription factor modules might be essential for targeting CENP-A to a favorable chromatin environment. In order to address these questions, it is essential to determine the exact composition of NuRD-dependent CID mistargeting complex. Interestingly, our Xlink-IP-MS approach indicated that MEP-1 is also a putative CID interacting partner. MEP-1 is the component of an alternative dNuRD complex so called dMec in *Drosophila*. Thus, the potential role of dMec complex in this mechanism should be investigated. The future investigation on NuRD complex will also help to better understand its involvement in CID misincorporation. Remarkably, due to potential contribution to the detrimental CENP-A mislocalization mechanism and genome instability, NuRD complex is a promising oncogenic target.

CAF-1 complex should also be further examined by several approaches to definitely rule out that CAF-1 is involved in CID ectopic incorporation. I, therefore, hesitate to make a final conclusion about the absence of CAF-1-mediated CID loading. First of all, the physical interaction between CID and CAF-1 needs to be further assessed by reciprocal co-IP's. Additional replicates with larger sample size are also required to check mislocalization of overexpressed CID upon CAF-1 depletion. Another necessary experiment is p180-tethering at an ectopic site by LacO/LacI system to analyze *de novo* CID deposition. Moreover, the stability and ectopic loading behavior of endogenous CID might also be tested upon CAL1 knockdown and CAF-1 induction.

Another interesting future research direction will be to identify the molecular details of hyd-dependent regulation of CID. Hyd-mediated degradation should be further proven by standard methods, such as cycloheximide chase or radioactive labeling. Moreover, by

proteasome inhibition with MG132 treatment will show if CID is indeed subject to proteasomal degradation upon hyd overexpression. To address CID ubiquitination by hyd one could be using HA or Flag tagged ubiquitin in combination with CID pulldowns. In order to exclude the ubiquitinated CID-interacting partners, which might be pulled down by native co-IP, denaturing co-IP should be performed. Instead of hyd overexpression, hyd depletion could be considered in order to avoid background ubiquitination by hyd E3 ligase. *In vitro* ubiquitination assay will also help to address this issue. In order to specifically address the catalytic role of hyd in CID ubiquitination, catalytic inactive mutant should be created and tested. Ectopic loading of CID should also be further assessed upon hyd depletion. Future research will help to understand these promising roles of hyd E3 ligase and its homologues in regulating genome stability by establishing homeostatic CID levels.

7 MATERIALS AND METHODS

7.1 Materials

All chemicals used in this study were purchased from Applichem, Baker, Invitrogen/Life technologies, Polysciences, Merck, Roche, Roth and Sigma. For details, see table 7.1.

Table 7.1 Chemicals

Chemicals	Provider
30% Acrylamide solution	Sigma
Agar bacteriology grade	Applichem
Agarose Ultra Pure	Sigma
Ampicillin	Sigma
APS	Applichem
Bromophenolblue	AppliChem
BSA	Applichem
DAPI	AppliChem
Dimethyl Sulfoxide (DMSO)	Baker
ECL	Thermo Fisher
EDTA	Applichem
Ethanol abs.	AppliChem
Ethidium bromide	Applichem
N-Ethylmaleimide	Sigma
Formaldehyde 37%	Baker
Glycerol	Applichem
2-Propanol	AppliChem
Kanamycin	Sigma
KCl	AppliChem
Milk Powder	AppliChem
Mounting medium	Polysciences
β-Mercaptoethanol	AppliChem
Methanol	ZMBH
MgCl ₂	Applichem
NP-40	AppliChem
PFA	Applichem

Phenol/Chloroform	AppliChem
Phenylmethylsulfonylfluoride (PMSF)	Roth
Protease inhibitor cocktail complete EDTA-free	Roche
Sodium dodecyl sulfate	Roth
Sodium chloride	Sigma
Sodium citrate	AppliChem
TEMED	AppliChem
Trichostatin A	Sigma
Trisethanolamine	AppliChem
Tris	Roth
Triton X-100	Merck
Trizol	Invitrogen
Tween 20	AppliChem

Table 7.2 Tissue culture reagents

Reagents	Provider
Cellfectin II	Invitrogen
Colcemid	PAA
Copper Sulfate	Grüssing
Fetal Bovine Serum (FBS)	Biochrom AG
Hygromycin B solution	Invitrogen
MG132	Santa Cruz Biotechnology
Penicillin Streptomycin	Invitrogen
Schneider's <i>Drosophila</i> medium	Invitrogen
TMR-Star	New England Biolabs
TMR Block	New England Biolabs

Table 7.3 Buffers and solutions

Buffer	Ingredients
SDS-PAGE and western blotting	
Separation gel (8.25%)	0.375 M Tris-HCl pH 8.8 8.25% acrylamide/bisacrylamide 30:0.8% 0.1% SDS 0.05% APS 0.05% TEMED in ddH ₂ O
Separation gel (10.5%)	0.375 M Tris-HCl pH 8.8 10.5% acrylamide/bisacrylamide 30:0.8% 0.1% SDS 0.05% APS 0.05% TEMED in ddH ₂ O
Stacking gel	0.123 M Tris-HCl pH 6.8 4.4% acrylamide/bisacrylamide 30:0.8% 0.1% SDS

	0.03% APS 0.1% TEMED in ddH ₂ O
4x Laemmli sample loading buffer	50 mM Tris-HCl pH 6.8 10% glycerol 2% SDS 0.5% β -Mercaptoethanol 0.02% Bromophenolblue in ddH ₂ O
1x SDS gel running buffer	25 mM Tris 190 mM glycine 0.1% SDS in ddH ₂ O
Transfer Buffer	25 mM Tris 192 mM Glycine 0.1 % SDS 20 % Methanol in ddH ₂ O
10x TBS	30 g/l Tris 88 g/l NaCl 2 g/l KCl pH 7.5 in ddH ₂ O
Blocking buffer	1x TBS 0.1% Tween-20 5% Milk powder
Washing buffer	1x TBS 0.1% Tween-20
Ponceau	0.2% Ponceau 3% TCA
Mild stripping buffer	15 g/l glycine 0.1% SDS 1% Tween-20 pH 2.2 in ddH ₂ O
Agarose gel electrophoresis	
50x Tris-acetate-EDTA (TAE)	242 g/l Tris-HCl 18.6 g/l EDTA pH 7.7 adjusted with acetic acid in ddH ₂ O
Yeast two hybrid	
SC-Leu/His-plates	6.7 g yeast nitrogen base without aa (Difco) 2 g drop out mix lacking histidine and leucine dissolved in 400 ml ddH ₂ O, autoclaved 20 g Bacto Agar (Difco) dissolved in 300 ml ddH ₂ O, autoclaved Solutions mixed at 70°C 100 ml of 1M sterilized glucose (20%)

	adjusted to 1l using ddH2O
LiSorb	100 mM lithium acetate (Sigma) 10 mM Tris-HCl pH 8.0 1 mM EDTA (Sigma) 1 M sorbitol (Merck)
LiPEG	100 mM lithium acetate (Sigma) 10 mM Tris-HCl pH 8.0 1 mM EDTA (Sigma) 40% PEG3350 (polyethylene glycol, Sigma) filter sterilized
Solution A	0.5 M NaH ₂ PO ₄ /Na ₂ HPO ₄ pH7.0 0.1% SDS 10 mM KCl (added dropwise) 1 mM MgCl ₂ (added dropwise) heat solution to 40°C
Solution B	400 mg low melting agarose dissolved in 30 ml ddH ₂ O solution used at 50°C
Solution C	40 mg X-Gal dissolved in 1 ml Dimethyl formamide made fresh each time
Immunofluorescence	
Metaphase spreads Hypotonic swelling solution	0.5 % (w/v) Sodium citrate in ddH ₂ O
PBS blocking solution	1x PBS 0.1% Triton X 100 5% Milk powder
PBS permeabilization solution	1x PBS 0.1% Triton X-100
Cell Lysis and co-immunoprecipitation	
RIPA cell lysis buffer for whole cell extracts	50 mM Tris-HCl (pH7.5) 150 mM NaCl 1% NP-40 0.5% Sodium dodecylsulfate 0.1% SDS 2 mM PMSF
GFP-binder co-IP lysis buffer	20 mM Tris-HCl (pH 7.5) 1 M NaCl 1% NP-40 1 mM PMSF 1µg/ml Aprotinin/leupeptin 0.5 µg/ml Pepstatin 1 x Roche complete protease inhibitor cocktail
GFP-binder co-IP IP buffer/wash buffer	20 mM Tris-HCl (pH 7.5) 250 mM NaCl 1% NP-40 2 mM PMSF 1µg/ml Aprotinin/leupeptin

	0.5 µg/ml Pepstatin 1 x Roche complete protease inhibitor cocktail
Xlink IP buffer/wash buffer (for GFP-binder)	50 mM Tris-HCl pH 8 150 mM NaCl 1 % NP-40 0.5 % Na-Doc 10 mM NaF 0.1 % SDS 40 mM NEM 1 mM EDTA 1 x Roche complete protease inhibitor cocktail
V5 co-IP IP buffer/wash buffer	50 mM Tris-HCl pH 7.5 150 mM NaCl 1 % Triton X-100 10 mM NaF 2 mM PMSF 20 mM NEM 1µg/ml Aprotinin/leupeptin 0.5 µg/ml Pepstatin
His IP buffer/wash buffer (for His-Trap)	20 mM Sodium phosphate buffer pH 7.5 500 mM NaCl 1 % NP-40 20 mM Imidazole 2 mM PMSF 20 mM NEM 1µg/ml Aprotinin/leupeptin 0.5 µg/ml Pepstatin
His IP elution buffer (for His-Trap)	20 mM Sodium phosphate buffer pH 7.5 500 mM NaCl 1 % NP-40 500 mM Imidazole 2 mM PMSF 20 mM NEM 1µg/ml Aprotinin/leupeptin 0.5 µg/ml Pepstatin

Table 7.4 Equipment and lab materials

Equipment/materials	Provider
Agarose gel trays	Workshop ZMBH
Balance	Sartorius, Kern EG
Bioruptor	NextGen
Blotting materials	BioRad
Coverslips (18 x 18 mm)	Thermo Scientific
Cytospin	Thermo
Deltavision microscope	Olympus/GE Healthcare
Film development system	Dr. Goos Suprema
Fly vials	Gosslein

FUJI Medical X-Ray Film	Fujifilm
Micropipettes	Gilson
Microwave	Sharp
Nanodrop	A260 Nanodrop
Nitrocellulose membrane (0.45 µm)	Amersham Biosciences
PCR-cycler	Biorad
Petri dishes	Greiner Bio-one
Pipette tips	Sarstedt, TipOne
pH-meter	Sartorius, Kern EG
Protein gel equipment	Biorad
Power supplies	Biorad, EMBL PS143
PVDF transfer membrane	GE Healthcare
Superfrost® Plus Slides	Thermo Fisher Scientific
Tabletop centrifuges	Eppendorf
TransBlot Turbo Transfer System	BioRad
Vortex	Scientific industries
Waterbath	Memmert
Whatman Paper	Roth
-80°C freezer	Heraeus
1.5 and 2 ml reaction tubes	Sarstedt
15 and 50 ml tubes	Sarstedt
0.2 ml PCR reaction tubes	Sarstedt
25 cm ² flask (cell culture)	Orange Scientific
75 cm ² flask (cell culture)	Orange Scientific
150 cm ² flask (cell culture)	Orange Scientific

Table 7.5 Primary and secondary antibodies

Antibody	reacts with	Dilution (IF//WB)	Source
Primary antibodies			
CID	rabbit	- // 1/2000	Active Motif
CID	chicken	1/500	P. Heun
CAL1	rabbit	- // 1/2500	AG Erhardt
CENP-C	Guinea pig	1/5000 // -	AG Erhardt
Actin	mouse	- // 1/5000	Millipore
H3	rabbit	- // 1/1000	Abcam
H4-Acetyl	rabbit	- // 1/500	Milliporemerck
alpha tubulin	mouse	1/1000 // 1/5000	Sigma
V5	mouse	1/1000 // 1/5000	Invitrogen
His	rabbit	1/1000 // 1/2000	Abcam
GFP	mouse	1/500 // 1/2500	Roche
GFP	chicken	1/200 // -	Abcam

Lamin	mouse	- // 1/5000	Dev. Stud. Hybrod. bank Iowa
RbAp48	rabbit	- // 1/20000	A. Brehm
HA	rabbit	- // 1/1000	Abcam
Mi-2	rabbit	1/200 // 1/8000	A. Brehm
MTA1-like	Guinea pig	- // 1/2500	A. Brehm
Hyd (EDD-M19)	goat	- // 1/200	SantaCruz
Ubiquitin (FK2)	mouse	- // 1/1000	Millipore
p180	Guinea pig	1/200 // 1/1000	Vermjer Lab
Secondary Antibodies			
Anti-rabbit HRP	rabbit	- // 1/5000	Abcam
Anti-mouse HRP	mouse	- // 1/10000	Abcam
Anti-rat HRP	rat	- // 1/5000	Abcam
Anti-goat HRP	goat	- // 1/5000	Abcam
Anti-guinea pig HRP	Guinea pig	- // 1/2500	Abcam
Alexa Fluor 488 goat IgG	chicken	1/500 // -	Invitrogen
Alexa Fluor 488 goat IgG	mouse	1/500 // -	Invitrogen
Alexa Fluor 488 goat IgG	rabbit	1/500 // -	Invitrogen
Alexa Fluor 546 goat IgG	rabbit	1/500 // -	Invitrogen
Alexa Fluor 546 goat IgG	guinea pig	1/500 // -	Invitrogen
Alexa Fluor 546 goat IgG	mouse	1/500 // -	Invitrogen
Alexa Fluor 647 goat IgG	rabbit	1/500 // -	Invitrogen
Alexa Fluor 647 goat IgG	guinea pig	1/500 // -	Invitrogen
Alexa Fluor 647 goat IgG	mouse	1/500 // -	Invitrogen

Table 7.6 Enzymes

Enzymes	Provider
Restriction enzymes	New England Biolabs
2x Dream <i>Taq</i> Master Mix	Fermentas
<i>Pfu</i> X polymerase	Jena Biosciences
Gibson Assembly Master Mix	New England Biolabs
T4 DNA ligase	New England Biolabs
Q5 DNA Polymerase	New England Biolabs
λ - Phosphatase	New England Biolabs
DNAseI	New England Biolabs
Benzonase	Sigma

Table 7.7 Kits

Kits	Provider
NucleoSpin Gel and PCR Cleanup	Macherey-Nagel
NucleoSpin Plasmid Purification	Macherey-Nagel
NucleoBond PC 100	Macherey-Nagel

dES-TOPO TA Cloning Kit	Invitrogen
MEGAscript® RNAi Kit	Ambion
RevertAid H Minus First Strand cDNA Synthesis Kit	Fermentas
dART RT Kit	Roboklon

Table 7.8 DNA vector constructs used for stable cell lines

Name	Source
pMT-CID-V5-His	AG Erhardt
pMT-CID-EGFP	P. Heun (Heun et al., 2006)
pMT-ΔN-CID-EGFP	AG Erhardt
pMT-CAL1-V5-His	AG Erhardt
pMT-Caf1-V5-His (RbAp48)	AG Erhardt
pmCherryTub	AG Erhardt
pHygro	AG Erhardt
pMM5	AG Erhardt
pMM6	AG Erhardt
pMM5-CAL1	AG Erhardt
pMM6-CAL1	AG Erhardt
pMM5-RDX	AG Erhardt
pMM6-RDX	AG Erhardt
pMM5-CID	AG Erhardt
pMM6-CID	AG Erhardt
pMM5-RbAp48	In this study
pMM6-RbAp48	In this study
pMM5-p180	In this study
pMM6-p180	In this study
pMM5-p180 ¹⁻⁴⁷⁶	In this study
pMM6-p180 ¹⁻⁴⁷⁶	In this study
pMT-CID-B3(A)-GFP	AG Erhardt
pMT-p180-V5-His	In this study
pLAP-empty	AG Erhardt
pMT-GFP-LacI-hygro	P.Heun (Mendiburo et al., 2011)
pMT-RbAp48-GFP-LacI-hygro	In this study
pMT-Flag-HA-hyd-hygro	A.Imhof (Barth et al., 2014)
pMT-RbAp48-MUT-V5-his	E. Laue (Algarni et al., 2014)

Table 7.9 Primers

Name	Sequence
pMT-F	CATCTCAGTGCAACTAAAG
pMT-R	TAGAAGGCACAGTCGAGG
cidqpcr-fw	TCACCGAAGGCGCCCTATTGG

MB154_qPCR_V5-His_R	GATGACCGGTACGCGTAGA
MB47_Act5D_FW	ATGTGTGACGAAGAAGTTGC
MB48_Act5D_RV	AGGATCTTCATCAGGTAGTC
T7-brown-for	taatacgactcactatagggagctctccttcgtgccgt
T7-brown-rev	taatacgactcactatagggatcaatagtaaccactgcggtgaat
CAF1-105_dsRNA_F	CTAATACGACTCACTATAGGGAGGCCCTTTCCCAAGGAATATGC
CAF1-105_dsRNA_R	CTAATACGACTCACTATAGGGAGTTCAGCATCCAACTCGGGTT
For_p180 dsRNA	ctaatacgactcactataggcaggcagaggattccaaacaaa
Rev_p180 dsRNA	ctaatacgactcactataggcagtggtcaggcgagtctccttt
p180-F	atgcacgctggcgttgtaaga
p180-R	atccgagagcatcaccacatcat
p180-Rev-RT	tctccagcggttcctcagat
p180-807-F	catgaaggcgggtcaaggagt
p180-1684-F	gaggtggactccaagaacga
p180-2557-F	catctcagcgacgaggaact
p180-BamHI-Mut-F	TGCGGCAGCGGATCGAACAACACATCCTAC
p180-BamHI-Mut-R	GTAGGATGTGTTGTTTCGATCCGCTGCCGCA
p180-BamHI-F	cgGGATCCgtATGCACGCTGGCGTTGTTAAG
N-p180-XhoI_R	tccgCTCGAGttaCAGACTCTTCCTGTTCAGG
Caf1-55-ORF-BamHI_F	cgGGATCCgtATGGTGGATCGCAGCGATAA
Caf1-55-ORF-XhoI_R	tccgCTCGAGTTAAGCGGTATTGGTTTCTAACTCG
Mi2_T7_F	CTAATACGACTCACTATAGGGAGctagaaaagcccagtgccag
Mi2_T7_R	CTAATACGACTCACTATAGGGAGgctccagcaactaaaacgc
p55-SpeI_F	AGGactagtATGGTGGATCGCAGCGATAATG
p55-NotI_R	TTTgcggccgctAGCGGTATTGGTTTCTAAC
Hyd_T7_F	ctaatacgactcactatagggagagcgaccgaataagtcagag
Hyd_T7_R	ctaatacgactcactatagggagagccacacgaccagaggttatc
HYD_Seq_-500_F	TTGCAGGACAGGATGTGGTG
HYD_Seq_950_F	ACGACGCTGGATAAGCAAAG
HYD_Seq_1750_F	TAACACGAACTCTGGCGTAG
HYD_Seq_2500_F	GTACCATTGTGCTTCGTGAT
HYD_Seq_3000_F	CGTTAGCAGCATCGATTTG
HYD_Seq_3663_F	CCACAAAGGACACGACTGCA
HYD_Seq_4250_F	GCAGTGCATCGGAGAACTCT
HYD_Seq_5000_F	ATCAAGAGGTGCAGAGGAGC
HYD_Seq_5750_F	TATGGGATCCAATTGACGCC
HYD_Seq_6570_F	CTGAAGCATTAATGGCCACA
HYD_Seq_7250_F	GTGCTAAGATCCCCAACTTG
HYD_Seq_8000_F	GGGCGTAAAATTAAGTTCCA
HYD_Seq_8500_F	AGGGATTCCAACCATTGCCA
T7_2_MTA1-like_F	CTAATACGACTCACTATAGGGAGACTGTGATGATTTTCGTTGTAC
T7_2_MTA1-like_R	CTAATACGACTCACTATAGGGAGATACATGTGGAAGACCACCGA

Table 7.10 *E.coli* strains

Name	Genotype
DH5 α	F- Phi80dlacZ DeltaM15 Delta(lacZYA-argF)U169 deoR recA1 endA1 hsdR17(rK-mK+)poa supE44 lambda-thi-1

Table 7.11 Yeast strains

Name	Genotype
SGY37VIII	MATa trp1 his3 leu2 ura3-52::URA3-lexA-op-LacZ (Geissler et al., 1996)

Table 7.12 Fly strains

Name	Genotype	Source
GMR-Gal4 driver	GMR/GMR; w ¹¹¹⁸	AG Erhardt
UAS-CID	GMR/CyO; UAS::CID/TM3,Sb	(Mathew et al., 2014)
CAP-G	P{w[+mC]=EP}CapG[EP2346]/CyO	(Mathew et al., 2014)
HydRNAi (hyd ^{GD14227})	w ¹¹¹⁸ ; P{GD14227}v44675	VDRC
Hyd ¹⁵ mutant	kniri ⁻¹ hyd ¹⁵ ; e ¹ /TM3, Sb ¹	Bloomington

7.2 Methods

All the methods in this study were performed according to standard AG Erhardt protocols.

7.2.1 Molecular Biology Techniques

7.2.1.1 Molecular cloning

All methods concerning standard molecular biology techniques were essentially performed as described in (Sambrook & W Russell, 2001). If necessary, details are given within the following protocols listed in this section.

7.2.1.2 Preparation of double-stranded RNA for RNA interference studies

Double-stranded RNA (dsRNA) was made using the Ambion MEGAscript kit according to the manufacturers protocol. This usually yielded dsRNA with a concentration of 0.2 – 1.5 μ g RNA/ μ l. Prepared dsRNA was aliquoted and frozen at -20°C.

7.2.1.3 Inducible gene constructs: the pMT-V5-His vector system

Most proteins analysed in this study were expressed from the CuSO₄-inducible pMT-V5-His vector (Life technologies). A detailed description of the vector cloning system can be found on the Life technologies/Invitrogen website (DES-TOPO TA expression kit). Briefly, the open reading frame (ORF) of interest was PCR- amplified with a forward and a reverse primer excluding the stop codon (to allow for a C-terminal epitope V5-his tag). The amplified ORF carried Adenine (A) overhangs at the 3'end and was ligated with the linearized vector (containing 5' Thymine (T) overhangs). Alternatively, the cloning was also performed by

restriction enzyme digestion approach. Briefly, the ORF of genes were amplified with primers containing restriction enzyme digest site overhangs. Then, both the insert and the vector were digested with the same restriction enzymes. Vector backbone and insert were then ligated by T4 DNA ligase. In addition, for Y2H, pMM5 and pMM6 constructs were used (Schramm, Elliott, Shevchenko, & Schiebel, 2000). The pMM5 vector expresses fusions of the LexA-DNA binding domain, whereas the pMM6 vector expresses fusions with the Gal4TA domain. RbAp48 and p180 were cloned into pMM5 and pMM6 vectors using BamHI and XhoI restriction sites. For p180 cloning, single BamHI cut site within the ORF of p180 was mutated by silent point mutagenesis.

The ligation reaction was transformed into bacteria (*E. coli*, DH5 α) to obtain clones. Single colonies were screened for the insertion using a gene-specific forward primer and a vector-specific reverse primer. PCR positive clones were sent for sequencing by GATC. Positive clones were co-transfected into *Drosophila* S2 cells, together with the pCopia-hygro plasmid allowing the creation of stable cell lines expressing the gene of interest. Some vectors had already available hygromycin or puromycin resistant markers without requirement of phygro co- transfection.

7.2.1.4 Mutagenesis

Mutants were generated by site-directed mutagenesis of plasmid DNA. Plasmids carrying the ORF to be mutated, were amplified with primers that carry the point mutation to be introduced, flanked by 10-15 nucleotides on each site that were perfectly complementary to the insert sequence. The PCR was performed with Pfu-X Polymerase (Jena Biosciences). The program that was set according to the manufacturer's protocol of the enzyme. Afterwards, the parental plasmid was removed by digesting with the methylation-dependent restriction enzyme DpnI for 2h at 37°C. The undigested DNA was transformed into bacteria. The next day, colonies were picked and sent for sequencing.

7.2.1.5 RNA Isolation and RT-PCR

One million cells were resuspended in 100 μ l Trizol, incubated for 5 min, supplemented with 20 μ l chloroform, vortexed, further incubated for 3 min and centrifuged at 12000 x g for 15 min at 4°C. The aqueous phase was supplemented with 50 μ l isopropanol, incubated for 10 min at RT and centrifuged for 15 min at 12000 x g at 4°C. One ml of 75% EtOH was added and nucleic acids were pelleted by 10 min at 7500 x g at 4°C. The pellet was air dried and resuspended in 20 μ l H₂O. Genomic DNA was removed by DNaseI (NEB) treatment. cDNA synthesis was performed using the RevertAidTM H Minus cDNA synthesis kit or dART RT kit. PCR with specific primers for actin and the CID-V5-his was performed and agarose gels were analysed on a Biorad Gel Doc XR system. Analysis of differences in expression levels was performed semi-quantitatively in the non-saturated range.

7.2.1.6 Yeast two hybrid

The yeast two hybrid (Y2H) system was originally introduced by Fields and Song (Fields & Song, 1989). It is based on the fact that the transcriptional activator Gal4 is only active when its two components, the DNA binding domain Gal4DNA and the acidic transactivation domain Gal4TA, are joined together. By fusing two candidate proteins either to the DNA binding or the transactivation domain alone, the activity of the transcription factor can be taken as read-out for protein interactions. The reconstituted Gal4 activates the transcription of the LacZ reporter gene encoding β -galactosidase. Since β -galactosidase metabolizes X-

Gal (5-bromo-4-chloro-3-indolyl- β -D-galactosidase) and thereby produces a blue dye, the interaction of the two candidate proteins can be visualized. In this study the bacterial DNA-binding protein LexA was used instead of the Gal4 DNA binding domain. At first step, competent cells of the yeast strain SGY37VIII, which carry the LacZ gene under the control of a LexA-operator, were prepared as described previously (Knop *et al.*, 1999). In the following, 0.1-05 μ g of pMM5 constructs (fusion with LexA-DNA binding domain) and/or pMM6 constructs (fusion with Gal4TA domain) were transformed into 15 μ l of competent SGY37VIII cells. After the addition of 100 μ l of LiPEG, cells were vortexed and incubated for 20 min at RT. 10 μ l DMSO (Fisher Scientific, Loughborough, UK) were added and cells were incubated for 10 min at 42°C. Afterwards, cells were harvested at 3000 g/3 min, resuspended in 200 μ l of sterile YPD and plated onto SC-Leu/His plates. Plates were incubated for 2 days at 30°C and were then transferred to 4°C for up to 15 days. In the following, transformants were plated onto SC-selective plates in a grid-like pattern. For this 200 μ l sterile YPD were inoculated and incubated o/n at 30°C. On the next day, 5 μ l of cells were spotted onto SC-selective plates and incubated for 3-4 hrs at 30°C. Cells were then tested for protein interaction by overlaying them with X-Gal top agar. Top agar was prepared by mixing 50 ml of solution A and 30 ml of solution B, filling up to 100 ml and adding 1 ml of solution C. Plates were not moved within the first 30 min after the overlay and kept at RT. Afterwards plates were incubated at 30°C. Cells with very strong two-hybrid interaction partners turned blue within minutes. However, plates were checked every 30 min for up to 12 hrs to detect weak interaction partners.

7.2.2 Tissue culture methods using *Drosophila* S2 cells

Drosophila Schneider 2 (S2) cells were used as in vitro model in this study. S2 cells are versatile tool to analyze the underlying mechanisms of centromere formation. This is due to the fact that your gene of interest can be easily depleted by performing RNA interference (RNAi), which can then be combined with powerful microscopy and/or biochemical approaches (Rogers & Rogers, 2008).

7.2.2.1 Growing and maintaining S2 cells

S2 cells were grown and maintained under sterile conditions in tissue culture flasks (Orange scientific). Cells were grown as a semi-adherent monolayer at 25°C in the dark in 10% fetal bovine serum-containing medium (SM), supplemented with 2 % penicillin and streptomycin mixture. Cells were splitted usually twice per week.

7.2.2.2 Thawing *Drosophila* S2 cells

Frozen S2 cells (10^7) were quickly thawed in a 30°C water bath and centrifuged. After removal of old medium, cells were resuspended in 1 ml fresh complete serum medium and transferred into a 25 cm² flask carrying 4 ml of fresh complete serum medium. Thawed cells usually take one to two weeks to recover.

7.2.2.3 Freezing S2 cells

A running stock of S2 cells should be replaced on a regular basis (for example every 3 month) with freshly thawed cells. Newly created stable cell lines should be frozen as soon as they are stable (after 6 weeks). Therefore cells were frozen for long term storage at -80°C (S2 cells can be stored for decades at -80°C or -160°C) in a mixture of fresh SM, DMSO and conditional medium (CM = medium wherein cells have been grown for several days). Cells were grown to maximum confluence in a 150 ml flask, washed off with a 10 ml pipette and

centrifuged for 5 min at 1000 x g. Cells were resuspended in the cryogenic medium (2.25 ml CM, 2.25 ml fresh SM, 500 µl DMSO). Aliquots of 1 ml were prepared in 2 ml cryotubes, transferred into a Mr. Freezer containing fresh 2- propanol and stored at -80°C for short term and at nitrogen tank for long term.

7.2.2.4 Transfection of S2 cells

Transfection was performed in 6-well plates. 1.5 Mio cells were plated into 2 ml fresh SM. Cells settled 1h to over night (o/N) until they reach 80-90 % confluency. Prior to transfection two solutions were prepared: a) 200 µl serum-free medium (SFM) with 4 µl of Cellfectin II (Life technologies) and b) 200 µl SFM and up to 5 µg of the to-be transfected DNA (1 µg pCopia-Hygro + vector(s) of interest), mixed and incubated for 45 minutes. The transfection mixture was filled up to 1 ml with SFM. Cells were washed once with SFM, followed by 4 h of incubation in the transfection mixture. One ml 20% SM was added, cells were grown for one day, followed by addition of 1 ml SM. Cells were further grown for three days and 250 µg/ml Hygromycin B was added to start the selection process. Cells were kept in the same 6-well plate for up to 3 weeks, medium was replaced every 7 days. In the fourth week after transfection, cells were transferred into a 25 cm² flask. Hygromycin was applied for 6 weeks which usually resulted in transfection efficiencies of 80 – 100 %. After the selection period, cells were grown either without selection reagent or half concentration of selective reagent for months.

7.2.2.5 Drug treatment of S2 cells

Several experiments in this study were performed in the presence of drugs. To obtain mitotic chromosomes, cells were treated with the microtubule depolymerizer colcemid (3.3 µg/µl). To inhibit proteasome, 20 µg/µl MG132 was added to the medium. It should be mentioned that S2 cells are particularly hard to arrest in mitosis. Usually only 10-15, maximum 20% of cells can be kept in a mitotic state. Protein expression was induced with variable range of CuSO₄ between 0.05 mM and 1 mM mostly for overnight. To inhibit HDAC, 0.25 µM TSA treatment was performed for 24 hours.

7.2.2.6 RNAi in S2 cells

RNA interference (RNAi) was performed in 6-well plates. One Mio cells (80-100% confluence) were plated into 1 ml SM and settled o/N. On the next day, cells were washed with SFM twice. 20-25 µg of dsRNA was added to the cells in 1 ml SFM. After 1 h incubation, 2 ml 15% SM was added. RNAi was carried out for 4 days. If cells reached 100% confluence, cells were splitted (1 Mio/ml) and the dsRNA treatment was repeated.

7.2.3 Microscopy

7.2.3.1 Image acquisition on Deltavision microscope

Microscopy was performed on a DeltaVision(R) Core system (Applied Precision). Images were acquired with an Olympus UPlanSApo 100 x objective (n.a. 1.4) at binning 1 (fixed cells and spreads) or binning 2 (live cell imaging), or an Olympus PlanApo N 60 x at binning 1 (n. a. 1.42). If not stated otherwise, all images were deconvolved and maximum-projected using the Applied Precisions softWoRx 3.7.1 suite. Deconvolution was performed with the following settings: a) ratio conservative, 10 cycles, high noise filtering (fixed cells) or b) enhanced additive, 5 cycles, high noise filtering (chromosomes). Quick projection was performed at maximum intensity for fixed cells and at average setting for chromosomes.

7.2.3.2 Image quantification using ImageJ software

To determine the penetrance of observed phenotypes, cells were counted for the presence or the absence of the respective phenotypes. Single cell mean intensity quantifications were done using the ImageJ software. Signal intensities in the area of interest (in our case: nucleus) were determined by marking the nuclear area based on the DAPI staining. These regions of interest (ROI) were saved and used as reference area for the channel of interest. The mean intensities of the desired channel were then calculated by adjusting the threshold of the intensities by default settings and by analyzing the mean intensities relative to the saved ROIs of the DAPI channel. For determining the number and the intensities of centromeric dots of CID, a set of plugins (spot detection plugin) developed by the Nikon Imaging Centre, University Heidelberg (Peter Bankhead) was used. After marking the nuclear boundaries in the DAPI channel and saving them with the ROI tool, the spots in the channel of interest were enhanced using the DoG spot enhancer plugin. Subsequently, the threshold was adjusted using 'Li' instead of default settings. The number of spots with their mean intensities relative to the nuclear area was determined using the ROI particle analyzer plugin. The quantifications shown in this study are representative results of at least three independent experiments unless otherwise stated. The signal graph was plotted using the Graphpad prism 7 software. The statistical significance of the results was analyzed with the student's t test.

7.2.3.3 Indirect immuno-fluorescence (IF)

Exponential growing cells were washed once in PBS (3000 x rpm, 3 min) resuspended in 100 μ l PBS and plated out on a positively charged glass slide (Thermo Scientific). Cells were allowed to settle for 10 min at RT. Carefully, 100 μ l 4 % formaldehyde was added slowly onto the cells. Fixation was performed for 10 minutes. Fixed cells were washed twice in PBS and either stored at 4°C in PBS or further processed for indirect immunofluorescence (IF). For IF, cells were permeabilized for 5 min with 0.1% Triton X 100/PBS. Unspecific groups were blocked for 30 min with 5% milk in 0.1 % Triton X 100/PBS. Primary antibody was incubated in 50 μ l blocking solution for 1h at RT or o/N at 4°C. During antibody incubation, cells were covered with parafilm to avoid evaporation. Cells were washed 3 x in PBS-T. Then, they were incubated in secondary antibody solution for 1h at RT. After three washes in PBS-T, DNA was stained for five minutes with DAPI/PBS, mounting medium was applied and cells were covered with a glass coverslip. Cells were imaged at a DeltaVision Core system. If not stated otherwise, 12 μ m in Z were imaged with 0.3 μ l stack interval distance.

7.2.3.4 Preparation of mitotic spreads

To obtain mitotic chromosomes, 3×10^5 – 1×10^6 exponentially growing cells were arrested in mitosis with 3.3 μ g/ μ l colcemid. Cells were arrested for 1h – 2h, centrifuged for 3 min at 3000 x rpm, resuspended in 500 μ l hypotonic sodium citrate solution (0.5% Na-citrate in ddH₂O), and incubated for 7 min. 500 μ l of swelled cells were spun on positively charged slides in a Shandon 4 cytopspin (900 rpm, high acceleration, Thermo) for 10 min, fixed with 4 % PFA/PBS for 10 min and subsequently treated for IF according to 7.2.3.3.

7.2.4 Biochemical methods

All protocols concerning cell lysis and immuno-precipitation of protein(s) were performed at 4°C. Buffers and solutions used for protein analysis are listed in Table 7.3.

7.2.4.1 Preparation of S2 cell lysates

To analyze the entire complement of cellular protein, whole cell extracts (WCE) were prepared. Usually $10^6 - 10^7$ cells were washed in PBS, and lysed in RIPA buffer containing 250 µl/ml benzonase (Sigma) for 10 min. Cell lysates were sonicated 3 x in a Bioruptor (30 sec sonication / 30 sec break, Level 5). Cells lysates were supplemented with 4 x Laemmli sample loading buffer (SLB) and analysed on SDS-PAGE (4.2.5.3). Alternatively, after wash with PBS, cells were directly supplemented with 2x laemmli buffer (40 µl/1Mio) and sonicated. Before SDS-PAGE gel run, they were boiled at 95°C for 5 min.

7.2.4.2 Co-immunoprecipitation of GFP-tagged proteins

GFP fusion proteins (like CID-GFP) were precipitated with the GFP-binding protein (GBP) covalently bound to NHS-sepharose (Morey, Barnes, Chen, Fitzgerald-Hayes, & Baker, 2004). Cells were usually lysed in GFP-IP high salt lysis buffer and then salt concentration was 4 times diluted. However, in GFP-co-IP to detect CID-NuRD interaction, lysis was performed in 250 mM NaCl-containing IP buffer since the physical interactions in this complex are not very stable. To prevent protein degradation, PMSF (2 mM), Roche Complete (1x) and aprotinin/leupeptin/pepstatin were added freshly to the lysis buffer. PTM state was conserved using Na-fluoride (10 mM), and N-ethyl maleimide (20-40 mM). Lysis was essentially performed as described in 7.2.4.1. The lysate was centrifuged for 30 min at high speed (13000 x rpm). The supernatant was diluted if high salt lysis buffer was used. Then the diluate or supernatant was transferred to a fresh reaction tube carrying 50 µl of NHS-GBP (equilibrated in lysis buffer). For the analysis of CID- binding proteins, co-immuno precipitation (Co-IP) was performed for 2 – 3 h. Beads were collected by centrifugation (3000 rpm, 1 min) and washed 6 x in 1 ml (Co)-IP buffer. Proteins were eluted in 2 volumes 2 x SLB for 5 min at 95°C and separated by SDS-PAGE followed by western blot (WB) or mass spectrometry (MS) analysis.

7.2.4.3 Xlink-IP

Xlink-IP protocol was performed based on (Kast & Klockenbusch, 2010). Briefly, 10^8 cells were washed in PBS and incubated in 10 ml 0.4% PFA at RT for 7 min with mild agitation. Then cells were centrifuged, and PFA was removed. 0.5 ml 1.25 mM ice cold glycine-PBS was added to quench the reaction. After centrifuge and removal of glycine-PBS, cells were lysed in 1 ml Xlink IP buffer for 30-60 min at 4°C on rotator. Sonification of 50 cycles (10 sec ON, 5 sec OFF) was performed. The lysates were centrifuged at 13000 rpm for 30 min and then transferred to the GBP beads (equilibrated). GBP-binder protocol was performed as described in 7.2.4.2. Elution was done with 50 µl 4x laemmli at 65°C for 10 min to keep Xlinks or at 95°C for 10 min to reverse Xlinks. The working of the protocol was confirmed by WB and coomassie staining, and samples were sent for MS analysis.

7.2.4.4 Co-immunoprecipitation of V5 or His-tagged proteins

$1.0-2.0 \times 10^8$ S2 cells expressing V5-tagged proteins were washed with cold PBS and then lysed in a V5-IP buffer. Of particular note, cells were treated for 8 h with 20 µg/µl of the proteasome inhibitor MG132 (Santa Cruz Biotechnology) for detection of poly-ubiquitinated

proteins. To prevent protein degradation, PMSF (2 mM), Aprotinin (1 µg/ml), Leupeptin (0.5 µg/ml) and Pepstatin (1 µg/ml) were added freshly to the lysis buffer. After incubating the cells at 4°C for 20 min, the lysate was centrifuged for 30 min at high speed. Subsequently, the supernatant was transferred to a precooled tube containing 1 µg of V5-antibody covalently coupled to agarose G beads (Roche). The Co-Immunoprecipitation (Co-IP) was performed for 2-3 hrs. Beads were then collected by centrifugation (1200 rpm, 5 min) and washed 6 x in 20 volumes of lysis buffer. Proteins were eluted in 2 volumes 2 x SLB for 5 min at 95°C and separated by SDS-PAGE followed by western blot (WB). On the other hand, His IP was performed based on His-SpinTrap protocol according to the manufacturer's instructions (GE Healthcare).

7.2.4.5 SDS PAGE and western blot analysis

Sodium dodecyl-sulfate (SDS) poly-acrylamide gel electrophoresis (PAGE) is a standard technique (Sambrook & W Russell, 2001). Briefly, denatured protein samples were separated on SDS PAGE gels (7-15%) with the Biorad TetraCell system. Separated proteins were transferred onto a nitrocellulose membrane (0.45 µm) using a Tris/ glycine/ methanol buffer (TGM). Wet or semi-dry blotting was performed according to the size of the proteins of interest. Nitrocellulose membranes were blocked for 30 min with 5% milk powder in TBS containing 0,1 % Tween 20. Primary antibodies were incubated for 1 h at RT or o/N at 4°C in blocking solution. After 3 washes in TBS-Tween, secondary antibodies were incubated for 1 h at RT. Commercial secondary antibodies were coupled to horseradish peroxidase (HRP). Signal detection was performed exploiting chemiluminescence (ECL solution).

7.2.4.6 Mass spectrometry of proteins and data analysis

ΔNCID co-IP MS was performed in collaboration with Sabine Merker from ZMBH Mass Spec facility. Xlink IP-MS study was performed in collaboration with ex-member Dr. Bernd Hessling from ZMBH Mass spec facility. Protein samples that were prepared for mass spectrometry (MS) analysis were isolated according to 7.2.4.2 or 7.2.4.3, and separated on SDS-PAGE. Proteins present in the gel were visualized with colloidal coomassie staining. After this step, gel was submitted to the facility and the routine protocols were applied. Gel pieces have been cut out and digested with Trypsin using the Digest Pro Robotic System from Intavis. Peptides have been separated on an in-house packed C18 reversed-phase column of 25 cm length using an 120 min gradient from 3% to 36% ACN and directly injected to an Q-Exactive HF mass spectrometer.

Data analysis was carried out by MaxQuant (version 1.5.3.30). In total 12671 peptides and 1791 proteins could have been identified by MSMS based on an FDR cutoff of 0.01 on peptide level and 0.01 on protein level. Match between runs option was enabled to transfer peptide identifications across Raw files based on accurate retention time and m/z. Quantification was done using a label free quantification approach based on the MaxLFQ algorithm. A minimum number of 2 quantified peptides was required for protein quantification, requantify option was activated, to enable quantification of proteins with very high ratios. In total 1787 proteins could have been quantified. MaxQuant raw output files have been filtered and visualized using in-house compiled R-scripts. Proteins were filtered by stringent threshold parameters (LFQ>2, peptide count increase > 4). The interesting candidate protein complexes were determined using String pathway analysis online tool.

7.2.5 Fly Genetics

7.2.5.1 Fly culture

Fly stocks were kept on standard medium at 18°C. To prevent mite contamination, food vials were exchanged every 3-4 weeks. While performing crosses, the vials were shifted to 25-29°C if required.

7.2.5.2 Virgin collection

Female virgins were collected within 8-15 hours after the culture had been cleared of adults. To speed up development, the vials were kept at 25°C during the day. Under these conditions, newly hatched flies stay virgins for roughly 8 hrs. Since flies stay virgins for approximately 16 hrs at 18°C, vials were transferred to 18°C o/n. Virgins were selected based on their light body colour, the dark spot in their translucent abdomen and/or their unexpanded wings. The flies were held back for 4-5 days to check for larvae in the holding vial. Confirmed virgins were used in matings.

7.2.5.3 Genetic interaction using CID overexpression flies

The GAL4/UAS-System is a versatile tool to specifically overexpress your gene of interest in a certain tissue. In our case, we used a flyline that overexpresses a UAS-CID transgene, due to a GMR-GAL4 driver, exclusively in the fly eye. This overexpression (o/e) is known to cause a severe rough eye phenotype (Heun et al., 2006; Jäger et al., 2005). Genetic interactors of CID can be identified based on their ability to enhance or suppress this phenotype (Jäger et al., 2005). To test whether *hyd* and CID genetically interact, virgins of *cid* o/e flies were mated with males of *hyd*¹⁵ mutant flies. Since stronger phenotypes are only observed at higher temperatures, the crosses were incubated at 29°C to produce progeny. Adults were removed before hatching started. F1-flies that simultaneously carry the *hyd*¹⁵ mutation and overexpress CID were analyzed for a suppression or enhancement of the rough eye phenotype. To do so, the heads of these F1 flies were imaged on a Leica M420 macroscope system (Wetzlar, Germany). The same protocol was also applied for the reciprocal cross.

7.2.5.4 Induction of RNAi in flies

As the binary UAS/GAL4 system allows targeted gene expression, it is the technique of choice to induce RNAi in flies. Depending on the driver, RNAi is either only switched on in a certain tissue or alternatively at a specific developmental stage from embryo to adult. In this study *hyd* RNAi was induced in the eye by GMR-Gal4 driver. The reciprocal crosses were kept at 29°C. The eyes of the emerging F1 generation were imaged using a Leica M420 macroscope system (Wetzlar, Germany).

8 APPENDICES

Table 8.1 Pairwise comparison of enriched proteins detected in Δ NCID co-IP-MS

Proteins enriched for Δ NCID/RbAp48 vs Δ NCID (LFQ ratio > 2)	Proteins enriched for Δ NCID vs Δ NCID/RbAp48 (LFQ ratio > 2)
AttD	CG14299
CG11897	sno
CG10126-RB	anon-EST:Liang-2.45
Gclc	CG43367
ImpL3	Spc105R
EndoA;endoA	fzy
Psa	tefu
CG8728-RA	Set1
pins	Pi3K68D
Gpo-1	CG1646
fs(1)Yb	Mekk1
CG10214	Fancd2
CG42553-RA	Zyx
CG3967	MED26
Git	Acf1
Paf-AHalp	asp
Nc73EF	AOX3
Usp5	CG9425
Coprox	Zcchc7
TBCB	CG15618
smt3	CG4554
Rae1	CG2260
Caf1	Bruce
tsr	Cap-D2
CG8223	Msp300
Cat	CG12499
CG3501	Ufd4
UQCR-C1	garz
CG8036	Rpl1
CG12909	lgs
CG17544-RA	PEK
bur	MBD-R2
CG1910	tho2
Wibg	kz
CG10565	rudhira
ATPCL	CG11870-RD
RpL38	CG2747
PpD3	RhoGAP19D
	spoon
	CG3016
	Sfmbt
	CG42684
	nonC
	shtd
	vir
	PIG-T
	Lk6

	spg
	osa
	stc
	Mio
	Cul3
	defl
	CG2875-RB
	eIF4G2
	Usp32
	CG8611
	Iva
	Ulp1
	hyd
	kis
	I(1)G0196
	Nipped-B
	I(2)k09022
	Sin3A
	mon2
	CG8771
	ttm50
	Midasin
	CG15445-RD
	Nipped-A
	DnaJ-1
	sec8
	woc
	CG16940-RC
	c11.1
	poe
	ABCB7
	Ge-1
	row
	Dlg5
	faf
	MED14
	lid
	Sec71
	Nup214
	CG15099
	CG8370
	cal1
	Cp190
	Tor
	Bap170
	rod
	CG4538-RA
	CG1234
	Gl
	RpA-70
	anon-73Bb
	sip2
	Rpn3
	BubR1

Table 8.2 Known or candidate CID interacting partners detected in Xlink-IP-MS compared to (Barth et al., 2014)

Prot. names	Peptide count .B3A	Peptide count .B3A-RbAp 48	Peptide count .CID	Peptide count. GFP only	LFQ CID vs GFP > 2	centromeric or CID interacting partner	centromeric candidate in Barth et al	LFQ>2 in Barth et al	Literature
Cap-G	2	5	5	0	Yes	Yes	No	Yes	genetic interaction
Incenp	3	3	3	0	Yes	Yes	No	Yes	
cal1	5	6	5	0	Yes	Yes	Yes	Yes	centromeric chaperone
asp	4	4	4	0	Yes	Yes	Yes	Yes	
Spt6	3	6	8	0	Yes	Yes	No	Yes	FACT complex
His4r;His4	12	17	17	10	Yes	Yes	No	Yes	nucleosome core complex
dre4	13	19	24	6	Yes	Yes	No	Yes	FACT complex
His2B	9	17	18	6	Yes	Yes	No	Yes	nucleosome core complex
Top2	22	37	42	11	Yes	Yes	No	Yes	chromosome length in C-elegans
Ckl1alpha	13	12	12	5	Yes	Yes	No	Yes	mitotic condensin function, ectopic CENP-A degradation
hyd	24	26	37	3	Yes	Yes	Yes	Yes	genetic and physical interaction, preliminary data
His2Av	6	8	9	3	Yes	Yes	No	Yes	nucleosome core complex, dna damage repair
His3	8	8	8	4	Yes	Yes	No	Yes	nucleosome core complex
Ssrp	10	13	15	7	Yes	Yes	No	Yes	FACT complex
Caf1	12	20	17	7	Yes	Yes	Yes	Yes	acetylation, nuclear import, centromeric targeting
Nap1	14	14	14	10	Yes	Yes	No	Yes	sister chromatid cohesion, CENP-B binding
mod	13	13	13	7	Yes	Yes	No	Yes	CAL-1 binding, centromere clustering, chromosome segregation
AGO2	16	18	18	7	Yes	Yes	No	Yes	assembly of centromeric heterochromatin
cid	0	0	2	1	Yes	Yes	Yes	Yes	
Hat1	5	8	9	4	Yes	Yes	Yes	Yes	acetylation, nuclear import, centromeric targeting
Kap-alpha1	3	3	3	1	Yes	Yes	No	Yes	transcriptional

									repressor of kinetochore attachment
REG	1	2	3	1	Yes	Yes	Yes	Yes	
Hsp70Bb	3	4	4	1	Yes	Yes	Yes	Yes	spindle length, kinetochore proteins
Srp54k	2	5	5	2	Yes	Yes	No	Yes	
prod	1	1	2	0	Yes	Yes	Yes	Yes	mitotic chromosome condensation
CG14695	3	3	3	0	Yes	Yes	No	Yes	
BEAF-32	1	1	2	0	Yes	Yes	No	Yes	chromatin insulator, genome organization
Ns3	12	13	13	2	Yes	Yes	No	Yes	
CG7518	7	7	7	0	Yes	Yes	Yes	Yes	
Nup50	6	6	6	1	Yes	Yes	No	Yes	
CklIbeta	5	3	5	1	Yes	Yes	No	Yes	mitotic condensin function, ectopic CENP-A degradation
SRPK	5	8	8	1	Yes	Yes	No	Yes	spindle microtubule assembly
CG1309	1	4	4	0	Yes	Yes	No	Yes	
RagC-D	5	5	5	1	Yes	Yes	Yes	Yes	
smt3	1	3	4	1	Yes	No	No	Yes	SUMO ortholog
Top1	3	2	3	1	Yes	No	No	Yes	
His2A	2	2	2	1	Yes	No	No	Yes	nucleosome core complex
His1	7	8	11	5	Yes	No	No	Yes	
Dek	6	6	7	4	Yes	No	No	Yes	DAXX ortholog
CG1399	5	6	4	1	Yes	No	Yes	Yes	
Hcf	13	12	12	1	Yes	No	Yes	Yes	
Gnf1	2	5	5	0	Yes	No	No	Yes	
lswi	8	10	11	1	Yes	No	No	Yes	
l(2)35Df	2	4	5	1	Yes	No	No	Yes	
Chro	3	4	5	1	Yes	No	No	Yes	
kis	6	7	7	1	Yes	No	No	Yes	
Rfc4	2	5	4	0	Yes	No	No	Yes	
ball	4	4	4	0	Yes	No	No	Yes	
Rrp1	4	10	9	1	Yes	No	No	Yes	
mod(mdg4)	1	3	3	0	Yes	No	No	Yes	
Dis3	7	8	9	1	Yes	No	No	Yes	
Nlp	1	2	4	1	Yes	No	No	Yes	
Prosbeta1	3	6	6	1	Yes	No	No	Yes	
mip130	5	6	5	1	Yes	No	No	Yes	
dia	5	8	7	1	Yes	No	No	Yes	
E(bx)	3	1	3	0	Yes	No	No	Yes	
Sin3A	1	2	4	0	Yes	No	No	Yes	

CG6693	2	4	4	0	Yes	No	No	Yes	
Nup205	2	6	4	0	Yes	No	No	Yes	
Nup75	2	4	4	1	Yes	No	No	Yes	
Rpd3	2	3	3	0	Yes	No	No	Yes	
nito	6	6	9	1	Yes	No	No	Yes	
Nop56	6	7	8	1	Yes	No	No	Yes	
sle	4	5	5	1	Yes	No	No	Yes	
Ns1	5	5	5	0	Yes	No	No	Yes	
CG5033	3	6	5	1	Yes	No	No	Yes	
Sec63	9	8	9	3	Yes	No	No	Yes	
vig	2	3	3	0	Yes	No	No	Yes	
nop5	5	6	7	2	Yes	No	No	Yes	
Cklalpha	4	4	4	1	Yes	No	No	Yes	
CG16817	7	6	6	1	Yes	No	No	Yes	
tud	9	8	7	0	Yes	No	No	Yes	
par-1	6	6	5	1	Yes	No	No	Yes	
Spt-I	2	4	4	0	Yes	No	No	Yes	
CG32138	5	5	5	1	Yes	No	No	Yes	
CG8478	15	16	13	1	Yes	No	No	Yes	
CG31368	4	5	4	0	Yes	No	No	Yes	
CG42232	3	9	8	0	Yes	No	No	Yes	
CG7946	5	7	7	0	Yes	No	No	Yes	
Hsp23	13	15	17	3	Yes	No	No	Yes	
Hsp26	9	13	16	8	Yes	No	No	Yes	
Hsp27	7	9	11	2	Yes	No	No	Yes	
Mi-2	11	14	17	3	Yes	No	No	Yes	
sqd	13	13	13	3	Yes	No	No	Yes	
DnaJ-1	11	10	12	3	Yes	No	No	Yes	
Hsp68	26	30	30	16	Yes	No	No	Yes	
larp	25	26	24	8	Yes	No	No	Yes	
FK506-bp1	12	14	14	7	Yes	No	No	Yes	
Rpl35A	11	13	11	8	Yes	No	No	Yes	
mask	44	44	36	9	Yes	No	No	Yes	
Imp	13	12	11	2	Yes	No	No	Yes	
smid	7	8	9	2	Yes	No	No	Yes	
Hsp83	61	64	62	44	Yes	No	No	Yes	
Droj2	25	24	24	13	Yes	No	No	Yes	
mor	7	6	8	2	Yes	No	No	Yes	
CG4747	13	16	17	9	Yes	No	No	Yes	
CG9281	19	17	19	9	Yes	No	No	Yes	
ncd	14	12	18	9	Yes	No	No	Yes	
CG10289	8	10	9	3	Yes	No	No	Yes	
Su(var)205	5	5	5	4	Yes	No	No	Yes	
cora	22	24	26	11	Yes	No	No	Yes	
Fmr1	24	22	22	10	Yes	No	No	Yes	

emb	9	11	12	7	Yes	No	No	Yes	
Rm62	20	22	22	14	Yes	No	No	Yes	
bel	29	27	28	14	Yes	No	No	Yes	
Nat1	19	19	17	10	Yes	No	No	Yes	
La	5	5	7	3	Yes	No	No	Yes	
CG10565	11	12	13	4	Yes	No	No	Yes	
Arf79F	5	8	8	6	Yes	No	No	Yes	
porin	20	22	22	16	Yes	No	No	Yes	
Hop	21	25	24	12	Yes	No	No	Yes	
poe	33	39	33	11	Yes	No	No	Yes	
XNP	2	4	5	0	Yes	Yes	No	No	ATRX ortholog, DAXX complex
Cul3	1	1	2	0	Yes	Yes	No	No	CID ubiquitin ligase
ial	2	3	3	0	Yes	Yes	No	No	kinetochore, spindle, SAC, anaphase promotion
PP2A-B	3	3	3	1	Yes	Yes	No	No	meiotic centromere
Spc105R	6	4	3	1	Yes	Yes	No	No	outer kinetochore
BubR1	15	10	11	0	Yes	Yes	No	No	outer kinetochore
rod	1	2	2	0	Yes	Yes	No	No	outer kinetochore, SAC

Table 8.3 GO terms for each sample in Xlink-IP-MS

Go term for B3(A)	GO term for B3(A)/RbAp48	GO term for CID
mRNA 3'-UTR binding	Isopeptidebond	nucleosome
Keep	Keep	Nucleosomecore
Stressresponse	nucleosome	Keep
Keep	Nucleosomecore	Systemic lupus erythematosus
translational initiation	Keep	Keep
Initiationfactor	Ublconjugation	Ribosome
regulation of translation	ribosome	ribosome
microtubule organizing center organization	translational initiation	Stressresponse
ribosome	Stressresponse	Ribosomalprotein
Ribosome	Ribosome	structural constituent of ribosome
Ribonucleoprotein	Initiationfactor	Ribonucleoprotein
RNA-binding	Ribosomalprotein	DNA geometric change
translation	structural constituent of ribosome	translation
Ribosomalprotein	Ribonucleoprotein	nuclear chromosome
ribonucleoprotein complex	translation initiation factor activity	translational initiation
3D-structure	translation	microtubule organizing center organization
RNA binding	microtubule organizing center organization	structural molecule activity

cytosol	Chromosome	Initiationfactor
intracellular non-membrane-bounded organelle	3D-structure	translation initiation factor activity
Phosphoprotein	structural molecule activity	3D-structure
cytoskeleton organization	regulation of translation	DNAreplication
organelle organization	translation factor activity, nucleic acid binding	Chromosome
cellular component organization	RNA transport	RNA-binding
Discard	Proteinbiosynthesis	DNA-binding
Discard	ribonucleoprotein complex	ribonucleoprotein complex
	RNA-binding	small ribosomal subunit
	DNA-binding	chromosome
	intracellular non-membrane-bounded organelle	regulation of translation
	RNA binding	nucleolus
	cellular macromolecular complex assembly	intracellular non-membrane-bounded organelle
	macromolecular complex assembly	RNA transport
	cytosol	RNA binding
	Phosphoprotein	DNA binding
	cytoskeleton organization	chromatin organization
	biosynthetic process	nucleic acid binding
	nucleic acid binding	chromosome organization
	organelle organization	Nucleus
	macromolecular complex	biosynthetic process
	cellular component organization	Phosphoprotein
	intracellular organelle	macromolecular complex
	organelle	organelle organization
	macromolecule metabolic process	cytosol
	Proteomicsidentification	cytoskeleton organization
	catalytic activity	nucleus
	membrane	intracellular organelle
	Discard	organelle
	Discard	protein metabolic process
	Oxidoreductase	cellular component organization
		macromolecule metabolic process
		cell part
		Proteomicsidentification
		Discard
		catalytic activity
		membrane
		Discard
		vesicle-mediated transport
		catabolic process
		Membrane
		Oxidoreductase

Table 8.4 Pairwise comparisons of enriched proteins detected in Xlink-IP-MS

B3(A)-RbAp48 vs B3(A)	CID vs B3(A)	CID vs B3(A)-RbAp48	B3(A) vs B3(A)-RbAp48	B3(A) vs CID	B3(A)-RbAp48 vs CID
LanA	Nlp	E(bx)	E(bx)	spd-2	Caf1
LanB2	brm	brm	spd-2	Bruce	Bruce
LanB1	cid	cid	Ire1	Ire1	CG7182
woc	LanB2	hyd	Spc105R	Ufd4	mask
mod(mdg4)	LanA	Spt5	AGBE	mask	Ufd4
smt3	LanB1	Aac11		Sgt	GlyS
row	mod(mdg4)	MTA1-like		Spc105R	unc-45
Acf1	woc	Spt6		rhea	
RbAp48	row	dpa		lic	
His2A	smt3	Mi-2		BubR1	
His4r;His4	Acf1	mahj		Pax	
His2Av	Sin3A	smid		iPLA2-VIA	
His2B	His2A	MBD-R2		Droj2	
His1	His4r;His4	MEP-1			
Hsp27	His2B	Mcm7			
Hsp22	His2Av	Ctf4			
Top2	CG42232	ncd			
His3	Top2	Rpd3			
Ssrp	His1	FK506-bp1			
Rrp1	Hsp22	Non2			
CG42232	Ssrp	Hsc70-1			
Hsp26	His3				
dre4	Hsp27				
Hsp23	dre4				
sqd	Rrp1				
AGO1	dpa				
	RbAp48				
	Dek				
	Spt6				
	TFAM				
	hyd				
	Hsp26				
	Mi-2				
	MTA1-like				
	Aac11				
	Non2				
	Spt5				
	Rpd3				
	Mcm6				
	XNP				
	FK506-bp1				
	Mapmodulin				
	smid				
	Rcc1				
	sli				
	Mcm7				
	Su(var)205				
	CG1371				

9 BIBLIOGRAPHY

- Aguilera, C., Nakagawa, K., Sancho, R., Chakraborty, A., Hendrich, B., & Behrens, A. (2011). c-Jun N-terminal phosphorylation antagonises recruitment of the Mbd3/NuRD repressor complex. *Nature*, 469, 231. Retrieved from <http://dx.doi.org/10.1038/nature09607>
- Ahmad, K., & Henikoff, S. (2002). The histone variant H3.3 marks active chromatin by replication independent nucleosome assembly. *Molecular Cell*, 9(6), 1191–1200. [https://doi.org/10.1016/S1097-2765\(02\)00542-7](https://doi.org/10.1016/S1097-2765(02)00542-7)
- Allis, C. D., & Jenuwein, T. (2016). The molecular hallmarks of epigenetic control. *Nature Publishing Group*, 17(8), 487–500. <https://doi.org/10.1038/nrg.2016.59>
- Allshire, R. C., & Ekwall, K. (2015). Epigenetic Regulation of Chromatin States in *Schizosaccharomyces pombe*. *Cold Spring Harbor Perspectives in Biology*, 7(7). <https://doi.org/10.1101/cshperspect.a018770>
- Allshire, R. C., & Karpen, G. H. (2008). Epigenetic regulation of centromeric chromatin: old dogs, new tricks? *Nature Reviews Genetics*, 9(12), 923–937. <https://doi.org/10.1038/nrg2466>
- Alpsoy, A., Yasa, S., & Gündüz, U. (2014). Etoposide resistance in MCF-7 breast cancer cell line is marked by multiple mechanisms. *Biomedicine & Pharmacotherapy*, 68(3), 351–355. <https://doi.org/10.1016/j.biopha.2013.09.007>
- Alqarni, S. S. M., Murthy, A., Zhang, W., Przewloka, M. R., Silva, A. P. G., Watson, A. A., ... Laue, E. D. (2014). Insight into the architecture of the NuRD complex: Structure of the RbAp48-MTA1 subcomplex. *Journal of Biological Chemistry*, 289(32), 21844–21855. <https://doi.org/10.1074/jbc.M114.558940>
- Amor, D. J., Bentley, K., Ryan, J., Perry, J., Wong, L., Slater, H., & Choo, K. H. A. (2004). Human centromere repositioning “in progress.” *Proceedings of the National Academy of Sciences*, 101(17), 6542–6547. <https://doi.org/10.1073/pnas.0308637101>
- Amor, D. J., Kalitsis, P., Sumer, H., & Choo, K. H. A. (2004). Building the centromere: From foundation proteins to 3D organization. *Trends in Cell Biology*. <https://doi.org/10.1016/j.tcb.2004.05.009>
- Anderson, A. E., Karandikar, U. C., Pepple, K. L., Chen, Z., Bergmann, A., & Mardon, G. (2011). The enhancer of trithorax and polycomb gene Caf1/p55 is essential for cell survival and patterning in *Drosophila* development. *Development*, 138(10), 1957–1966. <https://doi.org/10.1242/dev.058461>
- Andrews, A. J., Chen, X., Zevin, A., Stargell, L. A., & Luger, K. (2010). The Histone Chaperone Nap1 Promotes Nucleosome Assembly by Eliminating Nonnucleosomal Histone DNA Interactions. *Molecular Cell*, 37(6), 834–842. <https://doi.org/10.1016/j.molcel.2010.01.037>
- Arimura, Y., Shirayama, K., Horikoshi, N., Fujita, R., Taguchi, H., Kagawa, W., ... Kurumizaka, H. (2014). Crystal structure and stable property of the cancer-associated heterotypic nucleosome containing CENP-A and H3.3. *Sci Rep*, 4, 7115. <https://doi.org/10.1038/srep07115> [pii]
- Athwal, R. K., Walkiewicz, M. P., Baek, S., Fu, S., Bui, M., Camps, J., ... Dalal, Y. (2015). CENP-A nucleosomes localize to transcription factor hotspots and subtelomeric sites in human cancer cells. *Epigenetics & Chromatin*, 8(1), 2. <https://doi.org/10.1186/1756-8935-8-2>

- Au, W. C., Dawson, A. R., Rawson, D. W., Taylor, S. B., Baker, R. E., & Basrai, M. A. (2013). A novel role of the N terminus of budding yeast histone H3 variant Cse4 in ubiquitin-mediated proteolysis. *Genetics*. <https://doi.org/10.1534/genetics.113.149898>
- Bade, D., Pauleau, A. L., Wendler, A., & Erhardt, S. (2014b). The E3 Ligase CUL3/RDX Controls Centromere Maintenance by Ubiquitylating and Stabilizing CENP-A in a CAL1-Dependent Manner. *Developmental Cell*, 28(5), 508–519. <https://doi.org/10.1016/j.devcel.2014.01.031>
- Bailey, A. O., Panchenko, T., Sathyan, K. M., Petkowski, J. J., Pai, P.-J., Bai, D. L., ... Foltz, D. R. (2013). Posttranslational modification of CENP-A influences the conformation of centromeric chromatin. *Proceedings of the National Academy of Sciences*, 110(29), 11827–11832. <https://doi.org/10.1073/pnas.1300325110>
- Barth, T. K., Schade, G. O. M., Schmidt, A., Vetter, I., Wirth, M., Heun, P., ... Imhof, A. (2014). Identification of novel Drosophila centromere-associated proteins. *Proteomics*, 14(19), 2167–2178. <https://doi.org/10.1002/pmic.201400052>
- Bartsch, J., Truss, M., Bode, J., & Beato, M. (1996). Moderate increase in histone acetylation activates the mouse mammary tumor virus promoter and remodels its nucleosome structure. *Proceedings of the National Academy of Sciences*, 93(20). Retrieved from <http://www.pnas.org/content/93/20/10741>
- Basta, J., & Rauchman, M. (2017). The Nucleosome Remodeling and Deacetylase Complex in Development and Disease. In *Translating Epigenetics to the Clinic* (pp. 37–72). <https://doi.org/10.1016/B978-0-12-800802-7.00003-4>
- Becker, P. B., & Hörz, W. (2002). ATP-Dependent Nucleosome Remodeling. *Annual Review of Biochemistry*, 71(1), 247–273. <https://doi.org/10.1146/annurev.biochem.71.110601.135400>
- Belotserkovskaya, R., Oh, S., Bondarenko, V. A., Orphanides, G., Studitsky, V. M., & Reinberg, D. (2003). FACT facilitates transcription-dependent nucleosome alteration. *Science*, 301(5636), 1090–1093. <https://doi.org/10.1126/science.1085703>
- Benito, J. M., Godfrey, L., Kojima, K., Hogdal, L., Wunderlich, M., Geng, H., ... Konopleva, M. (2015). MLL-Rearranged Acute Lymphoblastic Leukemias Activate BCL-2 through H3K79 Methylation and Are Sensitive to the BCL-2-Specific Antagonist ABT-199. *Cell Reports*. <https://doi.org/10.1016/j.celrep.2015.12.003>
- Bergmann, J. H., Jakubsche, J. N., Martins, N. M., Kagansky, A., Nakano, M., Kimura, H., ... Earnshaw, W. C. (2012). Epigenetic engineering: histone H3K9 acetylation is compatible with kinetochore structure and function. *Journal of Cell Science*, 125(2), 411–421. <https://doi.org/10.1242/jcs.090639>
- Bergmann, J. H., Rodríguez, M. G., Martins, N. M. C., Kimura, H., Kelly, D. A., Masumoto, H., ... Earnshaw, W. C. (2011). Epigenetic engineering shows H3K4me2 is required for HJURP targeting and CENP-A assembly on a synthetic human kinetochore. *EMBO Journal*, 30(2), 328–340. <https://doi.org/10.1038/emboj.2010.329>
- Black, B. E., & Cleveland, D. W. (2011). Epigenetic centromere propagation and the nature of CENP-A nucleosomes. *Cell*, 144(4), 471–479. <https://doi.org/10.1016/j.cell.2011.02.002>
- Blanko, E. R., Kadyrova, L. Y., & Kadyrov, F. A. (2016). DNA mismatch repair interacts with CAF-1- and ASF1A-H3-H4-dependent histone (H3-H4)₂tetramer deposition. *Journal of Biological Chemistry*, 291(17), 9203–9217. <https://doi.org/10.1074/jbc.M115.713271>

- Bodor, D. L., Mata, J. F., Sergeev, M., David, A. F., Salimian, K. J., Panchenko, T., ... Jansen, L. E. T. (2014). The quantitative architecture of centromeric chromatin. *eLife*, 2014(3), 1–26. <https://doi.org/10.7554/eLife.02137>
- Bodor, D. L., Valente, L. P., Mata, J. F., Black, B. E., & Jansen, L. E. T. (2013). Assembly in G1 phase and long-term stability are unique intrinsic features of CENP-A nucleosomes. *Molecular Biology of the Cell*, 24(7), 923–932. <https://doi.org/10.1091/mbc.E13-01-0034>
- Boltengagen, M., Huang, A., Boltengagen, A., Trixl, L., Lindner, H., Kremser, L., ... Lusser, A. (2015). A novel role for the histone acetyltransferase Hat1 in the CENP-A/CID assembly pathway in *Drosophila melanogaster*. *Nucleic Acids Research*, 44(5), 2145–2159. <https://doi.org/10.1093/nar/gkv1235>
- Bonev, B., & Cavalli, G. (2016). Organization and function of the 3D genome. *Nature Reviews Genetics*. <https://doi.org/10.1038/nrg.2016.112>
- Bönisch, C., Schneider, K., Pünzeler, S., Wiedemann, S. M., Bielmeier, C., Bocola, M., ... Hake, S. B. (2012). H2A.Z.2.2 is an alternatively spliced histone H2A.Z variant that causes severe nucleosome destabilization. *Nucleic Acids Research*, 40(13), 5951–5964. <https://doi.org/10.1093/nar/gks267>
- Bouazoune, K., & Brehm, A. (2006). ATP-dependent chromatin remodeling complexes in *Drosophila*. *Chromosome Research*. <https://doi.org/10.1007/s10577-006-1067-0>
- Brackertz, M., Boeke, J., Zhang, R., & Renkawitz, R. (2002). Two highly related p66 proteins comprise a new family of potent transcriptional repressors interacting with MBD2 and MBD3. *Journal of Biological Chemistry*, 277(43), 40958–40966. <https://doi.org/10.1074/jbc.M207467200>
- Brasen, C., Dorosz, J., Wiuf, A., Boesen, T., Mirza, O., & Gajhede, M. (2017). Expression, purification and characterization of the human MTA2-RBBP7 complex. *Biochimica et Biophysica Acta (BBA) - Proteins and Proteomics*, 1865(5), 531–538. <https://doi.org/10.1016/j.bbapap.2017.02.002>
- Bui, M., Pitman, M., Nuccio, A., Roque, S., Donlin-Asp, P. G., Nita-Lazar, A., ... Dalal, Y. (2017). Internal modifications in the CENP-A nucleosome modulate centromeric dynamics. *Epigenetics and Chromatin*, 10(1), 1–21. <https://doi.org/10.1186/s13072-017-0124-6>
- Buschbeck, M., & Hake, S. B. (2017). Variants of core histones and their roles in development , stem cells and cancer. *Nature Publishing Group*. <https://doi.org/10.1038/nrm.2016.166>
- Cairns, B. R., Lorch, Y., Li, Y., Zhang, M., Lacomis, L., Erdjument-Bromage, H., ... Kornberg, R. D. (1996). RSC, an essential, abundant chromatin-remodeling complex. *Cell*, 87(7), 1249–1260. [https://doi.org/10.1016/S0092-8674\(00\)81820-6](https://doi.org/10.1016/S0092-8674(00)81820-6)
- Canzonetta, C., Vernarecci, S., Iuliani, M., Marracino, C., Belloni, C., Ballario, P., & Filetici, P. (2016). SAGA DUB-Ubp8 Deubiquitylates Centromeric Histone Variant Cse4. *G3 & Genes/Genomes/Genetics*, 6(2), 287–298. <https://doi.org/10.1534/g3.115.024877>
- Chadwick, L. H., Chadwick, B. P., Jaye, D. L., & Wade, P. A. (2009). The Mi-2/NuRD complex associates with pericentromeric heterochromatin during S phase in rapidly proliferating lymphoid cells. *Chromosoma*, 118(4), 445–457. <https://doi.org/10.1007/s00412-009-0207-7>
- Cheeseman, I. M., Chappie, J. S., Wilson-Kubalek, E. M., & Desai, A. (2006). The Conserved KMN Network Constitutes the Core Microtubule-Binding Site of the Kinetochore. *Cell*, 127(5), 983–997. <https://doi.org/10.1016/j.cell.2006.09.039>

- Cheloufi, S., Elling, U., Hopfgartner, B., Jung, Y. L., Murn, J., Ninova, M., ... Hochedlinger, K. (2015). The histone chaperone CAF-1 safeguards somatic cell identity. *Nature*, 528(7581), 218–224. <https://doi.org/10.1038/nature15749>
- Chen, C.-C., Bowers, S., Lipinszki, Z., Palladino, J., Trusiak, S., Bettini, E., ... Mellone, B. G. (2015). Establishment of centromeric chromatin by the CENP-A assembly factor CAL1 requires FACT-mediated transcription. *Developmental Cell*, 34(1), 73–84. <https://doi.org/10.1016/j.devcel.2015.05.012>
- Chen, C. C., Dechassa, M. L., Bettini, E., Ledoux, M. B., Belisario, C., Heun, P., ... Mellone, B. G. (2014). CAL1 is the Drosophila CENP-A assembly factor. *Journal of Cell Biology*, 204(3), 313–329. <https://doi.org/10.1083/jcb.201305036>
- Chen, H., Ruiz, P. D., Novikov, L., Casill, A. D., Park, J. W., & Gamble, M. J. (2014). MacroH2A1.1 and PARP-1 cooperate to regulate transcription by promoting CBP-mediated H2B acetylation. *Nature Structural and Molecular Biology*, 21(11), 981–989. <https://doi.org/10.1038/nsmb.2903>
- Chen, P., Wang, Y., & Li, G. (2014). Dynamics of histone variant H3.3 and its coregulation with H2A.Z at enhancers and promoters. *Nucleus*, 5(1), 21–27. <https://doi.org/10.4161/nucl.28067>
- Cheng, H., Bao, X., Gan, X., Luo, S., & Rao, H. (2017). Multiple E3s promote the degradation of histone H3 variant Cse4. *Scientific Reports*, 7(1). <https://doi.org/10.1038/s41598-017-08923-w>
- Cherry, C. M., & Matunis, E. L. (2010). Epigenetic regulation of stem cell maintenance in the drosophila testis via the nucleosome-remodeling factor NURF. *Cell Stem Cell*, 6(6), 557–567. <https://doi.org/10.1016/j.stem.2010.04.018>
- Chioda, M., Vengadasalam, S., Kremmer, E., Eberharter, A., & Becker, P. B. (2010). Developmental role for ACF1-containing nucleosome remodellers in chromatin organisation. *Development*, 137(20), 3513–3522. <https://doi.org/10.1242/dev.048405>
- Choi, E. S., Cheon, Y., Kang, K., & Lee, D. (2017a). The Ino80 complex mediates epigenetic centromere propagation via active removal of histone H3. *Nature Communications*, 8(1), 529. <https://doi.org/10.1038/s41467-017-00704-3>
- Chou, D. M., Adamson, B., Dephoure, N. E., Tan, X., Nottke, A. C., Hurov, K. E., ... Elledge, S. J. (2010). A chromatin localization screen reveals poly (ADP ribose)-regulated recruitment of the repressive polycomb and NuRD complexes to sites of DNA damage. *Proceedings of the National Academy of Sciences*, 107(43), 18475–18480. <https://doi.org/10.1073/pnas.1012946107>
- Clancy, J. L., Henderson, M. J., Russell, A. J., Anderson, D. W., Bova, R. J., Campbell, I. G., ... Watts, C. K. W. (2003). EDD, the human orthologue of the hyperplastic discs tumour suppressor gene, is amplified and overexpressed in cancer. *Oncogene*, 22(32), 5070–5081. <https://doi.org/10.1038/sj.onc.1206775>
- Clapier, C. R., & Cairns, B. R. (2009). The Biology of Chromatin Remodeling Complexes. *Annual Review of Biochemistry*, 78(1), 273–304. <https://doi.org/10.1146/annurev.biochem.77.062706.153223>
- Cleveland, D. W., Mao, Y., & Sullivan, K. F. (2003). Centromeres and kinetochores: From epigenetics to mitotic checkpoint signaling. *Cell*, 112(4), 407–421. [https://doi.org/10.1016/S0092-8674\(03\)00115-6](https://doi.org/10.1016/S0092-8674(03)00115-6)
- Daubresse, G., Deuring, R., Moore, L., Papoulas, O., Zakrajsek, I., Waldrip, W. R., ... Tamkun, J. W. (1999). The Drosophila kismet gene is related to chromatin-remodeling factors and is required

- for both segmentation and segment identity. *Development*, 126(6), 1175 LP-1187. Retrieved from <http://dev.biologists.org/content/126/6/1175.abstract>
- DeLuca, J. G., Gall, W. E., Ciferri, C., Cimini, D., Musacchio, A., & Salmon, E. D. (2006). Kinetochore microtubule dynamics and attachment stability are regulated by Hec1. *Cell*, 127(5), 969–82. <https://doi.org/10.1016/j.cell.2006.09.047>
- Denslow, S. A., & Wade, P. A. (2007). The human Mi-2/NuRD complex and gene regulation. *Oncogene*, 26, 5433. Retrieved from <http://dx.doi.org/10.1038/sj.onc.1210611>
- Deyter, G. M. R., & Biggins, S. (2014). The FACT complex interacts with the E3 ubiquitin ligase Psh1 to prevent ectopic localization of CENP-A. *Genes and Development*, 28(16), 1815–1826. <https://doi.org/10.1101/gad.243113.114>
- Deyter, G. M. R., Hildebrand, E. M., Barber, A. D., & Biggins, S. (2017). Histone H4 Facilitates the Proteolysis of the Budding Yeast CENP-A⁴ Centromeric Histone Variant. *Genetics*, 205(1), 113 LP-124. Retrieved from <http://www.genetics.org/content/205/1/113.abstract>
- Dong, Q., Yin, F. X., Gao, F., Shen, Y., Zhang, F., Li, Y., ... Li, F. (2016). Ccp1 Homodimer Mediates Chromatin Integrity by Antagonizing CENP-A Loading. *Molecular Cell*, 64(1), 79–91. <https://doi.org/10.1016/j.molcel.2016.08.022>
- Doyen, C. M., Moshkin, Y. M., Chalkley, G. E., Bezstarosti, K., Demmers, J. A. A., Rathke, C., ... Verrijzer, C. P. (2013). Subunits of the Histone Chaperone CAF1 Also Mediate Assembly of Protamine-Based Chromatin. *Cell Reports*, 4(1), 59–65. <https://doi.org/10.1016/j.celrep.2013.06.002>
- Dunleavy, E. M., Roche, D., Tagami, H., Lacoste, N., Ray-Gallet, D., Nakamura, Y., ... Almouzni-Pettinotti, G. (2009). HJURP Is a Cell-Cycle-Dependent Maintenance and Deposition Factor of CENP-A at Centromeres. *Cell*, 137(3), 485–497. <https://doi.org/10.1016/j.cell.2009.02.040>
- Erdel, F., & Rippe, K. (2011). Chromatin remodelling in mammalian cells by ISWI-type complexes - Where, when and why? *FEBS Journal*. <https://doi.org/10.1111/j.1742-4658.2011.08282.x>
- Fachinetti, D., Han, J. S., McMahon, M. A., Ly, P., Abdullah, A., Wong, A. J., & Cleveland, D. W. (2015). DNA Sequence-Specific Binding of CENP-B Enhances the Fidelity of Human Centromere Function. *Developmental Cell*, 33(3), 314–327. <https://doi.org/10.1016/j.devcel.2015.03.020>
- Falk, S. J., Guo, L. Y., Sekulic, N., Smoak, E. M., Mani, T., Logsdon, G. A., ... Black, B. E. (2015). CENP-C reshapes and stabilizes CENP-A nucleosomes at the centromere. *Science*, 348(6235), 699–703. <https://doi.org/10.1126/science.1259308>
- Fasulo, B., Deuring, R., Murawska, M., Gause, M., Dorigi, K. M., Schaaf, C. A., ... Tamkun, J. W. (2012). The Drosophila Mi-2 Chromatin-Remodeling Factor Regulates Higher-Order Chromatin Structure and Cohesin Dynamics In Vivo. *PLoS Genetics*, 8(8). <https://doi.org/10.1371/journal.pgen.1002878>
- Feinberg, A. P. (2018). The Key Role of Epigenetics in Human Disease Prevention and Mitigation. *New England Journal of Medicine*, 378(14), 1323–1334. <https://doi.org/10.1056/NEJMra1402513>
- Feng, Q., Cao, R., Xia, L., Erdjument-Bromage, H., Tempst, P., & Zhang, Y. (2002). Identification and functional characterization of the p66/p68 components of the MeCP1 complex. *Molecular and Cellular Biology*, 22(2), 536–46. <https://doi.org/10.1128/MCB.22.2.536-546.2002>

- Fields, S., & Song, O. (1989). A novel genetic system to detect protein–protein interactions. *Nature*, 340, 245. Retrieved from <http://dx.doi.org/10.1038/340245a0>
- Filipescu, D., Naughtin, M., Podsypanina, K., Lejour, V., Wilson, L., Gurard-Levin, Z. A., ... Almouzni, G. (2017). Essential role for centromeric factors following p53 loss and oncogenic transformation. *Genes and Development*, 31(5), 463–480. <https://doi.org/10.1101/gad.290924.116>
- Filipescu, D., Szenker, E., & Almouzni, G. (2013). Developmental roles of histone H3 variants and their chaperones. *Trends in Genetics : TIG*, 29(11), 630–40. <https://doi.org/10.1016/j.tig.2013.06.002>
- Flack, J. E., Mieszczanek, J., Novcic, N., & Bienz, M. (2017). Wnt-Dependent Inactivation of the Groucho/TLE Co-repressor by the HECT E3 Ubiquitin Ligase Hyd/UBR5. *Molecular Cell*, 67(2), 181–193.e5. <https://doi.org/10.1016/j.molcel.2017.06.009>
- Flanagan, J. F., Mi, L. Z., Chruszcz, M., Cymborowski, M., Clines, K. L., Kim, Y., ... Khorasanizadeh, S. (2005). Double chromodomains cooperate to recognize the methylated histone H3 tail. *Nature*, 438(7071), 1181–1185. <https://doi.org/10.1038/nature04290>
- Foltman, M., Evrin, C., De Piccoli, G., Jones, R. C., Edmondson, R. D., Katou, Y., ... Labib, K. (2013). Eukaryotic replisome components cooperate to process histones during chromosome replication. *Cell Reports*, 3(3), 892–904. <https://doi.org/10.1016/j.celrep.2013.02.028>
- Foltz, D. R., Jansen, L. E. T., Bailey, A. O., Yates, J. R., Bassett, E. A., Wood, S., ... Cleveland, D. W. (2009). Centromere-Specific Assembly of CENP-A Nucleosomes Is Mediated by HJURP. *Cell*, 137(3), 472–484. <https://doi.org/10.1016/j.cell.2009.02.039>
- Fu, J., Qin, L., He, T., Qin, J., Hong, J., Wong, J., ... Xu, J. (2011). The TWIST/Mi2/NuRD protein complex and its essential role in cancer metastasis. *Cell Res*, 21(2), 275–289. <https://doi.org/10.1038/cr.2010.118>
- Fujita, N., Jaye, D. L., Geigerman, C., Akyildiz, A., Mooney, M. R., Boss, J. M., & Wade, P. A. (2004). MTA3 and the Mi-2/NuRD complex regulate cell fate during B lymphocyte differentiation. *Cell*, 119(1), 75–86. <https://doi.org/10.1016/j.cell.2004.09.014>
- Fujita, N., Jaye, D. L., Kajita, M., Geigerman, C., Moreno, C. S., & Wade, P. A. (2003). MTA3, a Mi-2/NuRD complex subunit, regulates an invasive growth pathway in breast cancer. *Cell*, 113(2), 207–19. [https://doi.org/10.1016/S0092-8674\(03\)00234-4](https://doi.org/10.1016/S0092-8674(03)00234-4)
- Fujita, Y., Hayashi, T., Kiyomitsu, T., Toyoda, Y., Kokubu, A., Obuse, C., & Yanagida, M. (2007). Priming of Centromere for CENP-A Recruitment by Human hMis18 α , hMis18 β , and M18BP1. *Developmental Cell*, 12(1), 17–30. <https://doi.org/10.1016/j.devcel.2006.11.002>
- Fukagawa, T., & Earnshaw, W. C. (2014). The centromere: Chromatin foundation for the kinetochore machinery. *Developmental Cell*. <https://doi.org/10.1016/j.devcel.2014.08.016>
- Furuyama, T., Dalal, Y., & Henikoff, S. (2006). Chaperone-mediated assembly of centromeric chromatin in vitro. *Proceedings of the National Academy of Sciences*, 103(16), 6172–6177. <https://doi.org/10.1073/pnas.0601686103>
- Gaillard, P. H., Martini, E. M., Kaufman, P. D., Stillman, B., Moustacchi, E., & Almouzni, G. (1996). Chromatin assembly coupled to DNA repair: a new role for chromatin assembly factor I. *Cell*, 86(6), 887–896. [https://doi.org/S0092-8674\(00\)80164-6](https://doi.org/S0092-8674(00)80164-6) [pii]
- Geissler, S., Pereira, G., Spang, A., Knop, M., Souès, S., Kilmartin, J., & Schiebel, E. (1996). The spindle

- pole body component Spc98p interacts with the gamma-tubulin-like Tub4p of *Saccharomyces cerevisiae* at the sites of microtubule attachment. *The EMBO Journal*, 15(15), 3899–3911. Retrieved from <http://www.ncbi.nlm.nih.gov/pmc/articles/PMC452092/>
- Gibbons, R. J., Picketts, D. J., Villard, L., & Higgs, D. R. (1995). Mutations in a putative global transcriptional regulator cause X-linked mental retardation with α -thalassemia (ATR-X syndrome). *Cell*, 80(6), 837–845. [https://doi.org/10.1016/0092-8674\(95\)90287-2](https://doi.org/10.1016/0092-8674(95)90287-2)
- Goldberg, A. D., Banaszynski, L. A., Noh, K. M., Lewis, P. W., Elsaesser, S. J., Stadler, S., ... Allis, C. D. (2010). Distinct Factors Control Histone Variant H3.3 Localization at Specific Genomic Regions. *Cell*, 140(5), 678–691. <https://doi.org/10.1016/j.cell.2010.01.003>
- Gonzalez, M., He, H., Dong, Q., Sun, S., & Li, F. (2014). Ectopic centromere nucleation by CENP--a in fission yeast. *Genetics*, 198(4), 1433–1446. <https://doi.org/10.1534/genetics.114.171173> [pii]
- Green, C. M., & Almouzni, G. (2003). Local action of the chromatin assembly factor CAF-1 at sites of nucleotide excision repair in vivo. *EMBO Journal*, 22(19), 5163–5174. <https://doi.org/10.1093/emboj/cdg478>
- Grigoryev, S. A. (2018). Chromatin Higher-Order Folding: A Perspective with Linker DNA Angles. *Biophysical Journal*, 0(0). <https://doi.org/10.1016/j.bpj.2018.03.009>
- Gu, X. M., Fu, J., Feng, X. J., Huang, X., Wang, S. M., Chen, X. F., ... Zhang, S. H. (2014). Expression and prognostic relevance of centromere protein A in primary osteosarcoma. *Pathology Research and Practice*, 210(4), 228–233. <https://doi.org/10.1016/j.prp.2013.12.007>
- Gurard-Levin, Z. A., Quivy, J.-P., & Almouzni, G. (2014). Histone Chaperones: Assisting Histone Traffic and Nucleosome Dynamics. *Annual Review of Biochemistry*, 83(1), 487–517. <https://doi.org/10.1146/annurev-biochem-060713-035536>
- Guse, A., Carroll, C. W., Moree, B., Fuller, C. J., & Straight, A. F. (2011). In vitro centromere and kinetochore assembly on defined chromatin templates. *Nature*, 477(7364), 354–358. <https://doi.org/10.1038/nature10379>
- Hahn, M., Dambacher, S., Dulev, S., Kuznetsova, A. Y., Eck, S., Wörz, S., ... Schotta, G. (2013). Suv4-20h2 mediates chromatin compaction and is important for cohesion recruitment to heterochromatin. *Genes and Development*, 27(8), 859–872. <https://doi.org/10.1101/gad.210377.112>
- Hall, J. A., & Georgel, P. T. (2007). CHD proteins: a diverse family with strong ties. *Biochemistry and Cell Biology = Biochimie et Biologie Cellulaire*, 85(4), 463–76. <https://doi.org/10.1139/O07-063>
- Hamiche, A., & Shuaib, M. (2012). Chaperoning the histone H3 family. *Biochimica et Biophysica Acta - Gene Regulatory Mechanisms*. <https://doi.org/10.1016/j.bbagr.2011.08.009>
- Hatanaka, Y., Inoue, K., Oikawa, M., Kamimura, S., Ogonuki, N., Kodama, E. N., ... Ogura, A. (2015). Histone chaperone CAF-1 mediates repressive histone modifications to protect preimplantation mouse embryos from endogenous retrotransposons. *Proceedings of the National Academy of Sciences*, 112(47), 14641–14646. <https://doi.org/10.1073/pnas.1512775112>
- Hayashi, T., Fujita, Y., Iwasaki, O., Adachi, Y., Takahashi, K., & Yanagida, M. (2004). Mis16 and Mis18 are required for CENP-A loading and histone deacetylation at centromeres. *Cell*, 118(6), 715–729. <https://doi.org/10.1016/j.cell.2004.09.002>

- Hendrich, B., & Bird, A. (1998). Identification and Characterization of a Family of Mammalian Methyl-CpG Binding Proteins. *Molecular and Cellular Biology*, 18(11), 6538–6547. <https://doi.org/10.1128/MCB.18.11.6538>
- Henikoff, S. (2016). Mechanisms of nucleosome dynamics in vivo. *Cold Spring Harbor Perspectives in Medicine*, 6(9). <https://doi.org/10.1101/cshperspect.a026666>
- Henikoff, S., Ahmad, K., Platero, J. S., & van Steensel, B. (2000). Heterochromatic deposition of centromeric histone H3-like proteins. *Proceedings of the National Academy of Sciences of the United States of America*, 97(2), 716–21. <https://doi.org/10.1073/pnas.97.2.716>
- Henikoff, S., & Furuyama, T. (2012). The unconventional structure of centromeric nucleosomes. *Chromosoma*. <https://doi.org/10.1007/s00412-012-0372-y>
- Henikoff, S., & Gready, J. M. (2016). Epigenetics, cellular memory and gene regulation. *Current Biology*, 26(14), R644–R648. <https://doi.org/10.1016/j.cub.2016.06.011>
- Henikoff, S., & Smith, M. M. (2015). Histone variants and epigenetics. *Cold Spring Harbor Perspectives in Biology*, 7(1). <https://doi.org/10.1101/cshperspect.a019364>
- Heo, J.-I., Cho, J. H., & Kim, J.-R. (2013). HJURP Regulates Cellular Senescence in Human Fibroblasts and Endothelial Cells Via a p53-Dependent Pathway. *The Journals of Gerontology. Series A, Biological Sciences and Medical Sciences*, 68(17), 1–12. <https://doi.org/10.1093/gerona/gls257>
- Heun, P., Erhardt, S., Blower, M. D., Weiss, S., Skora, A. D., & Karpen, G. H. (2006). Mislocalization of the drosophila centromere-specific histone CID promotes formation of functional ectopic kinetochores. *Developmental Cell*, 10(3), 303–315. <https://doi.org/10.1016/j.devcel.2006.01.014>
- Hewawasam, G. S., Dhatchinamoorthy, K., Mattingly, M., Seidel, C., & Gerton, J. L. (2018). Chromatin assembly factor-1 (CAF-1) chaperone regulates Cse4 deposition into chromatin in budding yeast. *Nucleic Acids Research*, 1(March), 1–16. <https://doi.org/10.1093/nar/gky169>
- Hewawasam, G. S., Mattingly, M., Venkatesh, S., Zhang, Y., Florens, L., Workman, J. L., & Gerton, J. L. (2014). Phosphorylation by casein kinase 2 facilitates Psh1 protein-assisted degradation of Cse4 protein. *Journal of Biological Chemistry*, 289(42), 29297–29309. <https://doi.org/10.1074/jbc.M114.580589>
- Hewawasam, G., Shivaraju, M., Mattingly, M., Venkatesh, S., Martin-Brown, S., Florens, L., ... Gerton, J. L. (2010). Psh1 Is an E3 Ubiquitin Ligase that Targets the Centromeric Histone Variant Cse4. *Molecular Cell*, 40(3), 444–454. <https://doi.org/10.1016/j.molcel.2010.10.014>
- Hildebrand, E. M., & Biggins, S. (2016). Regulation of Budding Yeast CENP-A levels Prevents Misincorporation at Promoter Nucleosomes and Transcriptional Defects. *PLoS Genetics*, 12(3). <https://doi.org/10.1371/journal.pgen.1005930>
- Holliday, R., & Pugh, J. E. (1975). DNA modification mechanisms and gene activity during development. *Science (New York, N.Y.)*, 187(4173), 226–232. <https://doi.org/10.1126/science.1111098>
- Hori, T., Shang, W.-H., Toyoda, A., Misu, S., Monma, N., Ikeo, K., ... Fukagawa, T. (2014). Histone H4 Lys 20 Monomethylation of the CENP-A Nucleosome Is Essential for Kinetochores Assembly. *Developmental Cell*, 29(6), 740–749. <https://doi.org/10.1016/j.devcel.2014.05.001>
- Huang, H., Yu, Z., Zhang, S., Liang, X., Chen, J., Li, C., ... Jiao, R. (2010). Drosophila CAF-1 regulates

- HP1-mediated epigenetic silencing and pericentric heterochromatin stability. *Journal of Cell Science*, 123(16), 2853–2861. <https://doi.org/10.1242/jcs.063610>
- Jäger, H., Rauch, M., & Heidmann, S. (2005). The *Drosophila melanogaster* condensin subunit Cap-G interacts with the centromere-specific histone H3 variant CID. *Chromosoma*, 113(7), 350–361. <https://doi.org/10.1007/s00412-004-0322-4>
- Jansen, L. E. T., Black, B. E., Foltz, D. R., & Cleveland, D. W. (2007). Propagation of centromeric chromatin requires exit from mitosis. *Journal of Cell Biology*, 176(6), 795–805. <https://doi.org/10.1083/jcb.200701066>
- Jin, C., Zang, C., Wei, G., Cui, K., Peng, W., Zhao, K., & Felsenfeld, G. (2009). H3.3/H2A.Z double variant-containing nucleosomes mark nucleosome-free regions of active promoters and other regulatory regions. *Nature Genetics*, 41, 941. Retrieved from <http://dx.doi.org/10.1038/ng.409>
- Jing, R., Xi, J., Leng, Y., Chen, W., Wang, G., Jia, W., ... Zhu, S. (2017). Motifs in the amino-terminus of CENP-A are required for its accumulation within the nucleus and at the centromere. *Oncotarget*, 8(25), 40654–40667. <https://doi.org/10.18632/oncotarget.17204>
- Jones, P. A., Issa, J. P. J., & Baylin, S. (2016). Targeting the cancer epigenome for therapy. *Nature Reviews Genetics*. <https://doi.org/10.1038/nrg.2016.93>
- Kalluri, R., & Weinberg, R. A. (2009). The basics of epithelial-mesenchymal transition. *Journal of Clinical Investigation*. <https://doi.org/10.1172/JCI39104>
- Kanemaki, M., Kurokawa, Y., Matsu-Ura, T., Makino, Y., Masani, A., Okazaki, K. I., ... Tamura, T. A. (1999). TIP49b, a new RuvB-like DNA helicase, is included in a complex together with another RuvB-like DNA helicase, TIP49a. *Journal of Biological Chemistry*, 274(32), 22437–22444. <https://doi.org/10.1074/jbc.274.32.22437>
- Kasinathan, S., & Henikoff, S. (2017). Non-B-Form DNA Is Enriched at Centromeres. *Molecular Biology and Evolution*, 35(4), 949–962. Retrieved from <http://dx.doi.org/10.1093/molbev/msy010>
- Kast, J., & Klockenbusch, C. (2010). Optimization of formaldehyde cross-linking for protein interaction analysis of non-tagged integrin ?? 1. *Journal of Biomedicine and Biotechnology*, 2010. <https://doi.org/10.1155/2010/927585>
- Kaufman, P. D., Kobayashi, R., Kessler, N., & Stillman, B. (1995). The p150 and p60 subunits of chromatin assembly factor I: a molecular link between newly synthesized histones and DNA replication. *Cell*, 81(7), 1105–1114. [https://doi.org/S0092-8674\(05\)80015-7](https://doi.org/S0092-8674(05)80015-7) [pii]
- Kelly, A. D., & Issa, J.-P. J. (2017). The promise of epigenetic therapy: reprogramming the cancer epigenome. *Current Opinion in Genetics & Development*, 42, 68–77. <https://doi.org/10.1016/J.GDE.2017.03.015>
- Klare, K., Weir, J. R., Basilico, F., Zimniak, T., Massimiliano, L., Ludwigs, N., ... Musacchio, A. (2015). CENP-C is a blueprint for constitutive centromere-associated network assembly within human kinetochores. *Journal of Cell Biology*, 210(1), 11–22. <https://doi.org/10.1083/jcb.201412028>
- Krogan, N. J., Keogh, M. C., Datta, N., Sawa, C., Ryan, O. W., Ding, H., ... Greenblatt, J. F. (2003). A Snf2 Family ATPase Complex Required for Recruitment of the Histone H2A Variant Htz1. *Molecular Cell*, 12(6), 1565–1576. [https://doi.org/10.1016/S1097-2765\(03\)00497-0](https://doi.org/10.1016/S1097-2765(03)00497-0)

- Kunert, N., & Brehm, A. (2009). Novel Mi-2 related ATP-dependent chromatin remodelers. *Epigenetics*, 4(4), 209–211. <https://doi.org/10.4161/epi.8933>
- Kunert, N., Wagner, E., Murawska, M., Klinker, H., Kremmer, E., & Brehm, A. (2009). dMec: A novel Mi-2 chromatin remodelling complex involved in transcriptional repression. *EMBO Journal*, 28(5), 533–544. <https://doi.org/10.1038/emboj.2009.3>
- Kusam, S., & Dent, A. (2007). Common mechanisms for the regulation of B cell differentiation and transformation by the transcriptional repressor protein BCL-6. *Immunol Res*, 37(3), 177–186. <https://doi.org/IR:37:3:177> [pii]
- Lacoste, N., Woolfe, A., Tachiwana, H., Garea, A., Barth, T., Cantaloube, S., ... Almouzni, G. (2014). Mislocalization of the Centromeric Histone Variant CenH3/CENP-A in Human Cells Depends on the Chaperone DAXX. *Molecular Cell*, 53(4), 631–644. <https://doi.org/10.1016/j.molcel.2014.01.018>
- Lai, A. Y., & Wade, P. A. (2011). Cancer biology and NuRD: A multifaceted chromatin remodelling complex. *Nature Reviews Cancer*. <https://doi.org/10.1038/nrc3091>
- Lando, D., Endesfelder, U., Berger, H., Subramanian, L., Dunne, P. D., McColl, J., ... Laue, E. D. (2012). Quantitative single-molecule microscopy reveals that CENP-A(Cnp1) deposition occurs during G2 in fission yeast. *Open Biology*, 2(7), 120078. <https://doi.org/10.1098/rsob.120078>
- Larsen, D. H., Poinsignon, C., Gudjonsson, T., Dinant, C., Payne, M. R., Hari, F. J., ... Lukas, J. (2010). The chromatin-remodeling factor CHD4 coordinates signaling and repair after DNA damage. *Journal of Cell Biology*, 190(5), 731–740. <https://doi.org/10.1083/jcb.200912135>
- Lee, B. C. H., Lin, Z., & Yuen, K. W. Y. (2016). RbAp46/48LIN-53 Is Required for Holocentromere Assembly in *Caenorhabditis elegans*. *Cell Reports*, 14(8), 1819–1828. <https://doi.org/10.1016/j.celrep.2016.01.065>
- Lee, J. D. (2002). The ubiquitin ligase Hyperplastic discs negatively regulates hedgehog and decapentaplegic expression by independent mechanisms. *Development*, 129(24), 5697–5706. <https://doi.org/10.1242/dev.00159>
- Lewis, P. W., Elsaesser, S. J., Noh, K.-M., Stadler, S. C., & Allis, C. D. (2010). Daxx is an H3.3-specific histone chaperone and cooperates with ATRX in replication-independent chromatin assembly at telomeres. *Proceedings of the National Academy of Sciences*, 107(32), 14075–14080. <https://doi.org/10.1073/pnas.1008850107>
- Li, Y., Zhu, Z., Zhang, S., Yu, D., Yu, H., Liu, L., ... Zhu, M. (2011). Shrna-targeted centromere protein a inhibits hepatocellular carcinoma growth. *PLoS ONE*, 6(3). <https://doi.org/10.1371/journal.pone.0017794>
- Linger, J., & Tyler, J. K. (2005). The yeast histone chaperone chromatin assembly factor 1 protects against double-strand DNA-damaging agents. *Genetics*, 171(4), 1513–1522. <https://doi.org/10.1534/genetics.105.043000>
- Liu, W. H., Roemer, S. C., Port, A. M., & Churchill, M. E. A. (2012). CAF-1-induced oligomerization of histones H3/H4 and mutually exclusive interactions with Asf1 guide H3/H4 transitions among histone chaperones and DNA. *Nucleic Acids Research*, 40(22), 11229–11239. <https://doi.org/10.1093/nar/gks906>
- Loyola, A., & Almouzni, G. (2004). Histone chaperones, a supporting role in the limelight. *Biochimica et Biophysica Acta - Gene Structure and Expression*.

<https://doi.org/10.1016/j.bbaexp.2003.09.012>

Luo, J., Su, F., Chen, D., Shiloh, A., & Gu, W. (2000). Deacetylation of p53 modulates its effect on cell growth and apoptosis. *Nature*, 408(6810), 377–381. <https://doi.org/10.1038/35042612>

Ma, X. J., Salunga, R., Tuggle, J. T., Gaudet, J., Enright, E., McQuary, P., ... Sgroi, D. C. (2003). Gene expression profiles of human breast cancer progression. *Proc Natl Acad Sci U S A.*, 100, 5974–5979. <https://doi.org/10.1073/pnas.0931261100>

Maehara, K., Takahashi, K., & Saitoh, S. (2010). CENP-A Reduction Induces a p53-Dependent Cellular Senescence Response To Protect Cells from Executing Defective Mitoses. *Molecular and Cellular Biology*, 30(9), 2090–2104. <https://doi.org/10.1128/MCB.01318-09>

Magdinier, F., & Wolffe, A. P. (2001). Selective association of the methyl-CpG binding protein MBD2 with the silent p14/p16 locus in human neoplasia. *Proceedings of the National Academy of Sciences of the United States of America*, 98(9), 4990–4995. <https://doi.org/10.1073/pnas.101617298>

Maison, C., & Almouzni, G. (2004). HP1 and the dynamics of heterochromatin maintenance. *Nature Reviews Molecular Cell Biology*. <https://doi.org/10.1038/nrm1355>

Malik, H. S., & Henikoff, S. (2003). Phylogenomics of the nucleosome. *Nature Structural Biology*, 10, 882. Retrieved from <http://dx.doi.org/10.1038/nsb996>

Mansfield, E., Hersperger, E., Biggs, J., & Shearn, A. (1994). Genetic and molecular analysis of hyperplastic discs, a gene whose product is required for regulation of cell proliferation in *Drosophila melanogaster* imaginal discs and germ cells. *Developmental Biology*, 165(2), 507–526. <https://doi.org/10.1006/dbio.1994.1271>

Mansfield, R. E., Musselman, C. A., Kwan, A. H., Oliver, S. S., Garske, A. L., Davrazou, F., ... Mackay, J. P. (2011). Plant homeodomain (PHD) fingers of CHD4 are histone H3-binding modules with preference for unmodified H3K4 and methylated H3K9. *Journal of Biological Chemistry*, 286(13), 11779–11791. <https://doi.org/10.1074/jbc.M110.208207>

Marfella, C. G. A., & Imbalzano, A. N. (2007). The Chd family of chromatin remodelers. *Mutation Research - Fundamental and Molecular Mechanisms of Mutagenesis*, 618(1–2), 30–40. <https://doi.org/10.1016/j.mrfmmm.2006.07.012>

Marhold, J. (2004). The *Drosophila* MBD2/3 protein mediates interactions between the MI-2 chromatin complex and CpT/A-methylated DNA. *Development*, 131(24), 6033–6039. <https://doi.org/10.1242/dev.01531>

Marhold, J., Brehm, A., & Kramer, K. (2004). The *Drosophila* methyl-DNA binding protein MBD2/3 interacts with the NuRD complex via p55 and MI-2. *BMC Molecular Biology*, 5(1), 20. <https://doi.org/10.1186/1471-2199-5-20>

Mathew, V., Pauleau, A. L., Steffen, N., Bergner, A., Becker, P. B., & Erhardt, S. (2014). The Histone-Fold Protein CHRAC14 Influences Chromatin Composition in Response to DNA Damage. *Cell Reports*, 7(2), 321–330. <https://doi.org/10.1016/j.celrep.2014.03.008>

Mathieu, E. L., Finkernagel, F., Murawska, M., Scharfe, M., Jarek, M., & Brehm, A. (2012). Recruitment of the ATP-dependent chromatin remodeler dMi-2 to the transcribed region of active heat shock genes. *Nucleic Acids Research*, 40(11), 4879–4891. <https://doi.org/10.1093/nar/gks178>

- Matsuura, K., Huang, N. J., Cocce, K., Zhang, L., & Kornbluth, S. (2017). Downregulation of the proapoptotic protein MOAP-1 by the UBR5 ubiquitin ligase and its role in ovarian cancer resistance to cisplatin. *Oncogene*, 36(12), 1698–1706. <https://doi.org/10.1038/onc.2016.336>
- Maze, I., Noh, K. M., Soshnev, A. A., & Allis, C. D. (2014). Every amino acid matters: Essential contributions of histone variants to mammalian development and disease. *Nature Reviews Genetics*. <https://doi.org/10.1038/nrg3673>
- McKinley, K. L., & Cheeseman, I. M. (2016). The molecular basis for centromere identity and function. *Nature Reviews Molecular Cell Biology*. <https://doi.org/10.1038/nrm.2015.5>
- Mellone, B. G., & Allshire, R. C. (2003). Stretching it: Putting the CEN(P-A) in centromere. *Current Opinion in Genetics and Development*. [https://doi.org/10.1016/S0959-437X\(03\)00019-4](https://doi.org/10.1016/S0959-437X(03)00019-4)
- Mellone, B. G., Grive, K. J., Shteyn, V., Bowers, S. R., Oderberg, I., & Karpen, G. H. (2011). Assembly of drosophila centromeric chromatin proteins during mitosis. *PLoS Genetics*, 7(5). <https://doi.org/10.1371/journal.pgen.1002068>
- Melters, D. P., Bradnam, K. R., Young, H. A., Telis, N., May, M. R., Ruby, J. G., ... Chan, S. W. L. (2013). Comparative analysis of tandem repeats from hundreds of species reveals unique insights into centromere evolution. *Genome Biology*, 14(1). <https://doi.org/10.1186/gb-2013-14-1-r10>
- Mendiburo, M. J., Padeken, J., Fülöp, S., Schepers, A., & Heun, P. (2011). Drosophila CENH3 is sufficient for centromere formation. *Science*, 334(6056), 686–690. <https://doi.org/10.1126/science.1206880>
- Michael, K., Katja, S., Gislene, P., Wolfgang, Z., Barbara, W., Kim, N., & Elmar, S. (1999). Epitope tagging of yeast genes using a PCR-based strategy: more tags and improved practical routines. *Yeast*, 15(10B), 963–972. [https://doi.org/10.1002/\(SICI\)1097-0061\(199907\)15:10B<963::AID-YEA399>3.0.CO;2-W](https://doi.org/10.1002/(SICI)1097-0061(199907)15:10B<963::AID-YEA399>3.0.CO;2-W)
- Miga, K. H., Newton, Y., Jain, M., Altemose, N., Willard, H. F., & Kent, W. J. (2014). Centromere reference models for human chromosomes X and Y satellite arrays. *Genome Research*, 24(4), 697–707. <https://doi.org/10.1101/gr.159624.113>
- Mizuguchi, G., Shen, X., Landry, J., Wu, W. H., Sen, S., & Wu, C. (2004). ATP-Driven Exchange of Histone H2AZ Variant Catalyzed by SWR1 Chromatin Remodeling Complex. *Science*, 303(5656), 343–348. <https://doi.org/10.1126/science.1090701>
- Moggs, J. G., Grandi, P., Quivy, J.-P., Jonsson, Z. O., Hubscher, U., Becker, P. B., & Almouzni, G. (2000). A CAF-1-PCNA-Mediated Chromatin Assembly Pathway Triggered by Sensing DNA Damage. *Molecular and Cellular Biology*, 20(4), 1206–1218. <https://doi.org/10.1128/MCB.20.4.1206-1218.2000>
- Moncrieff, S., Moncan, M., Scialpi, F., & Ditzel, M. (2015). Regulation of hedgehog ligand expression by the N-end rule ubiquitin-protein ligase hyperplastic discs and the drosophila GSK3 β homologue, Shaggy. *PLoS ONE*, 10(9). <https://doi.org/10.1371/journal.pone.0136760>
- Moon, H. E., Cheon, H., & Lee, M. S. (2007). Metastasis-associated protein 1 inhibits p53-induced apoptosis. *Oncology Reports*, 18(5), 1311–1314.
- Moreno-Moreno, O., Medina-Giró, S., Torras-Llort, M., & Azorín, F. (2011). The F box protein partner of paired regulates stability of drosophila centromeric histone H3, CenH3 CID. *Current Biology*, 21(17), 1488–1493. <https://doi.org/10.1016/j.cub.2011.07.041>

- Moreno-Moreno, O., Torras-Llort, M., & Azorín, F. (2006). Proteolysis restricts localization of CID, the centromere-specific histone H3 variant of *Drosophila*, to centromeres. *Nucleic Acids Research*, 34(21), 6247–6255. <https://doi.org/10.1093/nar/gkl902>
- Morey, L., Barnes, K., Chen, Y., Fitzgerald-Hayes, M., & Baker, R. E. (2004). The Histone Fold Domain of Cse4 Is Sufficient for CEN Targeting and Propagation of Active Centromeres in Budding Yeast. *Eukaryotic Cell*, 3(6), 1533–1543. <https://doi.org/10.1128/EC.3.6.1533-1543.2004>
- Mori, J., Kawabata, A., Tang, H., Tadagaki, K., Mizuguchi, H., Kuroda, K., & Mori, Y. (2015). Human Herpesvirus-6 U14 Induces Cell-Cycle Arrest in G2/M Phase by Associating with a Cellular Protein, EDD. *PLOS ONE*, 10(9), e0137420. Retrieved from <https://doi.org/10.1371/journal.pone.0137420>
- Mosammaparast, N., Ewart, C. S., & Pemberton, L. F. (2002). A role for nucleosome assembly protein 1 in the nuclear transport of histones H2A and H2B. *EMBO Journal*, 21(23), 6527–6538. <https://doi.org/10.1093/emboj/cdf647>
- Müller, S., & Almouzni, G. (2014). A network of players in H3 histone variant deposition and maintenance at centromeres. *Biochimica et Biophysica Acta - Gene Regulatory Mechanisms*. <https://doi.org/10.1016/j.bbagr.2013.11.008>
- Müller, S., & Almouzni, G. (2017a). Chromatin dynamics during the cell cycle at centromeres. *Nature Reviews Genetics*. <https://doi.org/10.1038/nrg.2016.157>
- Murzina, N. V., Pei, X. Y., Zhang, W., Sparkes, M., Vicente-Garcia, J., Pratap, J. V., ... Laue, E. D. (2008). Structural Basis for the Recognition of Histone H4 by the Histone-Chaperone RbAp46. *Structure*, 16(7), 1077–1085. <https://doi.org/10.1016/j.str.2008.05.006>
- Musacchio, A., & Desai, A. (2017). A Molecular View of Kinetochore Assembly and Function. *Biology*, 6(1), 5. <https://doi.org/10.3390/biology6010005>
- Nakano, M., Okamoto, Y., Ohzeki, J., & Masumoto, H. (2003). Epigenetic assembly of centromeric chromatin at ectopic α -satellite sites on human chromosomes. *Journal of Cell Science*, 116(19), 4021 LP-4034. Retrieved from <http://jcs.biologists.org/content/116/19/4021.abstract>
- Natsume, R., Eitoku, M., Akai, Y., Sano, N., Horikoshi, M., & Senda, T. (2007). Structure and function of the histone chaperone CIA/ASF1 complexed with histones H3 and H4. *Nature*, 446, 338. Retrieved from <http://dx.doi.org/10.1038/nature05613>
- Nechemia-Arbely, Y., Fachinetti, D., Miga, K. H., Sekulic, N., Soni, G. V., Kim, D. H., ... Cleveland, D. W. (2017). Human centromeric CENP-A chromatin is a homotypic, octameric nucleosome at all cell cycle points. *The Journal of Cell Biology*, 216(3), 607–621. <https://doi.org/10.1083/jcb.201608083>
- Nicolson, G. L., Nawa, A., Toh, Y., Taniguchi, S., Nishimori, K., & Moustafa, A. (2003). Tumor metastasis-associated human MTA1 gene and its MTA1 protein product: Role in epithelial cancer cell invasion, proliferation and nuclear regulation. *Clinical and Experimental Metastasis*. <https://doi.org/10.1023/A:1022534217769>
- Niikura, Y., Kitagawa, R., & Kitagawa, K. (2017). CENP-A Ubiquitylation Is Required for CENP-A Deposition at the Centromere. *Developmental Cell*, 40(1), 7–8. <https://doi.org/10.1016/j.DEVCEL.2016.12.020>
- Niikura, Y., Kitagawa, R., Ogi, H., Abdulle, R., Pagala, V., & Kitagawa, K. (2015a). CENP-A K124Ubiquitylation Is Required for CENP-A Deposition at the Centromere. *Developmental Cell*,

32(5). <https://doi.org/10.1016/j.devcel.2015.01.024>

- Nye, J., Melters, D. P., & Dalal, Y. (2018). The Art of War: harnessing the epigenome against cancer [version 1; referees: 4 approved]. *F1000Research*, 7(141). <https://doi.org/10.12688/f1000research.12833.1>
- Ogiyama, Y., Ohno, Y., Kubota, Y., & Ishii, K. (2013). Epigenetically induced paucity of histone H2A.Z stabilizes fission-yeast ectopic centromeres. *Nature Structural & Molecular Biology*, 20, 1397. Retrieved from <http://dx.doi.org/10.1038/nsmb.2697>
- Ohkuni, K., Takahashi, Y., Fulp, A., Lawrimore, J., Au, W.-C., Pasupala, N., ... Basrai, M. A. (2016). SUMO-targeted ubiquitin ligase (STUbL) Slx5 regulates proteolysis of centromeric histone H3 variant Cse4 and prevents its mislocalization to euchromatin. *Molecular Biology of the Cell*, 27(9), 1500–1510. <https://doi.org/10.1091/mbc.E15-12-0827>
- Okada, M., Okawa, K., Isobe, T., & Fukagawa, T. (2009). CENP-H– containing Complex Facilitates Centromere Deposition of CENP-A in Cooperation with FACT and CHD1. *Molecular Biology of the Cell*, 20, 3986–3995. <https://doi.org/10.1091/mbc.E09>
- Olszak, A. M., Van Essen, D., Pereira, A. J., Diehl, S., Manke, T., Maiato, H., ... Heun, P. (2011). Heterochromatin boundaries are hotspots for de novo kinetochore formation. *Nature Cell Biology*, 13(7), 799–808. <https://doi.org/10.1038/ncb2272>
- Pauleau, A. L., & Erhardt, S. (2011). Centromere regulation: New players, new rules, new questions. *European Journal of Cell Biology*, 90(10), 805–810. <https://doi.org/10.1016/j.ejcb.2011.04.016>
- Pearson, C. G., Yeh, E., Gardner, M., Odde, D., Salmon, E. D., & Bloom, K. (2004). Stable kinetochore-microtubule attachment constrains centromere positioning in metaphase. *Current Biology*, 14(21), 1962–1967. <https://doi.org/10.1016/j.cub.2004.09.086>
- Pertceva, J. a, Dorogova, N. V, Bolobolova, E. U., Nerusheva, O. O., Fedorova, S. a, & Omelyanchuk, L. V. (2010). The role of Drosophila hyperplastic discs gene in spermatogenesis. *Cell Biology International*, 34(10), 991–6. <https://doi.org/10.1042/CBI20100105>
- Polo, S. E., Kaidi, A., Baskcomb, L., Galanty, Y., & Jackson, S. P. (2010). Regulation of DNA-damage responses and cell-cycle progression by the chromatin remodelling factor CHD4. *EMBO Journal*, 29(18), 3130–3139. <https://doi.org/10.1038/emboj.2010.188>
- Polo, S. E., Roche, D., & Almouzni, G. (2006). New Histone Incorporation Marks Sites of UV Repair in Human Cells. *Cell*, 127(3), 481–493. <https://doi.org/10.1016/j.cell.2006.08.049>
- Probst, A. V., & Almouzni, G. (2011). Heterochromatin establishment in the context of genome-wide epigenetic reprogramming. *Trends in Genetics*. <https://doi.org/10.1016/j.tig.2011.02.002>
- Przewlaka, M. R., & Glover, D. M. (2009). The Kinetochore and the Centromere: A Working Long Distance Relationship. *Annual Review of Genetics*, 43(1), 439–465. <https://doi.org/10.1146/annurev-genet-102108-134310>
- Qiu, J. J., Guo, J. J., Lv, T. J., Jin, H. Y., Ding, J. X., Feng, W. W., ... Hua, K. Q. (2013). Prognostic value of centromere protein-A expression in patients with epithelial ovarian cancer. *Tumour Biol*, 34(5), 2971–2975. <https://doi.org/10.1007/s13277-013-0860-6>
- Quénet, D., & Dalal, Y. (2014). A long non-coding RNA is required for targeting centromeric protein A to the human centromere. *eLife*, 3, e03254. <https://doi.org/10.7554/eLife.03254>

- Rai, A. N., Vargas, M. L., Wang, L., Andersen, E. F., Miller, E. L., & Simon, J. A. (2013). Elements of the Polycomb Repressor SU(Z)12 Needed for Histone H3-K27 Methylation, the Interface with E(Z), and In Vivo Function. *Molecular and Cellular Biology*, 33(24), 4844–4856. <https://doi.org/10.1128/MCB.00307-13>
- Ramírez, J., & Hagman, J. (2009). The Mi-2/NuRD complex: A critical epigenetic regulator of hematopoietic development, differentiation and cancer. *Epigenetics*, 4(8), 532–536. <https://doi.org/10.4161/epi.4.8.10108>
- Ranjitkar, P., Press, M. O., Yi, X., Baker, R., MacCoss, M. J., & Biggins, S. (2010). An E3 ubiquitin ligase prevents ectopic localization of the centromeric histone H3 variant via the centromere targeting domain. *Molecular Cell*, 40(3), 455–64. <https://doi.org/10.1016/j.molcel.2010.09.025>
- Ratnakumar, K., Duarte, L. F., LeRoy, G., Hasson, D., Smeets, D., Vardabasso, C., ... Bernstein, E. (2012). ATRX-mediated chromatin association of histone variant macroH2A1 regulates α -globin expression. *Genes and Development*, 26(5), 433–438. <https://doi.org/10.1101/gad.179416.111>
- Ray-Gallet, D., Quivy, J. P., Scamps, C., Martini, E. M. D., Lipinski, M., & Almouzni, G. (2002). HIRA is critical for a nucleosome assembly pathway independent of DNA synthesis. *Molecular Cell*, 9(5), 1091–1100. [https://doi.org/10.1016/S1097-2765\(02\)00526-9](https://doi.org/10.1016/S1097-2765(02)00526-9)
- Reddy, B. A., Bajpe, P. K., Bassett, A., Moshkin, Y. M., Kozhevnikova, E., Bezstarosti, K., ... Verrijzer, C. P. (2010). Drosophila Transcription Factor Tramtrack69 Binds MEP1 To Recruit the Chromatin Remodeler NuRD. *Molecular and Cellular Biology*, 30(21), 5234–5244. <https://doi.org/10.1128/MCB.00266-10>
- Reynolds, N., Salmon-Divon, M., Dvinge, H., Hynes-Allen, A., Balasooriya, G., Leaford, D., ... Hendrich, B. (2012). NuRD-mediated deacetylation of H3K27 facilitates recruitment of Polycomb Repressive Complex 2 to direct gene repression. *EMBO Journal*, 31(3), 593–605. <https://doi.org/10.1038/emboj.2011.431>
- Ribich, S., Harvey, D., & Copeland, R. A. (2017). Drug Discovery and Chemical Biology of Cancer Epigenetics. *Cell Chemical Biology*. <https://doi.org/10.1016/j.chembiol.2017.08.020>
- Roberts, S. M., & Winston, F. (1997). Essential functional interactions of SAGA, a *Saccharomyces cerevisiae* complex of spt, ada, and gcn5 proteins, with the snf/swi and srb/mediator complexes. *Genetics*, 147(2), 451–465.
- Rogers, S. L., & Rogers, G. C. (2008). Culture of *Drosophila* S2 cells and their use for RNAi-mediated loss-of-function studies and immunofluorescence microscopy. *Nature Protocols*, 3, 606. Retrieved from <http://dx.doi.org/10.1038/nprot.2008.18>
- Rosa, J. L. da, Holik, J., Green, E. M., Rando, O. J., & Kaufman, P. D. (2011). Overlapping Regulation of CenH3 Localization and Histone H3 Turnover by CAF-1 and HIR Proteins in *Saccharomyces cerevisiae*. *Genetics*, 187(1), 9–19. <https://doi.org/10.1534/genetics.110.123117>
- Rošić, S., & Erhardt, S. (2016). No longer a nuisance: Long non-coding RNAs join CENP-A in epigenetic centromere regulation. *Cellular and Molecular Life Sciences*. <https://doi.org/10.1007/s00018-015-2124-7>
- Rošić, S., Köhler, F., & Erhardt, S. (2014). Repetitive centromeric satellite RNA is essential for kinetochore formation and cell division. *Journal of Cell Biology*. <https://doi.org/10.1083/jcb.201404097>
- Roulland, Y., Ouarrhni, K., Naidenov, M., Ramos, L., Shuaib, M., Syed, S. H., ... Dimitrov, S. (2016).

- The Flexible Ends of CENP-A Nucleosome Are Required for Mitotic Fidelity. *Molecular Cell*, 63(4), 674–685. <https://doi.org/10.1016/j.molcel.2016.06.023>
- Sambrook, J., & W Russell, D. (2001). Molecular Cloning: A Laboratory Manual. *Cold Spring Harbor Laboratory Press, Cold Spring Harbor, NY*, 999. [https://doi.org/10.1016/0092-8674\(90\)90210-6](https://doi.org/10.1016/0092-8674(90)90210-6)
- Sansom, O. J., Maddison, K., & Clarke, A. R. (2007). Mechanisms of disease: methyl-binding domain proteins as potential therapeutic targets in cancer. *Nat Clin Pract Oncol*, 4(5), 305–315. Retrieved from http://www.ncbi.nlm.nih.gov/entrez/query.fcgi?cmd=Retrieve&db=PubMed&dopt=Citation&list_uids=17464338
- Schramm, C., Elliott, S., Shevchenko, A., & Schiebel, E. (2000). The Bbp1p-Mps2p complex connects the SPB to the nuclear envelope and is essential for SPB duplication. *EMBO J*, 19(3), 421–433. <https://doi.org/10.1093/emboj/19.3.421>
- Schuh, M., Lehner, C. F., & Heidmann, S. (2007). Incorporation of Drosophila CID/CENP-A and CENP-C into Centromeres during Early Embryonic Anaphase. *Current Biology*, 17(3), 237–243. <https://doi.org/10.1016/j.cub.2006.11.051>
- Schwartz, Y. B., & Cavalli, G. (2017). Three-dimensional genome organization and function in Drosophila. *Genetics*, 205(1), 5–24. <https://doi.org/10.1534/genetics.115.185132>
- Scott, K. C., & Sullivan, B. A. (2014). Neocentromeres: A place for everything and everything in its place. *Trends in Genetics*. <https://doi.org/10.1016/j.tig.2013.11.003>
- Scott, K. C., White, C. V., & Willard, H. F. (2007). An RNA polymerase III-dependent heterochromatin barrier at fission yeast centromere 1. *PLoS ONE*, 2(10). <https://doi.org/10.1371/journal.pone.0001099>
- Sequeira-Mendes, J., & Gutierrez, C. (2016). Genome architecture: from linear organisation of chromatin to the 3D assembly in the nucleus. *Chromosoma*. <https://doi.org/10.1007/s00412-015-0538-5>
- Serebriiskii, I., Estojak, J., Berman, M., & Golemis, E. A. (2000). Approaches to detecting false positives in yeast two-hybrid systems. *BioTechniques*, 28(2), 328–336.
- Sevim, V., Bashir, A., Chin, C. S., & Miga, K. H. (2016). Alpha-CENTAURI: Assessing novel centromeric repeat sequence variation with long read sequencing. *Bioinformatics*, 32(13), 1921–1924. <https://doi.org/10.1093/bioinformatics/btw101>
- Shang, W. H., Hori, T., Westhorpe, F. G., Godek, K. M., Toyoda, A., Misu, S., ... Fukagawa, T. (2016a). Acetylation of histone H4 lysine 5 and 12 is required for CENP-A deposition into centromeres. *Nature Communications*, 7. <https://doi.org/10.1038/ncomms13465>
- Shearer, R. F., Ionomou, M., Watts, C. K. W., & Saunders, D. N. (2015). Functional Roles of the E3 Ubiquitin Ligase UBR5 in Cancer. *Molecular Cancer Research*, 13(12), 1523–1532. <https://doi.org/10.1158/1541-7786.MCR-15-0383>
- Shelby, R. D., Monier, K., & Sullivan, K. F. (2000). Chromatin assembly at kinetochores is uncoupled from DNA replication. *Journal of Cell Biology*, 151(5), 1113–1118. <https://doi.org/10.1083/jcb.151.5.1113>
- Shibahara, K. I., & Stillman, B. (1999). Replication-dependent marking of DNA by PCNA facilitates CAF-1-coupled inheritance of chromatin. *Cell*, 96(4), 575–585. <https://doi.org/10.1016/S0092->

- Shimono, K., Shimono, Y., Shimokata, K., Ishiguro, N., & Takahashi, M. (2005). Microspherule protein 1, Mi-2??, and RET finger protein associate in the nucleolus and up-regulate ribosomal gene transcription. *Journal of Biological Chemistry*, 280(47), 39436–39447. <https://doi.org/10.1074/jbc.M507356200>
- Shrestha, R. L., Ahn, G. S., Staples, M. I., Sathyan, K. M., Karpova, T. S., Foltz, D. R., & Basrai, M. A. (2017). Mislocalization of centromeric histone H3 variant CENP-A contributes to chromosomal instability (CIN) in human cells. *Oncotarget*, 8(29), 46781–46800. <https://doi.org/10.18632/oncotarget.18108>
- Shuaib, M., Ouarrhni, K., Dimitrov, S., & Hamiche, A. (2010). HJURP binds CENP-A via a highly conserved N-terminal domain and mediates its deposition at centromeres. *Proceedings of the National Academy of Sciences of the United States of America*, 107(4), 1349–1354. <https://doi.org/10.1073/pnas.0913709107>
- Silva, M. C. C., Bodor, D. L., Stellfox, M. E., Martins, N. M. C., Hocheegger, H., Foltz, D. R., & Jansen, L. E. T. (2018). Cdk Activity Couples Epigenetic Centromere Inheritance to Cell Cycle Progression. *Developmental Cell*, 22(1), 52–63. <https://doi.org/10.1016/j.devcel.2011.10.014>
- Singh, N., Basnet, H., Wiltshire, T. D., Mohammad, D. H., Thompson, J. R., Heroux, A., ... Mer, G. (2012). Dual recognition of phosphoserine and phosphotyrosine in histone variant H2A.X by DNA damage response protein MCPH1. *Proceedings of the National Academy of Sciences*, 109(36), 14381–14386. <https://doi.org/10.1073/pnas.1212366109>
- Sitbon, D., Podsypanina, K., Yadav, T., & Almouzni, G. (2017). Shaping Chromatin in the Nucleus: The Bricks and the Architects. *Cold Spring Harbor Symposia on Quantitative Biology*, 33753. <https://doi.org/10.1101/sqb.2017.82.033753>
- Smeenk, G., Wiegant, W. W., Vrolijk, H., Solari, A. P., Pastink, A., & Van Attikum, H. (2010). The NuRD chromatin-remodeling complex regulates signaling and repair of DNA damage. *Journal of Cell Biology*, 190(5), 741–749. <https://doi.org/10.1083/jcb.201001048>
- Smits, A. H., Jansen, P. W. T. C., Poser, I., Hyman, A. A., & Vermeulen, M. (2013). Stoichiometry of chromatin-associated protein complexes revealed by label-free quantitative mass spectrometry-based proteomics. *Nucleic Acids Research*, 41(1). <https://doi.org/10.1093/nar/gks941>
- Song, J. J., Garlick, J. D., & Kingston, R. E. (2008). Structural basis of histone H4 recognition by p55. *Genes and Development*, 22(10), 1313–1318. <https://doi.org/10.1101/gad.1653308>
- Song, Y., He, F., Xie, G., Guo, X., Xu, Y., Chen, Y., ... Jiao, R. (2007). CAF-1 is essential for Drosophila development and involved in the maintenance of epigenetic memory. *Developmental Biology*, 311(1), 213–222. <https://doi.org/10.1016/j.ydbio.2007.08.039>
- Soshnev, A. A., Josefowicz, S. Z., & Allis, C. D. (2016). Greater Than the Sum of Parts: Complexity of the Dynamic Epigenome. *Molecular Cell*, 62(5), 681–694. <https://doi.org/10.1016/J.MOLCEL.2016.05.004>
- Sperlazza, J., Rahmani, M., Beckta, J., Aust, M., Hawkins, E., Wang, S. Z., ... Ginder, G. D. (2015). Depletion of the chromatin remodeler CHD4 sensitizes AML blasts to genotoxic agents and reduces tumor formation. *Blood*, 126(12), 1462–1472. <https://doi.org/10.1182/blood-2015-03-631606>

- Spruijt, C. G., Bartels, S. J. J., Brinkman, A. B., Tjeertes, J. V., Poser, I., Stunnenberg, H. G., & Vermeulen, M. (2010). CDK2AP1/DOC-1 is a bona fide subunit of the Mi-2/NuRD complex. *Molecular BioSystems*, 6(9), 1700. <https://doi.org/10.1039/c004108d>
- Stankovic, A., Guo, L. Y., Mata, J. F., Bodor, D. L., Cao, X.-J., Bailey, A. O., ... Jansen, L. E. T. (2017). A dual inhibitory mechanism sufficient to maintain cell cycle restricted CENP-A assembly. *Molecular Cell*, 65(2), 231–246. <https://doi.org/10.1016/j.molcel.2016.11.021>
- Steffen, P. A., & Ringrose, L. (2014). What are memories made of? How polycomb and trithorax proteins mediate epigenetic memory. *Nature Reviews Molecular Cell Biology*. <https://doi.org/10.1038/nrm3789>
- Stokes, D. G., & Perry, R. P. (1995). DNA-binding and chromatin localization properties of CHD1. *Molecular and Cellular Biology*, 15(5), 2745–2753. <https://doi.org/10.1128/MCB.15.5.2745>
- Stoler, S., Rogers, K., Weitze, S., Morey, L., Fitzgerald-Hayes, M., & Baker, R. E. (2007). Scm3, an essential *Saccharomyces cerevisiae* centromere protein required for G₂/M progression and Cse4 localization. *Proceedings of the National Academy of Sciences*, 104(25), 10571 LP-10576. Retrieved from <http://www.pnas.org/content/104/25/10571.abstract>
- Sullivan, B. A., Blower, M. D., & Karpen, G. H. (2001). Determining centromere identity: Cyclical stories and forking paths. *Nature Reviews Genetics*. <https://doi.org/10.1038/35084512>
- Sullivan, B. A., & Karpen, G. H. (2004). Centromeric chromatin exhibits a histone modification pattern that is distinct from both euchromatin and heterochromatin. *Nature Structural and Molecular Biology*, 11(11), 1076–1083. <https://doi.org/10.1038/nsmb845>
- Sullivan, L. L., Boivin, C. D., Mravinac, B., Song, I. Y., & Sullivan, B. A. (2011). Genomic size of CENP-A domain is proportional to total alpha satellite array size at human centromeres and expands in cancer cells. *Chromosome Research*, 19(4), 457. <https://doi.org/10.1007/s10577-011-9208-5>
- Sun, X., Clermont, P. L., Jiao, W., Helgason, C. D., Gout, P. W., Wang, Y., & Qu, S. (2016). Elevated expression of the centromere protein-A(CENP-A)-encoding gene as a prognostic and predictive biomarker in human cancers. *International Journal of Cancer*, 139(4), 899–907. <https://doi.org/10.1002/ijc.30133>
- Suzuki, A., Badger, B. L., & Salmon, E. D. (2015). A quantitative description of Ndc80 complex linkage to human kinetochores. *Nature Communications*, 6. <https://doi.org/10.1038/ncomms9161>
- Tachiwana, H., Kagawa, W., Shiga, T., Osakabe, A., Miya, Y., Saito, K., ... Kurumizaka, H. (2011). Crystal structure of the human centromeric nucleosome containing CENP-A. *Nature*. <https://doi.org/10.1038/nature10258>
- Tachiwana, H., Müller, S., Blümer, J., Klare, K., Musacchio, A., & Almouzni, G. (2015). HJURP involvement in de novo CenH3(CENP-A) and CENP-C recruitment. *Cell Reports*, 11(1), 22–32. <https://doi.org/10.1016/j.celrep.2015.03.013>
- Tagami, H., Ray-Gallet, D., Almouzni, G., & Nakatani, Y. (2004). Histone H3.1 and H3.3 Complexes Mediate Nucleosome Assembly Pathways Dependent or Independent of DNA Synthesis. *Cell*, 116(1), 51–61. [https://doi.org/10.1016/S0092-8674\(03\)01064-X](https://doi.org/10.1016/S0092-8674(03)01064-X)
- Takayama, Y., Sato, H., Saitoh, S., Ogiyama, Y., Masuda, F., & Takahashi, K. (2007). Biphasic Incorporation of Centromeric Histone CENP-A in Fission Yeast. *Molecular Biology of the Cell*, 19(2), 682–690. <https://doi.org/10.1091/mbc.E07-05-0504>

- Talbert, P. B., & Henikoff, S. (2010). Histone variants--ancient wrap artists of the epigenome. *Nat Rev Mol Cell Biol*, 11(4), 264–275. <https://doi.org/nrm2861> [pii]\n10.1038/nrm2861
- Talbert, P. B., & Henikoff, S. (2016). Histone variants on the move: substrates for chromatin dynamics. *Nature Reviews Molecular Cell Biology*, 18, 115. Retrieved from <http://dx.doi.org/10.1038/nrm.2016.148>
- Tamkun, J. W., Deuring, R., Scott, M. P., Kissinger, M., Pattatucci, A. M., Kaufman, T. C., & Kennison, J. A. (1992). brahma: A regulator of Drosophila homeotic genes structurally related to the yeast transcriptional activator SNF 2 SWI 2. *Cell*, 68(3), 561–572. [https://doi.org/10.1016/0092-8674\(92\)90191-E](https://doi.org/10.1016/0092-8674(92)90191-E)
- Timinszky, G., Till, S., Hassa, P. O., Hothorn, M., Kustatscher, G., Nijmeijer, B., ... Ladurner, A. G. (2009). A macrodomain-containing histone rearranges chromatin upon sensing PARP1 activation. *Nature Structural and Molecular Biology*, 16(9), 923–929. <https://doi.org/10.1038/nsmb.1664>
- Toh, Y., & Nicolson, G. L. (2009). The role of the MTA family and their encoded proteins in human cancers: molecular functions and clinical implications. *Clinical & Experimental Metastasis*, 26(3), 215–227. <https://doi.org/10.1007/s10585-008-9233-8>
- Tomaić, V., Pim, D., Thomas, M., Massimi, P., Myers, M. P., & Banks, L. (2011). Regulation of the Human Papillomavirus Type 18 E6/E6AP Ubiquitin Ligase Complex by the HECT Domain-Containing Protein EDD. *Journal of Virology*, 85(7), 3120–3127. <https://doi.org/10.1128/JVI.02004-10>
- Tomonaga, T., Matsushita, K., & Yamaguchi, S. (2003). Overexpression and Mistargeting of Centromere Protein-A in Human Primary Colorectal Cancer Overexpression and Mistargeting of Centromere Protein-A in Human Primary, 3511–3516.
- Torchy, M. P., Hamiche, A., & Klaholz, B. P. (2015). Structure and function insights into the NuRD chromatin remodeling complex. *Cellular and Molecular Life Sciences*. <https://doi.org/10.1007/s00018-015-1880-8>
- Toto, M., D'Angelo, G., & Corona, D. F. V. (2014). Regulation of ISWI chromatin remodelling activity. *Chromosoma*. <https://doi.org/10.1007/s00412-013-0447-4>
- Tsukuda, T., Fleming, A. B., Nickoloff, J. A., & Osley, M. A. (2005). Chromatin remodelling at a DNA double-strand break site in *Saccharomyces cerevisiae*. *Nature*, 438(7066), 379–383. <https://doi.org/10.1038/nature04148>
- Turner, B. M. (2002). Cellular memory and the histone code. *Cell*. [https://doi.org/10.1016/S0092-8674\(02\)01080-2](https://doi.org/10.1016/S0092-8674(02)01080-2)
- Tyagi, M., Imam, N., Verma, K., & Patel, A. K. (2016). Chromatin remodelers: We are the drivers!! *Nucleus*, 7(4), 388–404. <https://doi.org/10.1080/19491034.2016.1211217>
- Tyler, J. K., Bulger, M., Kamakaka, R. T., Kobayashi, R., & Kadonaga, J. T. (1996). The p53 subunit of Drosophila chromatin assembly factor 1 is homologous to a histone deacetylase-associated protein. *Molecular and Cellular Biology*, 16(11), 6149–6159. <https://doi.org/10.1128/MCB.16.11.6149>
- Tyler, J. K., Collins, K. A., Prasad-Sinha, J., Amiot, E., Bulger, M., Harte, P. J., ... Kadonaga, J. T. (2001). Interaction between the Drosophila CAF-1 and ASF1 Chromatin Assembly Factors. *Molecular and Cellular Biology*, 21(19), 6574–6584. <https://doi.org/10.1128/MCB.21.19.6574-6584.2001>

- Valente, V., Serafim, R. B., de Oliveira, L. C., Adorni, F. S., Torrieri, R., da Cunha Tirapelli, D. P., ... Carlotti, C. G. (2013). Modulation of HJURP (Holliday Junction-Recognizing Protein) Levels Is Correlated with Glioblastoma Cells Survival. *PLoS ONE*, 8(4). <https://doi.org/10.1371/journal.pone.0062200>
- Van Attikum, H., Fritsch, O., & Gasser, S. M. (2007). Distinct roles for SWR1 and INO80 chromatin remodeling complexes at chromosomal double-strand breaks. *EMBO Journal*, 26(18), 4113–4125. <https://doi.org/10.1038/sj.emboj.7601835>
- Varga-Weisz, P. D., Wilm, M., Bonte, E., Dumas, K., Mann, M., & Becker, P. B. (1997). Chromatin-remodelling factor CHRAC contains the ATPases ISWI and topoisomerase II. *Nature*, 388(6642), 598–602. <https://doi.org/10.1038/41587>
- Voullaire, L. E., Slater, H. R., Petrovic, V., & Choo, K. H. (1993). A functional marker centromere with no detectable alpha-satellite, satellite III, or CENP-B protein: activation of a latent centromere? *American Journal of Human Genetics*, 52(6), 1153–1163. Retrieved from <http://www.ncbi.nlm.nih.gov/pmc/articles/PMC1682274/>
- W., S. J., Mehdi, S. T., Mario, T., G., S. A. P., J., L. M., Lou, B., ... P., M. J. (2016). The MTA1 subunit of the nucleosome remodeling and deacetylase complex can recruit two copies of RBBP4/7. *Protein Science*, 25(8), 1472–1482. <https://doi.org/10.1002/pro.2943>
- Waddington, C. H. (1942). The epigenotype. *Endeavour*, (1), 18–20. <https://doi.org/10.1093/ije/dyr184>
- Wade, P. A., Geggion, A., Jones, P. L., Ballestar, E., Aubry, F., & Wolffe, A. P. (1999). Mi-2 complex couples DNA methylation to chromatin remodelling and histone deacetylation. *Nature Genetics*, 23(1), 62–66. <https://doi.org/10.1038/12664>
- Waldmann, T., & Schneider, R. (2013). Targeting histone modifications - epigenetics in cancer. *Current Opinion in Cell Biology*, 25(2), 184–189. <https://doi.org/10.1016/j.ceb.2013.01.001>
- Wang, G. G., Allis, C. D., & Chi, P. (2007). Chromatin remodeling and cancer, Part II: ATP-dependent chromatin remodeling. *Trends in Molecular Medicine*, 13(9), 373–80. <https://doi.org/10.1016/j.molmed.2007.07.004>
- Wang, G., Tang, X., Chen, Y., Cao, J., Huang, Q., Ling, X., ... Lin, X. (2014). Hyperplastic discs differentially regulates the transcriptional outputs of hedgehog signaling. *Mechanisms of Development*, 133, 117–125. <https://doi.org/10.1016/j.mod.2014.05.002>
- Wang, X., Singh, S., Jung, H.-Y., Yang, G., Jun, S., Sastry, K. J., & Park, J.-I. (2013). HIV-1 Vpr protein inhibits telomerase activity via the EDD-DDB1-VPRBP E3 ligase complex. *The Journal of Biological Chemistry*, 288(22), 15474–80. <https://doi.org/10.1074/jbc.M112.416735>
- Waterborg, J. H. (2012). Evolution of histone H3: emergence of variants and conservation of post-translational modification sites. *Biochem Cell Biol*, 90(1), 79–95. <https://doi.org/10.1139/o11-036>
- Wilson, B. G., & Roberts, C. W. M. (2011). SWI/SNF nucleosome remodellers and cancer. *Nature Reviews Cancer*, 11, 481. Retrieved from <http://dx.doi.org/10.1038/nrc3068>
- Winkler, D. D., Zhou, H., Dar, M. A., Zhang, Z., & Luger, K. (2012). Yeast CAF-1 assembles histone (H3-H4)2tetramers prior to DNA deposition. *Nucleic Acids Research*, 40(20), 10139–10149. <https://doi.org/10.1093/nar/gks812>

- Xia, L., Huang, W., Bellani, M., Seidman, M. M., Wu, K., Fan, D., ... Baylin, S. B. (2017). CHD4 Has Oncogenic Functions in Initiating and Maintaining Epigenetic Suppression of Multiple Tumor Suppressor Genes. *Cancer Cell*, 31(5), 653–668.e7. <https://doi.org/10.1016/j.ccell.2017.04.005>
- Xue, Y., Wong, J., Moreno, G. T., Young, M. K., Côté, J., & Wang, W. (1998). NURD, a novel complex with both ATP-dependent chromatin-remodeling and histone deacetylase activities. *Molecular Cell*, 2(6), 851–861. [https://doi.org/10.1016/S1097-2765\(00\)80299-3](https://doi.org/10.1016/S1097-2765(00)80299-3)
- Yadon, A. N., & Tsukiyama, T. (2011). SnapShot: Chromatin remodeling: ISWI. *Cell*. <https://doi.org/10.1016/j.cell.2011.01.019>
- Yang, J., Zhang, X., Feng, J., Leng, H., Li, S., Xiao, J., ... Li, Q. (2016). The Histone Chaperone FACT Contributes to DNA Replication-Coupled Nucleosome Assembly. *Cell Reports*, 14(5), 1128–1141. <https://doi.org/10.1016/j.celrep.2015.12.096>
- Yang, X.-J., & Seto, E. (2008). The Rpd3/Hda1 family of lysine deacetylases: from bacteria and yeast to mice and men. *Nature Reviews Molecular Cell Biology*, 9, 206. Retrieved from <http://dx.doi.org/10.1038/nrm2346>
- Yoo, Y. G., Kong, G., & Lee, M. O. (2006). Metastasis-associated protein 1 enhances stability of hypoxia-inducible factor-1?? protein by recruiting histone deacetylase 1. *EMBO Journal*, 25(6), 1231–1241. <https://doi.org/10.1038/sj.emboj.7601025>
- Yoshida, T., Hazan, I., Zhang, J., Ng, S. Y., Naito, T., Snippert, H. J., ... Georgopoulos, K. (2008). The role of the chromatin remodeler Mi-2 β in hematopoietic stem cell self-renewal and multilineage differentiation. *Genes and Development*, 22(9), 1174–1189. <https://doi.org/10.1101/gad.1642808>
- Yu, Z., Zhou, X., Wang, W., Deng, W., Fang, J., Hu, H., ... Li, G. (2015). Dynamic phosphorylation of CENP-A at Ser68 orchestrates its cell-cycle-dependent deposition at centromeres. *Developmental Cell*, 32(1), 68–81. <https://doi.org/10.1016/j.devcel.2014.11.030>
- Zasadzińska, E., Barnhart-Dailey, M. C., Kuich, P. H. J. L., & Foltz, D. R. (2013). Dimerization of the CENP-A assembly factor HJURP is required for centromeric nucleosome deposition. *EMBO Journal*, 32(15), 2113–2124. <https://doi.org/10.1038/emboj.2013.142>
- Zhang, W., Aubert, A., Gomez de Segura, J. M., Karuppasamy, M., Basu, S., Murthy, A. S., ... Laue, E. D. (2016). The Nucleosome Remodeling and Deacetylase Complex NuRD Is Built from Preformed Catalytically Active Sub-modules. *Journal of Molecular Biology*, 428(14), 2931–2942. <https://doi.org/10.1016/j.jmb.2016.04.025>
- Zhao, H., Winogradoff, D., Bui, M., Dalal, Y., & Papoian, G. A. (2016). Promiscuous Histone Mis-Assembly Is Actively Prevented by Chaperones. *Journal of the American Chemical Society*, 138(40), 13207–13218. <https://doi.org/10.1021/jacs.6b05355>

LIST OF ABBREVIATIONS

µg	microgram
µl	microliter
µm	micrometer
ac	Acetyl
ATRX	Alpha Thalassemia/Mental Retardation Syndrome X-Linked
bp	base pairs
Bw	brown
CALI	Chromosome alignment defect I
CATD	CENP-A targeting domain
CCAN	Constitutive Centromere Associated Network
CDE	Centromere DNA element
CENP-A	Centromeric Protein-A
CENP-C	Centromeric Protein-C
Ci	Cubitus interruptus
CID	Centromere identifier
cm	centimeter
°C	Degrees Celsius
Co-IP	Co-Immunoprecipitation
CUL3	Cullin 3
DAPI	4, 6-Diamidin-2-phenylindol
Daxx	Death-domain associated protein
ddH ₂ O	Double distilled water
DNA	Deoxyribonucleic acid
dsRNA	Double-stranded RNA
<i>E. coli</i>	<i>Escherichia coli</i>
EDTA	Ethylenediaminetetraacetic acid
FACT	Facilitates chromatin transcription
FBS	Fetal bovine serum
g	grams
GFP	Green fluorescent protein
HAC	Human artificial chromosome
H2A	Histone 2A
H2B	Histone 2B
H3	Histone 3
H4	Histone 4
HECT	Homologous to E6AP Carboxy terminus
HFD	Histone fold domain
Hh	Hedgehog
HJURP	Holliday junction-recognition protein
h	hour
hyd	Hyperplastic discs
IF	Immunofluorescence

kb	Kilobase pairs
kDa	KiloDalton
LacI	Lac inhibitor
LacO	Lac operon
M	Molar
me	Methyl
min	minutes
ml	mililitre
mRNA	Messenger RNA
NLS	Nuclear localization signal
NuRD	Nucleosome remodeling and deacetylase
o/e	overexpression
o/n	overnight
ORF	Open reading frame
PAGE	Poly-acrylamide gel electrophoresis
PBS	Phosphate buffered saline
PCR	Polymerase chain reaction
PFA	Paraformaldehyde
Psh1	Pob3/Spt16 histone associated
PTM	Posttranslational modification
qPCR	Quantitative PCR
RDX	Roadkill
RNA	Ribonucleic acid
RNAi	RNA interference
RNAPII	RNA polymerase II
ROI	Region of interest
rpm	Revolution per minute
RT	Room temperature
RT-PCR	Reverse transcription PCR
S2	<i>Drosophila</i> Schneider 2 cell line
SDS	Sodium-dodecyl sulfate
SFM	Serum-free medium
SM	Serum-containing medium
TF	Transcription factor
UAS	Upstream activating sequence
Ubi	Ubiquitin
UV	Ultraviolet
VDRC	Vienna <i>Drosophila</i> RNAi Center
WB	Western blot
WT	Wild type
Xlink	crosslink
Y2H	Yeast two hybrid

LIST OF FIGURES

Figure 1.1 The epigenetic information in the cell.....	16
Figure 1.2 Centromeres are functionally conserved primary constriction sites for kinetochore assembly during chromosome segregation.....	20
Figure 1.3 Loading pathways of H3 variants in mammals by their specific chaperone complexes	24
Figure 1.4 Chromatin localization and stoichiometric composition of mammalian multi-subunit NuRD complex;.....	29
Figure 3.1 There is a physical interaction between CID and RbAp48 subunit of CAF1 complex.....	35
Figure 3.2 Newly synthesized CID incorporation is reduced upon RbAp48 depletion....	37
Figure 3.3 RbAp48 tethering does not recruit CID as abundantly as p180 at ectopic LacO array.	38
Figure 3.4 Ectopically-expressed CID protein levels do not change dramatically upon knockdown of CAF1 subunits.....	39
Figure 3.5 Nuclear levels of ectopically-expressed CID does not decrease upon p180 RNAi.....	40
Figure 3.6 Hyd is enriched among the interacting partners of Δ NCID.....	42
Figure 3.7 X-linked CID containing complexes are pulled down and detected.....	44
Figure 3.8 Data quality for the Xlink-IP-MS experiment.....	46
Figure 3.9 Core components of NuRD complex are enriched among the interacting partners of CID.....	47
Figure 3.10 CID has a physical interaction with NuRD complex, which is stronger than B3 (A).....	48
Figure 3.11 Ectopically-expressed CID co-localizes with Mi-2 on the chromatin.....	49
Figure 3.12 Ectopically-expressed CID protein levels decrease upon Mi-2 knockdown.	50
Figure 3.13 Nuclear levels of ectopically-expressed CID decreases upon HDAC inhibition.	52
Figure 3.14 Ectopic CID localization is reduced upon Mi-2 and MTA1 depletion.....	53
Figure 3.15 NuRD-binding incompetent RbAp48 mutant lacks MTA1-like interaction, while retaining interactions with p180 and CID.....	55
Figure 3.16 Ectopic B3 (A) localization is reduced upon NuRD-binding incapable RbAp48 mutant overexpression.....	56
Figure 3.17 Nuclear localization of ectopically-expressed CID decreases upon MTA1-like knockdown.....	57
Figure 3.18 Nuclear localization of ectopically-expressed B3 (A) is abrogated upon NuRD-binding incapable RbAp48 mutant overexpression.....	58
Figure 3.19 CID physically and genetically interacts with hyd	60
Figure 3.20 CID is poly-ubiquitinated and destabilized upon hyd induction.	62
Figure 3.21 Cellular levels of nuclear localization-deficient CID constructs are upregulated under hyd depletion.....	64
Figure 3.22 Endogenous nuclear and total cellular CID levels increased upon hyd depletion.....	66
Figure 3.23 Centromeric CID levels at mitotic chromosomes increased upon hyd depletion.....	67
Figure 3.24 Newly synthesized CID incorporation is reduced upon hyd depletion.	68
Figure 4.1 Potential working modal for NuRD complex-mediated misincorporation of overexpressed CID	80

LIST OF TABLES

Table 7.1 Chemicals.....	85
Table 7.2 Tissue culture reagents.....	86
Table 7.3 Buffers and solutions.....	86
Table 7.4 Equipment and lab materials.....	89
Table 7.5 Primary and secondary antibodies.....	90
Table 7.6 Enzymes.....	91
Table 7.7 Kits.....	91
Table 7.8 DNA vector constructs used for stable cell lines.....	92
Table 7.9 Primers.....	92
Table 7.10 <i>E.coli</i> strains.....	94
Table 7.11 Yeast strains.....	94
Table 7.12 Fly strains.....	94
Table 8.1 Pairwise comparison of enriched proteins detected in Δ NCID co-IP-MS.....	102
Table 8.2 Known or candidate CID interacting partners detected in Xlink-IP-MS compared to (Barth et al., 2014).....	104
Table 8.3 GO terms for each sample in Xlink-IP-MS.....	107
Table 8.4 Pairwise comparisons of enriched proteins detected in Xlink-IP-MS.....	109

ACKNOWLEDGMENTS

I would like to thank first of all Sylvia for her support and supervision. Thank you Anne Laure for all the nice suggestions, corrections of my thesis and feedback. Andrea, thanks for all your technical support and assistance. The rest of the AG Erhardt members, you were always friendly, nice, helpful and funny. That makes the social lab environment always warm. Thanks for sharing this nice atmosphere and working together.

I am also very thankful to my TAC committee members Prof. Frauke Melchior and Prof. Bernd Bukau for their suggestions and feedback. They taught me to look more critically into my project. I also thank Prof. Marina Lusic for being the 4th referee.

I would like to particularly thank MSc student Alex Wilhelm for his enthusiasm and dedication into the project. He spent great effort on this project and made huge contributions. Dr. Bernd Hessling from ZMBH facility also majorly contributed to this study with Xlink-IP-MS results, interpretation and analysis. Dr. Sabine Merker from ZMBH facility collaborated with us for the Δ NCID co-IP. Collectively, I am very pleased to Dr. Thomas Ruppert and all the co-workers of ZMBH Mass Spec facility for their service. Imaging facility and Dr. Holger Lorenz were also very helpful with the microscopy image quantification.

I am especially thankful to all the other collaborators who made this work possible. Prof. Ernest Laue and Dr. Wei Zhang from Cambridge University gifted the very important RbAp48-mutant construct and did a major contribution to this study. Prof. Alex Brehm from Marburg University gave us the essential NuRD antibodies. Prof. Axel Imhof from Ludwig Maximilian University Munich sent the hyd construct, which was crucial for this study. Collaborators made the life easier for me; therefore, I am deeply thankful to them.

All of the friends in Heidelberg also made the life so pleasant. Abhi and Ana, it was so nice to be friend with you guys. I enjoyed so much during our conversations. And Abhi, you are quite an interesting person that I will always remember during my life. Gurkan, Ayca, Yashar, Takumi, all of you were so special. I loved the craziness of the friends from theatre group. Daniel, you were also an amazing friend. Atalay and Firat, I always look forward to our lunch time chats and basketball. There were so many special friends and memories that always made me smile in Heidelberg.

I also cannot be more thankful to my beloved family. Even though we are far from each other, they always made me feel home when I hear their voices. They are the most important contributor of this study because of growing me up with their love.

Lastly, I thank you my darling. You were always with me during these hard times. You always motivated me to achieve this success, and never let me surrender. You also showed me understanding and gave your love. I am so lucky to have such a fantastic partner.

